AN ABSTRACT OF THE THESIS OF

Jeremy D. Craner for the degree of Master of Science in
Geology presented on March 24, 2006.
Title: Hydrogeologic Field Investigation and Groundwater Flow Model of the Southern
Willamette Valley, Oregon.

Abstract approved:

_____

Roy Haggerty

Elevated groundwater nitrate (NO_3^-) concentrations in the Southern Willamette

Valley (SWV) caused the Oregon Department of Environmental Quality (ODEQ) to

declare a Groundwater Management Area (GWMA) in Spring, 2004. To better

understand direction of groundwater flow, groundwater age, and nitrate transport

pathways of the SWV we developed a steady-state numerical groundwater flow model

using MODFLOW with MODPATH. Model development was supplemented by field

investigations of local outcrops, pump and slug tests, and laboratory analyses to

determine groundwater age and groundwater chemistry.

Field work included the construction/collection of cross-sections and stratigraphic

columns; 12 slug tests and 3 pump tests to determine hydraulic conductivity and

storativity; 10 groundwater ages using CFC-11, CFC-12, and CFC-113; 3 wells

instrumented to collect long-term continuous water level measurements; 42 wells selected

for quarterly manual water level measurements; and 14 groundwater samples to

determine pH, dissolved oxygen, specific electrical conductance, chloride, sulfate, and nitrate concentrations.

Slug tests determined horizontal hydraulic conductivities (K_x) from 4.19 x 10^{-8} m/s to 4.62 x 10^{-4} m/s. Pump tests determined K_x-values from 3.59 x 10^{-4} m/s to 7.22 x 10^{-3} m/s, vertical hydraulic conductivities (K_v) from 3.48 x 10^{-6} m/s to 3.84 x 10^{-6} m/s, and storage coefficients from 0.05 to 0.15. Groundwater age ranged from 13 years to >50 years, with the greatest ages resulting from wells that penetrated the semi-confining Willamette Silt. Groundwater ages were compared to model particle travel times using MODPATH and used as calibration targets. Groundwater ages along with nitrate, chloride, sulfate, and dissolved oxygen concentrations were used to reconstruct past contaminant loading and observe data trends. Spatial distributions of hydraulic conductivity were estimated using wells with specific capacity data and an empirical relationship ($T = 158.48sc$, where T = transmissivity (ft^2/d) and sc = (gal/min/ft); $R^2 = 0.61$) between wells in the study area that contained both specific capacity and aquifer test data.

The calibrated groundwater flow model is intended to help make management decisions, establish monitoring programs, and to be used as an outreach education tool. Model simulations were run in key areas to demonstrate model capabilities and create visual aids for outreach education. This study suggests it may take 10's of years to see measurable declines of groundwater nitrate in some locations. It is our hope that educating stakeholders about local groundwater flow along with stressing the use of Best Management Practices (BMPs) will result in better decision making and lead to a reduction of groundwater nitrate concentration in the SWV.

Hydrogeologic Field Investigation and Groundwater Flow Model of the Southern
Willamette Valley, Oregon

by
Jeremy D. Craner

A THESIS

submitted to

Oregon State University

in partial fulfillment of
the requirements for the
degree of

Master of Science

Presented March 24, 2006
Commencement June 2006

Master of Science thesis of Jeremy D. Craner
presented on March 24, 2006.

APPROVED:

_____

Major Professor, representing Geology

_____

Chair of the Department of Geosciences

_____

Dean of the Graduate School

I understand that my thesis will become part of the permanent collection of Oregon State
University libraries. My signature below authorizes release of my thesis to any reader
upon request.

_____

Jeremy D. Craner, Author

ACKNOWLEDGEMENTS

TABLE OF CONTENTS

TABLE OF CONTENTS (Continued)

LIST OF FIGURES

LIST OF FIGURES (Continued)

LIST OF FIGURES (Continued)

LIST OF TABLES

LIST OF APPENDICES

LIST OF APPENDIX FIGURES

LIST OF APPENDIX TABLES

1. INTRODUCTION

A Groundwater Management Area (GWMA) was declared in the Southern Willamette Valley (SWV), Oregon on May 10, 2004 in response increased concern about groundwater nitrate (NO_3^-) contamination, making it one of three designated in Oregon. According to the Groundwater Quality Protection Act of 1989, the Department of Environmental Quality (DEQ) must declare a GWMA if nitrate levels at or above 7 mg/L, a level 70% of the Maximum Measurable Limit (MML) are confirmed in a widespread area and suspected to originate from non-point (diffuse or unconfined) sources (Eldridge, 2004). A GWMA unites local residents and environmental planners in the process of restoring and protecting groundwater quality, anticipating that people who live and work in the area maintain a groundwater resource they can safely utilize (Eldridge, 2004).

In Oregon, approximately 70% of all state residents and over 90% of rural residents rely on groundwater as their primary drinking water source (Oregon Department of Environmental Quality, 2001). Broad and Nebert (1990) and Gonthier (1985) indicate more than 80 percent of the groundwater used in the Willamette Basin is pumped from the alluvial aquifer. In most rural areas of the SWV, groundwater is the sole source of water for irrigation, consumption, and basic household needs. Groundwater is the most likely source for meeting future water needs, especially in rural areas, because many streams are administratively closed to new appropriations in summer (Bastasch, 1998). Since the SWV is one of the fastest growing regions in Oregon (Population Research Center, 2005) it is in our best interest to protect this vital, increasingly important resource.

With this expanding population, groundwater is becoming increasingly important. Further allocation of surface water and groundwater resources in some areas is unable to occur without affecting aquatic habitat, reducing base flow levels in local rivers and streams, and ultimately losing water from aquifer storage when the aquifer and stream are hydraulically connected. Regulating the use of groundwater is difficult and further development of groundwater resources is likely to impact surface water bodies, however, this is the only water resource available in rural areas of the SWV. Policy makers and water quality regulators are left with making difficult decisions about how to protect and manage water resources in this area.

A GWMA Committee composed of local stakeholders and public drinking water experts was formed to strategize with state agencies to determine what non-mandating measures are appropriate to help reduce existing contamination and to prevent further contamination of local groundwater. The GWMA Committee, local state and government agencies, scientists, and stakeholders have repeatedly asked questions like these about groundwater flow: (1) "Which direction is it moving?" (2) "How fast is it moving?" (3) "Which areas are most susceptible to anthropogenic contamination?" (4) "Where is the nitrate coming from?" (5) "If we change our management practices now, how long before we see a decline in groundwater nitrate levels?" (6) "Can my well be affected by my neighbors' practices?" These are all relevant yet difficult questions to answer. This study was conducted to address some of these questions with field studies and the development of a groundwater flow model of the SWV.

This study focused strictly on the movement of groundwater with nitrate and the development of a numerical groundwater flow model. This study was complimented by

field investigations, groundwater sampling, and laboratory analyses to determine groundwater age and chemistry. Rinella and Janet (1998) and Wentz et al. (1998) discuss surface water contamination issues in the Willamette Valley.

Project Objectives

- to develop a calibrated, up-to-date, steady-state numerical groundwater flow model to be used as a tool to help address groundwater quality and quantity issues in the SWV

- to interact with residents of the SWV through personal contact and web presentations in order to explain how groundwater moves and assist people in understanding how their behavior affects groundwater quality

- to collect model-specific data required for the development of a groundwater flow model that accurately represents the SWV. This included: the development of a groundwater monitoring network to collect water level measurements for model calibration, the construction of stratigraphic columns and cross-sections to gain a better understanding of stratigraphic relationships, the collection of groundwater samples for CFCs and pH, dissolved oxygen, sulfate, nitrate, chloride, and specific electrical conductance to determine groundwater age and chemistry, and to conduct pump and slug tests to best estimate aquifer parameters.

Research Questions

- How does geology affect groundwater flow in the SWV?

- What is the range of hydraulic conductivity for each hydrogeologic unit in the SWV?

- What is the age of groundwater in the SWV?

- Is the average age of groundwater constant throughout the SWV or does it change as geologic units and well depth changes?

- Does groundwater chemistry change with time?

2. BACKGROUND

2.1 Nitrate in Groundwater

Local groundwater is susceptible to anthropogenic contamination (e.g., nitrate or NO_3^-) due to the highly permeable soil and alluvial aquifer that exist in the SWV. Groundwater is vulnerable to contamination by nitrate because (1) nitrate application is ubiquitous, and (2) nitrate is highly mobile in water. Major sources of nitrate in watersheds of the United States include inorganic fertilizer, animal manure, and atmospheric deposition (Puckett, 1994). Leaching of excess nitrate from contaminated groundwater to surface water bodies where seepage rates are high along stream and river banks can cause problems such as eutrophication, which can drastically alter submerged aquatic vegetation and decrease dissolved oxygen levels, both required by fish and shellfish to survive (Gardner and Vogel, 2005). Nitrates high solubility and anionic form (negative charge) gives it the ability to leach through soils and contaminate groundwater (Nolan, 2001).

Elevated levels of nitrate in drinking water are a public health concern. High concentrations of nitrate can result in methemoglobinemia, or "blue baby syndrome," that can cause low oxygen levels in the blood of infants and can be fatal (Spalding and Exner, 1993). Ingestion of nitrate in drinking water has been linked to spontaneous abortions

and non-Hodgkin's lymphoma (Nolan, 2001). A variety of studies indicate that the development of cancers, birth defects, growth restriction, hypertension, and respiratory tract infections have been associated with excess nitrate intake (studies cited in Kite-Powell, 2003; Vick, 2004). The U.S. Environmental Protection Agency (U.S. EPA) has established a Maximum Contaminant Level (MCL) of 10 mg/L for nitrate as nitrogen (N) for public drinking water sources (U.S. Environmental Protection Agency, 2005).
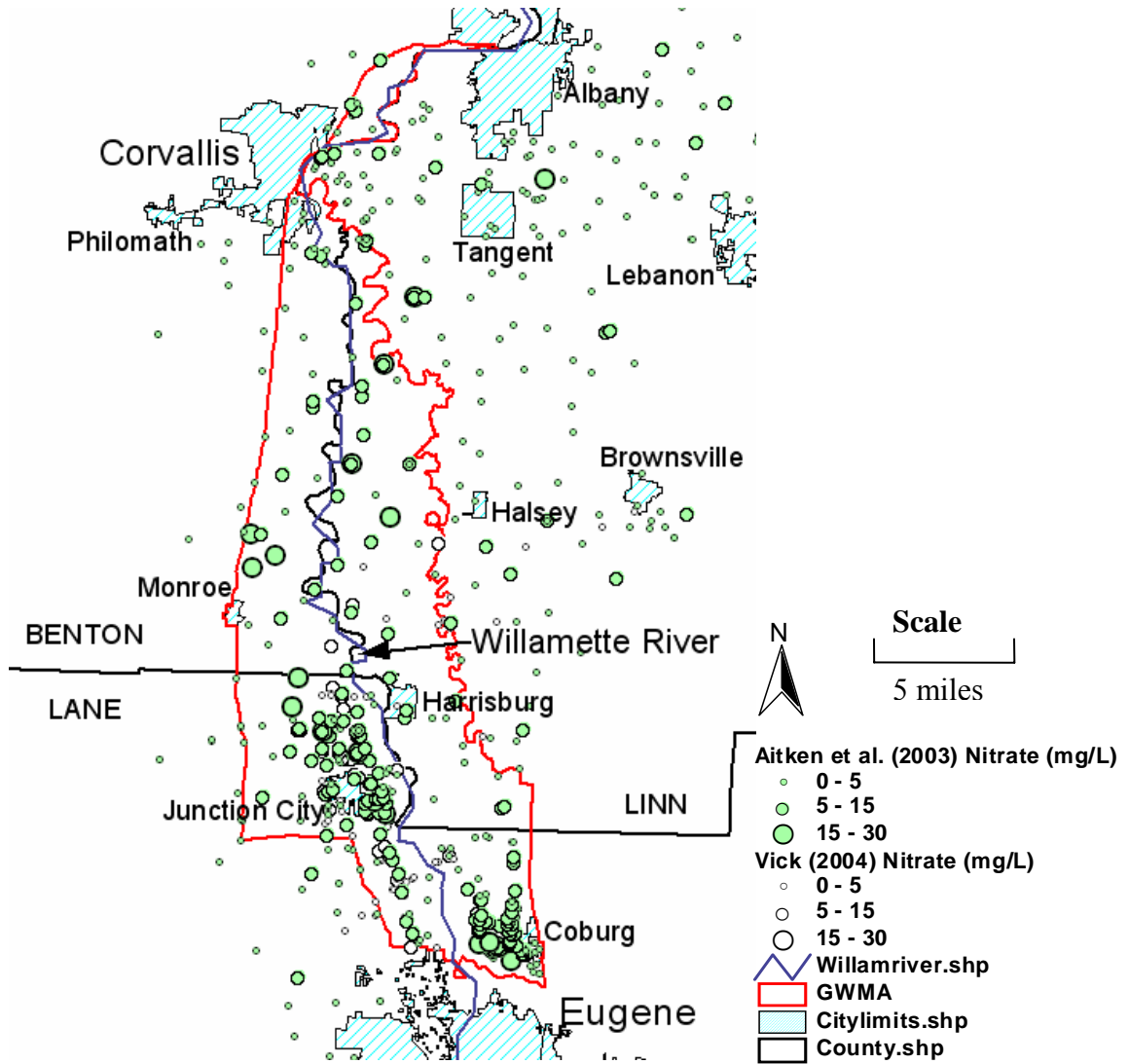
Figure 1: Nitrate concentrations of the SWV from recent groundwater studies.

Various forms of nitrogen exist in the environment. Nitrate is the main form of nitrogen that occurs in groundwater, but dissolved nitrogen also occurs as ammonia (NH_3), ammonium (NH_4^+), nitrogen (N_2), nitrite (NO_2^-), nitrous oxide (N_2O), and organic nitrogen (nitrogen that is incorporated into organic substances) (Kendall and Aravena, 1999). Nitrates are either taken up by plants to help form plant proteins, or are broken down by the actions of heterotrophic bacteria in the presence of an organic carbon source to form nitrogen gas (Canter, 1997).

Of local importance, a study conducted by Iverson (2002) suggests that in areas that contain a sufficient thickness of the semi-confining unit Willamette Silt, a geochemical reduction-oxidation boundary is preventing nitrate from entering the underlying aquifer through autotrophic denitrification, a process that is increasingly recognized for its ability to eliminate or reduce nitrate concentrations in groundwater (Korom, 1992). Another local study by Argihi (2004) suggests nitrate attenuation in the Willamette Silt is due to iron (II) reducing nitrate abiotically to nitrite, a non-biological mechanism occurring near the reduction-oxidization boundary. Nevertheless, the regionally extensive Willamette Silt has the capacity in some locations to reduce the amount of nitrate leaching into the groundwater by acting as a nitrogen sink. Vick (2004) used isotopes of nitrate and other chemical indicators in an attempt to determine sources of nitrate in drinking water wells in the SWV. Specific sources of nitrate were not conclusively found. The results of these studies become important when considering how to manage and protect the groundwater in the Willamette Valley.

Several studies have been conducted in the past 70 years documenting groundwater contamination in the SWV. These studies are reviewed by Vick (2004) and

by Cole and Oregon Department of Environmental Quality (ODEQ) (2004). Recent

groundwater assessments were conducted in the Willamette Basin by the U.S. Geological

Survey by Hinkle (1997) and Wentz et al. (1998). Recent assessments of groundwater

quality in the SWV were conducted in 2000-2002 by ODEQ (Aitken et al., 2003;

Eldridge, 2004) and by Vick (2004) in 2003 (see Figure 1). Results from ODEQ studies

in the SWV indicate that nitrate was detected between 3 and 10 mg/L in 41% of 476

wells, with 11% of 476 wells exceeding 10 mg/L. Vick (2004) sampled 120 wells and

found a mean nitrate concentration of 4.81 mg/L. Shallow groundwater unaffected by

human activities commonly contains less than 2 mg/L of nitrate (Mueller and Helsel,

1996).

It is believed that a combination of point and non-point sources is responsible for

the degraded groundwater quality in the SWV. Common point sources in this area

include confined animal feeding operations (CAFOs), gravel pits, and industrial

stormwater. Common non-point sources include malfunctioning septic systems,

fertilizers, and the reapplication of animal waste to fields.

2.2 Study Area

The SWV lowland is bounded to the west by the Coast Range, to the east by the

Cascade Range, to the south by the Coast and Cascade Ranges, and to the north by the

Salem Hills (see Figure 2). The Coast Range contains peaks that exceed 4,000 ft (1219

m) and the Cascade Range contains peaks that exceed 10,000 ft (3048 m). The GWMA

covers approximately 223 mi^2 (571 km^2) of the SWV and contains communities of

Junction City, Harrisburg, Monroe, and Coburg, along with portions of Linn (pop.

107,410), Benton (pop. 79,357), and Lane (pop. 331,594) counties (see Figure 1)

(Population Research Center, 2005). The SWV is one of the fastest growing regions in Oregon with an average total population growth of 12.5% from 1990-2000 (Population Research Center, 2005).

The Willamette Basin has a modified maritime climate regime characterized by cool, wet winters and warm, dry summers with about 75 percent of the annual precipitation occurring from October through March and less than 5 percent falling in July and August (Uhrich and Wentz, 1999). In the Willamette Valley, yearly precipitation ranges from 40 in to 50 in (102 cm to 127 cm) and mean monthly air temperatures range from 37°F to 41°F (3°C to 5°C) in January and 63°F to 68°F (17°C to 20°C) in August (Uhrich and Wentz, 1999). Specifically, average yearly precipitation and temperature in Corvallis and Eugene is 44 in (112 cm) and 52.8°F (11.6°C), and 49 in (125 cm) and 53.2°F (11.8°C), respectively (Oregon Climate Service, 2005). Streamflow in the Willamette Basin reflects the seasonal distribution of precipitation, with 60 to 85 percent of runoff occurring from October through March, but less than 10 percent occurring during July and August (Wentz et al, 1998).

The Willamette River drains the SWV (see Figure and Figure 2), running from south to north, and is the 13th largest river in the conterminous United States (Wentz et al., 1998). Other major water bodies in the SWV lowland include Fern Ridge Lake, Long Tom River, Marys River, and Coast Fork of the Willamette River (all draining portions of the Coast Range), McKenzie River, Mohawk River, Muddy Creek, Calapooia River, and South Santiam River (all draining portions of the Cascade Range).

The geomorphology of the SWV is characterized by a series of gently sloping and relatively smoother terrace and floodplain surfaces (Roberts, 1984). Fluvial,

glaciofluvial, lacustrine, and slackwater sediments make up the complex basin-fill

material (Allision, 1978; Balster and Parsons, 1968; Glenn 1965). The SWV is typified

by very low relief and slightly incised valleys and contains scattered hills that have been

partially buried by alluvium (Balster and Parsons, 1968). The prominent alluvial fans on

the east side of the SWV were deposited by high-energy streams where they entered into

the Willamette Lowland from the Cascade Range creating coarse proximal and fine distal

facies (Woodward et al., 1998). The majority of the SWV is relatively flat-lying,

however the floodplain deposits that lie along the Willamette, South Santiam, and

McKenzie Rivers, generally have an undulating or rolling topography.

The upper Willamette River has been significantly modified today from the time

of Euro-American settlement in the 1840s, with a reduction of channel length by about 45

to 50 percent (Benner and Sedell, 1997 and Hulse et al., 2002). The Willamette River

was at one time more anastomosing and braided whereas today it is channelized and

confined (Hulse et al., 2002). Cut into the main lowland plain are trenches that ordinarily

are floored with young alluvium; these are occupied by the Willamette River and its

tributaries. Due to low-energy conditions, rivers in the SWV are unable to erode

significantly into the coarse sediment on the alluvial fans and are forced, mostly by

lateral sidecutting, to occupy channels in the distal portions of the fans (usually to the

west) (Woodward et al., 1998). The floodplain of the Willamette River is narrow in

relation to the total valley width. In the SWV, the Willamette River occupies the western

part of the valley floor and is incised about 15 ft to 25 ft (4.6 m to 7.6 m) below the

general level of the valley plain (Balster and Parsons, 1968). The relatively younger

stratigraphy of the SWV was developed by cutting and removing the older alluvial

material and redepositing new, highly permeable alluvial stratigraphy, generally along the Willamette and South Santiam Rivers during Holocene time.

Land use practices in the SWV affect the quality of local groundwater, including groundwater nitrate levels. Groundwater samples collected in the Willamette Valley by Hinkle (1997) indicated statistically significant correlations between high nitrate levels, local irrigation, and the presence of pesticides, all suggesting local land use does affect groundwater quality (Hinkle, 1997). Influence of land use on groundwater quality is exasperated when a highly permeable aquifer is overlain by well-drained soils, which describes much of the SWV. Practices such as cultivation vs. no cultivation (Sotomayor and Rice, 1996), timing of application of fertilizer and irrigation along with irrigation efficiency (Selker, 2004; Selker and Rupp, 2004; Feaga et al., 2004), and crop type produced (Selker and Rupp, 2004; Ross Penhallegon, Oregon State University Extension, pers. communication, 2004) can have a large effect on the amount of nitrate that is leached into the underlying aquifer. In addition, nitrogen fertilizer application rates for the Willamette Basin show an increase from 1945 through about 1980, which may result in increased future groundwater nitrate concentrations (Alexander and Smith, 1990). Other local groundwater nitrate contributors include improperly functioning septic systems and residential areas (Vick, 2004).

The Willamette Valley is one of the premier agricultural areas in the world due mainly to highly fertile soils, a mild climate, and a long growing season. Agriculture in the Willamette Valley dates back to the early 1800s when stock animals and a variety of crops including wheat, vegetables, and fruit orchards were first introduced (Uhrich and Wentz, 1999). Agricultural land comprises 22 percent of the entire Willamette Basin,

found predominantly in the Willamette Valley lowland (Wentz et al., 1998). Currently, agriculture is the chief industry within the SWV (Uhrich and Wentz, 1999). In 2002, SWV farms covered over 1,400,000 acres (NASS, 2002). Main crops of the SWV include grass seed, hazelnuts, peppermint, tree and small fruits, and a variety of vegetables (Ross Penhallegon, Oregon State University Extension, pers. communication, 2004). Also of agricultural importance, thirty-three permitted confined animal feeding operations (CAFOs) are present across the SWV (Aitken et al., 2003).

Market changes have recently contributed to a major shift in the types of crops most farmers grow. This has required the farmers of the SWV switch to growing grass seed and other non-row crops to make a profit and maintain maximum production and economic viability. Crop-type changes result in the application of different types and amounts of fertilizers and other chemicals, as well as different irrigation practices. This change in land use subsequently affects nitrogen loading to the groundwater.
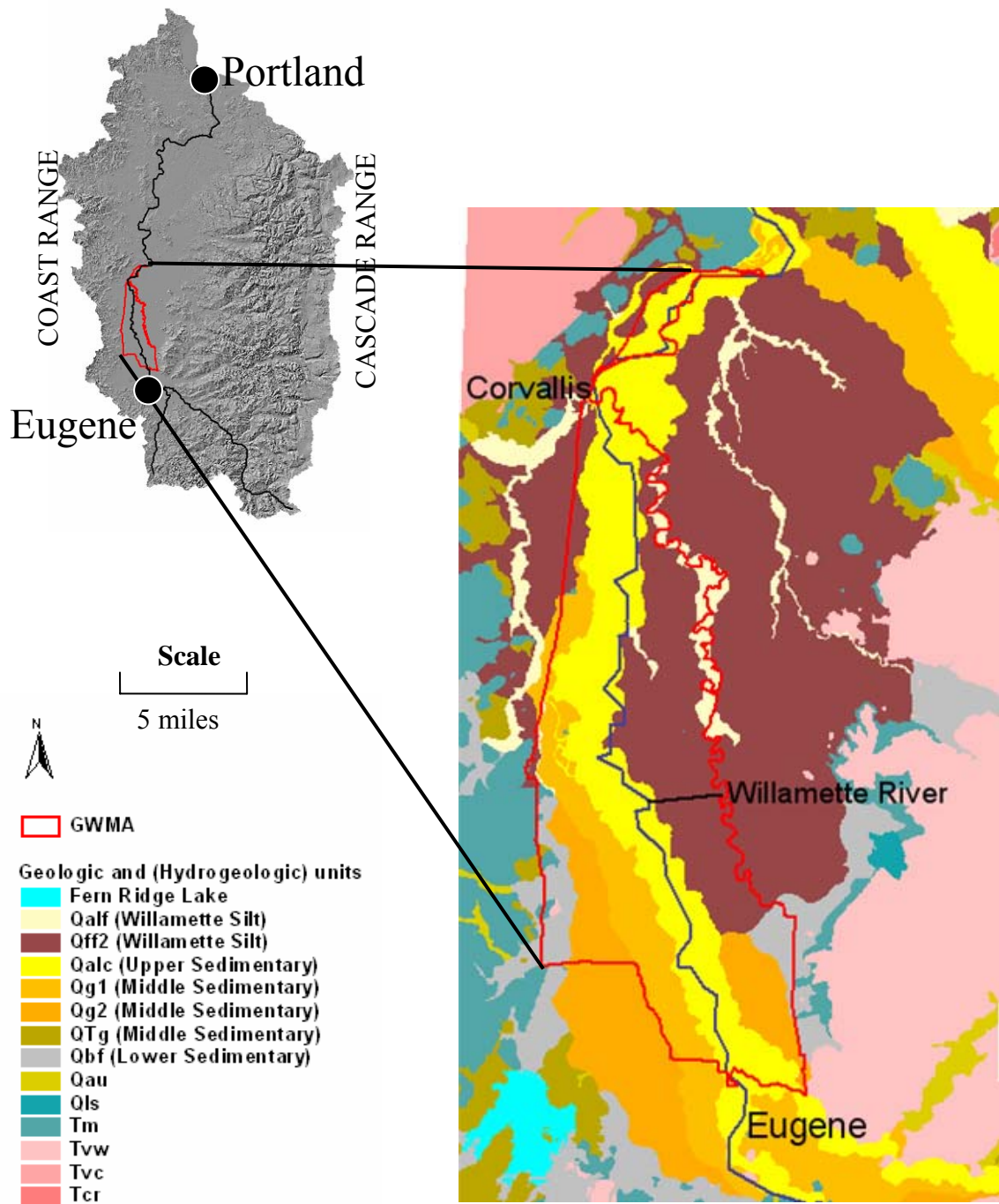
Figure 2: Regional view of the Willamette Basin and SWV including geologic and hydrogeologic units. Geologic units are those of O'Connor et al. (2001).

2.3 Geology

A variety of geologic events have resulted in forming what the Willamette

Lowland and SWV is today. Tectonic activity resulted in uplift, folding, and faulting

along of the Cascade and Coast Ranges and along the north-south axis of a regional

synclinorium creating subsidence between these two ranges and establishing the

Willamette Lowland as a depositional basin for continental sediment from flanking

mountain ranges (Yeats et al., 1996; Gannett and Caldwell, 1998). The Coast Range is

composed of uplifted Tertiary marine sedimentary rocks and related marine volcanic and

intrusive rocks and the Cascade Range is an accumulation of volcanic lavas and debris

erupted from continental volcanoes (see Figure 2). Tertiary marine strata and the older

Cascade volcanic rocks interfinger at depth (contact poorly constrained) beneath the

Willamette Lowland to form the bedrock foundation (Conlon et al., 2005). The

Willamette Lowland is a north-south oriented structural depression that is 145 miles (233

km) long, averages 10 to 15 miles (16 to 24 km) in width, and has been a topographic low

for at least 15 million years (O'Connor et al., 2001). Folded and faulted basalt (Columbia

River Basalt Group) divide the lowland into four separate structural basins, one of which

includes the SWV (Woodward et al., 1998). Detailed geologic history and geologic

descriptions of the basement rocks located within the Coast and Cascade Ranges can be

found in Piper (1942), Graven (1990), Yeats et al. (1996), Gannett and Caldwell (1998),

Woodward et al. (1998), and O'Connor et al. (2001).

Various studies have looked at the unconsolidated deposits of the SWV. Piper

(1942) completed one of the earliest studies focusing on hydrogeology and groundwater

resources of the Willamette Basin, along with the first attempt at mapping the basin-fill

deposits. Allison (1953) described in detail the geology of the Albany quadrangle.

Balster and Parsons (1968) described geomorphic surfaces of the Willamette Valley and

their relationships to soil types. Frank (1973), (1974), and (1976) focused on the

groundwater and hydrogeology of the Eugene-Springfield, Corvallis-Albany, Harrisburg-

Halsey areas, respectively. Roberts (1984) looked at the stratigraphic relationships and

evolutional history of the sedimentary fill of the SWV near Monroe. Graven (1990)

described the structure and tectonics of the SWV. A regional description of the

hydrogeologic units of the Willamette Lowland, including the SWV, was described by

Gannett and Caldwell (1998) and Woodward et al. (1998). Quaternary geologic units of

the SWV were mapped by O'Connor et al. (2001) based on stratigraphic, topographic,

pedogenic, and hydrogeologic properties. And finally, an up-to-date report integrating

data from previous studies with newly collected data to provide a conceptual framework

of the groundwater flow system in the Willamette Basin to help resource managers

evaluate the impacts of groundwater management decisions was provided by Conlon et

al. (2005). These studies are the most important with regard to geology, hydrogeology,

and groundwater/surface water flow systems in the SWV (emphasis placed on more

recent work) and will be referred to throughout this report.
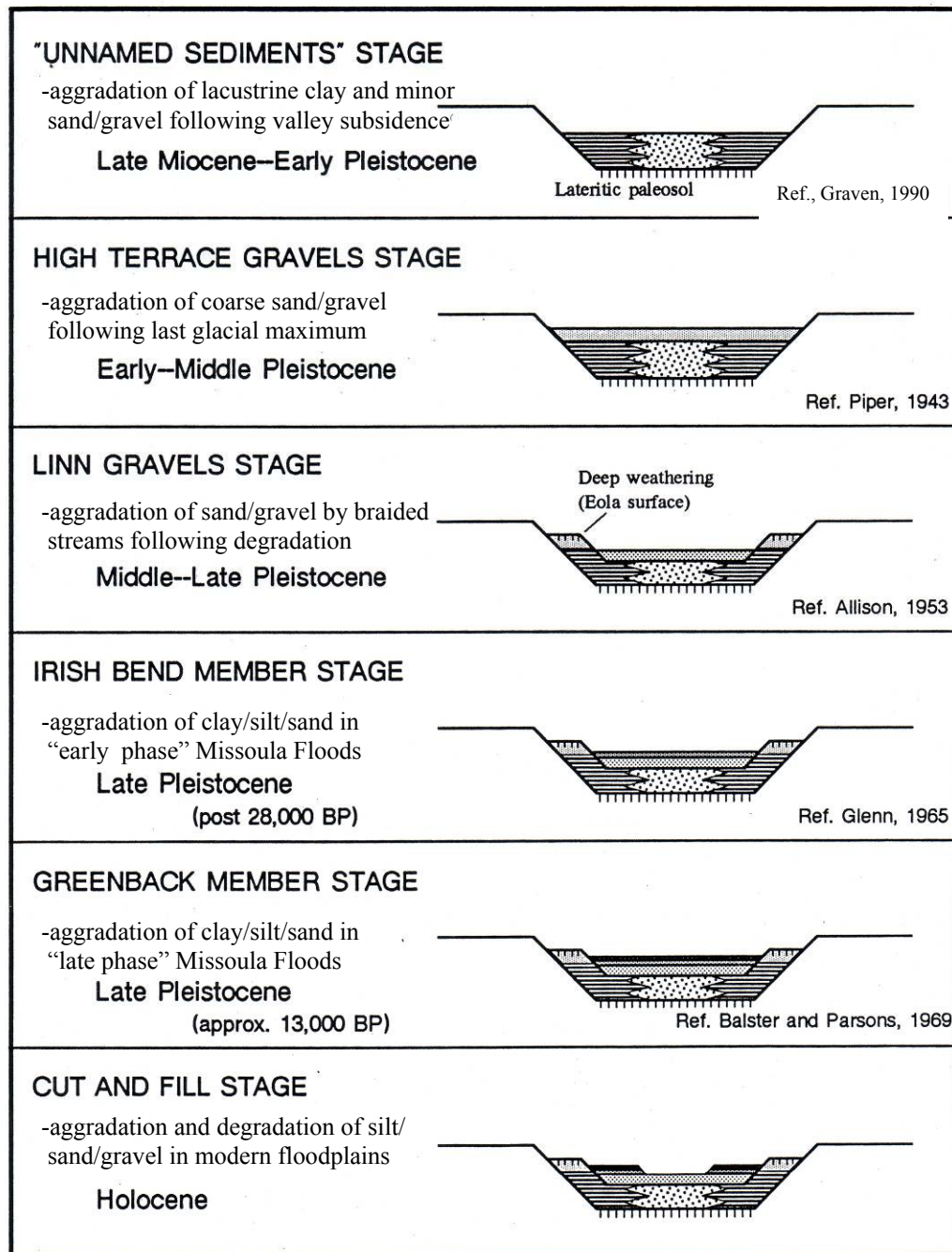
Figure 3: Schematic Neogene and Quaternary stratigraphic history of the SWV. Modified from Graven (1990).

2.4 Basin-fill Hydrogeologic Units

In this section we will characterize the designated basin-fill hydrogeologic units of the SWV and their hydraulic properties. Geologic units associated with each hydrogeologic unit will also be described. Geologic units were divided into five hydrogeologic units based on permeability, past studies, and data collected during this study.

The basin-fill material in SWV has undergone several episodes of aggradation and degradation. Figure 3 shows sequential conceptual models of aggradation and degradation within the unconsolidated basin-fill sediments. The basin-fill material deepens from north to south in the SWV and generally has a Cascade Range provenance due to its high gradient streams and bedrock material.

Various nomenclatures have been used for the basin-fill deposits. O'Connor et al. (2001) and Graven (1990) provide tables that contain informal and formal nomenclature, assigned ages, and inferred deposit genesis of bedrock and basin-fill units linking major past and current studies. For this study, a stratigraphic table was developed to help clarify nomenclature and stratigraphic relationships of geologic and hydrogeologic units (see Figure 4) from Gannett and Caldwell (1998) and Woodward et al. (1998), O'Connor et al. (2001), Conlon et al. (2005), and this study.

Hydraulic properties described in this section for the basin-fill hydrogeologic units were derived exclusively from Table 1 of Conlon et al. (2005), where transmissivity, hydraulic conductivity, and storativity values were estimated from previous studies. For comparison purposes, transmissivity was converted to hydraulic conductivity by dividing transmissivity by aquifer thickness, where aquifer thickness was

estimated as the well screen interval. This usually produces a maximum value of

hydraulic conductivity. The storage coefficient is also estimated in Table 1 of Conlon et

al. (2005), which is defined as the volume of water released from storage per unit surface

area of the aquifer per unit change in head.

		GEOLOGIC UNITS			HYDROGEOLOGIC UNITS		
		Piper (1942)	Frank (1973, 1974, 1976)	O'Connor et al. (2001)	Gannett and Caldwell, 1998	Conlon et al. (2005)	This study
QUATERNARY	Holocene	Younger Alluvium	Younger Alluvium	Qalc / Qalf	Willamette Aquifer	Upper Sedimentary unit (USU)	Upper Sedimentary unit (USHU)
	Pleistocene	Older Alluvium	Older Alluvium	Qg1; silt, clay, and minor sand; Missoula Flood Deposits (Qff1, Qff2); W. Basin provenance silt; Qg2	Willamette Silt unit	Willamette Silt unit (WSU); Middle Sedimentary unit (MSU)	Willamette Silt unit (WSHU); Middle Sedimentary unit (MSHU)
		Terrace Deposits	Terrace Deposits	QTg, QTt			
TERTIARY	Pliocene	Consolidated Rocks (sed. + volcanic)	Condolidated Rocks		Willamette Confining unit	Lower Sedimentary unit (LSU)	Lower Sedimentary unit (LSHU)
	Miocene		Little Butte Volcanic series		Columbia River Basalt unit	Columbia River Basalt unit	CRB (not in model)
	Oligocene		Eugene Form.		Basement Confining unit	Basement Confining unit (BCU)	Basement Confining unit (BCHU)
	Eocene		Spencer + Tyee Formations; Siletz River vol.				

Figure 4: Historic correlation chart containing the geologic and hydrogeologic units of the Southern Willamette Valley, Oregon. Modified from Figure 1 in O'Connor et al. (2001) and Figure 3 in Conlon et al. (2005).

2.4.1 Basement Confining Hydrogeologic Unit

The Basement Confining hydrogeologic unit (BCHU) is discussed in this section however no specific work was conducted during this study on this unit. This unit was used as impermeable boundary due to its low permeability, low porosity, and low well yield (Conlon et al., 2005). The unit includes the Tertiary marine sedimentary rocks and Eocene volcanic rocks of the Coast Range, and volcanic and volcaniclastic rocks of the Western Cascade area (Gannett and Caldwell, 1998). The unit underlies the SWV and Willamette Basin, and is exposed in the Coast Range and Western Cascades. High salinity is common in groundwater within the Tertiary marine sedimentary rocks (Piper, 1942 and Woodward and others, 1998). Arsenic is also a common problem within portions of the BCHU (Conlon et al., 2005).

Well yields are commonly less than 5 gal/min (3.15×10^{-4} m^3/s), suitable for most domestic uses. Fracture zones in this unit, however, can produce higher well yields (Conlon et al., 2005). Estimates of horizontal hydraulic conductivity (K_x) from Table 1 in Conlon et al. (2005) for this unit range from 10^{-5} ft/d to 10^{-2} ft/d (10^{-11} m/s to 10^{-8} m/s) and the storage coefficient (S) range from 5×10^{-5} to 3×10^{-3}.

2.4.2 Lower Sedimentary Hydrogeologic Unit

The spatially extensive Lower Sedimentary hydrogeologic unit (LSHU) overlies the BCHU and consists primarily of fine-grained, distal alluvial fan, low-gradient stream, and lake deposits. Drillers' logs describe this unit as "blue" or "grey" with varying combinations of clay, silt, sand, and "shale." This unit is thought to have been deposited in Pliocene and Pleistocene time; however, a constrained age of deposition has not been determined (O'Connor, et al, 2001). The LSHU is volumetrically the largest unit in the

basin-fill sequence and predominates at depth with a thickness up to 350 ft (107 m) (Gannet and Caldwell, 1998).

The fine-grained LSHU deposits are a regional confining unit because of their widespread occurrence and low permeability (Woodward et al., 1998). Distal alluvial fan sediments were mostly deposited by Cascade Range streams and proximal alluvial fan sediments were deposited by Coast Range streams (Conlon et al., 2005). This unit occurs in the lower part of the basin fill and dominates the entire sequence in areas distant from major alluvial fans (Gannett and Caldwell, 1998). The basin-fill deposits along the margins of the Willamette lowlands in the SWV, including those along the Long Tom River and adjacent to the Cascade Range foothills north of Springfield, appear to fill marginal topographic lows created by extensive deposition of coarse-grained deposits from the McKenzie and Willamette Rivers in the central axis of the SWV (O'Connor et al., 2001).

Hydrologic properties of the LSHU allow sustainable amounts of water to be pumped from portions of this unit. Spatially sparse lenses of sand and gravel exist within this unit and some municipal wells (e.g., Junction City) are able to pump large volumes of water from this unit (Oregon Department of Human Services; Oregon Department of Environmental Quality, 2005). Many newer wells drilled in the SWV are taping this lower unit in hopes of reducing the chance of contamination in their well water. Few wells have been drilled deep enough to penetrate the LSHU to the underlying unit, so geologic and hydrogeologic information is sparse. Estimates of hydrologic properties from Table 1 in Conlon et al. (2005) include K_x-values from 0.02 ft/d to 220 ft/d

$(7.06 \times 10^{-8}$ m/s to 1.39×10^{-4} m/s), a vertical hydraulic conductivity (K_v) value of 0.10

ft/d (3.52×10^{-7} m/s), and a S from 5×10^{-5} to 2×10^{-1}.

2.4.3 Middle Sedimentary Hydrogeologic Unit

The Middle Sedimentary hydrogeologic unit (MSHU) contains three geologic

units described by O'Connor et al. (2001): QTg, Qg_1, and Qg_2. This section describes

each of these units. Generally, the MSHU is composed of alluvial unconsolidated to

semi-consolidated sand and gravel. Sand and gravel deposits up to 250 ft (76 m) thick lie

mostly on the lower permeability LSHU and extend up into local drainages. The MSHU

mostly overlies the LSHU and is overlain by the Upper Sedimentary and Willamette Silt

hydrogeologic units, described in later sections of this study.

The QTg geologic unit is the oldest geologic unit (probably deposited between 2.5

and 0.5 Ma) within the MSHU (O'Connor et al., 2001). These are weathered, high

terrace, alluvial sands and gravels that exist along the margins of the SWV. The QTg

geologic unit ranges in thickness from 0-200 ft (0-60 m), has a planar to undulating

surface, and contains thick, strongly-developed soils and a surface that can reach 328 ft

(100 m) above modern floodplains (O'Connor et al., 2001).

The early Pleistocene age Qg_2 geologic unit comprises the majority of the MSHU.

Generally, this unit is made up of unconsolidated to semi-consolidated sand and gravel

deposited in broad braidplains and meandering floodplain environments along the

McKenzie and South Santiam Rivers in the SWV (O'Connor et al., 2001). Qg_2 contains

planar to slightly undulating terrace surfaces slightly higher than geologic unit Qg_1.

River exposures show weather resistant ledges of sand and gravel (O'Connor et al.,

2001). Much of the alluvial material of the Qg_2 geologic material is made up of the three

alluvial fans that stretch out from major tributaries (mainly the Willamette, McKenzie, and South Santiam Rivers) created by streams originating in the once glaciated terrain of the Cascade Range. These alluvial fans are named the Lebannon, Springfield, and Stayton Fans in Woodward et al. (1998). Proximal, coarse deposits that grade laterally into and interfinger with progressively finer distal sediments toward the center of the SWV were first recognized by Piper (1942) and have probably existed since uplift of the Western Cascade sub-providence (Gannett and Caldwell, 1998). These alluvial fans were deposited during Pleistocene time during large-volume depositional "pulses," (O'Connor et al., 2001; Conlon, 2005). Growth of these large alluvial fans last took place during Pleistocene time with incision and reworking of fan material by streams and rivers occurring since this time (Gannett and Caldwell, 1998).

The late Pleistocene age Qg_1 geologic unit is also contained within the MSHU. This is a relatively thin but widespread unit of sand and gravel that is generally overlain by Qalc and underlain Qg_2, the LSHU, or the BSHU. Qg_1 contains alluvial sand and gravel deposited in broad braidplains and is traced upstream as alluvial fills in the McKenzie and South Santiam River drainages within the SWV (O'Connor et al., 2001). Qg_1 forms low terraces and the surfaces of large fans where Cascade Range tributaries enter the valley. This geologic unit seems to have a slightly more defined braidplain morphology than the older Qg_2 geologic unit (O'Connor et al., 2001).

The permeable sand and gravel of the MSHU is an important groundwater source in the SWV. The terrace deposits and related pediment gravel are thoroughly weathered and nearly impervious, yielding water slowly at most places (Piper, 1942). The QTg geologic unit is not a regionally important source of groundwater due to its

elevated and generally thin extent, and because it usually lies above the regional water table (Piper, 1942; Gannett and Caldwell, 1998; O'Connor et al., 2001). The more permeable bodies of sand and gravel in the Qg_1 and Qg_2 (usually coarse channel facies) serve as preferential flow paths which appear to be thoroughly interconnected and allow free movement of groundwater (Piper, 1942). Deeper and older sand and gravel of the MSHU is more cemented and compact than units near the surface, probably resulting in lower permeability with depth (O'Connor et al., 2001). Generally, drillers' logs report "loose" sand and gravel near the surface and progressively "cemented" sand and gravel with depth. While conducting field reconnaissance it appeared that the Qalc geologic unit was more permeable than the Qg_1 and Qg_2 geologic units, and past studies in the area have also made this same distinction (Piper, 1942; Frank, 1973, 1974, and 1976).

According to Table 1 in Conlon et al. (2005), the MSHU (only containing the Qg_2 geologic unit, not Qg_1 and Qg_2 as in this study) has hydrogeologic properties of K_x from 0.002 ft/dto 2,230 ft/d (7.06 x 10^{-9} m/s to 7.87 x 10^{-3} m/s), K_v from 2 ft/d to 6.8 ft/d (7.06 x 10^{-6} m/s to 2.40 x 10^{-6} m/s), and a S from 2 x 10^{-4} to 2 x 10^{-1}. Since these values are specifically for the pre-Missoula Flood sand and gravel deposits, the MSHU of this study likely has hydrologic conductivity values greater than the lowest values reported. In the SWV, the majority of this unit is overlain by about 20 ft (6 m) of the WSHU, resulting in unconfined to semi-confined conditions, making the storage coefficient probably greater than 1 x 10^{-3} (Conlon, et al., 2005).

2.4.4 Willamette Silt Hydrogeologic Unit

The Willamette Silt hydrogeologic unit (WSHU) is a semi-confining to confining unit and usually overlies the MSHU. In the SWV, this unit includes the Qff_2 and Qalf

geologic units comprised of unconsolidated clay, silt, minor sand, and minor gravel 15 to 13.5 ka (O'Connor et al., 2001). Generally, this hydrogeologic unit has relatively uniform lithology composed mostly of clay and silt. The WSHU thins and decreases in grain size southward and ranges in thickness from 0 ft to 30 ft (0 m to 9.1 m) in the SWV. Locally, this unit also corresponds (in addition to those illustrated in Figure 4) to the "Willamette Silt" of Allison (1953), the "River Bend Unit III" of Glenn (1965), and the "Irish Bend" and "River Bend" Members of Roberts (1984) and Balster and Parsons (1968; 1969).

The WSHU is the result of late Pleistocene glacial-outburst floods from the upper Columbia River drainage. The source of the floodwater was Lake Missoula, a late Wisconsin glacial lake that formed when a lobe of the Cordilleran ice sheet impounded the Clark Fork River in western Montana, creating an ice-dam that failed periodically producing giant glacial-outburst floods (Gannett and Caldwell, 1998). Allison (1953) was the first to name this unit the Willamette Silt and along with Bretz (1925a; 1925b) were the first scientists to suggest the catastrophic flood hypothesis to describe large-scale depositional and erosional features in the northwest. These flood waters inundated the Willamette Valley on their way to the Pacific Ocean sporadically depositing rhythmic bedded fine-grained deposits from the proglacial "Willamette Lake," named by Allison (1978) as the lake which laid down a large portion of these deposits.

The number of floods that reached the SWV is difficult to estimate, however Glenn (1965) concluded approximately ten floods achieved a stage of at least 148 ft (45 m) above sea level at the River Bend section in the SWV. A developmental model has evolved that includes two distinct phases of flood deposition from the Columbia River

into the Willamette Valley (Allison, 1933, 1935, 1978; Glenn, 1965; Roberts, 1984; McDowell, 1991). In the first phase, a thick body of low-energy, silty to sandy deposits was laid down, probably by multiple floods. The second phase, resulting from a single very large flood, resulted in erosion and deposition of smaller volumes of sandy to bouldery high-energy deposits near gaps where the flood entered the valley and silty low energy deposits across the valley floor (McDowell, 1991). In the SWV, the upper, nearly perfect horizontal surface of the Willamette Silt hydrogeologic unit contains these silty, low energy deposits from the second phase. The largest flood(s) left deposits and ice-rafted erratics as far south as Eugene up to an altitude of 400 ft (122 m) (Allison, 1935). Following the catastrophic floods, the WSHU unit has been generally eroded away in the present flood plains of the Willamette River and its major tributaries (Gannett and Caldwell, 1998).

It is difficult to assign hydrologic property values to the WSHU because few wells exist within this unit and varying depositional catastrophic event have created spatial variability of the unit. The WSHU generally has high porosity but low permeability (Iverson, 2002 and Conlon et al., 2005). This unit is rarely used as an aquifer in the SWV, but in the past has provided a water supply for early settlers of the Willamette Valley (Piper, 1942). According to Table 1 in Conlon et al., (2005), the WSHU contains hydrogeologic properties of K_x from 0.1 ft/d to 8 ft/d (3.53×10^{-7} m/s to 2.82×10^{-5} m/s), K_v from 4×10^{-4} ft/d to 1×10^{-2} ft/d (1.41×10^{-9} m/s to 3.53×10^{-8} m/s), and a S from 0.2 to 0.3.

2.4.5 Upper Sedimentary Hydrogeologic Unit

The Upper Sedimentary hydrogeologic unit (USHU) consists chiefly of the Holocene geologic unit Qalc, described by O'Connor et al. (2001). This unit overlies contains unconsolidated floodplain deposits of clay, silt, sand, and minor gravel and overlies all other hydrogeologic units except the WSHU. In the SWV, the USHU is typically less than 16 ft (5 m) thick, and is thin or absent where the Willamette River flows on or near bedrock (O'Connor et al., 2001).

The USHU contains many distinctive features. This unit is exposed at the surface throughout its extent, has variable surface morphology, and is derived primarily of volcanic rock from active meandering and anastomosing channels of the Willamette River and South Santiam River in the SWV (O'Connor et al., 2001). Annual flooding occurs over portions of these active stream channels, depositing silty to sandy overbank facies (O'Connor et al. (2001). Drillers' logs and bank exposures show this sand and gravel unit contains tortuous ribbons of well-sorted sand and gravel separated horizontally and vertically by fine-grained overbank deposits, which may influence groundwater flow, solute transport, hyporheic flow, and groundwater/surface water interactions (O'Connor et al., 2001). On a basin-wide scale, this well-sorted, loose, and highly permeable unit can probably be considered a homogeneous unit for most groundwater analysis purposes (O'Connor et al., 2001).

Beneath the floodplains of the Willamette River and its principle tributaries, the USHU is highly permeable at most places (Piper, 1942). This sand and gravel unit typically has higher yields than the other geologic units in the Willamette Valley (Piper, 1942; Frank, 1973, 1974, 1976). Woodward et al. (1998) also use specific capacity,

hydraulic conductivity, and transmissivity data to demonstrate that the Holocene floodplain deposits have a greater permeability than the underlying alluvial units of the Willamette aquifer (primarily units Qg_1 and Qg_2) (O'Connor et al., 2001). This unit is characterized by high permeability, high porosity, and high well yield, as well as being the most productive aquifer in the region. Large diameter wells in this unit are capable of producing 10,000 gal/min (6.31 m^3/s x 10^{-1}) and commonly yield several thousand gal/min (Conlon et al., 2005). Frank (1976) reported wells with the highest yield in the area are in this unit, producing upwards of 700 gal/min (4.42 x 10^{-2} m^3/s). According to Table 1 in Conlon et al. (2005) the generally unconfined USHU (containing the Qalc and Qg_2 geologic units, not solely the Qalc as in this study) has hydrogeologic properties of K_x from 0.03 ft/d to 2.45 x 10^4 ft/d (1.06 x 10^{-7} m/s to 8.64 x 10^{-2} m/s), K_v of 2.0 ft/d (7.06 x 10^{-6} m/s), and a S from 3 x 10^{-3} to 2 x 10^{-1}. Modeling, specific capacity data, and aquifer tests were used to derive these estimates of hydraulic properties from past studies Conlon et al. (2005).

2.5 Hydrologic Budget

Due to the wet winters and dry summers, the heterogeneous geology and different soil types, the variety of rivers, streams, and lakes (most of which are controlled by dams), and varied land use throughout the Willamette Valley, a complex hydrologic system exists that varies both spatially and temporally. This section discusses the components of the hydrogeologic budget of the SWV. Recharge, evapotranspiration, groundwater/surface water interaction, groundwater elevations, horizontal and vertical groundwater flow, and well discharge are discussed and quantified.

2.5.1 Recharge

Water is recharged to the groundwater system in the SWV via precipitation, redistributed and reapplied by irrigation, and from river or stream seepage. Aquifers in the area are recharged principally by direct infiltration of precipitation during late autumn and winter, where the first rains replenish the soil moisture lost during summer. Average precipitation for the SWV is about 47 in/yr (119 cm/yr) (Oregon Climate Service, 2005). A portion of the water that infiltrates into the ground is retained in the unsaturated zone to replace soil moisture that was lost during the summer months. Water that does not infiltrate into the ground is usually lost to overland flow or evapotranspiration, which is highest in the summer. Recharge is most likely greater where the fine-grained Willamette Silt hydrogeologic unit is absent. The Willamette Silt is saturated with water where confined and provides a diffuse source of recharge to the underlying aquifer and to the rivers and streams in the area (Iverson, 2002). Groundwater age estimates calculated in Conlon et al. (2005) and this study also support greater recharge where no Willamette Silt is present. The lower permeability basement rock that surrounds the valley allows water to run via overland flow to the valley sediments, adding another means of recharge to the valley aquifers. Large-scale underground flow paths may also exists from the basement rock surrounding the SWV, providing an unknown but most likely minimal recharge source to the basin-fill aquifer. Most recharge is returned as discharge to streams in the Willamette Basin (Conlon et al., 2005).

Irrigation water that is pumped from a local aquifer and applied to a local field is an indirect form of recharge in the SWV. Crops that require water to mature in the summer months require irrigation. Irrigation water that is not used by plants or taken up

by evapotranspiration recharges the underlying aquifer. Approximately 90 percent of groundwater is withdrawn from the USHU and MSHU in the SWV (Karl Wozniak, pers. communication, Oregon Water Resources Department, 2003). Most irrigation occurs near the Willamette River in the well-drained soils where row crops, peppermint, tree and small fruits, and hazelnuts are grown (Ross Penhallegon, pers. communication, Oregon State University Extension, 2004). Irrigation usage depends on crop type, current weather conditions, and time of year. Irrigation is the largest use of groundwater, accounting for about 81 percent of annual groundwater withdrawals in the lowland (Conlon et al., 2005). Basin-wide estimates of water usage are estimated in Woodward et al. (1998) and Conlon et al. (2005).

Estimates of mean annual recharge based on precipitation, generalized surficial geology, land-use, and land-cover were made by Woodward et al. (1998) using past studies by Frank (1973, 1974, and 1976) for the SWV. These estimates varied from about 21.4 in (54.4 cm) (about 58 percent of mean annual precipitation) within the floodplain deposits to about 18.1 in (46 cm) (about 42 percent of mean annual precipitation) where floodplain deposits are not present, excluding the Columbia River basalt aquifer (Woodward et al., 1998; Lee and Risley, 2002). Recently, overall annual mean recharge estimates based on watershed modeling using the Precipitation-Runoff Modeling System (PRMS) (Leavesley et al., 1983) were made within the Willamette Basin (Lee and Risley, 2002). Estimates within the lowland were approximately 16 in (40.6 cm), about 27 percent of mean annual precipitation, which occurs mostly from November to April when rainfall is large and evapotranspiration is small (Conlon et al., 2005; Lee and Risley, 2002). PRMS recharge estimates are less than those estimated by

RASA (Woodward et al., 1998) because the geologic and soils data, which affect the

infiltration rates, were more generalized in the PRMS models developed by Laenen and

Risley (1997) than in the RASA study (Lee and Risley, 2002). Conlon et al. (2005)

estimates about 28 percent of precipitation infiltrates as recharge in the Willamette

Lowland. Recharge to the lowland area occurs locally and supplies the water for most

groundwater resources in this area (Conlon et al., 2005).

2.5.2 Evapotranspiration

Evapotranspiration in the SWV occurs from the unsaturated zone as water

percolates to the water table and from the saturated zone when the water table is within

the rooting depth of plants (Conlon et al., 2005). Since groundwater levels often occur

within a few feet of the ground surface, evapotranspiration can be a significant avenue of

discharge (Gannett and Woodward, 1997). Due to the variation of water level elevations

and extreme wet and dry seasons that exist within the SWV, evapotranspiration is a

seasonal process and is difficult to quantify. Average temperature of the SWV is about

52.9°F (11.6°C), but fluctuates annually on average between about 42°F and 63.3°F

(5.6°C and 17.4°C) (Oregon Climate Service, 2005). Piper (1942) first reported the most

extreme water level elevation fluctuations of the Willamette Valley in the SWV, a

minimum of 3.5 ft (1.1 m) and maximum of 28 ft (8.5 m). These were both recorded

under unconfined aquifer conditions and were natural. During the summer months when

temperature is highest, and evaporation is highest, water tables are lowest, precipitation is

lowest, and transpiration from plants is highest. Crop type, soil holding capacity, and

land cover can all affect evapotranspiration rates and are known to vary considerably in

the SWV.

A variety of past studies in the Willamette Valley have attempted to quantify evapotranspiration. Frank (1973) estimated mean annual Class A pan evaporation at Fern Ridge Reservoir to be 38.30 in (97.28 cm). Price (1967a) estimated evapotranspiration of the entire Willamette Valley to be about 20 in/yr (51 cm/year) and suggested that evapotranspiration in the flood plain of the French Prairie area to be about equal to the rate of evaporation from open-water bodies. Groundwater flow models developed by Woodward et al. (1998) support 15 in/yr to 16 in/yr (38 cm/year to 41 cm/yr) of evapotranspiration and also suggest a total potential evapotranspiration of about 25 in/yr (64 cm) in the lowland. Model simulations using PRMS indicate potential evapotranspiration in the SWV from about 40 in/yr to 60 in/yr (102 cm/yr to 152 cm/yr) (Lee and Risley, 2002).

Recent studies in the SWV indicate shallow water levels suggest evapotranspiration from the saturated zone is possible over an area of about 1,100 mi^2 (2848 km^2) (Conlon et al., 2005). Using the PRMS watershed model an average annual rate of residual evaporation for 1995-1996 is 28 in/yr (71 cm/yr) (Conlon et al., 2005). But, it is noted that actual evapotranspiration is less than 28 in/yr (71 cm/yr) because no long term water level declines exist in this area as one would expect with a recharge rate of 16 in/yr (41 cm/yr). For water budget purposes, evapotranspiration from the saturated zone is assumed to be 50 percent of the recharge rate, or 8 in/yr (20 cm/yr) (Conlon et al., 2005).

Total potential evapotranspiration was estimated for the SWV at the Oregon State University AgriMet site at the Hyslop Farm near Corvallis, OR. Daily reference-crop evapotranspiration (or potential evapotranspiration) was estimated using the Kimberly-

Penman method for alfalfa. Average yearly potential evapotranspiration from April 1990

through November 2005 at the AgriMet site was about 45 in/yr (114 cm/yr) (Oregon

Climate Service, 2005).

2.5.3 Groundwater/Surface Water Interaction

Seepage, or the exchange of water between surface water bodies and

groundwater, occurs to some extent in every river or stream in the SWV. Groundwater is

discharged naturally from the area by seepage and spring flow to streams, by

evapotranspiration, by underflow, and artificially through wells (Frank, 1974).

Groundwater is discharged to streams in the summer and fall as a result of the lowering

of river stage and dewatering of the highly permeable alluvial sediments along the river

plain, creating a gaining stream. Losing streams can occur in the area when the elevation

of the stream is above the water table, causing seepage from the stream to the nearby

aquifer. This usually occurs in the winter and fall. Losing streams provide recharge to

the groundwater flow system; gaining streams provide an important component of

streamflow (Conlon et al., 2005).

Within the Willamette Lowland, groundwater usually discharges to streams but its

contribution to annual streamflow is relatively small (Conlon et al., 2005). High rainfall

during the winter results in both runoff and groundwater discharge contributing to

streamflow, while during the dry summers groundwater is the main component of

streamflow and discharges at a low rate to streams (Conlon et al., 2005). As precipitation

events become more frequent in late autumn and winter, soil moisture will saturate to

field capacity and water will infiltrate to the aquifer and raise the water table, increasing

the gradient toward nearby groundwater discharge areas. Discharge to and recharge from

streams, rivers, and lakes in the SWV are highly dependent upon the amount of precipitation that has fallen (or amount infiltrated) and the stage height of the rivers, lakes, and streams. These seasonal affects can also vary spatially.

Difficulty exists in estimating gains and losses of streams in the SWV. Quantifying gains and losses to the groundwater system in the Willamette Bain is difficult due mainly to large flows and flow regulation (dams) (Conlon et al., 2005). Accuracy is also limited by temporal and spatial variation in streamflow, changes in out-of-stream withdrawals, and accuracy of stream-discharge measurements (Lee and Risley, 2002). In addition to the difficulties in estimating gains and losses of streams, other water users along these streams must be accounted for. Stream diversions for public supply and irrigation purposes as well as tributary inflow points are known to exist along many of the streams within the SWV and must be accounted for when estimating the amount of water a stream has gained or lost along a specific stream reach (see Appendix 2 Lee and Risley, 2002).

On a smaller scale, gains and losses along streams in the SWV have been shown to occur via hyporheic flow. A relative "gain" within a stream can occur very near a "loss" in a stream (see Figure 15 and 16 in Conlon et al., 2005). Alternating gains and losses in the South Santiam and Willamette Rivers may indicate shallow, hyporheic flow along short flow paths.

Some amount of measurement uncertainty exists when estimating stream gains and losses. Seepage measurement uncertainty is 3 percent for Acoustic Doppler Current Profiler (ADCP) measurements and 5 percent for current-meter measurements (Lee and Risley, 2002). Since seepage contributes only a small percentage of total streamflow and

is difficult to measure in the field, few calculations of stream gains and losses in the SWV indicate total seepage greater than the measurement uncertainty (Conlon et al, 2005). This is an important point to remember when using seepage estimates as calibration targets during groundwater model calibration.

Even though total seepage is rarely greater than the measurement uncertainty, a few past studies have attempted to quantify stream seepage rates along specific stream reaches in the SWV. Gaining reaches were exhibited by comparing water levels in wells near streams to stream stage near Corvallis, OR, and also by measurement of the difference of stream flow at two different locations along specific stream reaches (Conlon et al., 2005). Seepage measurements along rivers in the Willamette Basin are reported in Woodward et al. (1998), Lee and Risley (2002), Conlon et al. (2005), temporal studies within the SWV along the Willamette and South Santiam Rivers (among others) in Lee and Risley (2002), and seepage data studied cumulatively in Conlon et al. (2005).

Specific studies of stream gains and losses along designated stream reaches of the SWV are discussed in detail below. Gains and losses of reaches along the Middle Fork Willamette and Willamette River collected from April, May, July, and August are shown in Figure 14 of Lee and Risley (2002). The Jasper to Springfield reach showed small net losses. The Harrisburg reach indicated a significant net gain. The rest of the stream reaches showed minimal gains and losses within the measurement uncertainty. The measurements showed a general trend where the gains were greater or the loss less in the spring than in the summer, however the Harrisburg reach showed the opposite trend (Lee and Risley, 2002). Gains and losses of reaches along the South Santiam River were small and all within the measurement uncertainty (Lee and Risley, 2002), however a prior study

by Leanen and Risley (1997) along RM 7.7 to RM 3.3 showed a loss greater than the measurement uncertainty of 130 ft^3/s (3.68 m/s). An up-to-date table containing seepage estimates of selected streams within the Willamette Basin is shown in Appendix C of Conlon et al. (2005). It was generally found from seepage estimates during low-flow periods that streams crossing the proximal part of the buried alluvial fans lose water to the aquifer, whereas streams crossing the distal portions of the fans gain water from the aquifer (Woodward et al., 1998).

Groundwater elevation contours indicate gaining stream reaches (indicated by the contours bending upstream) in much of the SWV. The bending of these contours generally are sharp across the deep, narrow floodplains underlain by the less permeable Willamette Silt hydrogeologic unit and shallow across the broad, shallow floodplain of the Willamette River and major tributaries underlain by more permeable Upper Sedimentary and Middle Sedimentary hydrogeologic units (Conlon et al., 2005). Small gains along streams flowing on the Willamette Silt hydrogeologic unit are the result of a poor hydraulic connection between streams and the underlying sand and gravel aquifer, whereas large gains along streams with permeable streambeds are expected (Conlon et al., 2005). Pumping nearby streams can impact local stream stage, but impacts are expected to be small due to upward flow being limited by the lower hydraulic conductivity Willamette Silt hydrogeologic unit (where it exists) (Iverson, 2002; Conlon et al., 2005).

2.5.4 Groundwater Elevations

Fluctuating groundwater elevations in the SWV affect aquifer storage and stream seepage, both important to the hydrogeologic budget of the area. Water elevation maps,

an extensive well inventory, and a water elevation observation network were first developed in the Willamette Valley by Piper (1942). An equilibrium exists due to high water levels in the rainy season when recharge from precipitation exceeds discharge to local streams and low water levels during the dry season when discharge by pumping, evapotranspiration, and leakage to streams exceeds recharge (Conlon et al., 2005). In the SWV, long-term hydrographs show that groundwater elevations are in equilibrium (Woodward et al., 1998; Conlon et al., 2005), with water levels remaining relatively constant since at least the early 1960's (see Figure 18c. in Woodward et al., 1998). The recovery of water levels each winter to about the same elevation indicates that the aquifer is supported mainly by water from direct infiltration of local precipitation (Woodward et al., 1998).

Groundwater within the Willamette aquifer generally occurs under unconfined or semi-confined conditions, making the potentiometric surface equal or nearly equal to the water table (Woodward et al., 1998). The water table is found within 5 ft to 20 ft (1.5 m to 6 m) of the land surface in the SWV (Conlon et al., 2005). Where the Willamette Silt hydrogeologic unit exists and wells are drilled into the Middle Sedimentary hydrogeologic unit, water levels are within 10 ft (3 m) of land surface, closely approximating the water table in the silt (Conlon et al., 2005). Piper (1942) first recognized that the water table existed within the Willamette Silt and described it as "semi-perched," however, piezometer and monitoring well studies have shown full saturation below the initial water table (Conlon et al., 2005). Piper (1942) noted that from 1928 to 1936, both minimum (3.5 ft or 1 m) and maximum (28 ft or 8.5 m) water table fluctuations occurred in the SWV under unconfined, natural conditions.

Local groundwater elevations are directly affected by precipitation, groundwater pumping, and nearby river levels, thus affecting aquifer storage. Temporal changes in aquifer storage occur as the water table fluctuates, the direct result of seasonal changes in recharge and discharge. The water table is a dynamic surface that moves up and down in concert with local and regional groundwater recharge and discharge, precipitation, river/reservoir stage, and well-withdrawal (Woodward et al., 1998). Groundwater storage increases about 500,000 acre-ft (6.165×10^8 m^3) each winter in the SWV, mainly by infiltration of rain; storage declines an equal amount during the summer and autumn, mainly by drainage into the streams, and some discharged by withdrawals from pumping (Piper, 1942).

Recent average water table elevation maps have been constructed by Woodward et al. (1998) and Conlon et al., (2005). Piper (1942) and Frank (1974) also constructed water table elevation maps over all or portions of the SWV. The Conlon et al. (2005) and the Woodward et al. (1998) contours lie at nearly the same locations, with more detail illustrated in the Woodward et al. (1998) contour map.

Groundwater elevation information can be used to study response time to local precipitation and river stage changes. Groundwater elevation data for the entire Willamette Basin can be found in Orzol et al. (2000). This data set contains 265 wells with records from 1 to 70 years. Hydrographs of wells in the SWV (LANE 8725 and LINN 10841) are shown in Figures 22 and 23 of Conlon et al. (2005) along with daily precipitation and river stage information. Both wells show a direct, rapid response to precipitation and/or stream stage in early fall and to small rain events that occur throughout the rainy season. Quick aquifer response to precipitation events as well as

quick gradient reversal from fluctuating stream stage indicates fast infiltration rates and

good hydraulic connection between the streams and alluvial aquifer. A delay is noticed

at the beginning of the rainy season, reflecting the time necessary to bring soil moisture

to field capacity (Piper, 1942; Woodward et al., 1998; Conlon et al., 2005). Both wells

also show a gradual decline in water levels in the spring as well as following winter rain

events. These responses along with the direct correlation to individual storm events

indicate that recharge is local, infiltration rates are rapid, and recharge paths are short

(Conlon et al., 2005).

2.5.5 Horizontal Groundwater Flow

Horizontal hydraulic gradients within the SWV are usually less than 0.0028,

mostly due to the gently sloping surface and high permeability alluvial units (Conlon et

al., 2005). Using average values of hydraulic gradient, hydraulic conductivity, and

effective porosity of the Willamette aquifer, horizontal groundwater velocity ranges from

3 ft/d to 30 ft/d (0.9 m/d to 9.1 m/d), typical of sand and gravel aquifers (Woodward et

al., 1998). Groundwater moves in a general northwest direction on the east side of the

Willamette River and in a north-northeast direction on the west side of the Willamette

River, according to the water table contours found in Woodward et al. (1998) and Conlon

et al. (2005).

2.5.6 Vertical Groundwater Flow

The vertical component of groundwater flow in the SWV can be determined using

groups of nearby wells screened at different depths. Vertical flow in the SWV is

generally downward (negative) throughout most of the basin, mainly due to the localized

recharge of precipitation. An upward (positive) gradient exists under some streams in the

SWV, indicating discharge to streams. The largest negative gradient in the basin-fill sediments is between the less permeable Willamette Silt hydrogeologic unit and the Middle Sedimentary hydrogeologic unit (Conlon et al., 2005). Positive gradients are found along the streams entrenched within the Willamette Silt, indicating gaining streams (Conlon et al., 2005). Vertical gradients were calculated from water level data collected during this study from three locations, two of these locations were used to calculate vertical gradients in Conlon et al. (2005). These vertical gradient values for the SWV ranged from -0.18 to 0.07, comparable to those collected in the SWV by Conlon et al. (2005) of -0.15 to 0.48.

2.5.7 Well Discharge

Most groundwater use in the SWV falls into four categories: public supply, irrigation, industrial, and domestic. This water mostly originates from the alluvial sand and gravel aquifers. Other water exits the groundwater system via evapotranspiration and discharge to streams. Groundwater usage estimates were made for irrigation, public supply, and industrial use, but not for domestic use because domestic use is relatively small in a regional sense when compared to other uses (Conlon et al., 2005). Details on how these withdrawal estimates were calculated for each hydrogeologic unit are outlined in Conlon et al. (2005), pg. 32-37.

Of the total amount of groundwater pumped within the SWV, 83.6 percent is for irrigation, 14.9 percent is for public supply, and 1.5 percent is for industrial purposes (Conlon et al., 2005). Most pumpage is from the Upper and Middle Sedimentary hydrogeologic units, especially along the floodplain of the Willamette River where many irrigation wells exist (Conlon et al., 2005). The largest groundwater user in the SWV is

the Springfield Utility Board, providing water for the City of Springfield. Smaller cities

that use groundwater for public supply purposes in the SWV include: Monroe,

Brownsville, Harrisburg, Halsey, Veneta, and Junction City (Conlon et al., 2005).

Eugene is developing well fields to meet growing water demand (Conlon et al., 2005).

Groundwater is also pumped from local gravel pits. Some stakeholders near gravel pit

operations have been forced to deepen their wells in response to local decline in

groundwater elevations. Corvallis, Eugene, and Albany use surface water as their public

water supply source.

3. DATA COLLECTION

3.1 Stratigraphic Columns

Field work was conducted at four outcrops of the basin-fill sand and gravel units of the SWV to develop a better understanding of the stratigraphic relationships between geologic units. Four stratigraphic columns were developed, one at each outcrop (see Figure 5 and Figure 6). These four outcrops were selected based on (1) the extent of the exposure, and (2) the spatial location and geologic unit. Therefore, sites at the Green and White and Delta Sand and Gravel company operations were selected, as well as locations along the Willamette River at Irish Bend and Cartney Park.

Difficulty in determining specific geologic units exists due to few visual clues other than spatial and vertical position that distinguish one geologic unit from another. Differences in geologic material type and thickness are shown at each outcrop location.

Green and White Gravel Pit

Location	Age	Unit	Thickness

67.0 m amsl

- Undisturbed surface. Clayey silt to sand with frequent gravel to small cobble sized clasts scattered throughout unit. All clasts volcanic in origin. Root structure throughout.

1.2 m

- Upward fining, loose, fine gravel to small cobble sized clasts with a silt to fine to medium sand matrix. Fresh appearance. Nearly all clasts volcanic in origin (99%). Some large scale planar cross-bedding.

1.16 m

- Fresh, loose, fine to coarse gravel with clayey silt and sand matrix. More clay and silt in matrix and slightly more compacted than above unit.

1.74 m

- Covered, but most likely contains the same properties as described above.

62.9 m amsl - Local water table.

Green and White Gravel Pit — Holocene — Qalc

EXPLANATION

Deposit features

	Clay
	Silt
	Sand
	Gravel
	Pedogenesis
	Planar cross-bedding

Irish Bend

Location	Age	Unit	Thickness

83.8 m amsl - Undisturbed surface, silty clay soil.

1.0 m

- Massive silty clay unit with the same properties as the below unit but much lighter in color (light tan). Possibly deposited during a different depositional event than the below unit. Root structure throughout.

3.6 m

- Massive clayey silt dark tan in color. Unable to bedding structure in unit. Generally homogeneous.

- Fine to medium cross-bedded sub-angular sand.

- Upward fining, cemented, fine to coarse gravel with a clayey silty sand matrix. All clasts of volcanic origin. Some oxidization. Weathered appearance. Weathering rinds prominent.

2.2 m

- Some lenses of clayey silt with sand.

- "Concrete" appearance. Very compacted.

77.0 m amsl - Willamette River surface.

Irish Bend — Upper Pleistocene — Willamette Silt — Pleistocene — Qg2

Scale

5 miles

Corvallis

Willamette River

Eugene

Figure 5: Stratigraphic columns and lithologic descriptions at a Green and White gravel pit (Lat. 44.49300 N; Long. 123.26247 W) and near the Willamette River near Irish Bend (Lat. 44.36124 N; Long. 123.21841 W). Projection = UTM; Datum = NAD 83.

Cartney Park

85.3 m amsl
- Undisturbed surface. Finely bedded clayey silt.

- Generally homogeneous silty clay to clayey silt with some sub-rounded fine to medium grained sand. Similar in appearance to Willamette Silt unit. Most likely reworked and redeposited Willamette Silt overbank facies with sand from river channel. Root structure throughout.

1.5 m

- Minor cross-bedded silty sand.

- Upward fining, loose, fine to coarse gravel with fine to medium sand matrix. Compaction seems to increase moderately with depth. Fresh appearance. All clasts of volcanic origin.

1.2 m

- Covered, but most likely sand and gravel as described above.

82.6 m amsl
- Willamette River surface.

Location: Cartney Park
Age: Holocene
Unit: Qalc

EXPLANATION

Deposit features

⊟	Clay
⊟	Silt
⊡	Sand
⊡	Gravel
⊡	Pedogenesis
⊡	Planar cross-bedding

Delta Gravel Pit

115.8 m amsl
- Disturbed surface. Clayey silt soil.

- Upward fining, loose, fine to cobble sized clasts with fine to coarse sand matrix. Sand particles in matrix rounded to sub-rounded in shape. Least resistant to erosion. No weathering rind, fresh appearance. All clasts of volacanic origin.

- Upward fining, moderately compacted, fine to coarse gravel with silt to coarse sand matrix. "Dirtier" appearance. Large-scale planar cross-bedding. More resistant to erosion. Water exiting near bottom of contact with Qg1?. All clasts of volcanic origin.

- Upward fining, compacted, fine to coarse gravel with clay to coarse sand matrix. Large-scale cross-bedding. Weathering rinds prominent. All clasts of volcanic origin.

- Floor of pit
107.3 m amsl

Location: Delta Gravel Pit
Age: Holocene?, Pleistocene?
Unit: Qalc?, Qg1?
Thickness: 4.25 m, 4.25 m

Scale
5 miles

Corvallis
Willamette River
Eugene
N

Figure 6: Stratigraphic columns and lithologic descriptions at Cartney Park (Lat. 44.31849 N; Long. 123.21676 W) near the Willamette River and a Delta Sand and Gravel pit (Lat. 44.10617 N; Long. 123.10947 W). Projection = UTM; Datum = 83.

3.2 Water Level Network

A water level monitoring network consisting of 42 private wells and monitoring wells were established in the SWV during July and August 2004. The purpose of developing this network was to gather data for model calibration. Two GIS data sets were used when attempting to locate wells in the field: (1) a spatial set of all wells positively identified in the field by Oregon Water Resource Department (OWRD) staff, and (2) a synoptic data set of water level measurements previously collected by OWRD staff. The current water level monitoring network of the OWRD was then identified so that duplicate measurements did not occur. Monitoring wells installed with a push-probe by the ODEQ and Louis Arighi were also used for water level measurements (Arighi, 2004). Only wells with well logs that could be retrieved from the OWRD website and could be positively identified in the field were initially considered for the water level monitoring network. Wells were then selected that represented the aquifer in the SWV both vertically and spatially. A few wells nested by each other with open intervals at varying depths were selected for the water level monitoring network to determine local vertical gradients. Approximately 100 residents were visited to gain permission to collect quarterly (July, October, January, and April) water level measurements. If a resident was not home notes were left and phone calls made to try to establish contact. Measurements were collected in July and August 2004 as permission was being established from home and land owners. Some wells were added after July and August 2004 to fill in gaps where too few wells existed and as fieldwork progressed, developing connections with stakeholders. Synoptic measurements were again collected in October 2004 and January, April, July, and October 2005, and each round took approximately 2.5 days.

Water level measurements were taken with an electric tape marked at 5 ft (1.5 m) intervals. A hand-held tape marked at 0.01 ft (0.3 cm) intervals was used after a solid hold on the electric tape had been established. Methods used to take water level measurements, calibration criteria, expected accuracy, and techniques used to complete the water level inventory forms are located in Appendix E. Water level inventory forms provided by the OWRD are in Appendix C. If no obvious access to the water level in the well was found (i.e., an open casing) an access port was used to insert the electric tape. The measurement at each well was checked over time to ensure a static measurement was being made. If a static measurement could not be taken, notes were recorded on the water level inventory form.

Two OWRD digital recorders were used to collect long-term water level measurements and capture short-term effects like local pumping and recharge. The "Jacob's Well," LANE 8725, has been collecting water level measurements at 2-hour intervals since 10/22/1996. Data collection for this study started 8/21/2004. Equipment at LANE 8725 consists of an USGS Unidata Shaft Encoder 6509, SN# 1447 and an USGS Unidata Starlogger 6004B, SN# 3004. The second recorder, BENT 6612, was installed and the collection of water level measurements at 2-hour intervals for this study began 8/21/2004. Equipment at BENT 6612 consists of an OWRD Unidata Shaft Encoder, SN# 904 and an OWRD Unidata Starlogger 6004B, SN# 2785. The shaft encoder at both recorder stations was set to collect measurements below land surface. Data was downloaded, equipment checked for accuracy, and batteries checked every three months. An OWRD recorder well inventory sheet (located in Appendix C) was

completed and updated quarterly for each recorder station. Specific recorder information

can be found in Table 1.

Table 1: Recorder well locations, well construction, and stratigraphic position.

RECORDER OWRD well-log ID	Latitude	Longitude	Land Surface Elevation amsl (ft/m)	Perforated Interval Below Land Surface amsl (ft/m)	Hydro-geologic Unit
LANE 8725	44.15380 N	123.25023 W	341/104	No Perforations, 311/94.8	MSU
BENT 6612	44.28292 N	123.25028 W	295/90.9	247-237/ 75.3-72.2	LSU

Recorder LANE 8725 was planned to be decommissioned by the OWRD,

however an agreement was made to continue data collection for the purpose of this study.

The unused well BENT 6612 was located and permission granted by landowners to

install a recorder shelter and equipment. Throughout the duration of the project, other

water level data was sought out and collected. The OWRD currently collects quarterly

water level measurements from twelve different wells, and historic water level data has

been collected in fourteen wells within the SWV. This data was collected and organized

for use in this study. The Springfield Utility Board and Eugene Water and Electric Board

occasionally collect water level measurements from wells in the Eugene-Springfield area.

Data collected from wells that lie within the model domain were used during this study.
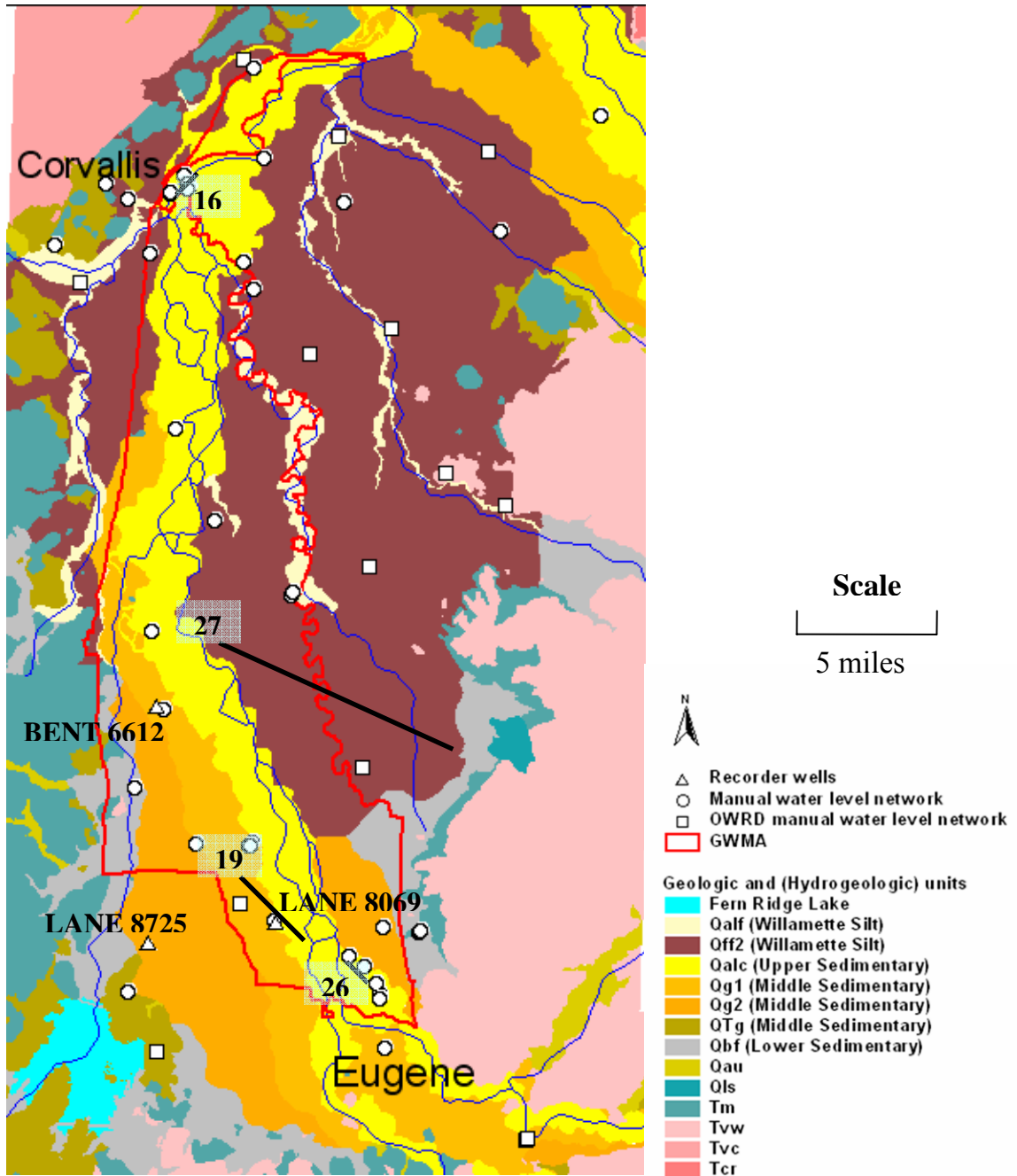
Figure 7: Water level network locations. Data found in Appendix I and Appendix J. Lines with numbers indicate cross-section locations and figure numbers within this report.

Some wells were not used as calibration targets due to their spatial or vertical extent residing outside of the final model boundaries. In all, 45 water level measurements were used within the model as calibration targets (see Figure 7). Average values collected from 7/1/2004 through 7/31/2005 were used as target values. These data are shown in Appendix I. All manual and recorder water level measurement data can be found in Appendix J.

Long-term water level measurements (measurements collected in two hour increments) were gathered from two continuous sources, BENT 6612 and LANE 8725 and are shown with daily precipitation data in Figures 10 and Figure 11, respectively. Other long-term data was collected at the Pump test #3 site where equipment was left installed and checked for maintenance and to download data. LANE 8069 was used at the Pump test #3 site to collect short-term measurements before and during the pump test and long-term measurements collected thereafter. These data can be observed with stream stage elevations from nearby gage locations (see Figure 8) and precipitation data from nearby rain gages (see Figure 9). All long-term water level measurement data are located in Appendix J.

Measurement error when calculating water level measurements can occur as a result of a number of factors. Water level measurements collected with an electric tape will give results within ± 0.04 ft (± 1.2 cm) for measurements less than 200 ft (70 m) in length (see details in Appendix E). The hand-held measurement tape used in this study contained markings every hundredth foot. A measuring point (MP) was established, usually the top of the well casing at the access port, and the distance from the MP to the land surface datum (LSD) was measured. The LSD along with the location of each well

was determined using a 7.5-minute quadrangle map with 5 ft to 10 ft contour intervals

and a Garmin GPS 12XL unit. GPS coordinates were recorded using the WGS-1984

datum. Horizontal error using a GPS and 7.5-minute quadrangle map is about 100+ ft

and vertical error using solely a 7.5 minute quadrangle map depends on the contour

interval and is about ±5 ft.
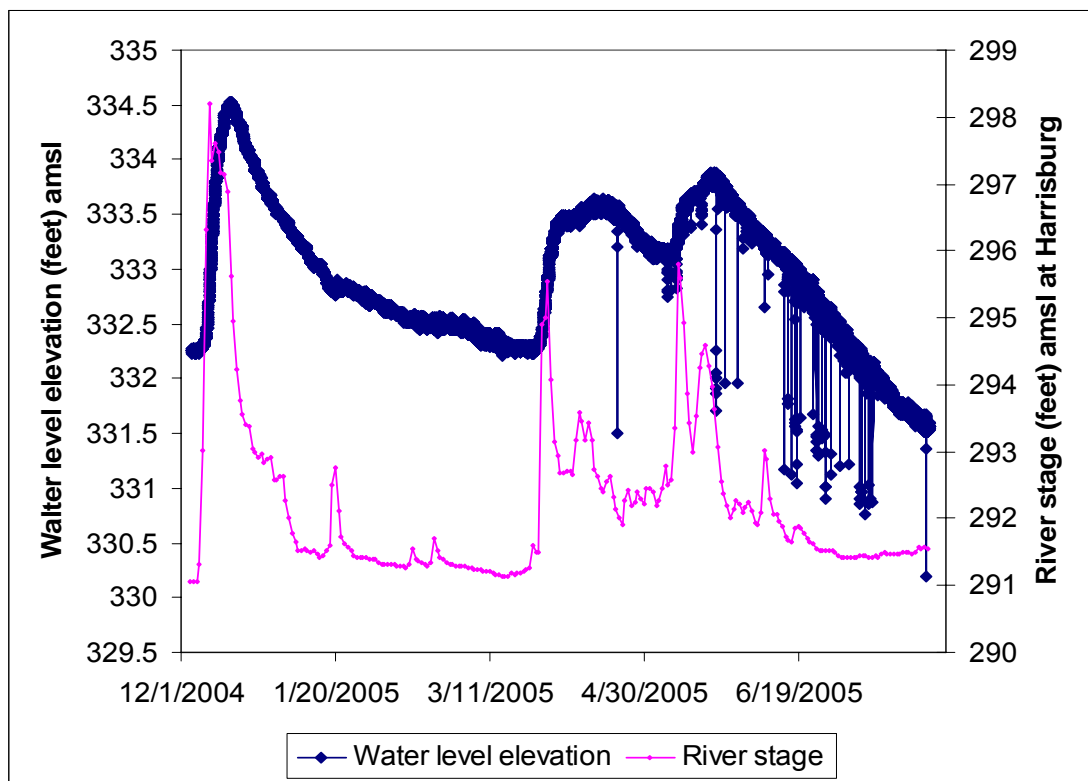
Figure 8: LANE 8069 water level elevation and Willamette River stage at Harrisburg.
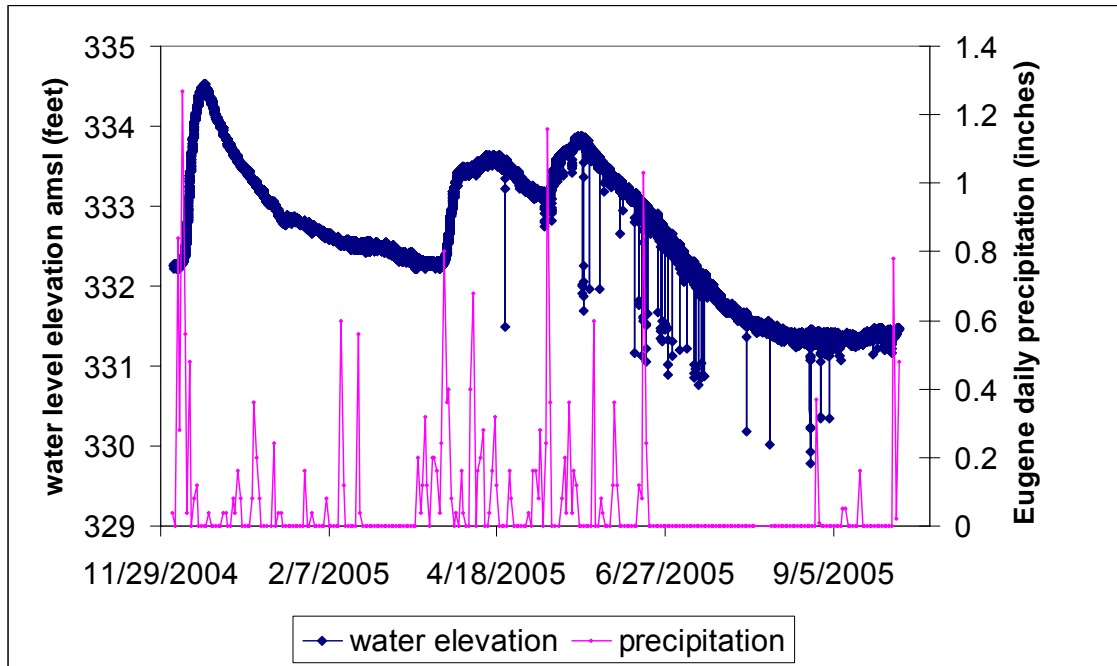
Figure 9: LANE 8069 water level elevation and daily precipitation at Eugene.
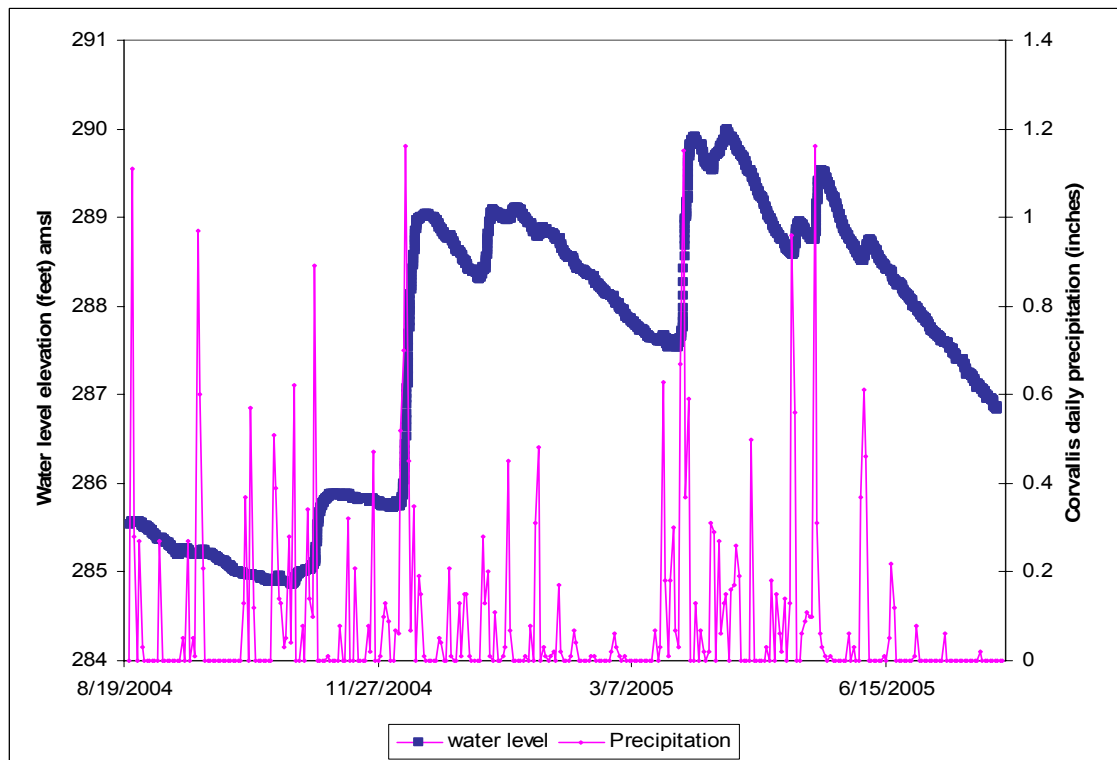
Figure 10: BENT 6612 water level elevation and daily precipitation at Corvallis.
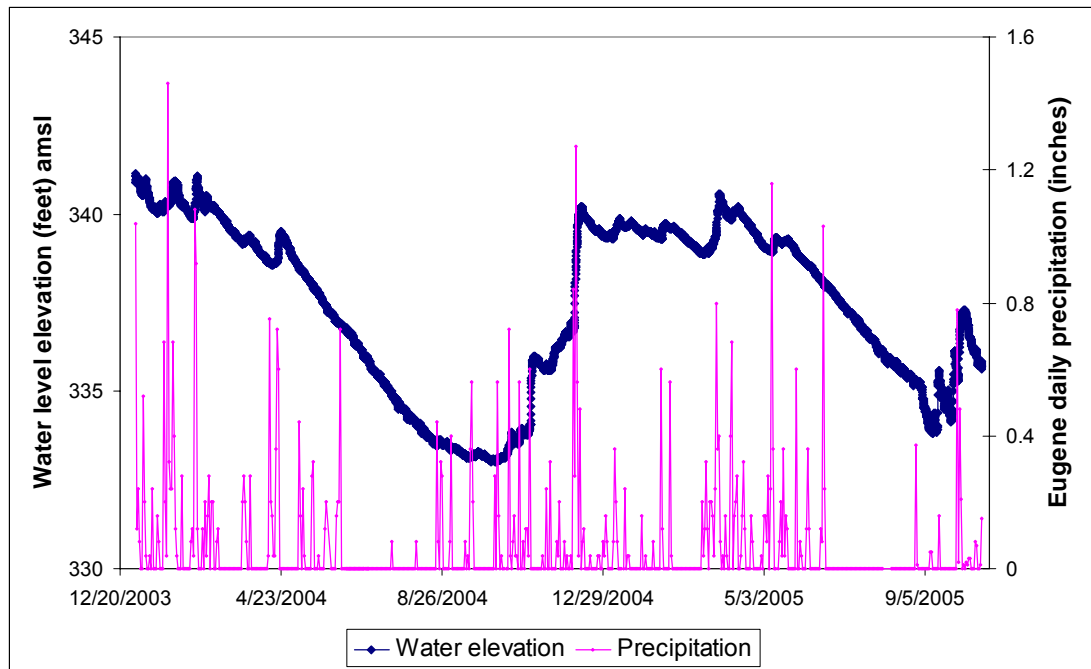
Figure 11: LANE 8725 water level elevation and daily precipitation at Eugene.

3.3 Aquifers Tests

3.3.1 Pump Tests

Three pump tests were conducted for estimation of hydraulic conductivity,

specific storage, and specific yield parameters for model input. Gathering previously

collected aquifer data along with collecting new data in the field was emphasized during

this study. Field reconnaissance was conducted throughout the SWV (specifically within

the GWMA) to locate areas that contained optimal characteristics for a pump test. Such

characteristics included (1) permission from landowner to conduct a pump test, (2)

location to store or dispose of water during pump test, (3) capacity (well and pump) to

produce $\geq$ 100 gal/min (6.31 x 10^{-3} m^3/s) for an extended period of time, (4) installation

of pressure transducers possible in wells nearby the potential pumping well so manual

measurements could be collected as the pump test was underway (used Theis equation to

determine drawdown potential with approximated hydraulic conductivity and pumping

rate), (5) ability to conduct the pump test when recharge from precipitation, rivers, and

other water bodies were minimal, and (6) ability to link wells in the field to their

appropriate well logs.

Various locations in the SWV were explored in order to locate sites conducive for

a complete and accurate pump test. Towns that used high-production wells to supply

water for their communities were initially targeted as potential pump test sites. In

addition to the high-production wells in these areas, the ability to disposal of water for an

extended period of time was also possible. Junction City and Coburg water supply wells

locations and pumping schedules were obtained from brief tours given by each cities

Public Works Director. Junction City wells contained air lines used to estimate water

levels, a method that is not accurate enough for accurate pump test results. Pressure

transducers were also not able to be installed in the wells. Field reconnaissance for other

wells to be used as monitoring wells near the high-production wells failed. Neither of

Coburg's wells was able to pump continuously for twenty-four hours (no water storage).

It was then thought the use of a numerical model such as MODFLOW could be used if

pumping rate from a well is known and drawdown in nearby wells measured over a

period of time to estimate aquifer parameters. However, field reconnaissance for

monitoring wells near the production wells for installation of pressure transducers failed.

Field reconnaissance for production and nearby monitoring wells north and south of

Coburg was then completed using GIS well locations established by the OWRD and

collection of local area well logs to contact landowners both at their residences and by phone. No sites that fit the required characteristics listed above for an accurate and complete pump test were located. The area surrounding OWRD recorder well BENT 6612 was explored for possible pump test sites using the same methods described for north and south Coburg produced no sites that could be used for a pump test.

A few sites were located where a complete and accurate pump test could be conducted. A variety of departments affiliated with Oregon State University operate and manage research facilities outside Corvallis city limits. The Lewis-Brown Horticultural, Botany Research and Plant Pathology, Vegetable Crops Research, Food Science Aquaculture Laboratory, and Hyslop Experimental Farms and Trysting Tree Golf Course were visited (all within a short distance from one another) and field reconnaissance conducted at each location. Another site was located southeast of Harrisburg, OR and field reconnaissance was conducted there as well. This included contacting farm or site managers, locating all wells within and surrounding the sites, inspecting wells to determine if pressure transducers could be installed in each well, linking well logs to wells located in the field, approximating pumping rates for each well (if available) were collected, gathering irrigation information, and determining locations to store or dispose of well water during the pump test. The Vegetable Crops Research Farm and the location southeast of Harrisburg, OR both contained the appropriate characterisitics to conduct an accurate and complete pump test.

3.3.1.1 Pump Test #1

The first pump test was conducted in the Upper Sedimentary hydrogeologic unit at the Vegetable Crops Research Farm east of Corvallis, OR. Figure 16 shows the

location of Pump test #1 (Site #1), the pumping well (GR-2800), and the monitoring wells (LINN 55017 and LINN 52897). Table 2 includes information on each well used during the pump test. Additional wells (other than pumping and monitoring wells) are shown in the cross-section; these wells were used specifically for cross-section development.

An attempt was made to install pressure transducers in the three wells nearest GR-2800. One well did not have the correct well-head geometry for installation of a pressure transducer, so two separate pressure transducers were installed in two monitoring wells. An OWRD Recorder Well Inventory Sheet (see Appendix C) was completed during and updated regularly after installation for both pumping and monitoring wells. These forms helped to organize and document each wells' activities prior, during, and after the pump test was completed.

A variety of equipment was used during Pump test #1. A Druck PDCR-1800 20 psi (Serial # 1153710) pressure transducer with Unidata Macrologger (Serial # 5451) and Unidata 960-1060 Barometric Pressure Instrument Model 6522A (Serial # 5321) was calibrated and installed 9/25/04 in LINN 52897 (monitoring well #2). A Global Water WL-15 15 ft Water Logger (Serial # 37018) was calibrated and installed in LINN 55017 (monitoring well #1) 9/25/04. A Global Water WL14 15 ft Water Logger (Serial # 3650) was installed in GR-2800 (pumping well #1) 9/28/04. All data loggers were programmed to collect water level measurements at 15 minute intervals. The wells were monitored prior to the pump test to ensure that the aquifer was static and no stresses were affecting the potential pump test site. Manual measurements were made to ensure the transducers did not drift and continued to take accurate measurements. A laptop computer was used

to download data and adjust data collection parameters using Starlog Software and Global Water Software. Existing permanent irrigation lines along with mobile irrigation piping was used to route water pumped by GR-2800 away from Site #1 and into the Willamette River. The SeaMetrics TX-81 turbine flow meter was used with a fitting from SeaMetrics to ensure accurate measurements and was installed in the outflow irrigation pipe.

Before the start of Pump test #1, data loggers in each well were set to collect water level data at one minute intervals and reset following the test to collect data every fifteen minutes about fifteen hours after the pump test began. Manual measurements were taken at GR-2800 and LINN 55017 immediately after the pump was started. The flow meter was not functioning properly and in an attempt to fix it the meter dislodged from the fitting, under pressure from the pumping water. This instant decrease in water pressure unexpectedly shut off the pump in GR-2800, thus no recovery data were recorded and the pump was shut off prematurely before steady-state conditions were reached. Nonetheless, drawdown data were recorded in wells GR-2800 and LINN 55017. No response to pumping was recorded in LINN 52897. Flow measurements were collected throughout Pump test #1 with a five-gallon bucket and eighty-five gallon garbage can.

Before the pump test, site managers were notified to ensure that no irrigation would occur during the time that the pump test was conducted. Two production wells exist to the northeast of Site 1 belonging to the Oregon State University Fish Disease Research Laboratory. Both wells sustained constant pumping rates before, during, and after the pump test.

Table 2: Well information for Pump test #1.

OWRD well-log ID	Distance From Pumping Well (ft/m)	Land Surface Elevation of Well amsl (ft/m)	Perforated Interval Below Land Surface amsl (ft/m)	Hydro-geologic Unit
GR-2800	N/A	212/64.6	No Perforations, 177/54	USU
LINN 55017	92/28	215/65.5	177-167/54-50.9	USU/LSU
LINN 52897	1125/342.9	214/65.2	186.5-176.5/56.8-53.8	USU/LSU?

Pump test #1 began at 16:22 on 9/30/04 and ended 6:45 10/1/04. Due to pumping well GR-2800 shutting off unexpectedly, only drawdown data were recorded. The sustained pumping rate throughout this test was 95 gal/min (5.99×10^{-3} m^3/s). The time immediately following the start of the pump was ignored and attributed to well-bore storage in the large diameter (2.5 ft) pumping well. Well-bore storage can also affect nearby monitoring wells, as shown in drawdown vs. time data for LINN 55017 in Figure 13.

Aquifer parameters were calculated using the method that best represents the conceptual model found at the field site of Pump test #1. Dawson and Istok (1991) was used as a reference, leading to the Neuman Match-Point Method (Neuman, 1974) being selected as the most representative model. The Neuman Match-Point Method is used specifically for transient, unconfined, partially and fully penetrated observation and pumping wells, and anisotropic aquifer conditions. A list of assumptions for this model are displayed in Dawson and Istok (1991), page 278. Storage coefficients were calculated using early time data only because the effects of gravity drainage above the water table on groundwater flow to the pumping well are negligible (Dawson and Istok, 1991).

The large diameter pumping well made it impossible to calculate K_v and S_y

(specific yield). However, data from observation well LINN 55017 allowed for the

estimation of T, K_x, K_v, and S_y as shown in Table 3. Only 0.12 ft (3.7 cm) of drawdown

occurred in LINN 55017 during the pump test. The value calculated for S_y is low given

the known aquifer characteristics and may be because flow in the saturated capillary

fringe above the water table is neglected (Kruseman and de Ridder, 2000). No "late-

time" data or delayed yield effects were recorded during Pump test #1. Drawdown vs.

time data for GR-2800 and LINN 55017 can be found in Figures 12 and 13, respectively.

An example of how these data were analyzed along with calculation specifics can be

found in Appendix G.

Table 3: Final aquifer property values for Pump test #1.

OWRD well-log ID	Drawdown, Neuman Match-Point			
	T (ft^2/d; m^2/s)	K_x (ft/d; m/s)	K_v (ft/d; m/s)	S_y
GR-2800	2.49 x 10^3; 2.68 x 10^{-3}	1.09 x 10^2; 3.95 x 10^{-4}	N/A	N/A
LINN 55017	3.64 x 10^4; 3.91 x 10^{-2}	1.59 x 10^3; 5.59 x 10^{-3}	9.87 x 10^{-1}; 3.48 x 10^{-6}	0.06
LINN 52897	N/A	N/A	N/A	N/A
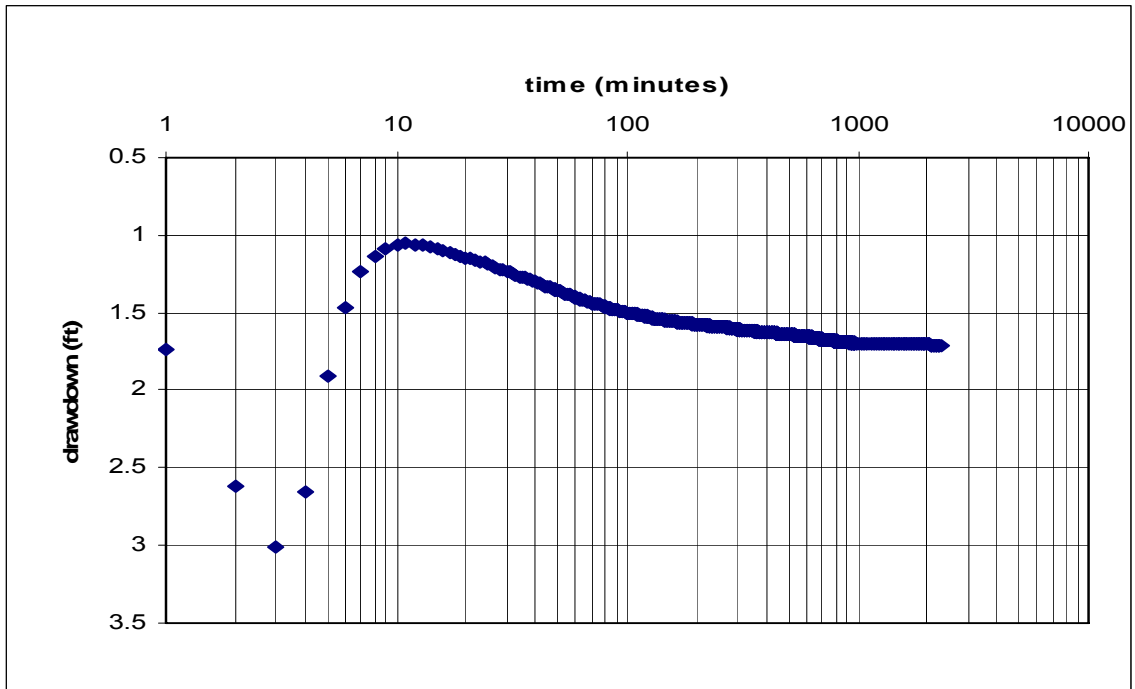
Figure 12: Pumping well (GR-2800) drawdown vs. time for Pump test #1.
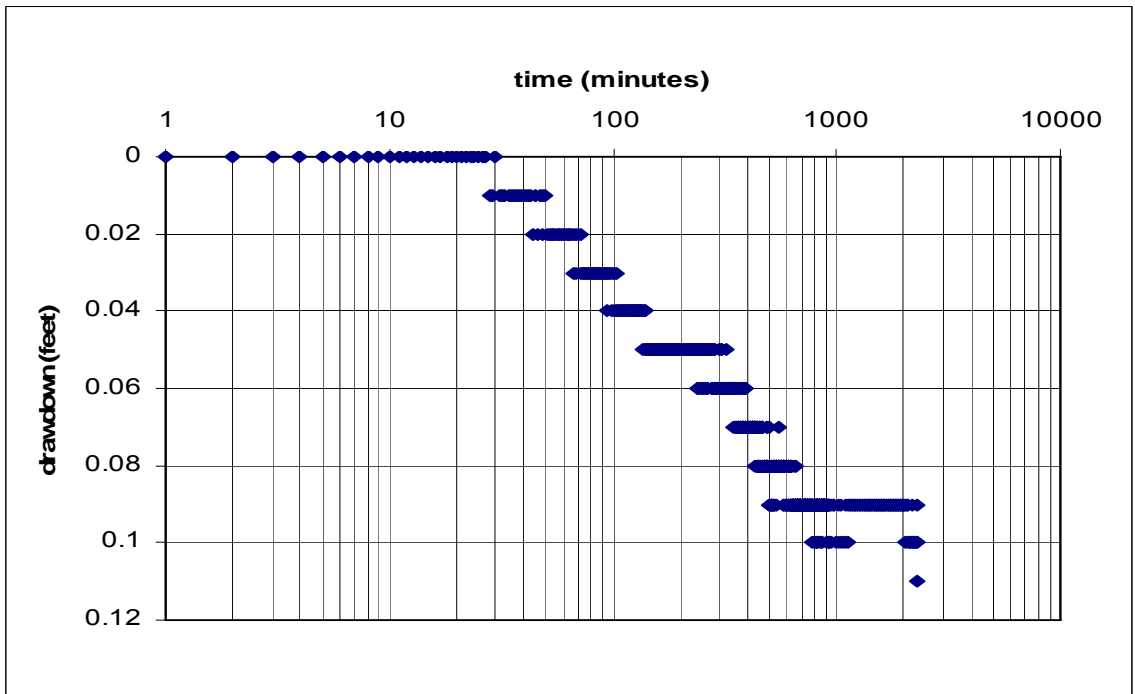
Figure 13: Monitoring well (LINN 55017) drawdown vs. time for Pump test #1.

3.3.1.2 Pump Test #2

Pump test #2 was conducted at the same site with the same monitoring and pumping wells as Pump test #1 (Site #1) from 8:00 10/5/04 to 17:30 10/7/04. A second test was conducted to collect recovery data from GR-2800 and LINN 55017 and to conduct a pump test for a longer period of time than Pump test #1 (to better stress the aquifer). Data loggers in all wells were set to collect data at one minute intervals prior to the start of Pump test #2, reset to take measurements every 15 minutes approximately six hours after the start of the test, then reset to collect measurements every one minute prior to shutting off the pump. Response to pumping was recorded in only one monitoring well, LINN 55017. Flow measurements were made using a five gallon bucket and eighty-five gallon garbage can (the flow meter was still inoperable).

Near steady-state conditions were met at the end of Pump test #2. The pump in GR-2800 was initially set at a pumping rate too high to sustain for an extended period of time. This led to the pump in the well pumping air periodically and required a decrease in pumping rate to 118 gal/min (7.44×10^{-3} m^3/s) 55 minutes into the test. The initial pumping rate was not measured. Since the initial pumping rate was not measured, the data collected after fifty-five minutes was used to estimate hydraulic properties.

The Neuman Match-Point Method was again used to analyze the drawdown data (Dawson and Istok, 1991) and the Theis Recovery Method (Theis, 1935) used to analyze the recovery data at each well. The Theis Recovery Method was selected to analyze the recovery data because Neuman (1975) showed that an unconfined aquifers delayed water table response to pumping is fully reversible and that the Theis Recovery Method is applicable in unconfined aquifers, but only for late time data when effects of elastic

storage have dissipated. Assumptions for this method can be found in Kruseman and de

Ridder (2000), p. 55-56 and 195.

Well-bore storage effects in the first few minutes of the test were attributed once

again to the large well diameter of GR-2800. No "late-time" data or delayed yield effects

were recorded during Pump test #2. During Pump test #2, a greater drawdown in LINN

55017 was measured (0.02 ft greater) than drawdown measured during Pump test #1. In

all, similar values of aquifer properties were calculated for Pump Test #1 (see Table 3)

and Pump Test #2 (see Table 4). A low specific yield value may once again be due to

flow in the saturated capillary fringe above the water table that is neglected (Kruseman

and de Ridder, 2000). Drawdown vs. time data for GR-2800 (see Figure 14) and LINN

55017 (see Figure 15) can be found below. An example of how these data were analyzed

along with calculation specifics can be found in Appendix G.

Table 4: Final aquifer property values for Pump test #2.

OWRD well-log ID	Drawdown, Neuman Match-Point				Recovery, Theis	
	T (ft^2/d; m^2/s)	K_x (ft/d; m/s)	K_v (ft/d; m/s)	S_y	T (ft^2/d; m^2/s)	K_x (ft/d; m/s)
GR-2800	2.33×10^3; 2.51×10^{-3}	1.02×10^2; 3.59×10^{-4}	N/A	N/A	2.35×10^4; 2.52×10^{-2}	1.03×10^3; 3.62×10^{-3}
LINN 55017	4.02×10^4; 4.32×10^{-2}	1.75×10^3; 6.18×10^{-4}	1; 3.84×10^{-6}	0.08	4.69×10^4; 5.05×10^{-2}	2.05×10^3; 7.22×10^{-3}
LINN 52897	N/A	N/A	N/A	N/A	N/A	N/A
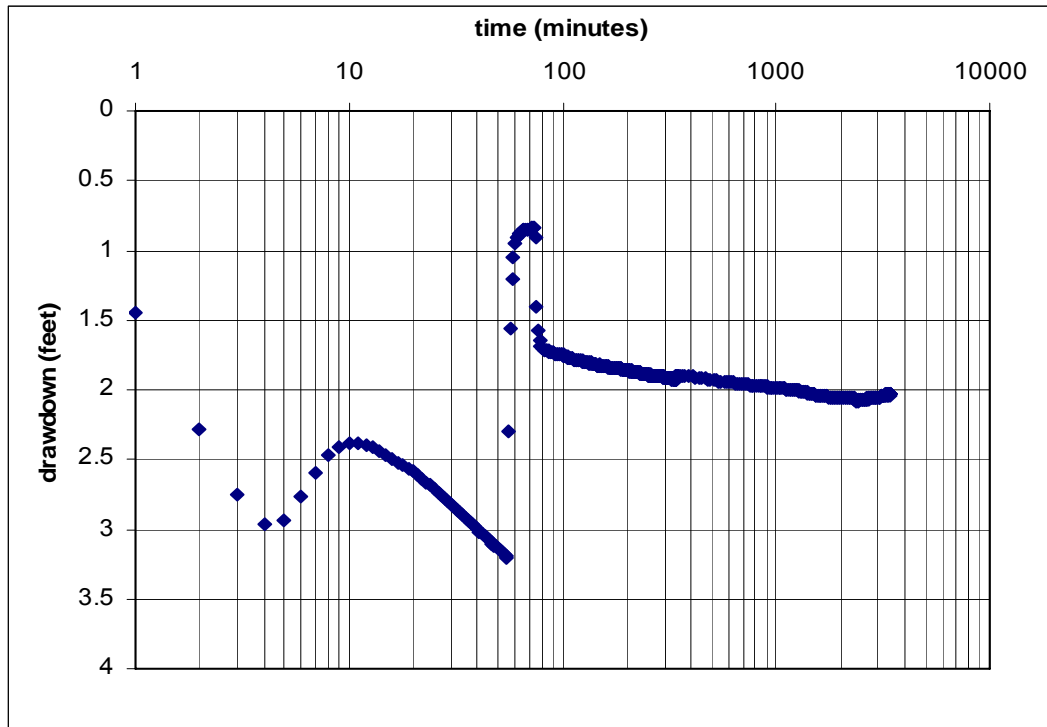
Figure 14: Pumping well (GR-2800) drawdown vs. time for Pump test #2.
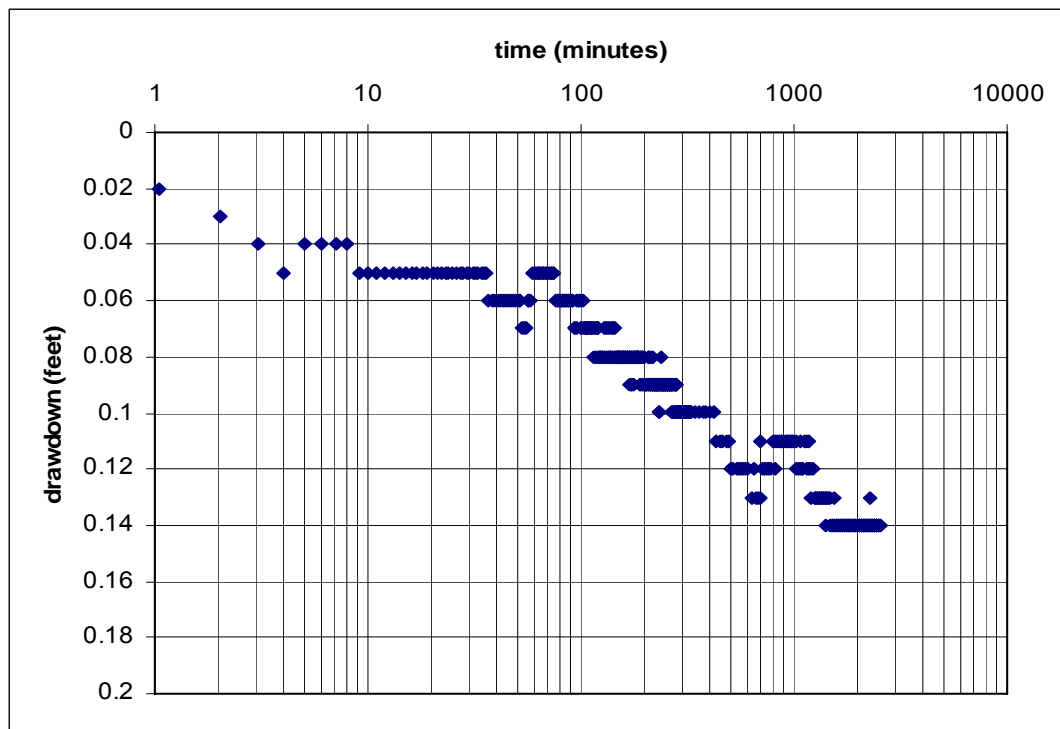
Figure 15: Monitoring well (LINN 55017) drawdown vs. time for Pump test #2.
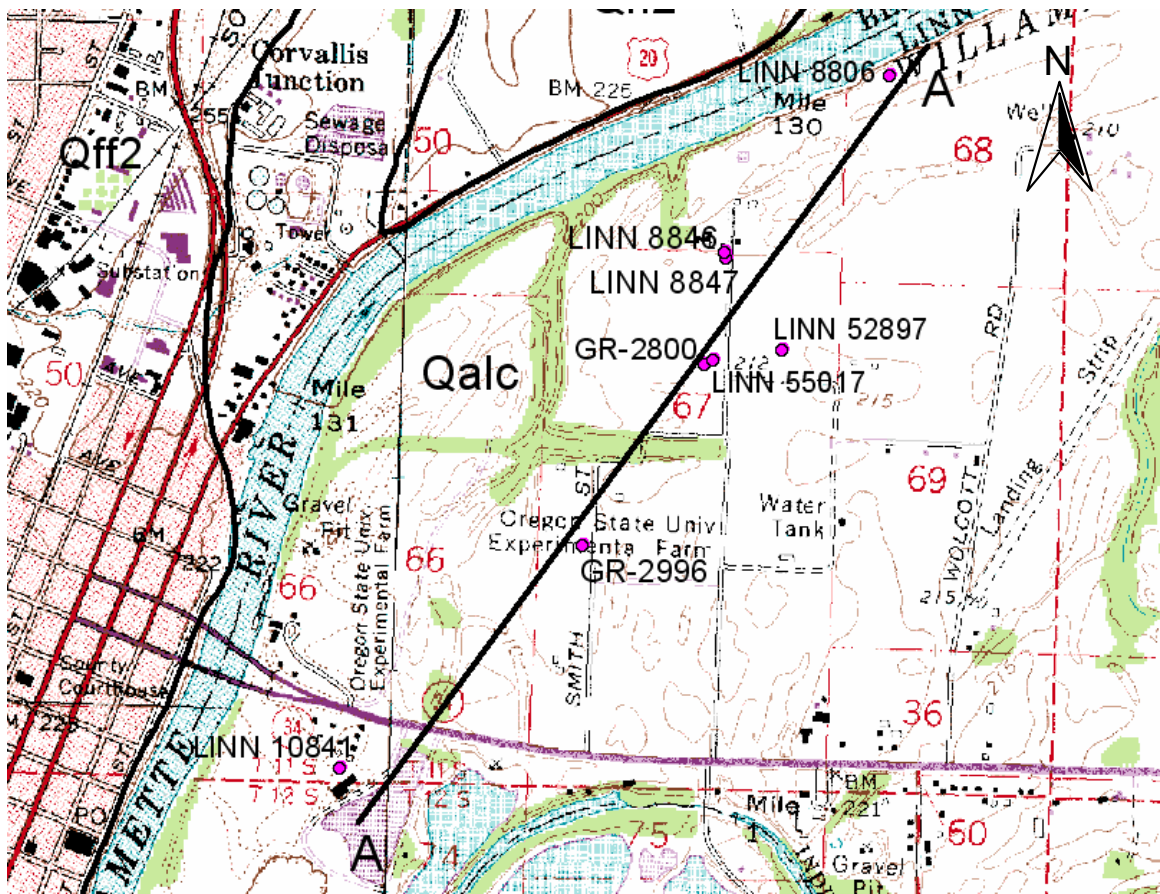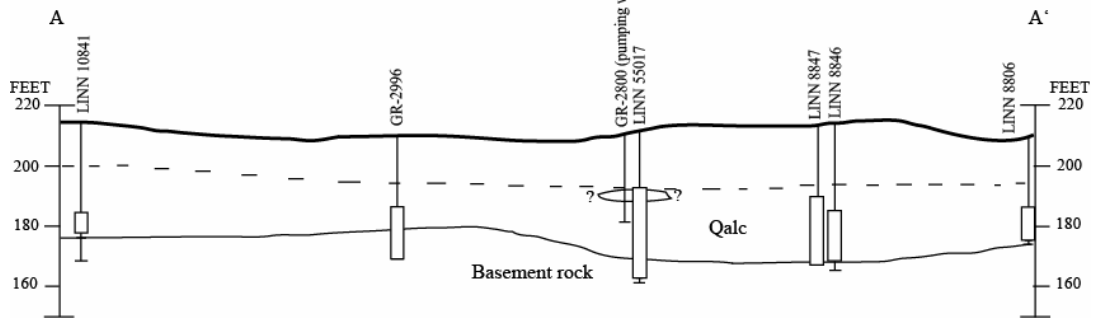
Figure 16: Map of location where Pump test #1 and Pump test #2 were conducted with cross-section (x50 vertical exaggeration). Dotted line represents bottom of overbank facies. Large-scale map view location found in Figure 7.

3.3.1.3 Pump Test #3

Pump test #3 was conducted at Site #2 southeast of Harrisburg, OR. Field

reconnaissance was conducted to locate all wells in the vicinity, link well logs to all local

wells, and to determine which wells may be in use during the pump test. Permission was

granted from the landowners to conduct a pump test using LANE 8101 as the pumping

well and LANE 8029 and the Sullivan well as monitoring wells. Monitoring well

information is located in Table 5. A map of Site #2, including monitoring wells,

pumping well, and wells used during cross-section construction are located in Figure 19.

The SeaMetrics TX-81 turbine flow meter was installed down gradient of the GE 15 H.P.

pump in LANE 8101 with a custom fitting provided by SeaMetrics. Seven-hundred

twenty feet of irrigation piping was transported from Corvallis to the field site and was

installed to transport the water pumped from LANE 8101 down gradient to a slough of

the Willamette River. The Druck pressure transducer and data logger used in Pump Test

#1 and Pump Test #2 were calibrated and installed in LANE 8069 12/4/04. The Global

Logger WL-15 used in Pump Test #1 and Pump Test #2 was calibrated and installed in

the Sullivan well 12/4/04. Background data were collected to observe water level

changes in the aquifer and to ensure minimal amounts of drift existed in the pressure

transducers. No instrumentation could be installed in LANE 8101 due to well-head

construction limitations.

Although December is not the optimal time to conduct an aquifer test, time

restraints and lack of precipitation for an extended period of time warranted conducting

such a test.

Table 5: Well information for Pump test #3.

OWRD well-log ID	Distance From Pumping Well (ft/m)	Land Surface Elevation of Well amsl (ft/m)	Perforated Interval Below Land Surface amsl (ft/m)	Hydrogeologic Unit
LANE 8101	N/A	347/105.8	No perforations, 326/99.4	MSU/USU
LANE 8069	417/127.1	346/105.5	317-326/96.6-99.4	MSU/USU
Sullivan well	251/76.5	348/106.1	318/96.9	MSU/USU

The pump test began 10:08 12/15/04 and ended 14:00 12/17/04. Data loggers in all wells were set to collect data at one minute intervals prior to the start of Pump test #3, reset to take measurements every fifteen minutes approximately four hours after the start of the test, then reset to collect measurements every one minute prior to shutting off the pump. Manual drawdown and recovery measurements were collected with an electric tape from the Sullivan well. Minimal drawdown was recorded at LANE 8069 and the Sullivan well.

Two observation wells, LANE 8069 and the Sullivan well, collected drawdown and recovery data for estimation of T, K_x, K_z, and S_y. The pumping well, LANE 8101, was maintained an average rate of 103 gal/min (6.50×10^{-3} m^3/s (see Figure D 7 in Appendix G). The timing of the test was not optimal, but recharge was expected to be minimal due to recently experiencing low amounts of local precipitation and an observed plateau of a previous rising Willamette River. After analysis of the data, it appears that two major things occurred that made the drawdown and recovery data difficult to

interpret: (1) the Willamette River did raise slightly during the test, causing local water tables to rise with it, and (2) the pumping rate was not great enough to cause substantial response in either the Sullivan well or LANE 8069, with the Sullivan well being the most difficult to interpret, mostly due to the well being closest to the Willamette River and furthest from the pumping well. The Neuman Match-Point Method was initially used but failed due to a lack of fit between the measured drawdown data and the Neuman curve data. The Theis Match-Point Method was then used to analyze the Sullivan well data and LANE 8069 data (Dawson and Istok, 1991).

Table 6 contains the aquifer parameter analysis results. Recovery data was smeared due to the steadily rising Willamette River and local water table. The data could not be interpreted with any confidence. Drawdown vs. time data can be found for the Sullivan well and LANE 8069 in Figure 17 and Figure 18, respectively. An example of how these data were analyzed along with calculation specifics can be found in Appendix G.

Table 6: Final aquifer property values for Pump test #3.

	Drawdown, Theis				Recovery, Theis	
OWRD well-log ID	T (ft^2/d; m^2/s)	K_x (ft/d; m/s)	K_v (ft/d; m/s)	S_y	T (ft^2/d; m^2/s)	K_x (ft/d; m/s)
Sullivan well	3.28 x 10^4; 3.53 x 10^{-2}	6.56 x 10^2; 2.32 x 10^{-3}	N/A	0.15	N/A	N/A
LANE 8069	7.08 x 10^4; 7.61 x 10^{-2}	1.42 x 10^3; 5.00 x 10^{-3}	N/A	0.05	na	N/A
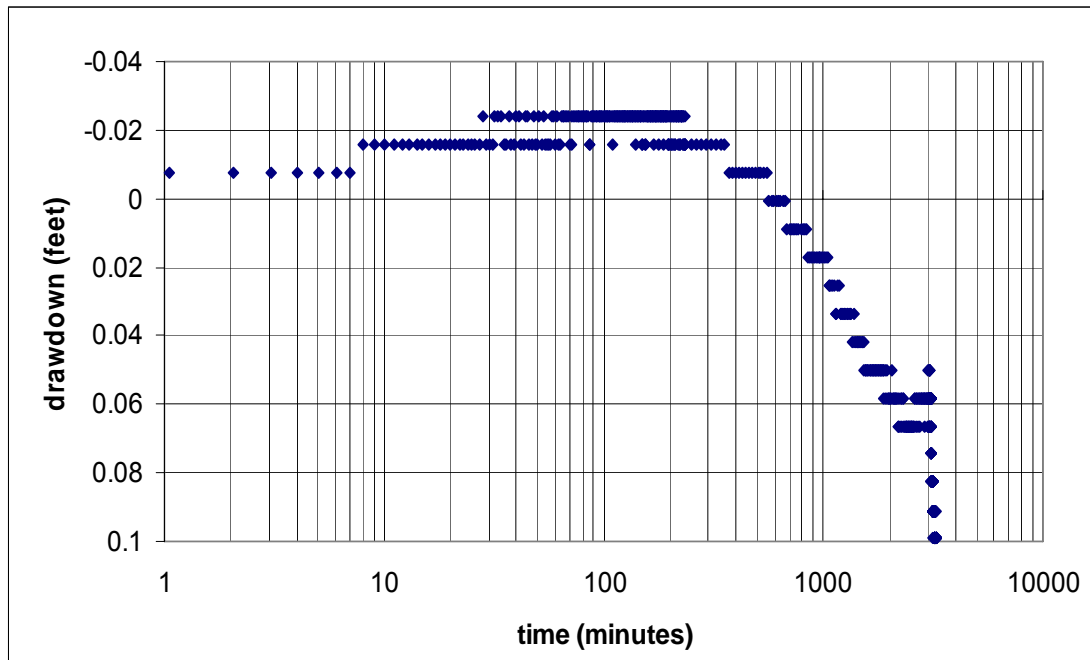
Figure 17: Monitoring well (Sullivan well) drawdown vs. time for Pump test #3.
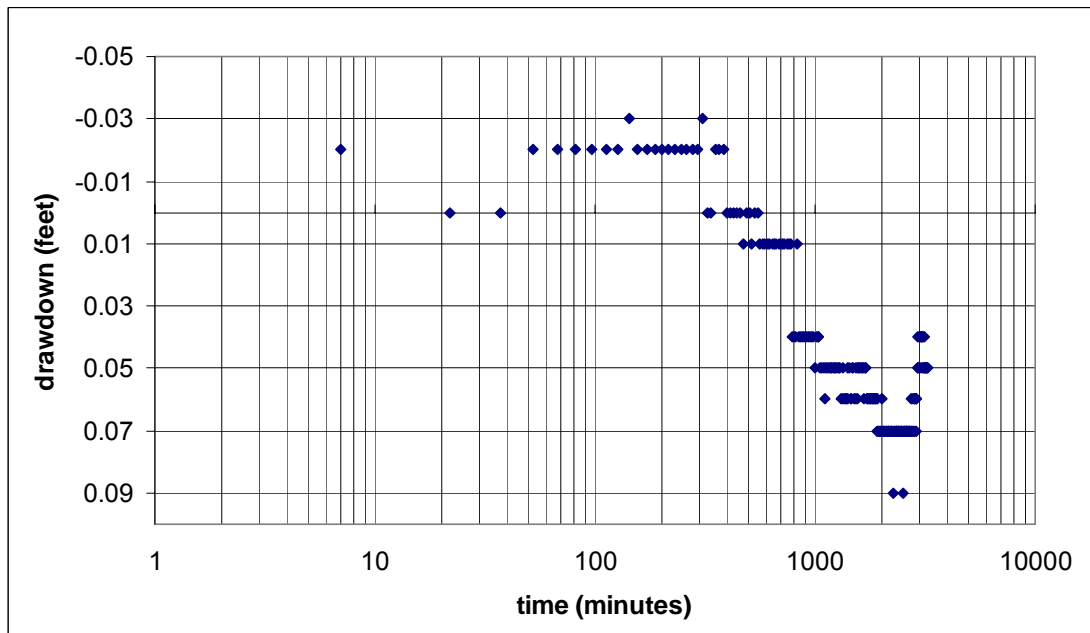
Figure 18: Monitoring well (LANE 8069) drawdown vs. time for Pump test #3.
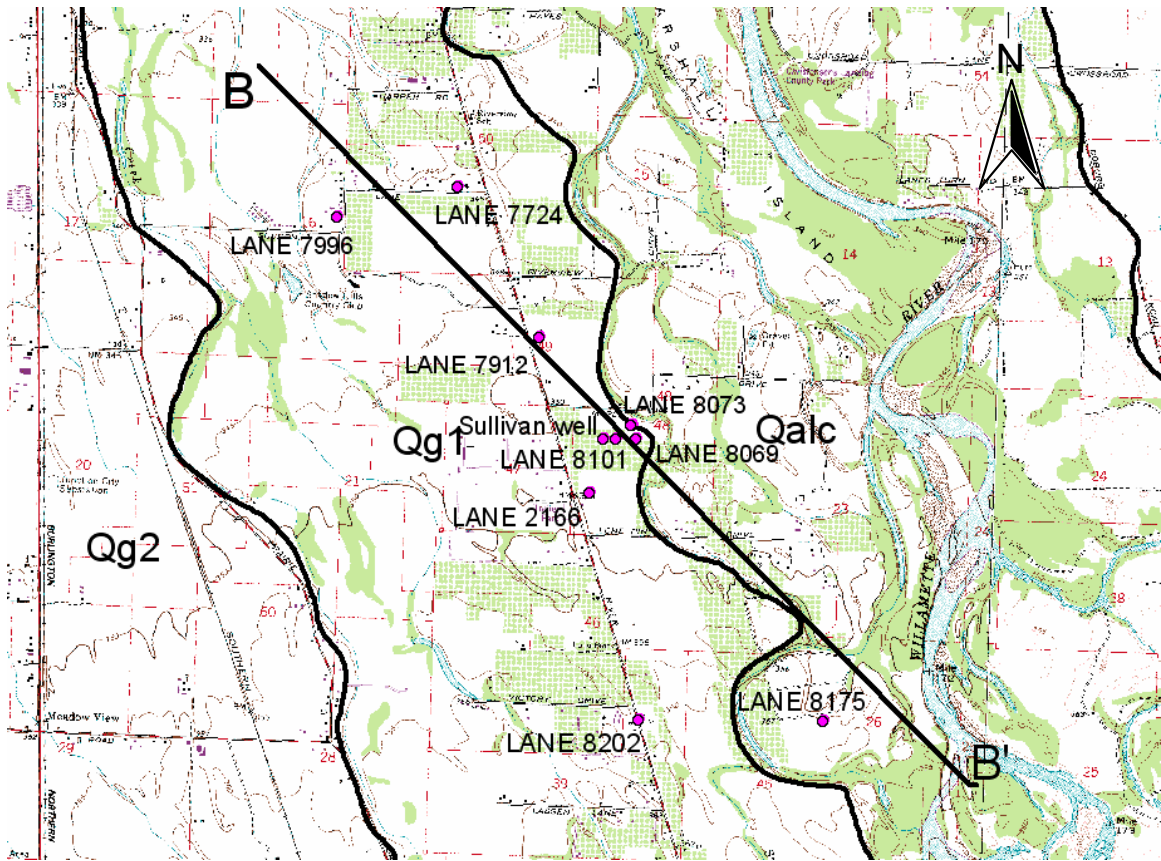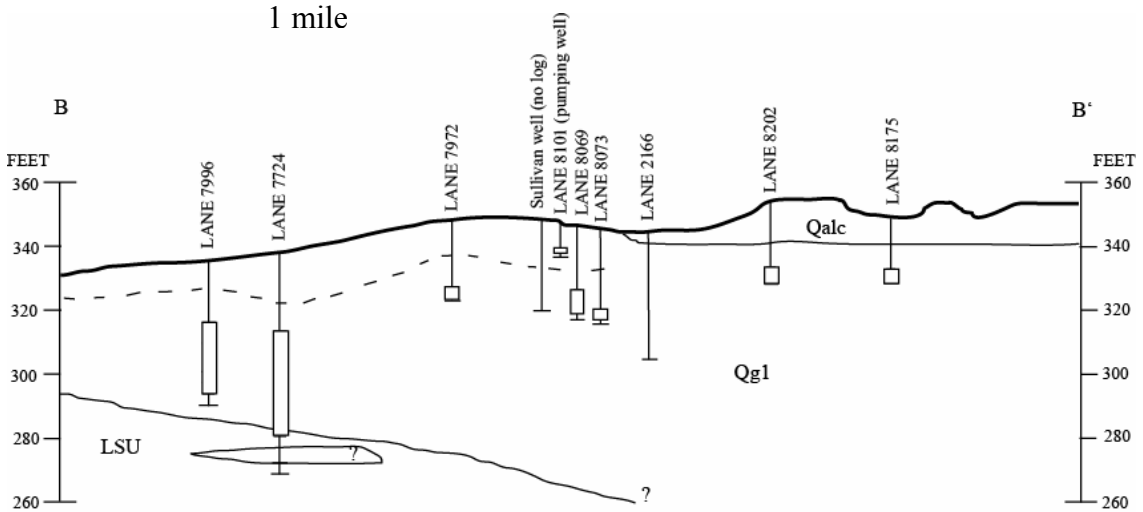
Figure 19: Map of location where Pump test #3 was conducted with cross-section (x50 vertical exaggeration). Dotted line represents bottom of overbank facies. Large-scale map view location found in Figure 7.

3.3.2 Slug Tests

Slug tests were conducted to obtain more estimates of aquifer properties throughout the SWV. Locations within the GWMA were initially targeted, along with wells in close proximity to each other at varying depths. Wells were selected based on (1) if permission from the landowner was granted, (2) if the well was located in the approximate desired spatial and vertical location, (3) if a positive correlation could be established between the well in the field and well log, and (4) if access into the well existed for insertion of electric tape, pressure transducer, or injection of water.

Five slug tests were conducted in summer 2004 on five different wells by injecting a known volume of water and measuring the decline in water level in each well over time with a stopwatch. This method proved to be inaccurate due to the high hydraulic conductivity of the tested strata, resulting in a rapid decline of water levels. Only one well, BENT 52470, of the initial five wells tested produced data that were able to be analyzed.

Slug tests were conducted on eleven more wells in the SWV in spring 2005. A Global Water WL-15 15 ft Water Logger, set to collect measurements every second, was calibrated and inserted into each well if access was available. An electric tape was used to collect water level measurements where well-head geometry prevented insertion of the pressure transducer. A known volume of water was either injected or removed as quickly as possible; either rising or falling water level values were recorded with the pressure transducer or electric tape. Kruseman and Ridder (2000) recommend that the water level in the well be displaced by about 10 cm to 50 cm. This was done whenever possible, however, domestic wells commonly have well-head geometries with small (~0.75 in or

1.9 cm) access ports which constrain how much water can be added to a well. Local well

logs were collected near each well selected for a slug test to aid in determining local

stratigraphic thicknesses. Table 7 includes information about the well and details about

each slug test.

Table 7: Slug test information. Well locations in Appendix I.

OWRD well-log ID	Well diameter (ft)	Land surface elevation, AMSL, (ft/m)	Depth to top of screen (ft/m)	Depth to bottom of screen (ft/m)	Water level measurement method	Volume of water injected or withdrew (gallons)
BENT 52470	0.0625	230/70.1	13.6/4.1	18.6/5.7	electric tape	+0.25
BENT 6612	0.67	295/89.9	48/14.6	58/17.7	transducer	+1
LANE 8725	0.67	343/104.5	30/9.1, no screen	30/9.1, no screen	transducer	+1
BENT 1192	0.5	282/86	39/11.9, no screen	39/11.9, no screen	electric tape	- unknown amount
BENT 51799	0.5	282/86	80/24.4	100/30.5	electric tape	+1
Funke Dist. (have log)	0.67	392/119.5	150/45.7	200/61	transducer	+1
Funke phouse (no log)	0.5	392/119.5	87/26.5, no screen	87/26.5, no screen	transducer	+1
LANE 7590	0.83	372/113.4	24/7.3	28/8.5	transducer	+2
LANE 7596	0.67	343/104.5	18/5.5	40/12.2	transducer	+1
LINN 13770	0.83	285/86.9	38/11.6	48/14.6	transducer	+1
LINN 2476	0.5	287/87.5	25/7.6	58/17.7	electric tape	+1
LINN 12120	0.5	215/65.5	260/79.2, no screen	260/79.2, no screen	transducer	+1
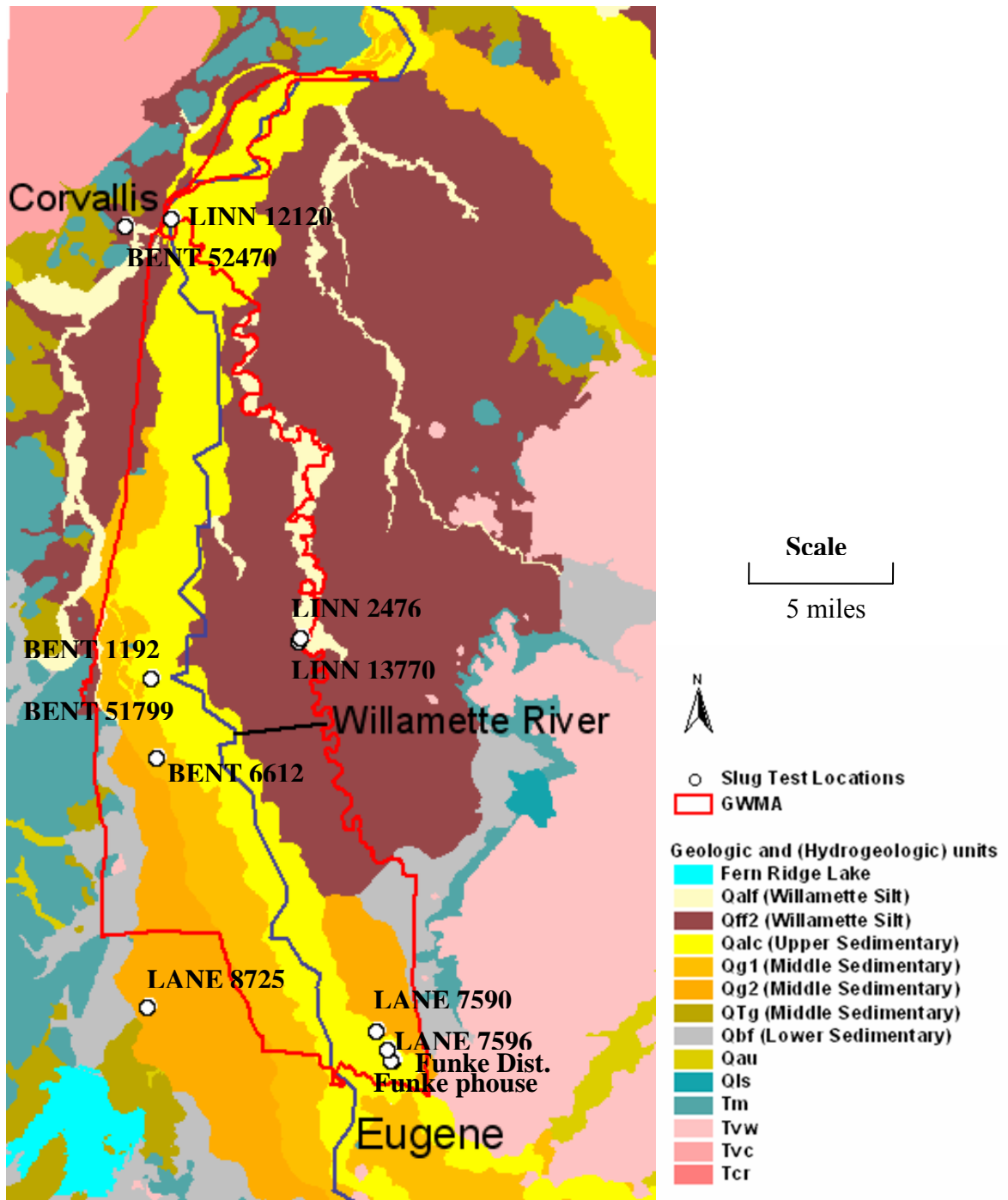
Figure 20: Slug test locations.

The method selected to analyze the slug test data, the Bouwer and Rice Method, was developed by Bouwer and Rice (1976) and assumptions can be located on p. 308 of Dawson and Istok (1991). Some of the slug test analysis were complicated by high hydraulic conductivities, large well radii, and limited access for installation of equipment and addition of an instantaneous volume of water making it difficult to mimic the assumptions that make the Bouwer and Rice Method possible. Many scientists are skeptical of slug tests, and advantages and disadvantages to this method are discussed in Butler (1998). Table 8 shows the results of slug test data analysis. Slug test data and an example calculation can be found in Appendix H.

Table 8: Slug test analysis results. Well locations in Appendix I.

OWRD well-log ID	"Average" elevation of open interval, AMSL, (ft; m)	Hydraulic conductivity, K_x, (ft/d; m/s)	Hydrogeologic Unit
BENT 52470, MW-2	213.9; 65.2	0.045; 4.84×10^{-8}	LSHU
BENT 6612	242; 73.8	17.1; 1.84×10^{-5}	LSHU
LANE 8725	313; 95.4	11.0; 1.18×10^{-5}	MSHU
BENT 1192	243; 74.1	13.3; 1.43×10^{-5}	MSHU
BENT 51799	192; 58.5	1.08; 1.16×10^{-6}	LSHU
Funke Dist. (have log, no OWRD log ID)	217; 66.1	12.1; 1.30×10^{-5}	MSHU
Funke phouse (no log)	305; 93	26.0; 2.80×10^{-5}	MSHU
LANE 7590	336; 102.4	430; 4.62×10^{-4}	MSHU
LANE 7596	314; 95.7	0.039; 4.19×10^{-8}	MSHU
LINN 13770	242; 73.8	40.1; 4.31×10^{-5}	MSHU
LINN 2476	247; 75.3	21.8; 2.34×10^{-5}	MSHU
LANE 12120	-45; 13.7	0.040; 4.30×10^{-8}	BCHU

3.4 Specific Capacity Analysis

We used specific capacity (*sc*), the ratio of well discharge to drawdown, to estimate transmissivity (*T*) (where $T = (ft^2/d)$ and $sc = (gal/min/ft)$). These data are abundant; almost every well log contains a record of drawdown for a given discharge. When aquifer test information is sparse, specific capacity information is commonly used as an alternative to estimate transmissivity. An analysis of wells that contain both specific capacity and aquifer test data was used to develop an empirical relationship between specific capacity and transmissivity (see Figure 21). The empirical relationship was then used to estimate transmissivity for wells that only contain specific capacity data. A similar empirical relationship has been developed for different aquifer types with large amounts of data (Meier et al., 1999; Razack and Huntley, 1992) with good success. These studies opted to use site specific data as opposed to using the general empirical relationship for unconfined ($T = 1500*sc$) and confined aquifers ($T = 2000*sc$) found in Dawson and Istok (1991).

Since few aquifer tests have been performed in the SWV, specific capacity data were used from Orzol et al. (2000) which contain well data collected and compiled by the OWRD and USGS. Orzol et al. (2000) contains two groups of field-located well data collected in the Willamette Basin: the "study" data set (containing 1,234 wells collected specifically for the study) and "non-study" data set (containing 4,752 wells collected during previous USGS and OWRD studies) (Orzol et al., 2000). These data sets were selected because they contain field-located wells in GIS format along with selected information from water-well reports, water-level data from wells, water-chemistry data

from selected wells, and borehole geophysical data from selected wells, as well as

specific capacity information and OWRD well-log ID's.

The "study" and "non-study" wells located within the SWV were sorted and

organized in order to select the most accurate specific capacity data and sustain enough

data spatially for data interpolation within the Middle and Lower Sedimentary

hydrogeologic layers. Two specific criteria were used: (1) the pumping duration must be

≥ 1 hour, and (2) the pumping method must be a pump or bailer type. These two criteria

were selected because, in general, the longer the specific capacity test the more accurate

the results and using a pump or bailer to remove water from a well is the most accurate

method. Results included 66 wells from the "non-study" data set and 63 well from the

"study" data set. Well logs were gathered using OWRD well-log ID's, average depth of

well screen determined, and the average elevation of well screen was determined using

the surface elevation of each well. Well screen thickness was also determined for each

well. A well screen thickness of 5 ft (1.5 m) was assigned to wells with a ≤ 5 ft screened

interval. Well screen thickness information was used to approximate hydraulic

conductivity, where T = hydraulic conductivity*well screen thickness.
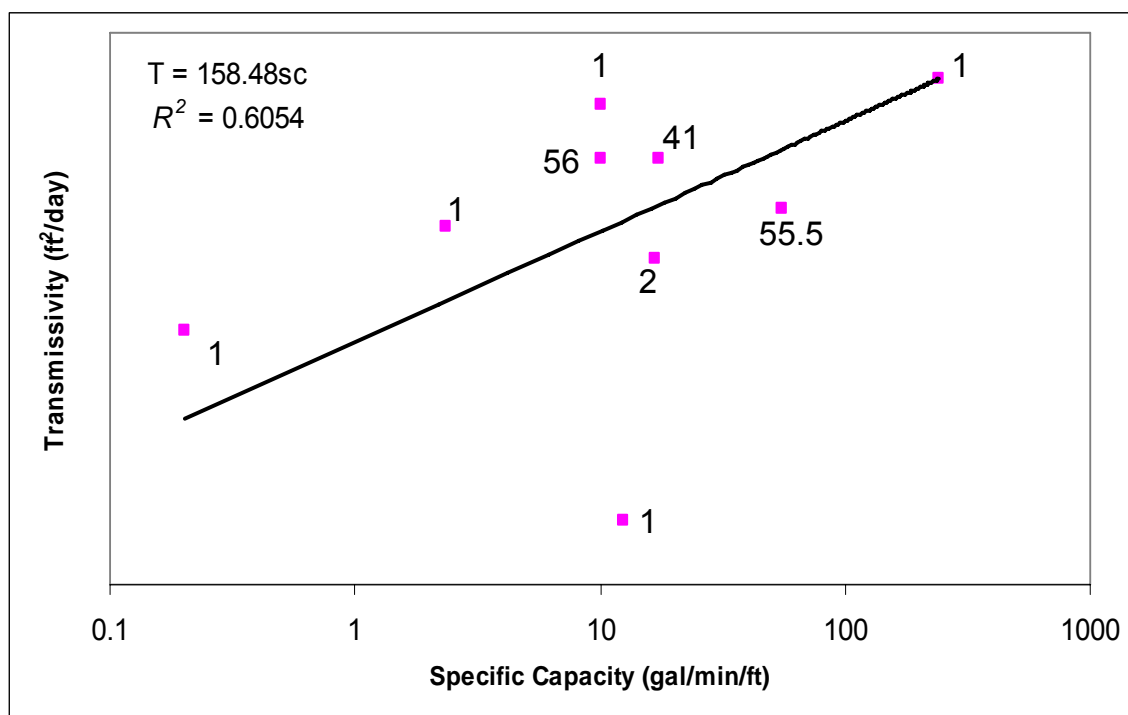
Figure 21: Transmissivity vs. specific capacity for selected wells of the SWV. The value beside each point represents the amount of time in hours that the specific capacity test was conducted.

The values of hydraulic conductivity derived for the "non-study" and "study" wells using the empirical relationship may overestimate the true hydraulic conductivity due to using a minimized value (the well screen thickness) for aquifer thickness. However, an underestimation of hydraulic conductivity may also result due to the low constant within the derived equation $T = 158.48*sc$ (compared to a constant value of 1500 or 2000 in Dawson and Istok, 1991). An $R^2 = 0.6054$ explains about 60 percent of the original variability with the model $T = 158.48*sc$. Therefore, this empirical relationship can be rewritten as $T = 158.48*sc \pm 40$ percent. This uncertainty must be remembered when using this type of data. The final estimates of hydraulic conductivity derived for wells located within the MSHU and LSHU are shown in Appendix I.

3.5 Groundwater Chemistry

Fifteen groundwater chemistry samples were collected from groundwater wells in the SWV and analyzed for nitrate (NO_3^-), chloride (Cl^-), sulfate (SO_4^{2-}), and pH. The purpose of our sampling was to supplement existing data and maintain ongoing water quality monitoring, not to sample the SWV extensively. Samples were collected in October, November, and December 2004 and July 2005. Only wells with submersible pumps were used and samples were collected immediately following well purging in order to minimize disturbance of the water column.

The methods used during the groundwater chemistry sampling process were the well-volume method where standard operating procedures for collection of representative groundwater samples were followed (Yeskis and Zavala, 2002). These procedures included: 1) completing an observation well form (Appendix C), including measuring depth to water in each sampling well (if possible); 2) calculating well casing volume and measuring pumping rate with a five gallon bucket; 3) pumping at least three well casing volumes before sampling at a constant rate; and 4) collecting measurements of water levels in the well (if possible), dissolved oxygen (mg/L), temperature (°C), and specific conductance (µS/cm) as well is being purged. Dissolved oxygen and temperature measurements were made with an YSI Model 52 dissolved oxygen meter, calibrated weekly. Specific conductance measurements were made using a Hanna Instruments 8733 Conductivity Meter, calibrated according to the operators manual. Stabilization criterion (the amount deviated from the original value, indicating water representative of the aquifer is being measured) for specific conductance of ±3 percent were met at each sampling location, except for samples N13, N14, and N15 where the conductivity meter

failed and temperature was used as a backup stabilization parameter during the sample collection.

All samples were delivered to Oregon State University Central Analytic Laboratory (CAL) for chemical analysis within 24 hours of collection. CAL has similar laboratory methods as those specified for: EPA Methods 300.0 for nitrate and chloride, EPA Methods 150.1 for pH, and EPA Methods 375.2 for sulfate. Lab information and equipment used for analysis can be found in Appendix A. Precision and accuracy information for CAL can be found in Appendix B.

Results of the analysis of groundwater chemistry sampling are shown in Table 9. Ten samples were collected along with CFC samples for comparison between groundwater chemistry and CFC-model ages (Section 3.6). Five samples were collected (one duplicate sample) in areas of local concern. Letters were sent to all the well owners that cooperated by allowing groundwater to be collected from their well (see Appendix D). In addition to the fifteen samples, one spike sample containing 10 mg/L of NO_3^- and one field blank containing pure deionized water were prepared and taken to CAL for analysis. These two samples along with the duplicate sample were prepared and/or collected to determine laboratory variability, to determine the potential for introduction of contaminants from ambient sources during sample collection, and to assess precision of the sample collection process. A high standard of quality assurance and quality control was maintained throughout the sampling process.

Mean values of parameters from field collected and CAL results are as follows: nitrate (5.5 mg/L), chloride (58.8 mg/L), sulfate (9.3 mg/L), final specific electrical conductance (567 μS/cm), final temperature (13.6°C), and pH (6.9). Duplicate samples

N10 and N11 only show a variability of 0.02 mg/L for nitrate and the remaining

parameters analyzed are equal to one another. The sample spike (S1), prepared to contain

10 mg/L of nitrate, was analyzed at CAL and returned a nitrate value of 10.59 mg/L.

This may indicate either the laboratory spike sample was developed incorrectly or that

the CAL may slightly overestimate nitrate concentrations. The field blank DI1,

containing pure deionized water, returned low concentrations of nitrate, sulfate, and

chloride, well within the detection and accuracy limits for each parameter as determined

by CAL (see Appendix B).

Nitrate can originate from a variety of sources and is discussed in detail in Section

2.1. The MCL for nitrate is 10 mg/L (U.S. Environmental Protection Agency, 2005).

Four samples, N4, N6, N7, and N10 contain concentrations >10 mg/L. Nitrate as well as

chloride, sulfate, and dissolved oxygen results were analyzed separately based on wells

that penetrated the Willamette Silt hydrogeologic unit vs. wells that did not penetrate the

Willamette Silt hydrogeologic unit. This may be the most prominent geologic distinction

and where present likely affects infiltration of water to the aquifer, decreasing the

possibility of surface contamination. Mean nitrate levels were greater where no

Willamette Silt exists (8.21 mg/L) than where Willamette Silt does exists (2.84 mg/L).

Basement material of the SWV contains volcanic and volcaniclastic rocks and

marine sedimentary rocks, which may be a source of chloride in some areas. Sewage and

septic systems as well as pesticide and fertilizer applications generally contain high

chloride content and can be introduced into groundwater (Woodward et al., 1998). The

National Secondary Drinking Water Regulations (secondary standards) for chloride is

250 mg/L (U.S. Environmental Protection Agency, 2005). Samples N3 and N13 contain

concentrations of chloride >250 mg/L. This study found that where Willamette Silt is present the mean chloride concentration is greater (116.37 mg/L) than where Willamette Silt is not present (5.04 mg/L).

Sulfate usually originates from the evaporative minerals gypsum and anhydrite; or from the oxidization of pyrite (Driscoll, 1986). Sulfate based fertilizers can also contribute sulfate to groundwater. The secondary standard for sulfate is 250 mg/L (U.S. Environmental Protection Agency, 2005). All samples collected during this study contain concentrations of sulfate <21 mg/L. Mean sulfate concentrations were slightly greater where Willamette Silt is present (10.32 mg/L) than where Willamette Silt is not present (6.63 mg/L). Sulfate is redox-sensitive (Hinkle, 1997) and can react under reducing or oxidizing conditions.

The solubility of air in water at 0°C at atmospheric pressure is about 29 mg/L; about 10 mg/L of this represents the oxygen portion (Driscoll, 1986). The maximum value of dissolved oxygen (DO) found in this study was 8.08 mg/L and minimum concentration was 0.10 mg/L. Reducing or low DO conditions (DO concentrations <1.0 mg/L) (Hinkle, 1997), readily exist in the SWV. Mean DO concentrations where Willamette Silt is not present were lesser (1.74 mg/L) than where Willamette Silt is present (5.71 mg/L).

The secondary standards recommended for pH are a range of 6.5 to 8.5 (U.S. Environmental Protection Agency, 2005). Wells N9 and N10 contain water with a pH slightly less than 6.5, or slightly acidic. All other wells contained water within the 6.5 to 8.5 range. Wells where Willamette Silt is present exhibited slightly larger pH values

(7.12) than wells where no Willamette Silt is present (6.76). If pH is low, the possibility

of denitrification occurring increases.

Specific electrical conductance measures the ability of the water to conduct

electrical current and can be used as a proxy to measure the total quantity of ions in

solution. The larger the specific electrical conductance, the more ions exist in solution.

Samples collected from wells where Willamette Silt is present contain greater specific

electrical conductance (836 µS/cm) compared to wells where no Willamette Silt is

present (393 µS/cm). Field and laboratory recorded data are included in Table 9.

Nitrate and dissolved oxygen concentrations are likely related to one another.

Figure 22 shows a linear relationship between nitrate and dissolved oxygen

concentrations. However, a past study by Vick (2004) of 120 wells in the SWV showed a

weak statistically significant trend between nitrate and dissolved oxygen concentrations

(P-value = 0.1531). Figure 23 shows an apparent relationship between nitrate

concentration, dissolved oxygen concentration, and average well depth. These

relationships indicate that denitrification may be occurring to varying degrees at varying

depths beneath land surface.
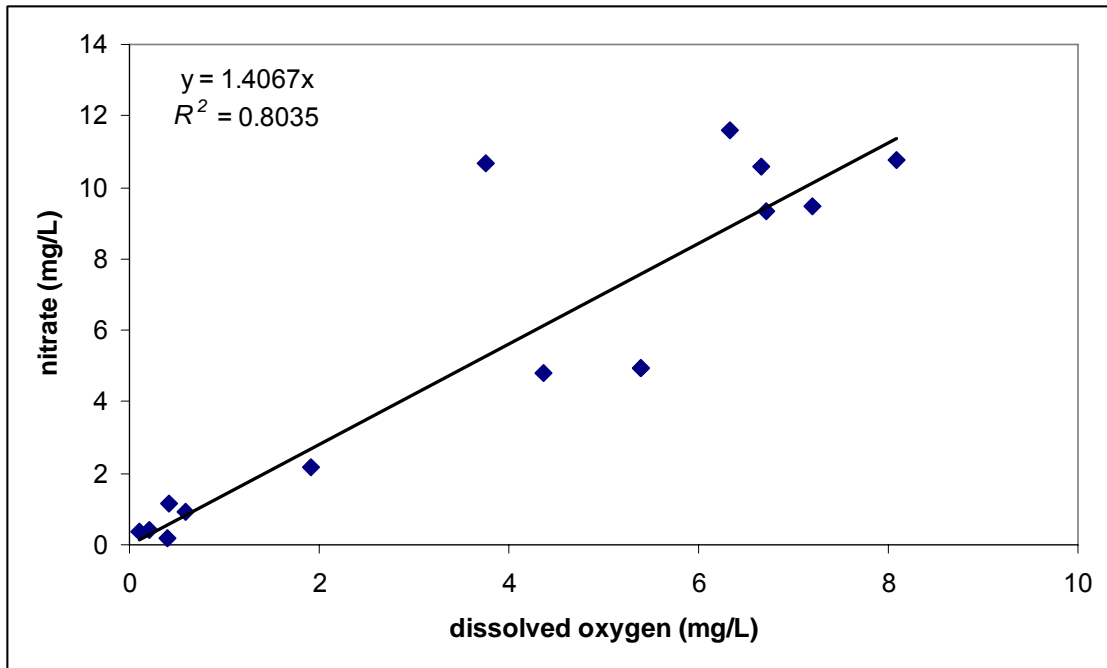
Figure 22: Nitrate concentration vs. dissolved oxygen concentration for sampled wells.
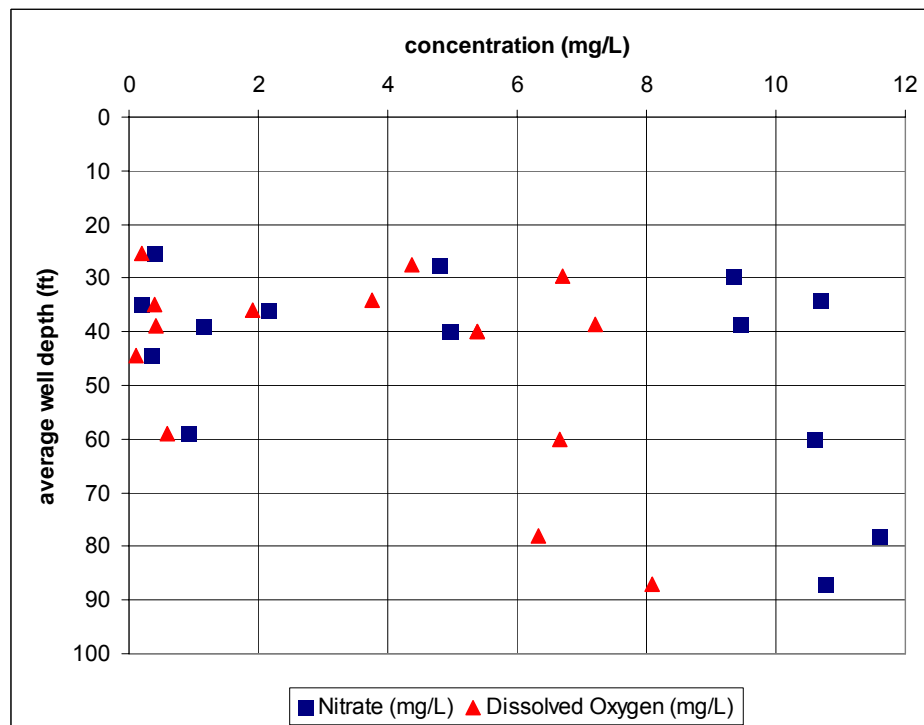
Figure 23: Average well depth vs. nitrate and dissolved oxygen concentrations for sampled wells.

Table 9: Groundwater chemistry data and results. Projection = UTM; Datum = NAD 83

OWRD Log id #	Lat. (UTM 11)	Long. (UTM W)	Sample #	Date	Site location	Willamette Silt?	Elevation amsl (ft)	Average open interval amsl (ft)	NO3-N (ppm)	Cl- (ppm)	SO4-S (ppm)	pH	*Dissolved oxygen (mg/l), final	*Specific electrical conductance (µS/cm), final	*Temp. (°C), final
LINN 14016	44.27186	123.07964	CFC1, N1	10/25/2004	Harrisburg transect	Y	323	297.5	0.40	10.80	7.07	7.20	0.20	190.5	13.4
LINN 14130	44.28580	123.13774	CFC2, N2	10/25/2004	Harrisburg transect	Y	308	272	2.16	36.30	1.83	7.20	1.92	254.0	13.4
LINN 50592	44.27190	123.06774	CFC3, N3	10/26/2004	Harrisburg transect	Y	321	282	1.14	273.90	2.51	7.30	0.43	no data	13.9
LINN 13346	44.31691	123.19436	CFC4, N4	10/26/2004	Harrisburg transect	Y	296	262	10.68	22.10	19.91	7.10	3.75	2116.7	13.4
LANE 8073	44.16798	123.15480	CFC5, N5	11/9/2004	South J.C.	N	347	319.5	4.80	5.50	4.35	6.60	4.37	1060.0	13.3
LANE 5698	44.13406	123.08700	CFC6, N6	11/16/2004	Coburg	N	383	305	11.60	4.50	3.65	7.00	6.33	280.7	13.1
LANE 7488	44.13507	123.09467	CFC7, N7	11/16/2004	Coburg	N	378	318	10.60	3.90	4.38	6.70	6.66	268.6	13.1
LINN 14105	44.28911	123.05962	CFC8, N8	11/20/2004	Harrisburg transect	Y	312	277	0.20	161.00	9.40	7.10	0.40	874.7	13.4
LANE 51456	44.14332	123.09749	CFC9, N9	12/14/2004	Coburg	N	373	343.5	9.33	5.00	8.60	6.40	6.71	292.9	13.4
no well log	44.13030	123.18580	CFC10, N10	12/14/2004	Coburg	N	392	305	10.78	4.39	4.70	6.40	8.08	257.3	12.5
LINN 10769	44.51138	123.18580	N11	7/19/2005	Oakville	Y	243	203	4.96	32.00	20.90	6.80	5.39	300.0	14.4
LINN 10769	44.51138	123.18580	N12	7/19/2005	Oakville	Y	243	203	4.94	33.00	20.90	6.80	5.39	300.0	14.4
LINN 14280	44.58324	123.18192	N13	7/19/2005	Albany	Y	225	180.5	0.35	278.00	10.60	7.20	0.10	1280.0**	16.6***
LANE 7719	44.20826	123.17538	N14	7/19/2005	Junction City	N	332	293.5	9.45	7.00	18.00	6.60	7.20	296.0**	13.0***
LANE 4237	44.20988	123.17321	N15	7/19/2005	Junction City	N	332	273	0.92	5.00	2.70	7.60	0.59	171.0**	13.0***
none	none	none	S1	9/14/2005	none	N/A	none	none	10.59	0.20	0.10	7.00	N/A	105.0**	N/A
none	none	none	D1	9/14/2005	none	N/A	none	none	0.01	0.10	0.10	5.90	N/A	3.8	N/A

*Based on average values collected during well purging.
**From CAL.
***Used as the steady-state parameter during sampling.

3.6 Groundwater Age with Chlorofluorocarbons

3.6.1 Background and Limitations

Chlorofluorocarbon (CFCs) dating of groundwater was developed by USGS

scientists because it is practical, cost-effective, and applicable to most shallow, young

groundwater systems (Epler, 1990; Busenberg and Plummer, 1991; 1992). An important

quantity in groundwater protection is the residence time of water in an aquifer; it relates

to both the travel time of a pollutant to arrive at a well and the time span required for self-

purification of a polluted aquifer after removal of pollutant inputs (Zoellmann et al.,

2001). Residence time, or groundwater age, is determined by relating measured

concentrations to known historical atmospheric concentrations coupled with expected

concentrations for water in equilibrium with air (Plummer, 1999). Figure 22 shows

historical CFC concentrations. Groundwater dating with CFC-11, CFC-12, and CFC-113

is possible because (1) the atmospheric mixing ratios of these compounds are known

and/or have been reconstructed over the past 50 years, (2) the Henry's Law solubilities in

water are known, and (3) concentration in air and young water are relatively high and can

be measured (Plummer and Busenberg, 2000).
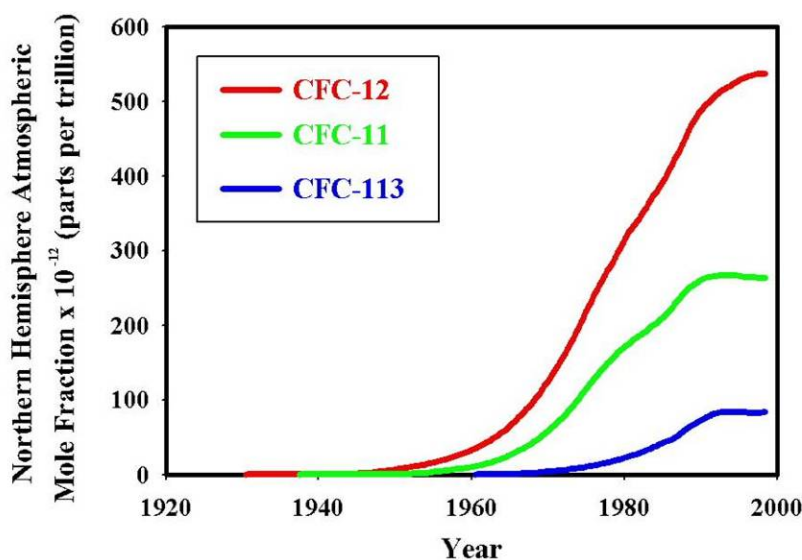
Figure 24: Atmospheric concentration of CFC-11, CFC-12, and CFC-113 vs. time (modified from http://www.rsmas.miami.edu/groups/tritium/).

CFC-11 (trichlorofluoromethane, $CFCl_3$), CFC-12 (dichlorodifluoromethane, CF_2Cl_2), and CFC-113 (trichlorotrifluoroethane, $C_2F_3Cl_3$), or CFCs, are stable, synthetic, halogenated alkanes, developed in the early 1930s as safe alternatives to ammonia and sulphur dioxide in refrigeration (Plummer and Busenberg, 2000). CFCs, better known to most as Freon™, are nonflammable, noncorosive, nonexplosive, noncarcinogenic, very low in toxicity, and have physical properties conductive to a wide range of industrial and refrigerant applications (Plummer, 1999). Primary uses of CFC-11 and CFC-12 include coolants in air-conditioning and refrigeration, blowing agents in foams, insulation, and packing materials, propellants in aerosol cans, and as solvents (Plummer and Busenberg, 2000). CFC-113 has been used primarily by the electronics industry in manufacture of semiconductor chips, in vapor degreasing and cold immersion cleaning of microelectronic components, and as a solvent in surface cleaning procedures (Jackson et al., 1992). Current estimates of atmospheric lifetimes of CFC-11, CFC-12, and CFC-113

are 45 ± 7, 87 ± 17, and 100 ± 32 years, respectively (Volk et al., 1997). CFC-12, CFC-11, and CFC-113 concentrations can be measured analytically making it possible to identify groundwater recharged since approximately 1941, 1947, and 1955, respectively (Plummer and Busenberg, 2000).

The age of groundwater is defined as the amount of time that has elapsed since the water became isolated from the earth's atmosphere (Freeze and Cherry, 1979). If detectable concentrations of CFCs are present in groundwater, at least some modern (since 1941) groundwater has entered the aquifer and thereby makes the aquifer more susceptible to anthropogenic contamination. CFC dating of groundwater is based on the assumption that historical CFC concentrations in the unsaturated zone, or in the air that was last in contact with the water, are known or can be calculated (Plummer and Busenberg, 2000). Although reference is often made to dating of groundwater, the age actually applies to the date of introduction of the chemical substance, and not the water (Plummer and Busenberg, 2000). CFCs pass the unsaturated zone diffusively before they enter the groundwater at dissolved concentrations according to Henry's Law (Weeks 1982 and Cook and Solomon, 1995). Since their release into the atmosphere, concentrations of CFCs are higher in the soil air above the water table than in the water below, thus maintaining a positive downward gradient of tracer (Ekwurzel et al., 1994). For most dating applications, CFC confinement is thought to occur fairly rapidly, sometime between the seasonal high and low water table (Cook and Solomon, 1997). Shallow groundwater remains closed to gas exchange because molecular diffusion coefficients of gases are some five orders of magnitude smaller in water than in air

(Plummer and Busenberg, 2000). Therefore, at the water table a CFC age of zero should be applied and ages should increase along groundwater flow paths.

Because the hydraulic conductivity of earth material is highly variable, considerable uncertainty often exists in calculated flow velocities and transport rates (Cook and Solomon, 1997). Nevertheless, environmental isotope methods, including the use of chlorofluorocarbons (CFCs), are now regarded as routine tools for solving a variety of problems in hydrology (Ekwurzel et al., 1994; Hinkle and Snyder, 1997; Plummer and Busenberg, 2000; Zoellmann et al., 2001; Zuber et al., 2004). Many processes occur during recharge and in the groundwater environment that can affect CFC concentrations beyond those set by air-water equilibrium and consequently affect interpretation of apparent age (Plummer and Busenberg, 2000). Table 10 highlights some of the most important processes and their affect on apparent age calculations. These limitations are important to remember when applying CFC-model ages. Hinkle (2005), in Appendix B of Conlon et al. (2005) gives a complete overview of local limitations along with analysis of the derivation of CFC-model ages for twenty-one wells within the Willamette Basin, ten of which are included in the SWV.

Property	Environment Most Affected	Description of Process	Effect on Apparent Age
Recharge temperature	Shallow water table	Temperature at the water table during recharge. Over-estimated... Under-estimated... ± 2°C, Less than or equal to1970 ± 1 year or less ± 2°C, 1970-1990, ± 1-3 years ± 2°C, >1990, >3 years	 Too young Too old
Excess air	Rapid, focused recharge; fractured rock.	Addition of air trapped and dissolved during recharge. Significant for post-1990 recharge.	Too young
Recharge elevation	Mountain recharge	Water recharged at high altitude dissolves less CFCs because of lower barometric pressure. Over-estimated... Under-estimated... ± 100 m not important ± 1000 m, < 1987, ± few years Significant for post-1990 recharge	 Too young Too old
Thickness of unsaturated zone	Unsaturated zone >10 m	Air in deep unsaturated zone is older than that of the modern troposphere. 0-10 m, error < 2 years 30 m, error 8 - 12 years.	Too old
Urban air	Eastern USA, Western Europe, urban areas	CFC mixing ratios in urban and industrialised areas can exceed regional values.	Too young
CFC contamination	Urban and industrial areas, sewage effluent	CFCs added to water from local anthropogenic sources, in addition to that of air-water equilibrium.	Too young (impossibly young)
Microbial degradation	Anaerobic environments, sulphate-reducing, methanogenic Fluvial and glacial drift sediment	No degradation in aerobic environments................... Sulphate-reducing, and fermentation: CFC-11, CFC-113 degraded, CFC-12 quasi-stable......................... Methanogenic: CFC-11≥CFC-113>>CFC-12	No effect CFC-11, CFC-113 Too old Too old
Sorption	Organic-rich sediment, peat	Sorption of CFCs onto particulate organic carbon and mineral surfaces. CFC-113>>CFC-11≥CFC-12	Too old
Mixed waters	Production wells, fractured rock	Mixing of young and older water in water pumped from open intervals in wells Apparent age of young fraction in mixture................ Apparent age of old fraction in mixture....................	 Too old Too young
Hydrodynamic dispersion	All groundwater environments	Generally small effect for CFCs. 1975 – 1993... <1975..	 Too old Too young

Table 10: Summary of processes that can modify apparent age (modified from Plummer and Busenberg, 2000).

The simplest and most common transport assumption in CFC-based dating is to assume piston flow (Plummer and Busenberg, 2000). The rate at which a parcel of water becomes isolated from the unsaturated zone air is, in part, a function of recharge rate, porosity of the unsaturated zone soil, aqueous and gaseous diffusion coefficients, and magnitude of water table fluctuations (Plummer and Busenberg, 2000). The addition of contaminant concentrations of CFCs to groundwater can usually be attributed to anthropogenic point sources such as discharge from septic tanks, leaking sewer lines, leakage from underground storage tanks, discharge or injection of industrial wastes, and recharge from rivers carrying effluent from sewage treatment plants (Plummer and Busenberg, 2000). As a general rule, if dissolved oxygen is less than about 0.5 mg/L, it is likely that CFC-11 has been at least partially degraded. However, reliable ages can often be obtained from CFC-12 and CFC-113 is such environments (Plummer and Busenberg, 2000).

3.6.2 Sampling of Chlorofluorocarbons

Field work was conducted in the SWV to locate wells that had optimum characteristics to collect a groundwater sample for analysis of CFCs. Requirements used during well selection in the field were (must have) (1) permission from the landowner, (2) submersible pump (suction-lift pumps can cause volatilization due to drop in pressure in the sample line caused by a vacuum and jet pumps use circulation of water to pump water, causing an increased chance of mixing and contamination), (3) approximate desired spatial location, (4) a well log that can be linked to the field located well, (5) a perforated interval of ≤ 5 ft to reduce the chances of well bore mixing, (6) a perforated interval at the desired depth, (7) a sampling point as close to the wellhead as possible for

attachment of a hose bib and copper piping upgradient any water treatment, pressure tanks, or holding tanks, (these systems can change the chemistry of a water sample), and 8) a sampling point upgradient polyvinyl chloride (PVC) that may contain glue in joints that could contaminate the sample (Laphan et al., 1995).

Exceptions to the requirements listed above had to be made while selecting wells for CFC sampling. This was because a limited number of wells exist in the SWV that fit all well criteria listed above. Many wells were located in a desired spatial location that contained preferred depth and perforated intervals, but contained a sampling point with a high probability of contaminating the sample. It seemed illogical to sample from a well where a good possibility of known contamination existed, even if all other optimum well criteria were met. Wells selected as CFC sampling sites contained sampling points that minimized contamination, contained a minimum amount of perforations, and were located in a desired spatial location. Wells with deeper perforated intervals along a transect between the Willamette River and Cascade Range were desired but did not exist. A selection of wells in the Coburg area were located with varying depths that fit the CFC sampling criteria.

Ten wells (total number restricted by budget) were selected for CFCs sampling. Five samples were collected between the Willamette River and the Cascade Range along a groundwater flow path to determine if CFC-model ages increase along a flow path. Four samples were collected in the Coburg area from wells nearby each other that contained well perforations at different depths in order to determine if CFC-model age increases with depth. One additional sample was collected SE of Junction City because

of its high quality sample collection characteristics and prior permission by the

landowner.

Sampling of water for CFC analysis was conducted after following the well-

volume method and standard operating procedures for collection of representative

groundwater samples (Yeskis and Zavala, 2002), also described in Section 3.5.

Collection of groundwater for analysis of CFCs was done according to protocol

developed by the USGS Reston Chlorofluorocarbon Laboratory using 125 mL glass

bottles with foil-lined caps (see Appendix A). A hose-bib and refrigeration grade copper

tubing were linked together and used as a sampling apparatus. All equipment was

washed with Liquinox and thoroughly rinsed with de-ionized water prior to each

sampling event. Before attaching the sampling apparatus to the sampling point at each

well location, Teflon tape was wrapped repeatedly around the threads to provide and air-

tight, low potential contamination source seal. A 2-liter glass beaker was used to carry

out the filling procedure. Three 125 mL samples were collected at each sampling

location. All thirty groundwater samples were packaged and sent to The Tritium

Laboratory (TTL), University of Miami/RSMAS for analysis of CFC-11, CFC-12, and

CFC-113. At each sampling location, CFC-11, CFC-12, and CFC-113 concentrations

were determined for each sample.

3.6.3 Calculation of CFC-model Age

To calculate the CFC-model age of groundwater, both the temperature of the

water table during recharge and the elevation of the water table during recharge are

required. Both of these parameters are approximated at the same vertical location below

land surface where the CFCs enter the groundwater and are isolated from the atmosphere.

The average recharge elevation is required only if the recharge elevation is > 656 ft (200 m). Since this elevation is much greater than all of the SWV, this parameter is not required. A recharge temperature at the water table of 8°C was determined by calculating the mean monthly temperatures from November 2003 through May 2004 (Oregon Climate Service, 2005). Hinkle and Snyder (1997) used dissolved-nitrogen and argon gases to calculate recharge temperatures at the water table near Portland, OR. They found mean and median recharge temperatures of 8°C, supporting estimates calculated for this study. This recharge temperature was supplied to TTL and CFC-model ages were calculated by staff. CFC-model calculations from TTL and specifics on how these CFC-model ages were calculated are located in Appendix F.

The ten wells sampled in the SWV were analyzed to determine concentrations of three CFCs: CFC-11, CFC-12, and CFC-113. Each sampling location along with final average CFC-model ages are shown in Figure 25. Cross-sections with CFC-model ages were also constructed for the Coburg (see Figure 26) and Harrisburg (see Figure 27) locations.

The CFC-model ages were determined using the CFC-11, CFC-12, and CFC-113 ages determined by TTL and considering subsurface processes that can affect these CFC-model ages. A CFC-model determined groundwater age represents a composite age because of the hydrodynamic dispersion in an aquifer and the mixing of different flow components in a well (Hinkle and Snyder, 1997). Degradation may occur in reducing environments by microbial processes (Hinkle, 2005), therefore dissolved oxygen measurements were collected and results reported in Table 11. According to Plummer and Busenberg (2000), when dissolved oxygen is less than about 0.5 mg/L, it is likely

that CFC-11 has been at least partially degraded, but reliable ages can often be obtained

from CFC-12 and CFC-113. CFC-11 also degrades faster than CFC-12 and degradation

of CFC-12 does not happen until methanogenic conditions are well established (Plummer

and Busenberg, 2000).

Three wells (CFC1, CFC3, and CFC8) contained water <1 mg/L dissolved

oxygen; other wells may contain water with <1 mg/L dissolved oxygen but as a lesser

total percentage than water with ≥1 mg/L dissolved oxygen. In this study, CFC-11 ages

are generally greater than CFC-12 ages (see Appendix F), suggesting some degradation

of CFC-11. CFC-113 is difficult to interpret because it also can exhibit biodegradation in

reducing environments. CFC-113 also sorbs to a greater degree than CFC-11 or CFC-12.

CFC-113 is also in liquid form at common environmental temperature (CFC-11 and

CFC-12 are gases), making CFC-113 able to contaminate groundwater more easily

(Plummer and Busenberg, 2000 and Hinkle, 2005). Little if any degradation of CFC-113

is shown (see Appendix F). In conclusion, CFC-12 is likely to give the most

representative CFC-model age of the three CFCs.

Five wells contained supersaturated CFC-12 concentrations, or concentrations

that are above present day atmospheric concentrations. Four wells contained

concentrations of CFC-113 below the detection limit (0.010 pmol/kg). CFC-11

concentrations for all wells were within the detection limits. When determining a single

CFC-model age for each well location using CFC-11, CFC-12, and CFC-113, the

maximum CFC-12 age was used where applicable to minimize the effect of possible

contamination during the sample collection process. If the CFC-12 age was

supersaturated, a combination of CFC-11 and CFC-113 ages were used to designate a

final CFC-model age. Where relatively large age differences existed between the CFC-11 and CFC-113 ages, a range of ages were assigned as the final CFC-model age for the specified well. Even though degradation of CFCs can occur and imply a groundwater age that is too old, CFC-model ages should be treated as minimum ages because CFC contamination is more likely to occur (Hinkle and Snyder, 1997).

Results indicate CFC-model age does not necessarily increase with well depth (see Figure 26) or along shallow groundwater flow paths (see Figure 27). This is suggestive of vertical and horizontal groundwater mixing; old and young groundwater mixing within the unconsolidated basin-fill sands and gravels. Varying CFC-11, CFC-12, and CFC-113 model ages in successive samples collected from the same well also suggest possible groundwater mixing. Groundwater ages slightly increase along an approximate groundwater flow path in the northern SWV (Hinkle, 2005). A greater amount of samples collected in Hinkle (2005) may assist in illustrating this point. CFC-model ages are greater from wells sampled where Willamette Silt is present (19 to >50 years) than samples collected from wells where no Willamette Silt is present (13 to 20 years) in this study (see Table). Final CFC-model ages from Hinkle (2005) are similar to final CFC-model ages of samples collected from wells that penetrate Willamette Silt.

Well owner	Sample #	Hydro-geologic unit	Well penetrating Willamette Silt?	Average well depth (ft)	Distance along flow path (miles)	DO (mg/L)	NO$_3$ (mg/L)	CFC-model age (years)	CFC-model "average" age (years)
Malpass	1, CFC1	MSU	Y	25.5	3.23	0.20	0.40	36-45	40.5
Malpass	2, CFC1								
Malpass	3, CFC1								
Knox	4, CFC2	MSU	Y	36	6.28	1.92	2.16	38	38
Knox	5, CFC2								
Knox	6, CFC2								
Dornhecker	7, CFC3	MSU	Y	39	2.70	0.43	1.14	35	35
Dornhecker	8, CFC3								
Dornhecker	9, CFC3								
Hargett	10, CFC4	MSU	Y	34	9.61	3.75	10.68	19-31	25
Hargett	11, CFC4								
Makos	12, CFC5	MSU	N	27.5	N/A	4.37	4.80	20	20
Makos	13, CFC5								
Makos	14, CFC5								
Gray	15, CFC6	MSU	N	78	N/A	6.33	11.60	17	17
Gray	16, CFC6								
Gray	17, CFC6								
Emerson	18, CFC7	MSU	N	60	N/A	6.66	10.60	18	18
Emerson	19, CFC7								
Emerson	20, CFC7								
Hanson	21, CFC8	MSU	Y	35	2.44	0.40	0.20	34	34
Hanson	22, CFC8								
McKluskie	23, CFC9	USU; MSU	N	29.5	N/A	6.71	9.33	18	18
McKluskie	24, CFC9								
McKluskie	25, CFC9								
Funke	26, CFC10	MSU	N	87	N/A	8.08	10.78	13-18	15.5
Funke	27, CFC10								
Funke	28, CFC10								

Table 11: Selected groundwater age and groundwater chemistry information. Well locations found in Table 9.
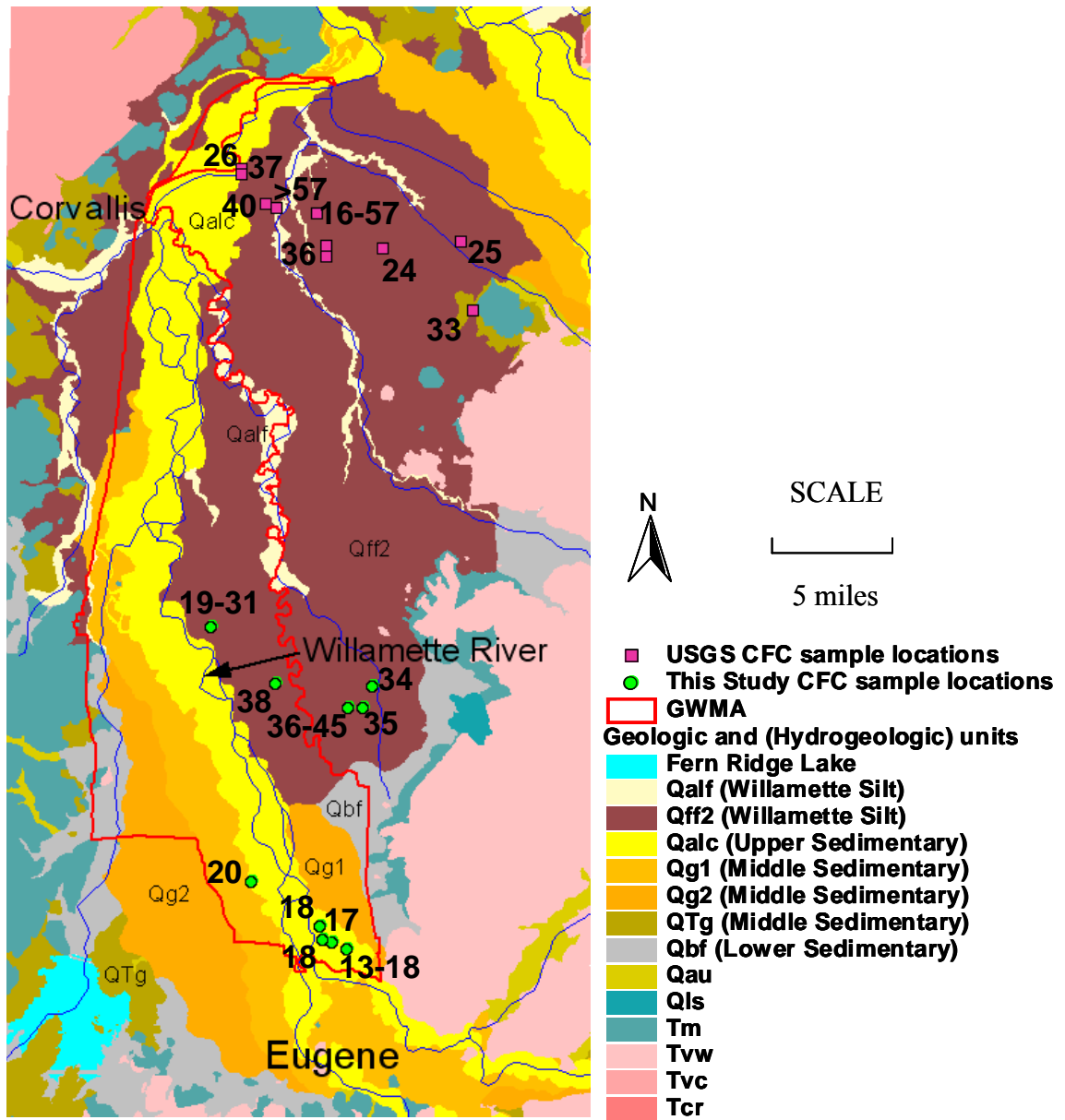
Figure 25: CFC sampling locations and associated groundwater ages (years) from Hinkle in Conlon et al. (2005) and this study.
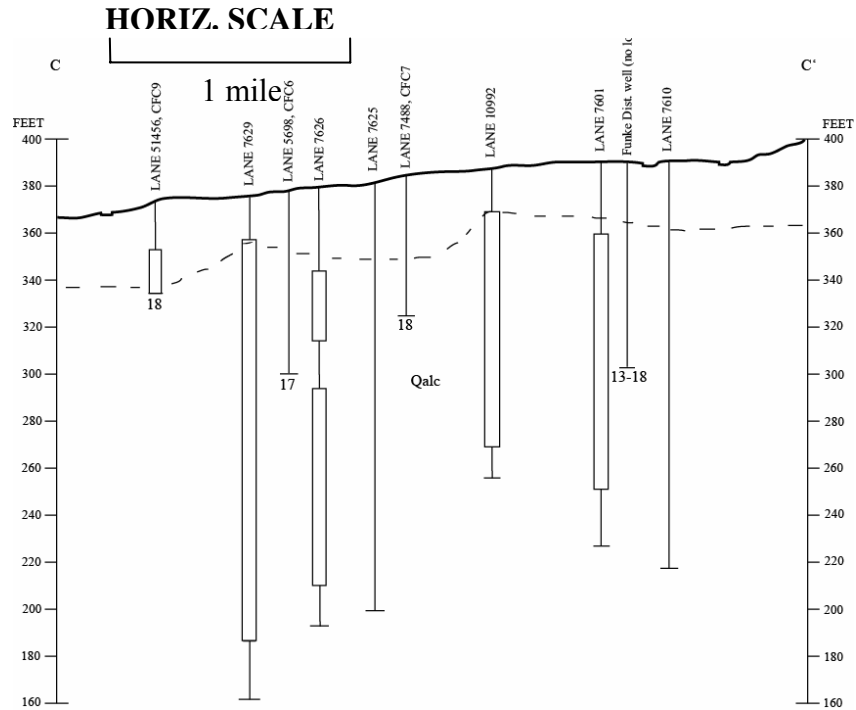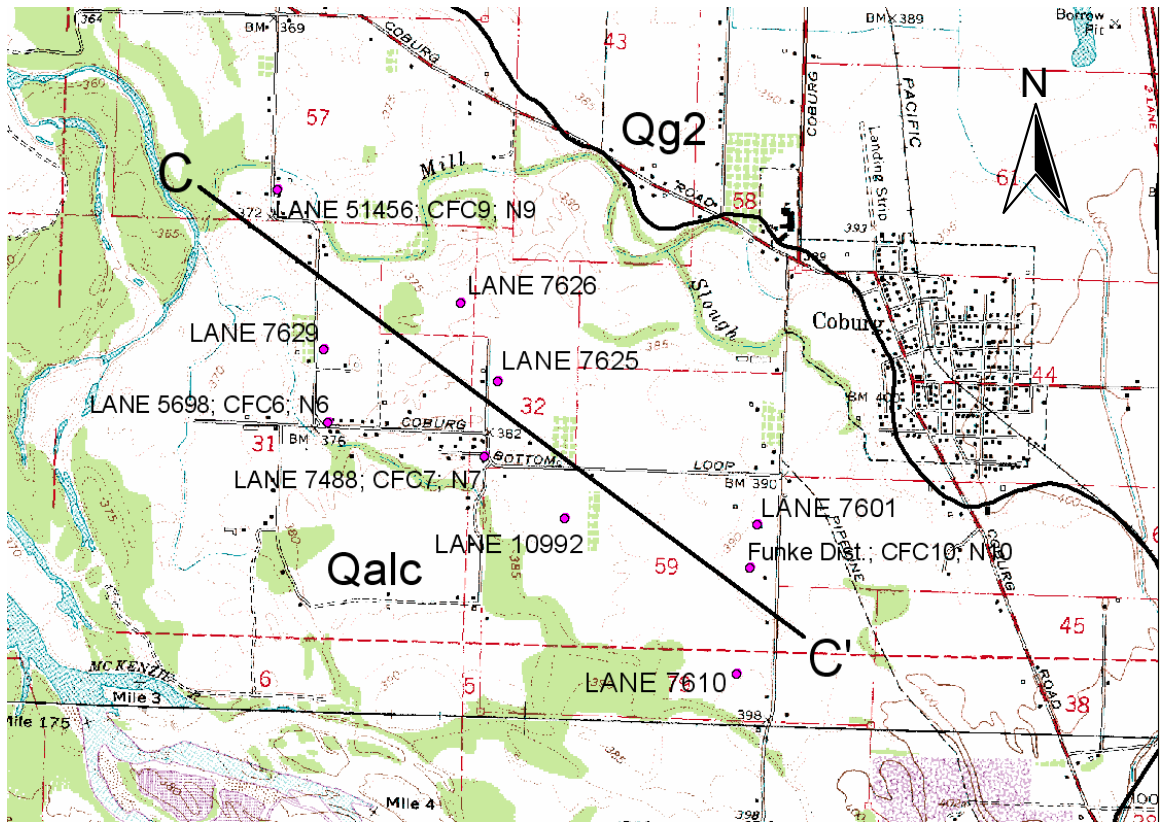
Figure 26: CFC sampling locations and cross-section in Coburg, OR area (x50 vertical exaggeration). Dotted line represents bottom of overbank facies. Large-scale map view location found in Figure 7.
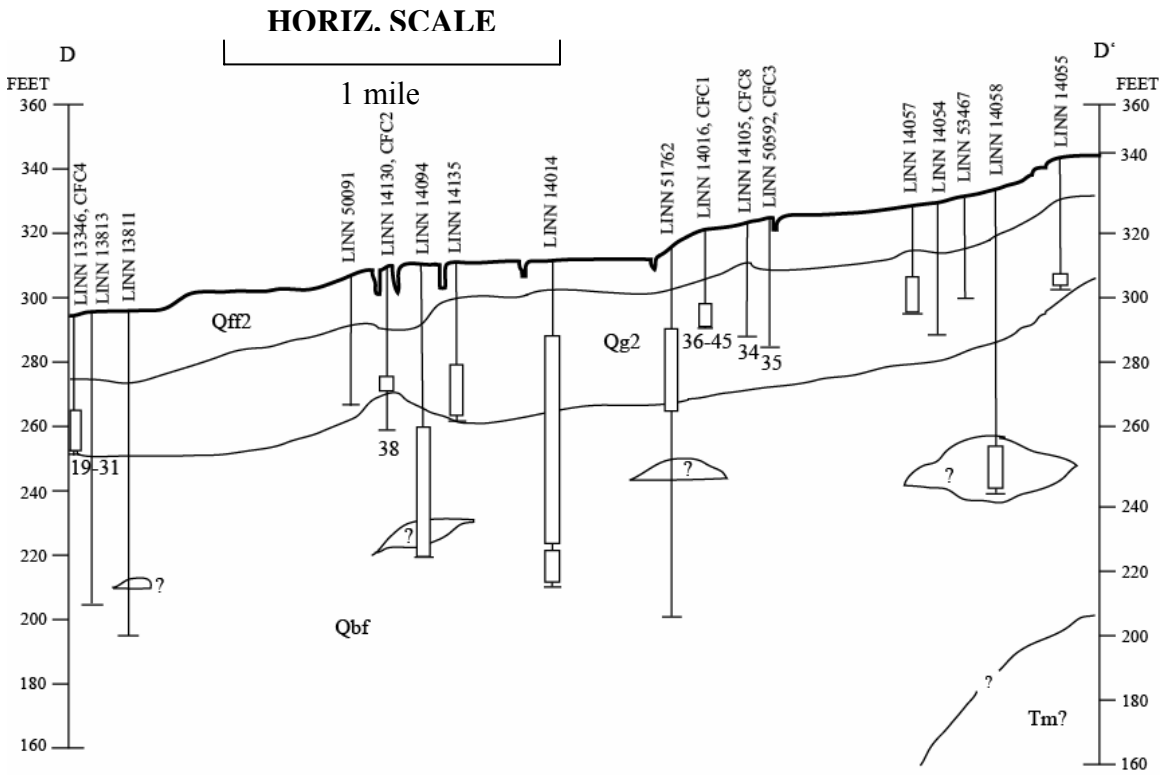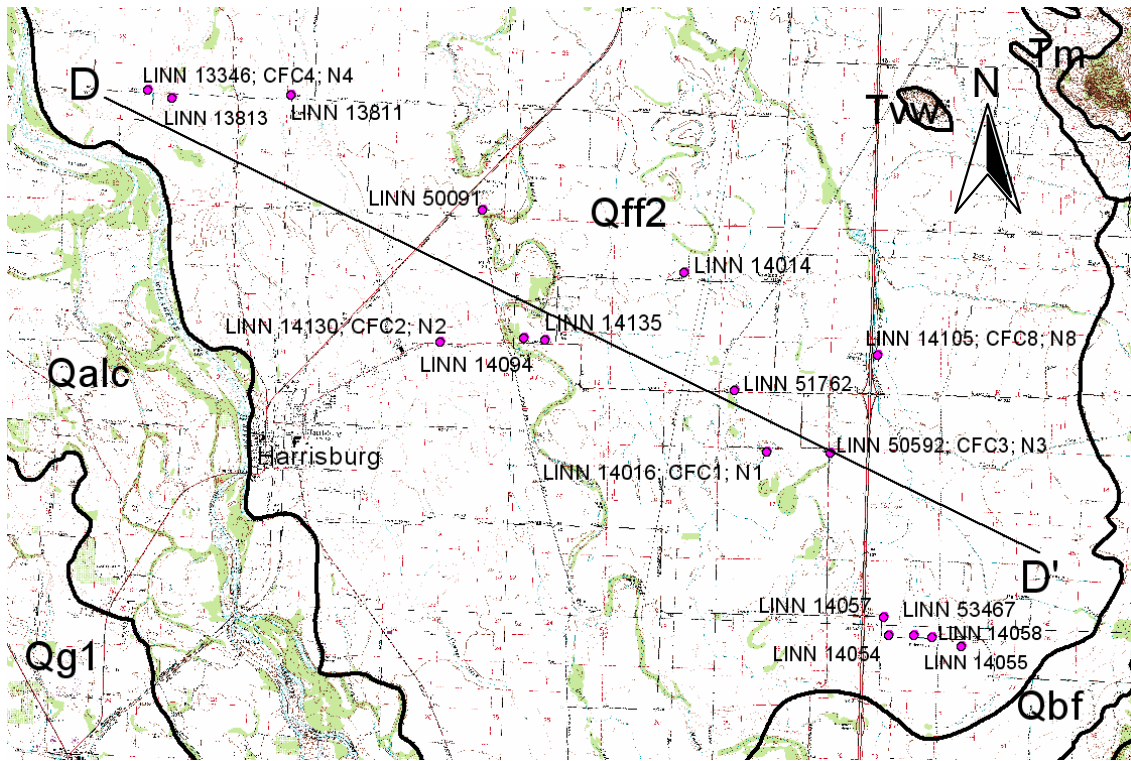
Figure 27: CFC sampling locations and cross-section in Harrisburg, OR area (x50 vertical exaggeration). Large-scale map view location found in Figure 7.

3.7 Modeling

Properly applied models are useful tools to assist in problem evaluation, design remedial strategy, conceptualize and study flow processes, provide additional information for decision making, and recognize limitations of data and guide collection of new data (Schwartz et al, 1990). Details of the model, along with a description of the work that was completed is provided below.

3.7.1 Purpose and Objective

A numerical groundwater flow model was developed to be used as a tool to aid in the estimation of groundwater travel times and directions in the GWMA and throughout the SWV. Indirectly, this model can also be used as a tool to solve water management problems likely to occur in the future and to gain a better understanding of the hydrologic flow system in the SWV. For purposes of this project, the model was constructed specifically to examine local water quality, not quantity issues. The model is intended to be used by local policy makers and scientists to help make management decisions. Water quality educators also seek a model that can be used as an outreach tool to help describe groundwater flow in a non-technical way to local stakeholders. This is important because the local stakeholders directly impact the amount of nitrate penetrating the water table. The GWMA Committee is currently developing an Action Plan that will contain recommendations to the Oregon DEQ to be used to educate and persuade local stakeholders to change their current behaviors and improve groundwater quality. Questions such as: (1) "What is the general direction and travel times of groundwater in the SWV?" (2) "Where is most of the nitrate coming from?" and (3) "How long will it take before we see a reduction of groundwater nitrate if we change our current BMPs and

install improved septic systems?" These questions are difficult to answer but frequently discussed by the GWMA Committee and others. A groundwater model has the ability to help answer some of these questions.

3.7.2 Model Description

3.7.2.1 Governing Equations and Model Code

The complexity of the hydrogeology and hydrologic system along with known three-dimensional components of groundwater flow within the SWV require a numerical three-dimensional groundwater flow model. MODFLOW along with MODPATH implemented within the graphical user interface GMS version 5.0 (Groundwater Modeling Software) (Brigham Young University, 2003) was used to model three-dimensional groundwater flow within the SWV. MODFLOW (Harbaugh et al., 2000), the most common numerical modeling tool in the hydrogeologic community (McDonald and Harbaugh, 2003; Clemo, 2005), was developed by the U.S. Geological Survey and contains a collection of groundwater simulation tools. MODPATH is a particle tracking program that works with MODFLOW to calculate groundwater velocities, flow path lines, and travel times.

A steady-state model was developed to study characteristics of the groundwater flow system in the SWV. A cell-centered model was developed to solve the finite difference form of the three-dimensional, steady-state groundwater flow equation for both unconfined and confined aquifers. Three of the four model layers contain homogeneous and anisotropic hydraulic conductivity values. One layer contains both heterogeneous and anisotropic hydraulic conductivity values. The groundwater flow equation describing this model is as follows (modified from Fetter, 2001):

$$\frac{\partial}{\partial x}\left(K_x \partial h / \partial x\right) + \frac{\partial}{\partial y}\left(K_y \partial h / \partial y\right) + \frac{\partial}{\partial z}\left(K_z \partial h / \partial z\right) = -R(x, y, z)$$

where h (L) is head; K (L/T) is hydraulic conductivity; $x, y,$ and z (L) are direction

in space; and R (L/T) is recharge. The Darcy equation was used to calculate flow

velocities.

3.7.2.2 Model Description

Much work was conducted by the U.S. Geological Survey in previous studies to

determine the extent and thicknesses of hydrologic and geologic units of the Willamette

Basin. It was determined early in this project that it would be redundant to use well logs

and other information to construct a "new" hydrogeologic framework already completed

with a high degree of quality by the U.S. Geological Survey. So, the three-dimensional

geometry of the basin-fill deposits of the SWV was constructed using a combination of

published and unpublished data from the U.S. Geological Survey as well as work done

during this study. The basement rock within the area was not modeled and is considered

impermeable in this study.

Published and unpublished data were used to develop the hydrogeologic

framework of the SWV. Published grid-type geologic thickness data were developed in

O'Connor et al. (2001) of the Quaternary age Qalc and Qg$_1$ units. Unpublished non-grid

type (isopach) hydrogeologic thickness data were developed in Gannett and Caldwell

(1998) and Woodward et al. (1998) for the Willamette confining unit, the Willamette

aquifer unit, and the Willamette Silt unit (the LSHU, the MSHU and USHU, and the

WSHU described in this study, respectively). Grid-type thickness data were obtained

from the U.S. Geological Survey used to derive the isopach maps mentioned above in an

unpublished form. This grid thickness data, along with a 10m digital elevation model

(DEM) (Oregon Statewide DEM Downloads, 2003) of the SWV, was used within the

geographical information systems (GIS) ArcView 3.3 to develop continuous contact

surfaces between the WSHU, USHU, MSHU, and LSHU as designated for this study.

All grid-type data was altered so that the grid size of each data set was 500 ft x 500 ft and

each grid vertices (intersection) lined up spatially. Each grid vertex along the

hydrogeologic contacts were made a point and exported into GMS where linear

interpolation was used to develop hydrostratigraphic units with varying thicknesses.

Natural pinch-outs exist at the contacts between basin-fill material and basement rock and

along map-view hydrogeologic unit contacts. Hydrostratigraphic errors were located and

corrected using the model checker in GMS. The model was then thoroughly checked and

errors found were corrected manually. Care was taken to ensure that the resulting

hydrostratigraphy best represented the known stratigraphic relationships of the SWV. .

3.7.2.3 Boundary Conditions and Fluxes

A variety of GIS data was collected for this study, some of which was used to

assign boundary conditions and designate the model domain. Digital 7.5-minute

quadrangle maps, aerial photographs, geologic units, and layers showing location of

streams and rivers, all in GIS form, were used to accurately assign natural boundary

conditions that exist in the SWV. Natural boundary conditions were used whenever

possible. Originally, modeling was considered over just the spatial extent of the GWMA

but difficulty in assigning accurate boundary conditions eventually lead to the modeling

of the entire SWV from the foothills of the basement rock in west to the foothills of the

basement rock to the east, with a combination of rivers, basement rock, Fern Ridge Lake,

and basin-fill sediments to the north and south. The contact between basin-fill deposits and basement rock was assigned a no flow boundary condition due to its very low permeability. Rivers, streams, and lakes were added as boundary conditions using spatial GIS data imported into GMS. Figure 28 shows all boundary conditions.
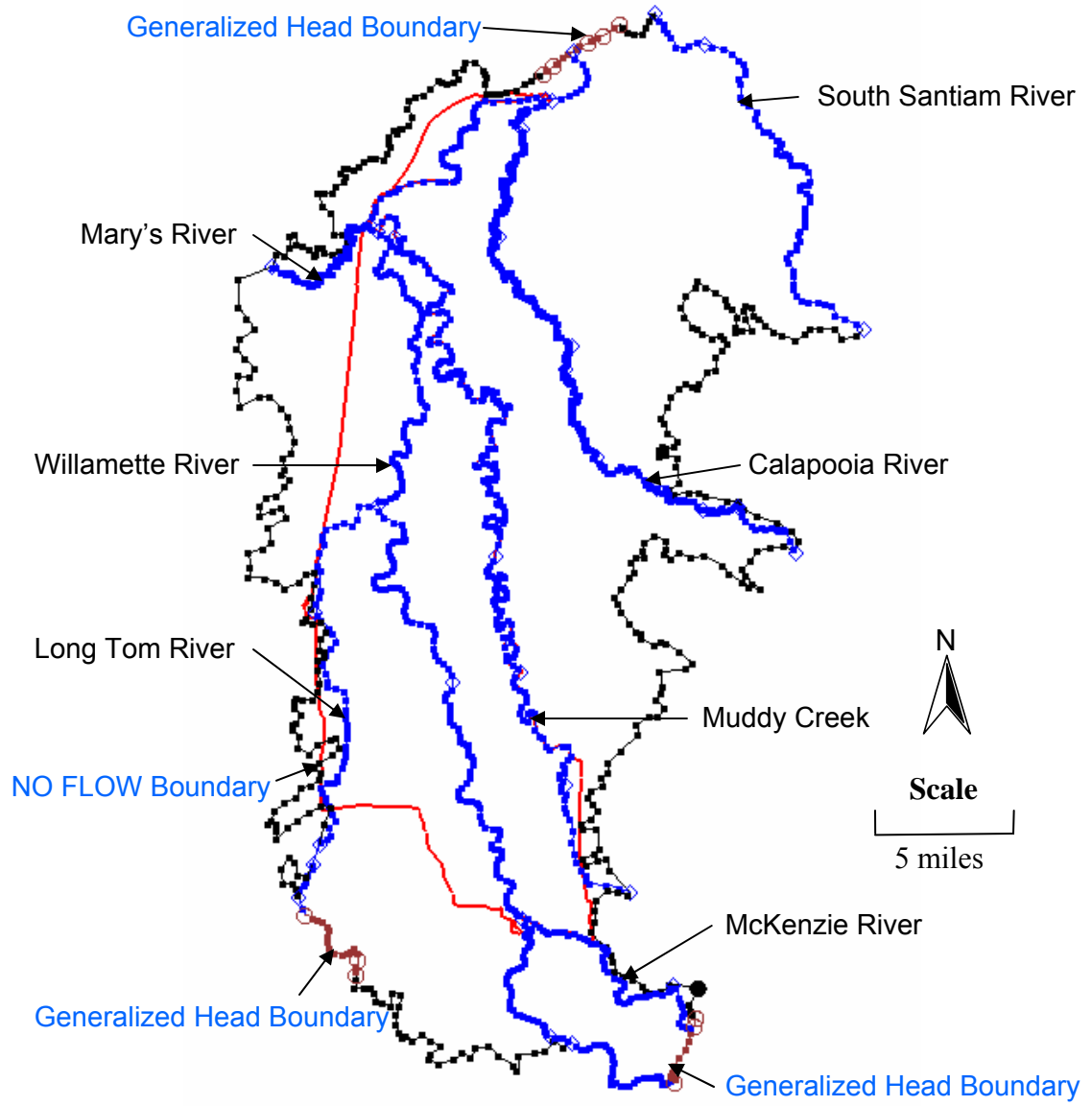
Figure 28: Model boundaries and local water bodies.

3.7.2.3.1 Rivers and Lakes

The river package within GMS-MODFLOW was used to simulate river stage, river depth, and seepage rate within the SWV model. An average constant river depth of 5 ft (1.5 m) was maintained throughout the entire model. For this steady-state model, fluxes and river stages were calculated from average daily data collected from 07/01/2004 through 07/31/2005, herein referred to as the average yearly amount. River stage data was collected from the U.S. Geological Survey and the U.S. Army Corp of Engineers (U.S. Geological Survey, 2005; U.S. Army Corps of Engineers, 2005) at every gage location within the model domain and input into the model as the river surface elevation. River elevation values were linearly interpolated between gage locations. River flow data was also collected at each gage location in the model domain and used to estimate seepage rates along stream reaches between gage locations. Seepage rates were initially estimated using the equation (modified from McDonald and Harbaugh, 1988):

$$C = \frac{K \times W}{M}$$

where C (L^2/T/L) is streambed conductance, K (L/T) is hydraulic conductivity, W (L) is width of the river, and M (L) is riverbed thickness. Estimates of the hydraulic conductivity of the riverbed sediments based on the hydraulic conductivity of each hydrogeologic unit that underlies each particular river or stream. The length of each reach is calculated in the river package. The width of each river or stream was estimated using 7.5-minute topographic maps. Riverbed thickness was estimated, varying slightly between water bodies. This gave initial estimates for seepage and the conductance was adjusted accordingly during the calibration process. Fern Ridge Lake water level data

were obtained from the U.S. Army Corps of Engineers (2005). The northeastern

shoreline was assigned as a generalized head boundary. Parameters for the generalized

head boundary include a water level elevation and seepage rate. The seepage rate was

estimated and average water level elevation found and assigned to the generalized head

boundary. Table 12 shows final seepage estimates for a given river or stream reach.

Table 12: Modeled water bodies and their final bed conductance values.

River/Stream	Final Conductance $(ft^2/d)/(ft)$; $(m^2/s/m)$
Willamette River	3000; 1.058×10^{-2}
Middle Fork Willamette River	3000; 1.058×10^{-2}
Long Tom River	1000; 3.538×10^{-3}
McKenzie River	3000; 1.058×10^{-2}
South Santiam River	4000; 1.411×10^{-2}
Marys River	50; 1.8×10^{-4}
Calapooia River	100; 3.53×10^{-4}
Muddy Creek (Lane County)	100; 3.53×10^{-4}

3.7.2.3.2 Evapotranspiration

The evapotranspiration (ET) package was used to simulate ET using an areal

coverage over the entire model domain. Parameters required for the package are

maximum ET rate, ET surface (the elevation where if the water table is at or above this

elevation, the maximum ET rate occurs), and extinction depth (the depth of the water

table below the ET surface elevation where ET ceases to exist) (McDonald and

Harbaugh, 1988). The average yearly maximum evapotranspiration rate was 45 in/year

(114 cm/year) at the Corvallis AgriMet site (Oregon Climate Service, 2005). The

extinction depth was assumed to be about the maximum rooting depth of most crops in

the area, which is about 5 ft (Woodward et al., 1998). The ET surface was designated as the surface elevation of the model using a 10 m DEM.

3.7.2.3.3 Recharge

An average yearly precipitation rate for Corvallis and Eugene is 28 in/year (71 cm/year) (Oregon Climate Service, 2005). According to Conlon et al. (2005), current recharge estimates developed using PRMS models of the Willamette Basin (Leavesley et al., 1983) were calculated that suggests about 27 percent of precipitation recharges the lowland areas. Therefore, a recharge rate of 7.6 in/year (19 cm/year) was assigned in an areal coverage over the entire model domain. It is noted that from 07/01/2004 to 07/31/2005 was exceptionally dry and that the average precipitation rate in the SWV is usually from 40 in/year to 45 in/year (102 cm/year to 114 cm/year) (Oregon Climate Service, 2005). The average annual recharge for the Willamette Basin lowland is 16 in/year (41 cm/year) (Conlon et al., 2005).

3.7.2.3.4 Water Usage

Total water usage (public supply, irrigation, industrial, and domestic) for the Willamette Basin was estimated in Conlon et al. (2005). Irrigation water usage was estimated using (1) land cover by crop type using 1992 LANDSAT satellite images, (2) lands irrigated with groundwater determined using water rights, (3) irrigation water needs estimated by multiplying these acreages by crop water requirements minus precipitation that fell during the irrigation season, (4) where groundwater and surface water usage coexist, groundwater withdrawals are estimated to account for 50 percent of annual irrigation water needs, and (5) withdrawals from wells were calculated by dividing irrigation water needs by the irrigation efficiency which was assumed to be 0.75 (King et

al., 1978 and Conlon et al., 2005). Further study was conducted in the central Willamette

Basin using water rights and LANDSAT to a more detailed study using water rights,

LANDSAT, and ground truth data and it was determined that methods (1) through (5)

overestimated water use, therefore irrigation water use values in the Willamette Basin

were multiplied by 0.6 (pers. communication, Terrence Conlon, U.S. Geological Survey,

July 26, 2005). Public supply groundwater withdrawals were based on monthly-use

reports, industrial withdrawals were estimated using water right data and other

supplemental information, and domestic use was not estimated because total groundwater

use for the category is small and overall is a small fraction of the hydrologic budget

(Conlon et al., 2005). Further explanation is found in the Well Discharge section of

Conlon et al. (2005).

Only the corrected total irrigation water use information was incorporated into the

model. The 7000 ft grid-type total irrigation water use data was converted to the exact

grid cell dimensions of the MODFLOW model using ArcView GIS. Then, this data was

converted into a data format that GMS recognized as pumping well information and was

assigned to pump water only from the MSHU (due to model and time constraints),

assuming all water is drawn from the MSHU. Water was pumped from each cell that

contained water usage information (see Figure 29). This hydrogeologic unit was selected

due to its great extent and thickness, along with composing the majority of the upper and

middle sedimentary unit where about 73 percent of all pumpage in the Willamette Basin

occurs (Conlon, 2005). Rates were assigned based on the information contained within

each grid cell. This method was conducted to remove water at varying rates uniformly

throughout the model.
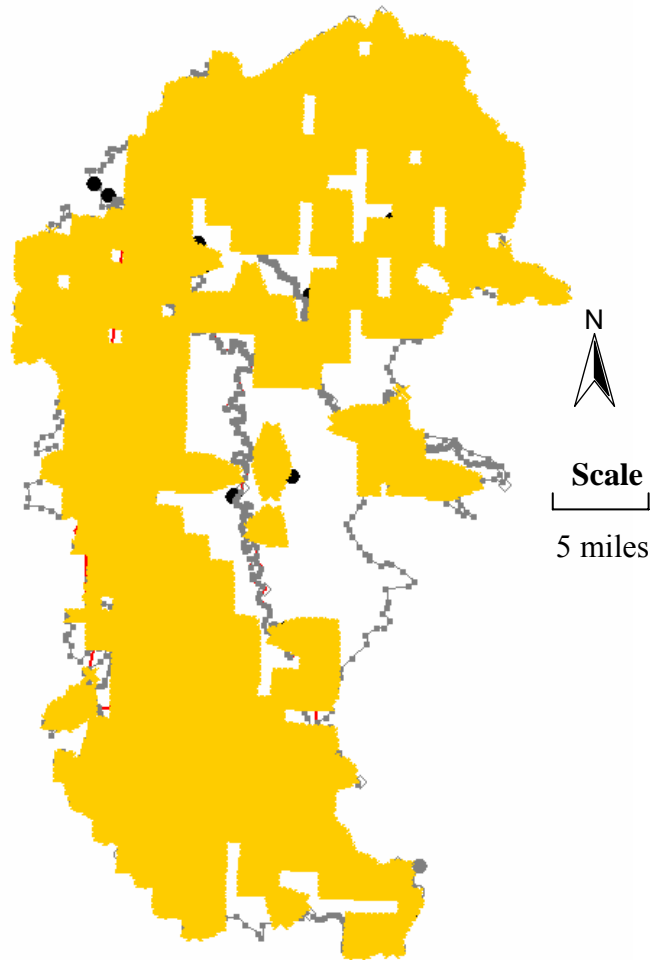
Figure 29: Spatial distribution of groundwater pumping wells within the Middle Sedimentary hydrogeologic unit.

3.7.2.3.5 Generalized Head Boundaries

Generalized head boundaries were assigned in the northern part of the model near Albany and in the southern part of the model near Springfield. Both locations were chosen based on geography and assigned along a single average water table contour derived from a water table map developed by Woodward et al. (1998). A head value was assigned along each generalized head boundary based on the value assigned for each

contour. A conductance value was also estimated and assigned, and was adjusted during

model calibration.

Table 13: Generalized head boundaries and final conductance values.

Generalized Head Boundary	Final Conductance $(ft^2/d)/(ft)$; $(m^2/s)/(m)$
Northern	50; 1.8×10^{-4}
Fern Ridge Lake	50; 1.8×10^{-4}
Southern	50; 1.8×10^{-4}

3.7.3 Discretization and Other Information

Four layers, each layer consisting of a different hydrogeologic unit, were

developed for the model (see Figure 30). The model was discretized into five-hundred by

five-hundred foot squares in the x- and y-direction within each model layer. These

dimensions were determined through trial and error to be the finest grid that could be

assigned to a model of this size within the capability of the computer being used. Layer

thickness was assigned based on the thicknesses of each hydrogeologic unit, as described

in the Section 3.7.2.2. Again, only basin-fill deposits were modeled.

Groundwater flow between units, or interblock transmissivity, was calculated

using the harmonic mean of transmissivity. The Layer Property Flow Package option

was used along with the preconditioned conjugate-gradient 2 (PCG2) solver. The PCG2

solver was chosen as the best solver option and was used based on its documented

accuracy and insensitivity to the values of relaxation parameter and convergence criterion

(Osiensky and Williams, 1997) as well as its ability to account for the water budget using

head-change and residual criteria (Hill, 2003). A value of 0.97 was used for the modified

incomplete Cholesky relation parameter.
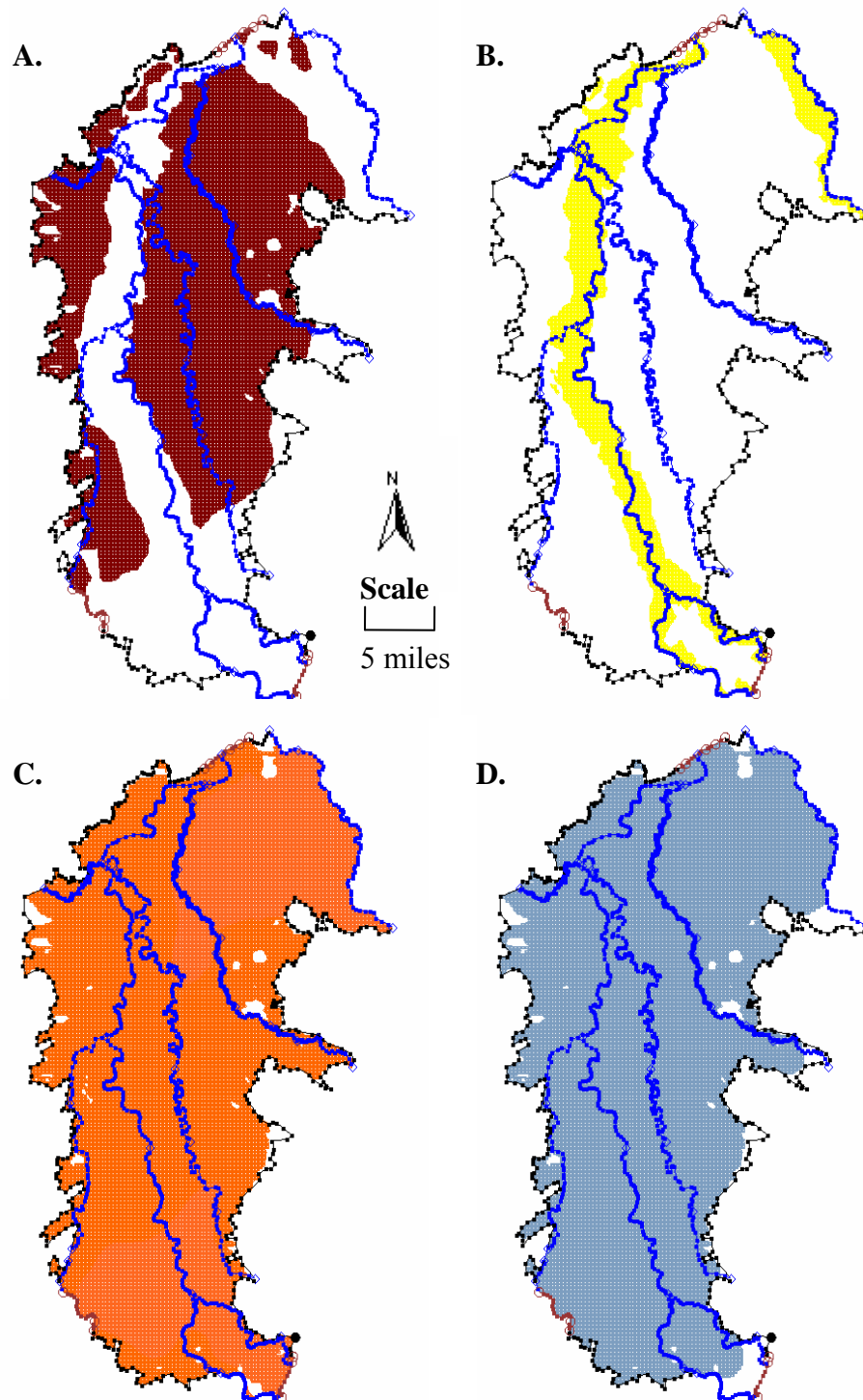
Figure 30: Discretization of each hydrogeologic unit. From top-left and rotating clockwise is the (A.) Willamette Silt; (B.) Upper Sedimentary; (C.) Middle Sedimentary; and (D.) Lower Sedimentary hydrogeologic units.

3.7.4 Aquifer System Properties

It is well known that values of aquifer properties (i.e., transmissivity, hydraulic conductivity, and storativity values) in most cases vary by orders of magnitude, making these values some of the most difficult to quantify. When transmissivity and hydraulic conductivity values are decided upon, they generally contain the greatest associated error in comparison to other assigned model parameters. Therefore much effort was spent conducting pump and slug tests during this study and contacting state and governmental agencies, local consulting firms, and public utility companies to determine if any aquifer tests had been conducted in the SWV. This data along with specific capacity information found on most well logs was used to estimate transmissivity and ultimately hydraulic conductivity of the model domain. The model that was developed was steady-state, meaning all fluxes and water levels are in equilibrium. Thus, storativity values were not required as model input.

This section discusses the initial hydraulic conductivity values assigned to each hydrogeologic unit and how they were assigned. Table 14 summarizes initial K_x and anisotropy ratios (K_x/K_v) values and the sources that these values were derived from.

3.7.4.1 Willamette Silt Hydrogeologic Unit

Few hydrogeologic data exist for the WSHU mostly due to its inability to transmit water, relative thinness compared to other hydrogeologic units, and that it overlies the more sought-after permeable sand and gravel resulting in few wells with screened intervals exposed to this unit. Homogeneous and anisotropic conditions were assigned to the entire WSHU. The initial K_x-value assigned was 1.0 ft/d (3.5 x 10^{-6} m/s) and the initial K_x/K_v assigned was 75. Two aquifer types can be assigned in GMS-MODFLOW.

A "convertible" aquifer can be either unconfined or confined depending on the height of the potentiometric surface. A "confined" aquifer is always saturated. This layer was assigned as "convertible."

3.7.4.2 Upper Sedimentary Hydrogeologic Unit

Surprisingly, few wells containing specific capacity or aquifer test data for the Upper Sedimentary hydrogeologic unit exist in the SWV. Most public supply and irrigation wells are drilled through into the underlying sand and gravel of the MSHU and LSHU. Pump test #1 and pump test #2 contained wells either completely or partially penetrating the USHU, resulting in estimates of hydraulic conductivity and storativity. One well containing specific capacity data associated with this unit was also established. An initial estimate for model input was made based on pump and specific capacity tests. Homogeneous and anisotropic conditions were assigned. The initial K_x-value assigned was 450 ft/d (1.59 x 10^{-3} m/s) and the initial K_x/K_v assigned was 150. This layer was assigned as "convertible."

3.7.4.3 Middle Sedimentary Hydrogeologic Unit

Most of the aquifer property information collected during this study fell within the MSHU due to its large spatial extent, large relative thickness, and hydrogeologic properties. This unit was separated into three geologically different areas (see Figure 31). An isopach map in GIS form containing the thickness of the Willamette Aquifer was used to designate these different areas (Woodward et al., 1998). Alluvial fans created by the large amount of material originating in the Cascade Range were deposited within the Willamette Basin and are included in the MSHU. Proximal and distal type facies were deposited due to the sediments loss of energy upon entering the Willamette Basin,

creating deposits with likely different hydrogeologic properties (Woodward et al., 1998).

Aquifer property data that lie within a certain area, selected as the 60 ft (18.3 m) contour

line for both the Lebanon and Springfield fans, were separated from the other data that

existed outside of the fan areas (see Figure 13 in Woodward et al., 1998 and Figure 31 in

this study).

Two-dimensional ordinary kriging (Zimmerman and Zimmerman, 1991) was used

to interpolate horizontal hydraulic conductivity values between points creating

heterogeneity, whereby three separate experimental and model variograms were

constructed. Separate experimental and model variograms were constructed for the

Lebanon fan, Springfield fan, and the rest of the MSHU, assigning each area a unique

intrinsic model. The experimental variogram was found by calculating the variance of

each point in the data set with respect to each of the other points and plotting the

variances vs. distance between points. Then, a model variogram was fit as best possible

to the experimental variogram to model the trend displayed with the experimental

variogram.

The model variograms were then used to interpolate K_x-values between data

points within each of the three distinct areas. The result developed heterogeneous K_x-

values within the MSHU that also accounted for geologic conditions (see Figure 31).

Isotropy was also added while conducting ordinary kriging within each specified area.

Heterogeneous and anisotropic values of hydraulic conductivity were used in this layer.

Initial values of hydraulic conductivity for each well location, the method used, and the

data source where the information was derived are shown in Appendix I. For the entire

MSHU, the initial K_x-value assigned ranged from 0.003 ft/d (1.06 x 10^{-8} m/s) to 505 ft/d

(1.78 x 10^{-3} m/s). The initial K_x/K_y-value assigned was 150. The mean K_x-value for this unit is 57.1 ft/d (2.01 x 10^{-4} m/s) and median K_x-value for this unit is 21.1 ft/d (7.44 x 10^{-5} m/s). This layer was assigned as "convertible."
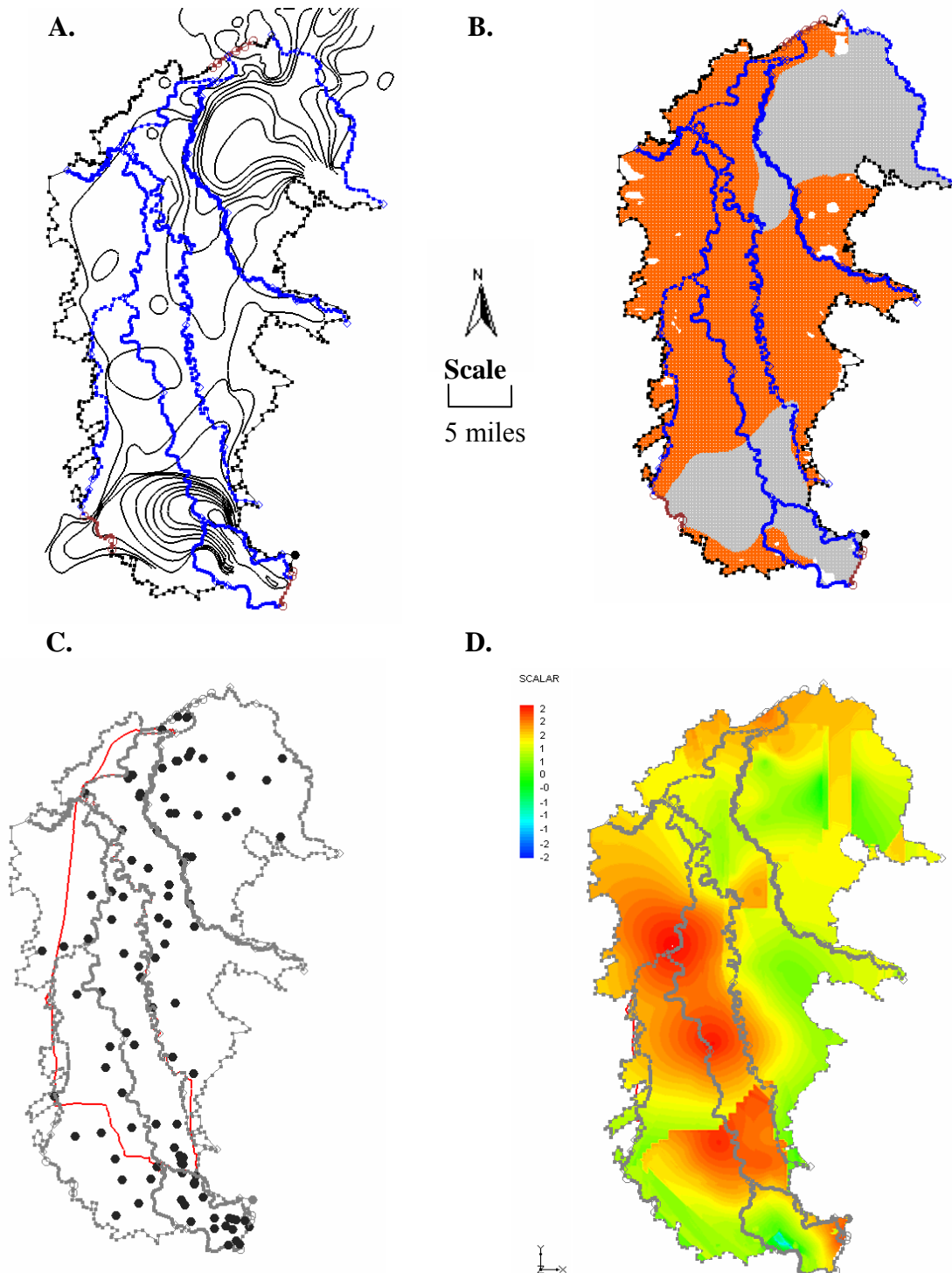
Figure 31: (A.) Thickness contours (20 ft) of the Willamette aquifer modified from Woodward et al. (1998); (B.) The Lebanon and Springfield Fans (in gray) within the MSHU; (C.) K_x-value well locations in the MSHU; (D.) Kriged K_x-values in $\log_{10}$ form for the MSHU.

3.7.4.4 Lower Sedimentary Hydrogeologic Unit

Aquifer property estimates for the LSHU were derived mostly from specific capacity information. Few wells are drilled into this unit because the highly productive MSHU usually overlies this unit and because the LSHU generally produces less water than the MSHU. Two-dimensional ordinary kriging was originally going to be used for this hydrogeologic unit, however, after constructing an experimental variogram for data associated with this unit it was found that very little variability vs. distance exists within this data set. Therefore, a single K_x-value using the geometric mean of the data set was initially assigned to the LSHU. The geometric mean is used when flow is uniform and hydraulic conductivity has a log-normal distribution, which the data displayed. Figure 32 displays the spatial distribution of K_x-values for the LSHU. Initial values of hydraulic conductivity for each well location, the method used, and the data source where the information was derived are shown in Appendix I. The initial K_x-value assigned was the geometric mean of 7.24 ft/d (2.55 x 10^{-5} m/s) and the initial K_x/K_y assigned was 50. This layer was assigned as "confined."
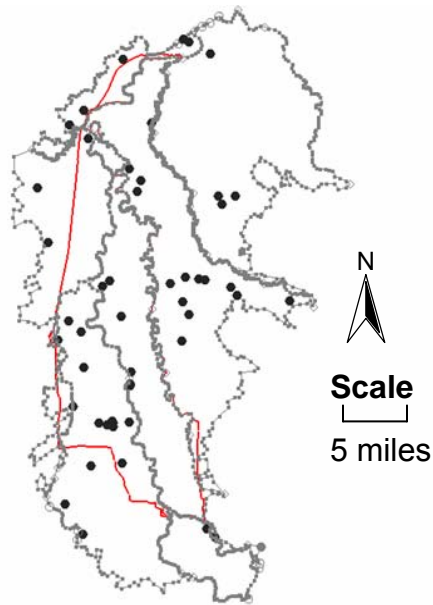
Figure 32: Spatial distribution of hydraulic conductivity values of the Lower Sedimentary hydrogeologic unit.

Table 14: Initial K_x and K_x/K_v estimates for each hydrogeologic unit and the sources from which each value was derived.

Hydrogeologic unit, Layer #	Horizontal hydraulic conductivity (K_x) (ft/d); (m/s)	Anisotropy ratio (K_x/K_v)	Sources
Willamette Silt, Layer 1	1.0; 2.1 x 10^{-4}	75	Woodward et al, 1998; Iverson, 2002
Upper Sedimentary, Layer 2	450; 9.53 x 10^{-2}	150	This study (pump tests and specific capacity)
Middle Sedimentary, Layer 3	0.003 – 505 (kriged) and 10.17 (geometric mean); 6.35 x 10^{-7} – 1.07 x 10^{-1} (kriged) and 2.15 x 10^{-3} (geometric mean)	150	Woodward et al., 1998; this study; sources cited in Appendix I.
Lower Sedimentary, Layer 4	7.24 ; 1.52 x 10^{-3} (geometric mean)	50	Woodward et al., 1998; this study; sources cited in Appendix I.

3.7.5 Calibration

Calibration was completed using a trial-and-error process, using data collected

from 07/1/2004 to 07/31/2005 and adjusting initial model parameters until simulated vs.

measured head values and simulated vs. measured seepage rates agreed reasonably with

one another. Parameters adjusted were: K_x, K_x/K_y, and general head and river

conductance. Following calibration, all K_x and K_x/K_y values were adjusted from their

initial estimates. Finalized K_x and K_x/K_y values for each hydrogeologic unit are shown in

Table 15. It is important to note that the initial MSHU K_x-values were multiplied by 14

and the initial LSHU K_x-values were multiplied by 8.

Table 15: Final optimized parameters for each hydrogeolgic unit.

Hydrogeologic unit, Layer #	Horizontal hydraulic conductivity (K_x), (ft/d); (m/s)	Anisotropy ratio (K_x/K_y)
Willamette Silt, Layer 1	0.027; 5.72 x 10⁻⁶	100
Upper Sedimentary, Layer 2	550; 1.16 x 10⁻¹	50
Middle Sedimentary, Layer 3	0.003 – 505 (**x14**) (kriged); 6.35 x 10⁻⁷ – 1.07 x 10⁻¹ (**x14**) (kriged)	50
Lower Sedimentary, Layer 4	7.24 (**x8**); 1.52 x 10⁻³ (**x8**)	75

The total water balance was checked after each model run. Final results show that the amount of water into the model approximately equals the amount of water out of the model (<-0.02 percent discrepancy, see Table 16), indicating mass balance and a properly running model. Forty-five measured field head values from 07/1/2004 to 07/31/2005 were averaged and used as calibration targets (see Appendix I and Figure 34). A graph of computed vs. observed head values is found in Figure 33. A target range of ±7 ft was assigned to each calibration target. A greater value was initially assigned at the start of the calibration process and was reduced as calibration progressed. The target range was justified due to the averaging of the measured head values and error associated with well position, surface elevation measurements, and field measurement of head values. Discussion of error can be found in Section 3.7.7. To quantify the error between simulated and measured head values ($N = 45$), mean error (ME), mean absolute error (MAE), and root mean squared error (RMS) were monitored, recorded, and reduced as much as possible during calibration. Final model error results were ME = -0.108 ft (0.033 m), MAE = 5.182 ft (1.579 m), and RMS = 6.750 ft (2.057 m).

River seepage (river gain or loss) was estimated from 07/1/2004 to 07/31/2005 along reaches between stream gages in the SWV. Past studies in the area measured "snapshots" in time, estimating river seepage for a small number of reaches during low and high flow periods in the SWV (Lee and Risley, 2002 and Conlon et al., 2005). Unfortunately most seepage calculations were less than the measurement uncertainty, therefore seepage along these stream reaches is difficult to quantify. Many factors can contribute to seepage error (discussed in Section 2.5.3). Even though detailed seepage rate studies in the past have been unable to quantify that seepage exists at the large reach

scale, river seepage estimates were calculated where possible. Seepage estimates were calculated and compared to simulated values along four reaches, one along the Long Tom River and three along the Willamette River. A comparison of the measured vs. simulated seepage rates indicate reasonable agreement following calibration. All measured gaining reaches have simulated gaining reaches and all measured losing reaches have losing simulated reaches, except for the Long Tom River. Further analysis was not conducted due to the many uncertainties associated with estimation of river seepage.

MODPATH, a particle tracking package that tracks particles as they move advectively with groundwater, was also used as a calibration tool and is discussed in Section 3.7.8 (Harbaugh et al., 2000).

Table 16: Volumetric budget for the model.

PARAMETER	IN (ft^3):	OUT (ft^3):
Storage =	0	0
Constant Head =	2179930.75	293471.6875
Wells =	0	59.611
River Leakage =	25014478	58818304
ET =	0	312852.4062
Head Dep. Boundaries =	1308599.875	1692182.75
Recharge =	32601918	0
TOTAL IN =	61104928	-61116872
IN - OUT =		-11944
PERCENT DISCREPANCY =		-0.02
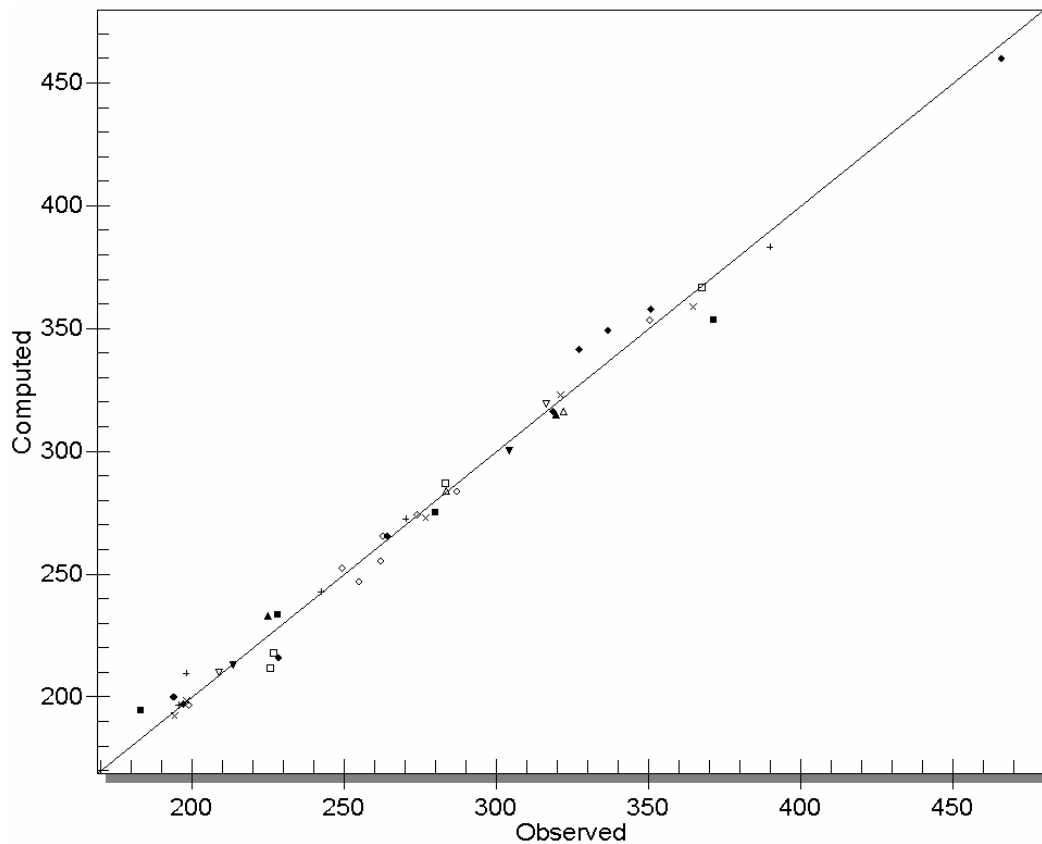
Figure 33: Computed hydraulic head (ft) vs. observed hydraulic head (ft).
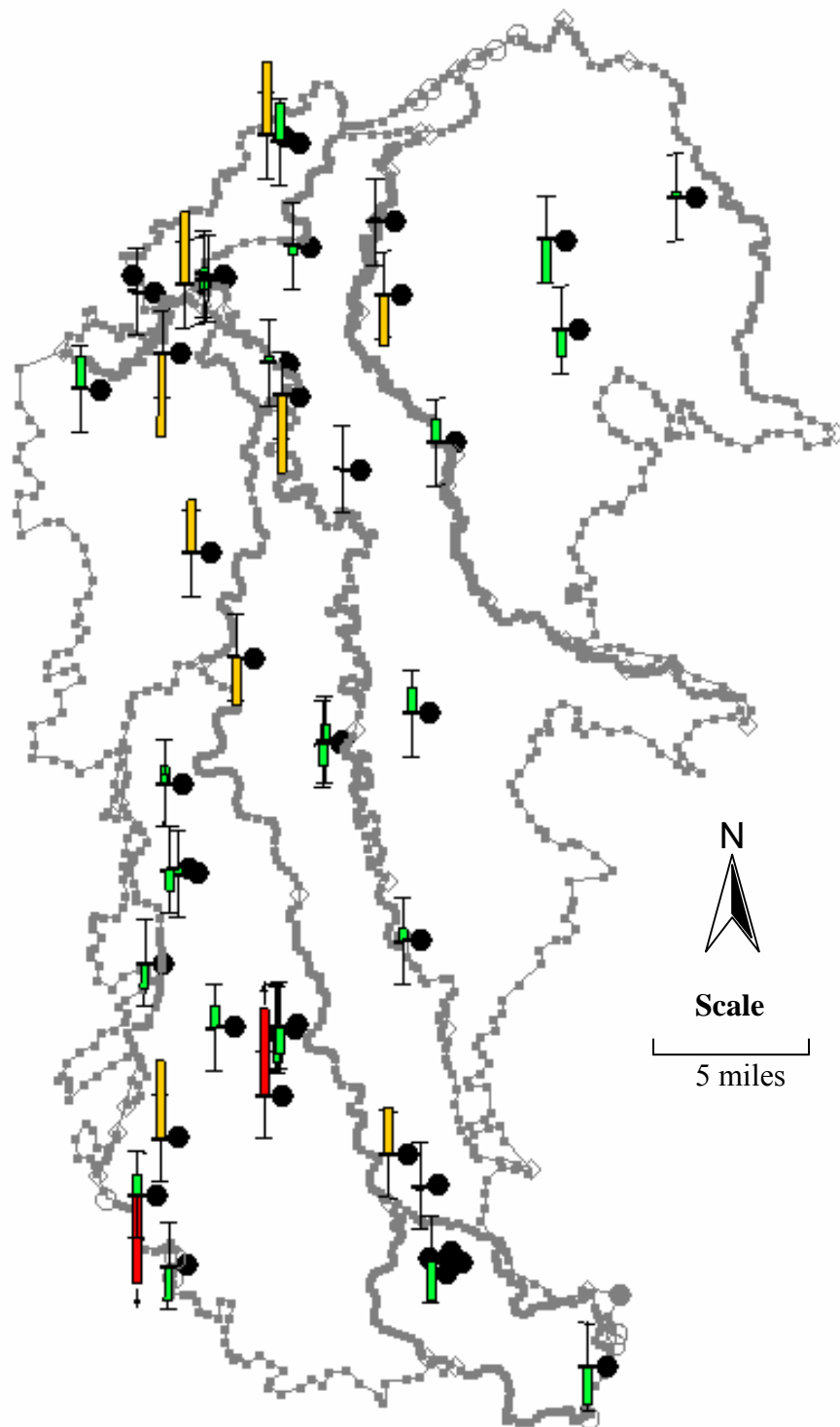
Figure 34: Head calibration targets ($N = 45$). Green indicates computed vs. observed values within ±7 ft. Yellow indicates error <200%. Red indicates error >200%.

Simulated head contour maps were developed for the USHU (Figure 35), MSHU (Figure 36), and LSHU (Figure 37). These maps illustrate the water table and/or potentiometric surface of the SWV. These contours also help to show the general direction of groundwater flow. These simulated head contours were then compared to water table contours from Conlon et al. (2005), which were based on field measurements collected during mid-November 1996. Figure 38 shows simulated head contours of the MSHU and the water table contours from Conlon et al. (2005). Figure 39 shows the simulated head contours of the LSHU and the water table contours from Conlon et al. (2005).

Results of the comparison between the simulated head contours of the MSHU and LSHU and the water table contours from Conlon et al. (2005) generally show that the location of the contours compare relatively well. Spacing between contours varies in places, but generally show similar zones of high and low hydraulic conductivity. Gaining streams are accentuated more in the Conlon et al. (2005) water table contours than the simulated head contours. This is likely a direct result of stream bed conductance. The LSHU was designated as a confined aquifer making the simulated head contours a potentiometric surface, not a water table surface. Nevertheless, the simulated head contours of the MSHU and LSHU vary little.
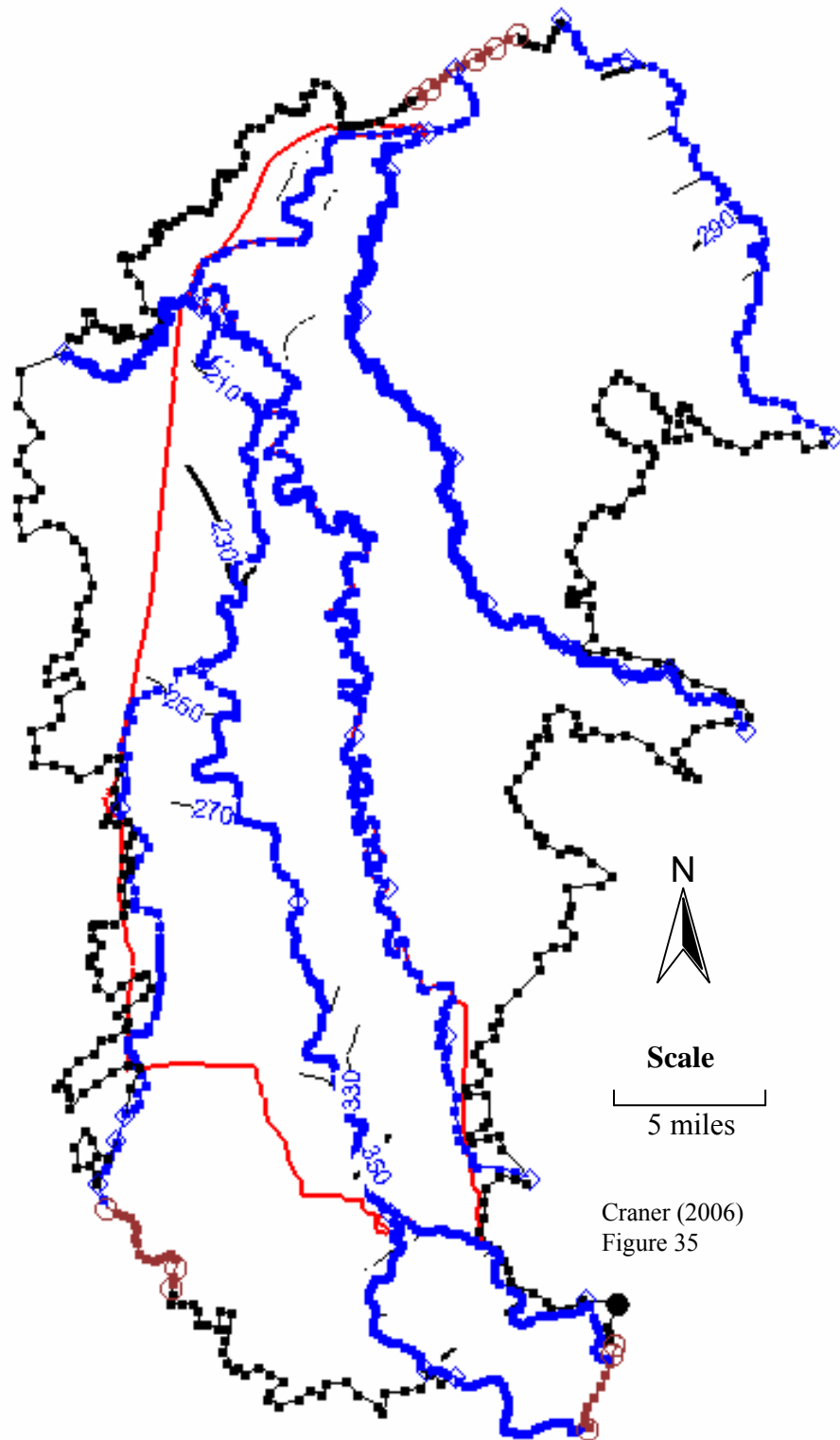
Figure 35: Simulated hydraulic head contours (ft) for the Upper Sedimentary hydrogeologic unit.
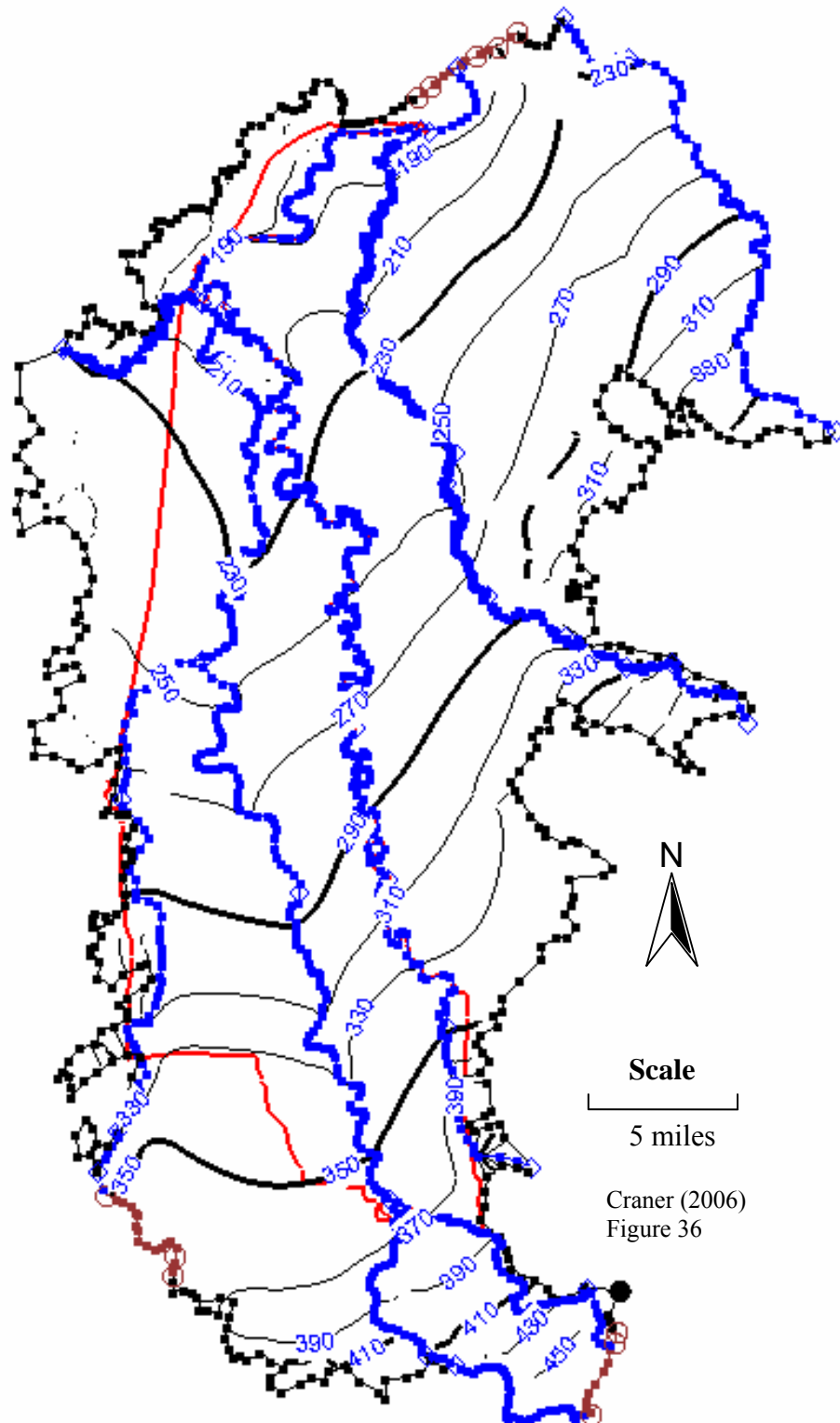
Figure 36: Simulated hydraulic head contours (ft) for the Middle Sedimentary hydrogeologic unit.
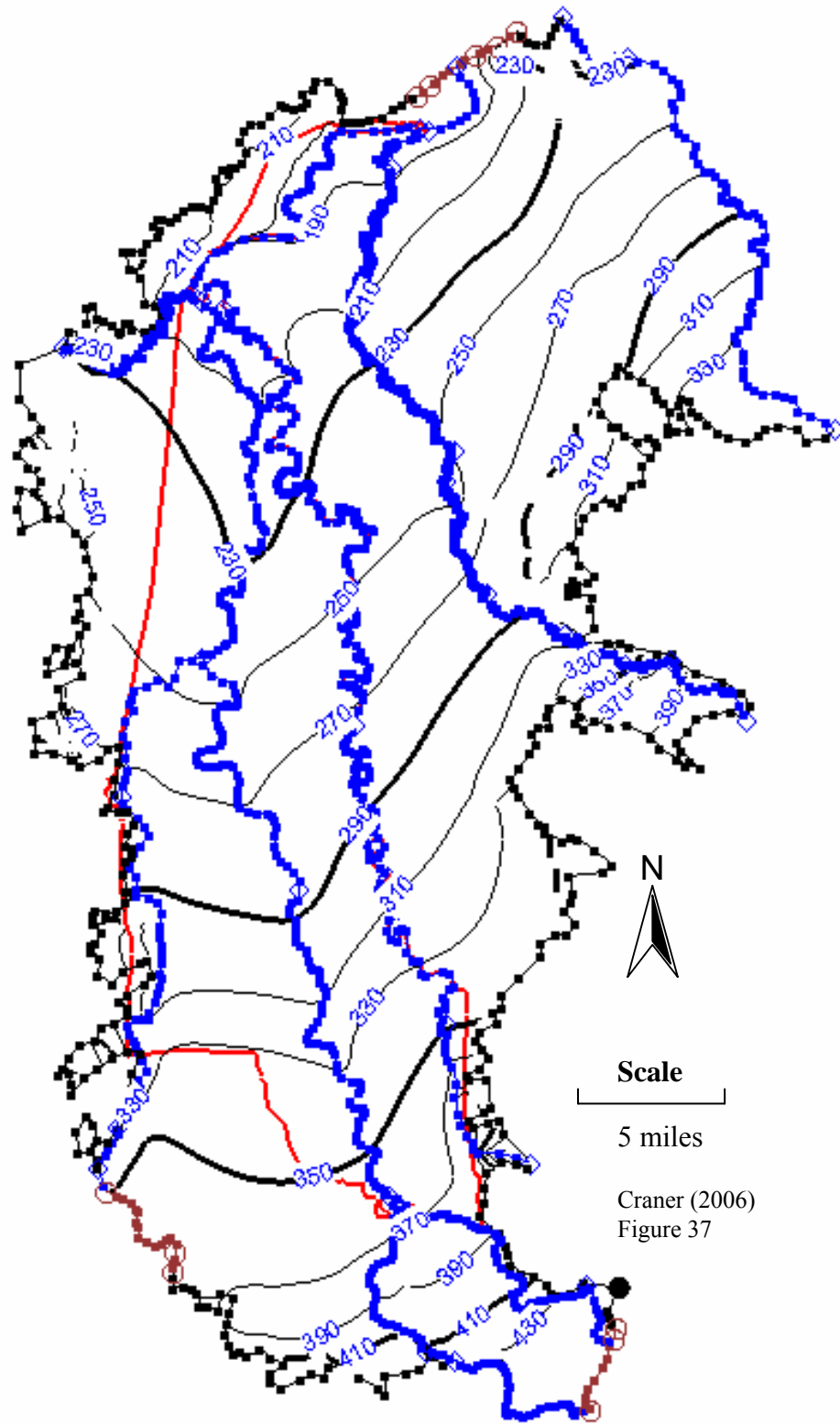
Figure 37: Simulated hydraulic head contours (ft) for the Lower Sedimentary hydrogeologic unit.
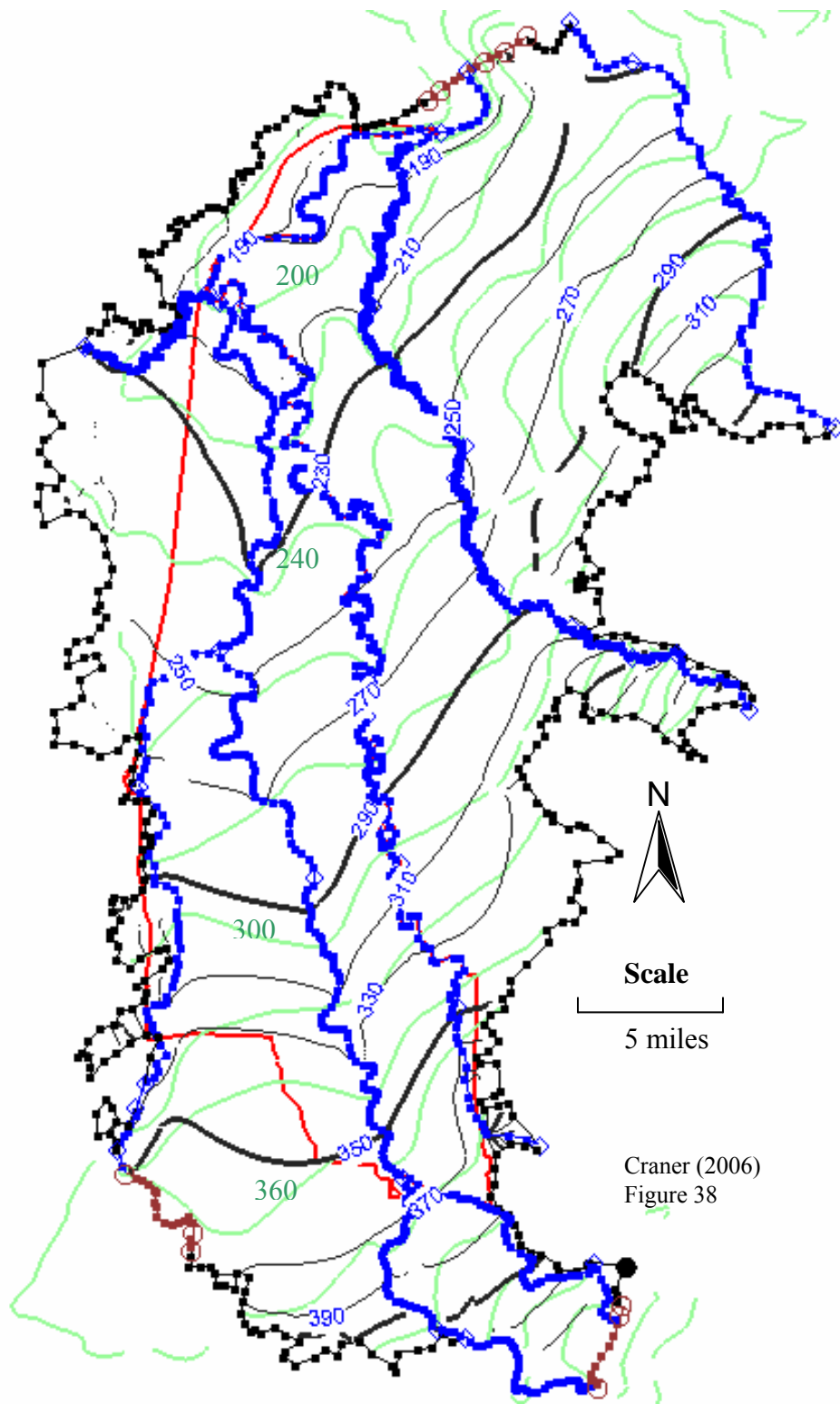
Figure 38: Simulated hydraulic head contours (ft) for the Middle Sedimentary hydrogeologic unit and Conlon et al. (2005) generalized water table contours (20 ft intervals) from measurements in mid-November 1996.
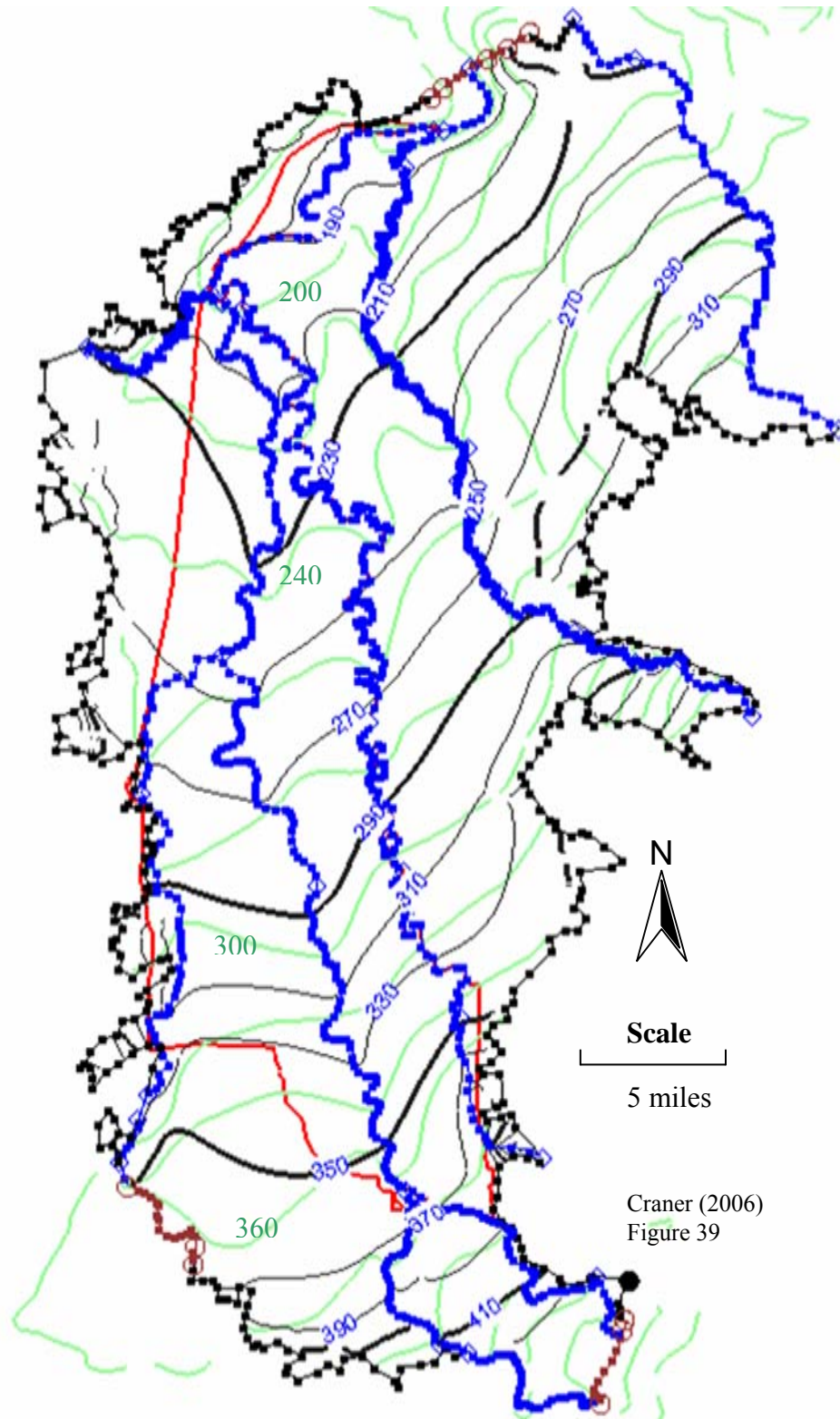
Figure 39: Simulated hydraulic head contours (ft) for the Lower Sedimentary hydrogeologic unit and Conlon et al. (2005) generalized water table contours (20 ft intervals) from measurements in mid-November 1996.

3.7.6 Sensitivity Analysis

A sensitivity analysis was conducted to quantify the uncertainty of specified model parameters. The model parameters analyzed during the sensitivity analysis were recharge rate, maximum ET rate, the horizontal hydraulic conductivity (K_x) and anisotropy ratio (K_x/K_y) of each hydrogeologic unit. The sensitivity analysis was conducted using the automated Sensitivity Analysis option in GMS-MODFLOW. Dimensionless composite scaled sensitivities were calculated. The composite scaled sensitivities are calculated for each parameter using scaled sensitivities. Scaled sensitivities are dimensionless quantities that can be used to compare the importance of different observations to the estimation of a simulated value (Hill, 1998). This nonlinear regression method accounts for the amount of information provided by the observations for the estimation of a particular parameter (Hill, 1998). Equations can be found in Hill (1998). For a selected parameter, the greater the value of composite scaled sensitivity, the greater the importance of the selected parameter.

Results indicate the recharge rate was by far the most sensitive parameter analyzed, followed by the K_x-value of the LSHU, maximum ET rate, and the K_x-value of the USHU (see Figure 40). The rest of the parameters have relatively low composite scaled sensitivity values. Recharge was assigned as a constant value over the entire model domain, however, recharge is seasonal due to the wet winters, dry summers, and variety of geologic units that exist in the SWV. Recharge is a difficult parameter to quantify but does not vary by several orders of magnitude like hydraulic conductivity. Recharge rates do not vary by >2 orders of magnitude, but hydraulic conductivity estimates may vary by more than 2 orders of magnitude.
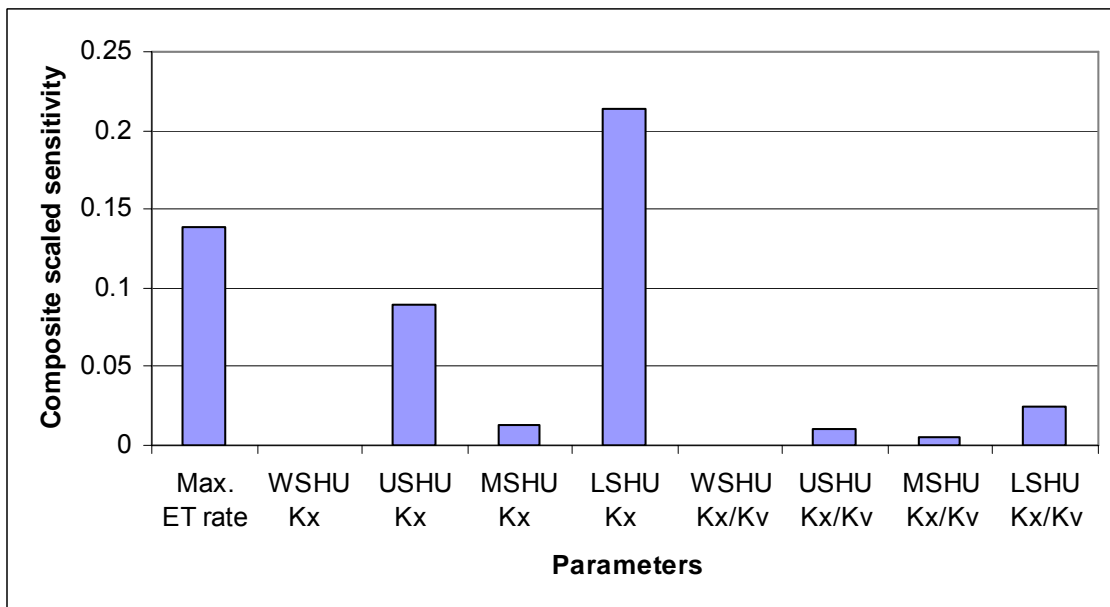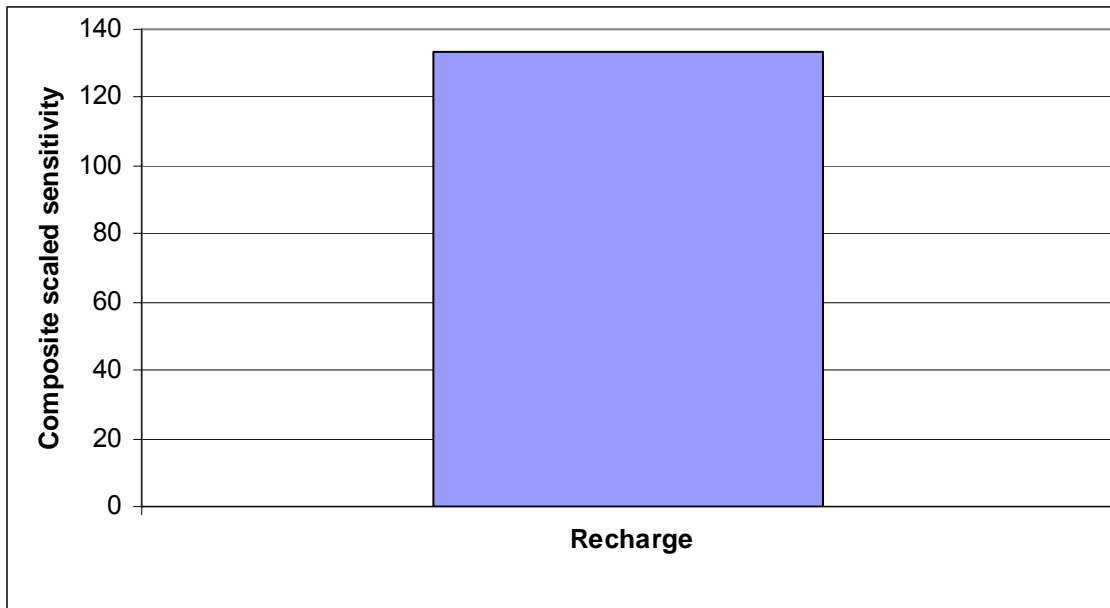
Figure 40: Composite scaled sensitivities vs. selected parameters. Note: We are skeptical of the final composite scaled sensitivity values produced by the model; see text.

The sensitivity analysis conducted during this study possibly produced unreasonable results. Specifically, the composite scaled sensitivity value for recharge is likely too large (see Figure 40). It is unlikely that recharge is nearly 1000 times more sensitive to a change in head than the other model parameters analyzed during the sensitivity analysis. The reasoning behind these results is currently unclear.

A grid size analysis was also conducted to determine how sensitive the model was to changes in grid cell size in the x- and y-directions. Cell sizes were increased from the original 500 ft x 500 ft to 1000 ft x 1000 ft and then to 2000 ft x 2000 ft grid cell size. The model was run after each increase in cell size and ME, MAE, and RMSE values of the simulated vs. observed head values were recorded, as well as river gains/losses along four stream reaches. River gains/losses varied little with increase in cell size. Table 17 compares the increase in cell size and associated error. Results indicate that grid cell size does increase associated error values, but the increase ME, MAE, and RMSE do not increase incrementally with an increase in grid cell size. This shows that recording all associated error values between simulated vs. observed head values during model analysis is important. The smallest grid size possible to be constructed for this model was 500 ft x 500 ft due to computer memory limitations. A grid size <500 ft x 500 ft may yield lower MAE and RMSE values and produce more precise results.

Table 17: Grid cell size sensitivity analysis.

Grid Cell Size (ft)	ME (mean error, ft; m)	MAE (mean absolute error, ft; m)	RMSE (root mean squared error, ft; m)
500 x 500	-0.108; 0.033	5.182; 1.579	6.750; 2.057
1000 x 1000	4.383; 1.336	8.787; 2.678	16.661; 5.078
2000 x 2000	8.079; 2.462	9.531; 2.905	22.394; 6.826

A separate sensitivity analysis was conducted on the interpolation of K_x-values in the MSHU. After separating this layer into three different areas and using ordinary kriging to interpolate K_x-values between data points, it was not apparent that this method adequately represented the geology of this layer. Therefore, the geometric mean was calculated for all K_x-values within this layer, resulting in a value of 10.17 ft/d (2.99×10^{-6} m/s). The geometric mean of the K_x-values was then assigned to the MSHU. The model was run and a comparison made between the calibrated model with the relatively more complex horizontal hydraulic conductivity values and the model with the geometric mean value for the entire layer. The model with the geometric mean value resulted in error calculations of simulated vs. observed heads of ME = 6.448 ft (1.965 m), MAE = 8.588 ft (2.618 m), and RMSE = 10.798 ft (3.291 m). River gains/losses were similar to the calibrated model. Overall, the model with the simplified K_x-value field altered the error values substantially in comparison to the calibrated model with the complex K_x-value field. However, no attempt was made to calibrate the simplified model, which would have improved the error. Currently it is not apparent which K_x-value field best represents the MSHU, therefore the original, more complex K_x-value field was used for the duration of this study.

3.7.7 Sources of Error

A variety of error results during the construction of a groundwater flow model. During calibration, the comparison between simulated vs. measured head values were used almost exclusively. Therefore the field location and measurement of the head values likely contribute the greatest amount of error in the model. Quantification of this error is described in Section 4.1. After using a 7.5-minute topographic map to determine

each well location, an effort was made to minimize the well elevation error by using a 10

m DEM to determine a more precise well elevation. This was done within GMS-

MODFLOW. All other data used to construct the model was assumed to have negligible

error in comparison to the measured head values.

3.7.8 Comparison of CFC-Model Age and MODPATH Travel Times

A comparison of CFC-model ages and particles tracked using MODPATH

(Harbaugh et al., 2000) was conducted to ensure conceptual integrity within the model.

Any tracer (i.e., CFCs) that provides direct age information is a valuable tool for

calibrating groundwater flow models (Ekwurzel et al., 1994). Transient tracers provide

time information that can be used to infer flow velocity and direction, extent of

hydrodynamic dispersion, and recharge/discharge rates (Ekwurzel et al., 1993).

Tritium/^{3}He and CFCs have been used as calibration targets with success (Plummer et al.,

1993; Reilly et al., 1994; Stute and Schlosser, 2000).

Fifty particles were released from the 10 wells sampled for CFCs during this

study and the 9 wells sampled for CFCs by the U.S. Geological Survey (Hinkle, 2005).

Particles were released from the average well screen elevation at each location and

tracked backward to their point of origin at the water table. A similar analysis was

conducted by the U.S. Geological Survey in the Portland, OR area with success (Hinkle

and Snyder, 1997). Travel times were calculated for each particle, averages determined,

and compared below in Table 18 with CFC-model ages for each well location. Effective

porosity values used for each model layer were: 0.4 (WSHU), 0.3 (USHU), 0.25

(MSHU), and 0.2 (LSHU).

Table 18: Comparison of average particle travel times calculated using MODFLOW-MODPATH and CFC-model age. *U.S. Geological Survey data from Hinkle (2005).

Well	Average particle travel time (years)	CFC-model age (years)*	Average particle travel length (ft)	MODPATH groundwater velocity (ft/year)
U.S. Geological Survey*				
LINN 14280	9.8	37	5346.38	543
LINN 4146	104.3	26	21636.1	207
LINN 8753	37.6	40	10979.1	292
LINN 8756	483.5	>57	54774.4	113
LINN 50097	89.4	0-57	33091	370
LINN 50852	67.4	16-57	26879.7	399
LINN 50103	61.4	36	25790.7	420
LINN 10510	55.8	24	16102.6	289
LINN 10391	70.4	25	23237.1	330
This study				
LINN 13346 (CFC4)	4.9	19-31	22504.9	4593
LINN 14130 (CFC2)	15.6	38	17208.2	1103
LINN 14016 (CFC1)	24.6	36-45	13635.4	555
LINN 50592 (CFC3)	18.7	35	10241.5	549
LINN 14105 (CFC8)	82.0	34	15057.5	184
LANE 8073 (CFC5)	15.6	20	31509.4	2020
LANE 51456 (CFC9)	3.2	18	8621.26	2661
LANE 7488 (CFC7)	12.4	18	21136	1711
LANE 5698 (CFC6)	11.2	17	19452.5	1737
Funke_Dist (CFC10)	4.3	13-18	8590.28	1984
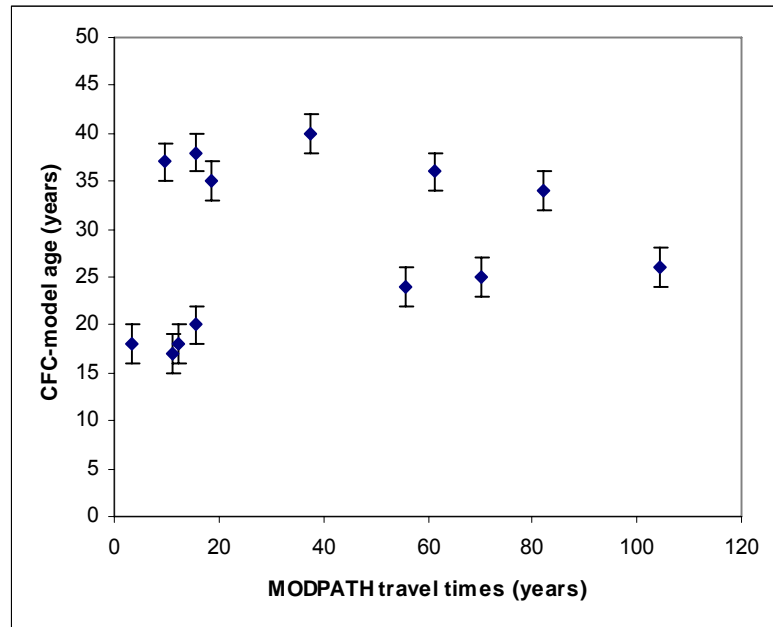
Figure 41: Graph comparing CFC-model ages (contains data with no age ranges) and particle travel times developed using MODFLOW-MODPATH.

MODPATH travel times represent how a conservative, non-sorbing tracer would travel though the saturated portion of the aquifer. Figure 41 indicates a discrepancy between CFC-model ages and MODPATH travel times at most well locations. This may be due to inaccuracies in the estimation of hydraulic conductivity, too few cells or layers, or the contamination or degradation of CFCs. Groundwater velocity values ranged from 3.01×10^{-1} ft/d to 1.26×10^{1} ft/d (1.06×10^{-6} m/s to 4.45×10^{-5} m/s). These groundwater velocities are about an order of magnitude smaller than the 3 ft/d to 30 ft/d (1.06×10^{-5} to 1.06×10^{-4} m/s) (typical of sand and gravel aquifers) calculated by Woodward et al. (1998). This discrepancy may be due to the small number of wells (N=19) observed or that most wells observed penetrated the WSHU and are open to the Qg_2 geologic unit which generally contains older sand and gravel with lower hydraulic conductivity values.

Figure 42 shows the starting and ending position of the 50 particles released from the 19

well locations and tracked backwards to their point of origins. Particle pathways show

the direction of groundwater flow, the length of each particle pathway, and the origin of

particles released from each well. Generally, Figure 42 indicates where water is coming

from when water is pumped from each well.
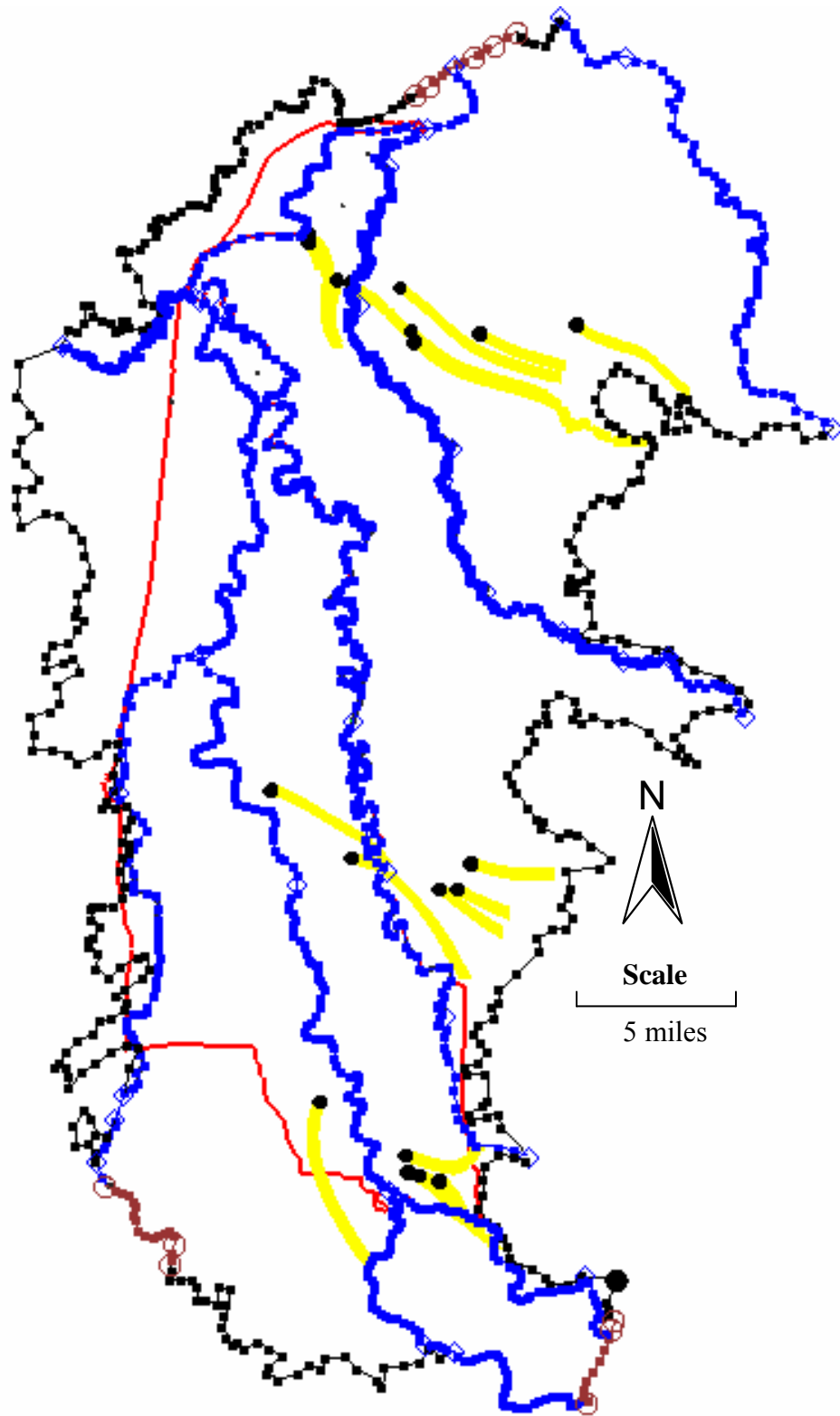
Figure 42: MODPATH particle pathways for well locations where CFC samples were collected.

3.7.9 Model Simulations

Once the numerical steady-state model was calibrated, example simulations showing the effects of pumping on groundwater/surface water and MODPATH particle transport were developed for 3 specified areas. These model simulations were run to demonstrate some capabilities of the current model and to develop visual aids for outreach education. It is important to remember that the model predictions reflect the error and uncertainty in the model and should not be considered exact. Effective porosity values used for each model layer were: 0.4 (WSHU), 0.3 (USHU), 0.25 (MSHU), and 0.2 (LSHU).

3.7.9.1 Coburg area

The Coburg area was selected because of known elevated groundwater nitrate concentrations (see Figure 1) likely due to the large percentage of residents with septic systems. One particle was released at the selected location per 500 ft x 500 ft cell at the water table and tracked down gradient. Releasing particles at the water table simulates how anthropogenic sources of contamination (i.e., nitrate) will travel advectively through the saturated subsurface. The particles terminate when they reach a model boundary or the water table.

Figure 43 shows the Coburg and Bottom Loop Road area, the potentiometric surface of the MSHU, and the particle starting and ending locations for particles released near the Bottom Loop Road. Arrows were placed every 1000 days to indicate particle direction and travel time. In map view, the particles travel down gradient and most terminate at the Willamette River. In cross-section, the particles travel horizontal just below the potentiometric surface within the MSHU. The particle travel times, indicated

by the location of the arrow along the selected particle pathway, indicate it takes <1000

days for some particles to reach the Willamette River whereas other particles take >1000

days.

This example simulation of the Coburg area can be used for local groundwater

management. Contaminant migration direction and travel time give local officials

estimates of where to monitor groundwater and the clean-up time of groundwater if

current management practices change. This model simulation may not represent the

exact groundwater flow direction and groundwater velocity at this location.
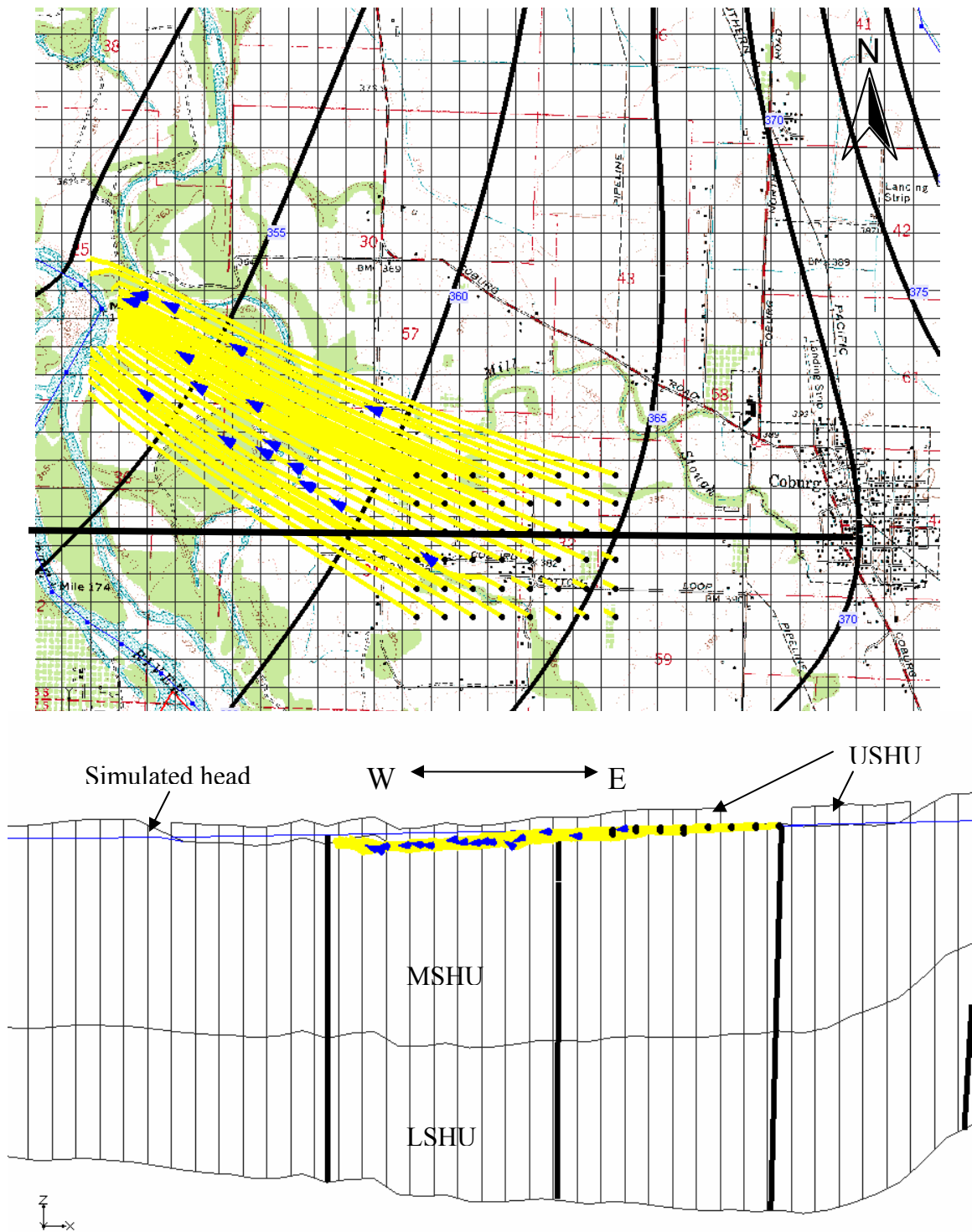
Figure 43: Simulated head contours (ft), particle pathways, and arrows showing travel time (placed every 1000 days) and flow direction in map and cross-sectional view (x20 vertical exaggeration) of the Coburg area. Grid size 500 ft x 500 ft. This model simulation may not represent the exact groundwater flow direction and groundwater velocity at this location.

3.7.9.2 Harrisburg area

The Harrisburg area was selected to observe effects of groundwater pumping on local groundwater/surface water and to observe capture zones as water is pumped from the MSHU or LSHU. The City of Harrisburg relies solely on groundwater as their water source. Harrisburg's geographic location nearby the Willamette River likely impacts the local water table. To observe the effect that the Willamette River has on groundwater pumping, two model simulations were run with a well placed west of the Willamette River and adjusted to pump 750 gal/min (4.7 x 10^{-2} m^3/s) from either the MSHU or LSHU. Ten particles were released at the well location and tracked backward to illustrate the location of the well capture zones.

Figures 44 and 45 show a map and cross-section view of the potentiometric surface, well location, and capture zone of the MSHU and LSHU near Harrisburg. Arrows were placed every 100 days in Figure 44 and every 1000 days in Figure 45 along the particle pathways to show flow directions and travel times.

Results of pumping from the MSHU indicate that most groundwater originates from the west side of the Willamette River (see Figure 44). The potentiometric surface of this unit is altered little during pumping. Due to the greater hydraulic conductivity of the MSHU compared to the LSHU, the capture zone is narrow and travel times faster. In cross-sectional view, the majority of the water pumped from the well is shown to travel down gradient from the MSHU, to the LSHU, and then to the MSHU where it is removed.

Results of pumping from the LSHU indicate that most groundwater is removed up gradient and passes beneath the Willamette River (see Figure 45). The potentiometric

surface of the LSHU is altered to a greater degree than pumping from the MSHU due to the increased depth of the well and lower hydraulic conductivity. In cross-sectional view, most pathways originate at the water table and travel to the LSHU where they move nearly horizontal to the pumping well.

This example simulation of pumping from a well at varying depths in the Harrisburg area can aid in determining well placement, well capture zones, and effects of pumping on the nearby Willamette River. When making groundwater management decisions travel times along particle pathways to a pumping well can help to understand the transient movement of water in the local aquifer. This model simulation may not represent the exact groundwater flow direction and groundwater velocity at this location.
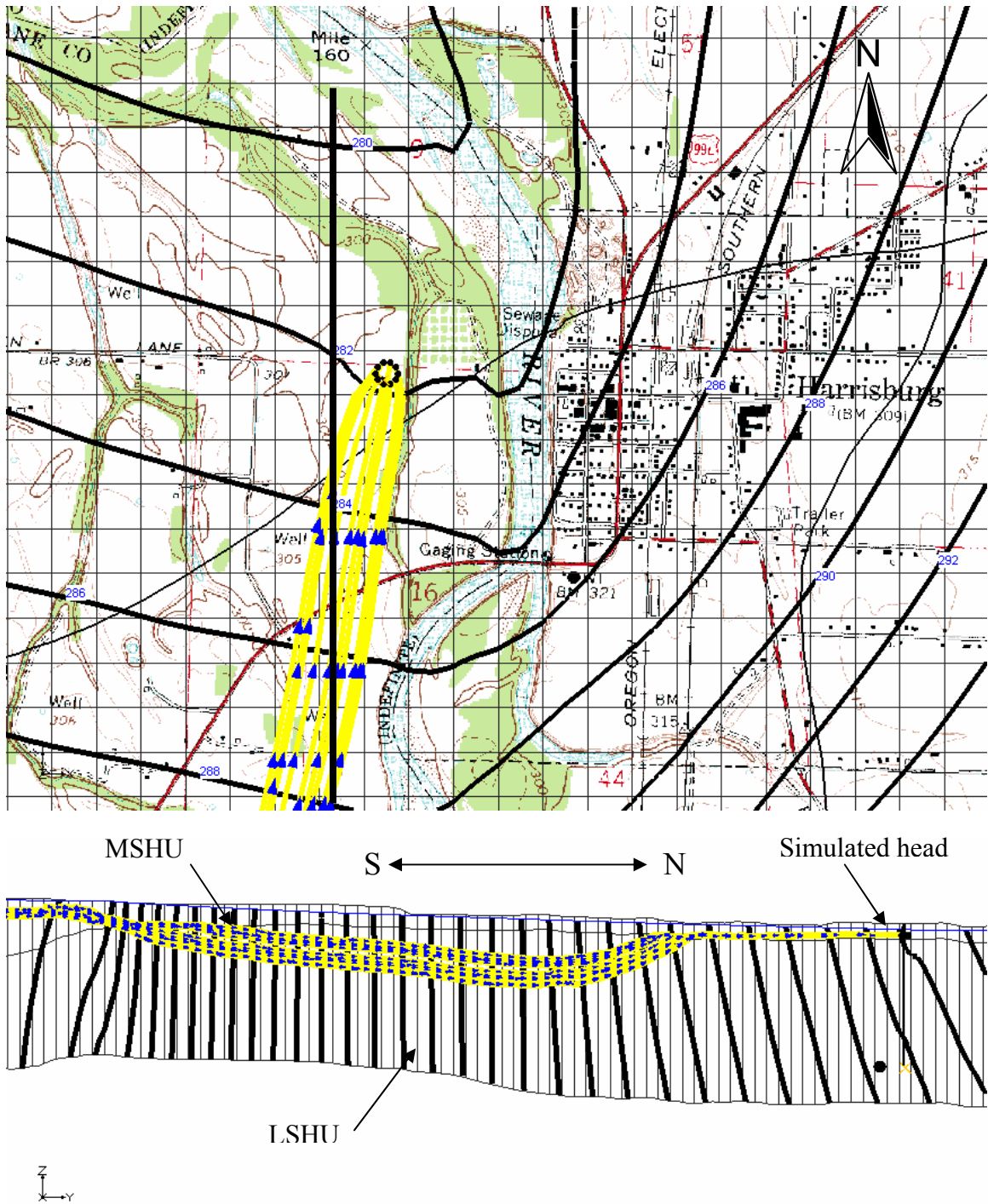
Figure 44: Simulated head contours (ft), capture zone, particle pathways, and arrows showing travel time (placed every 100 days) and flow direction in map and cross-sectional view (x20 vertical exaggeration) of the Harrisburg area, pumping from the MSHU. Grid size 500 ft x 500 ft. This model simulation may not represent the exact groundwater flow direction and groundwater velocity at this location.
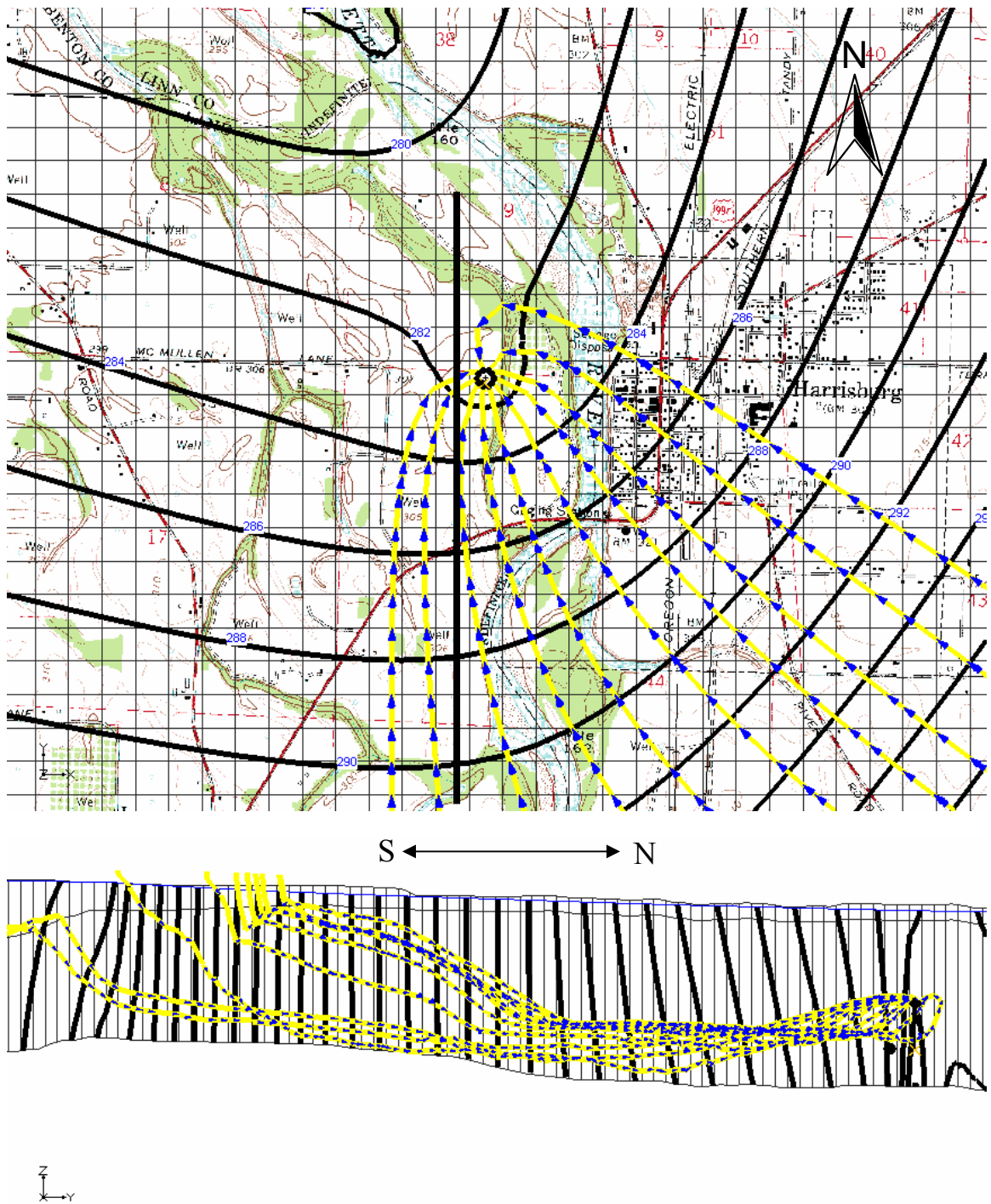
Figure 45: Simulated head contours (ft), capture zone, particle pathways, and arrows showing travel time (placed every 1000 days) and flow direction in map and cross-sectional view (x20 vertical exaggeration) of the Harrisburg area, pumping from the LSHU. Grid size 500 ft x 500 ft. This model simulation may not represent the exact groundwater flow direction and groundwater velocity at this location.

3.7.9.3 Southern Willamette Valley Travel Times

A groundwater travel time map was developed using MODFLOW-MODPATH. Particles were released at the potentiometric surface from randomly selected cells and tracked forward in the MSHU and LSHU as they moved through the saturated subsurface until reaching a model boundary or simulated head surface. The maximum age of the particle travel time was assigned to the particle starting location. This information was then linearly interpolated to a 2-D grid in GMS-MODFLOW and contoured using color. Two maps were produced, one for the MSHU and one for the LSHU, displaying the spatial distribution of the maximum ages of particles released at the simulated head surface of the SWV.

Travel times for selected cells within the MSHU (Figure 47) range from 7.19 x 10^{-4} years to 446 years ($N = 487$). The mean is 29.3 years and median is 5.19 years for these selected cells. Travel times for selected cells within the LSHU (Figure 48) range from 3.41 x 10^{-1} years to 798 years. The mean is 99.9 years and median is 50.0 years. Travel times are greater in the LSHU due to the layers relatively low hydraulic conductivity and stratigraphic position. Travel times nearby the Willamette River are generally lower than travel times nearby the foothills of the Coast and Cascade Ranges. This is likely due to the majority of recharge for the SWV consisting of rainfall, the greater hydraulic conductivity of the basin-fill sediments nearby the Willamette River, and the fact that most groundwater eventually discharges to the Willamette River. These features create short flow paths nearby the Willamette River and long flow paths at distance from the Willamette River.

These resulting maps can be used for land use and groundwater management.
Varying management practices can be devised for areas with low vs. areas with high
travel times. This model simulation may not represent the exact maximum groundwater
direction and travel time.
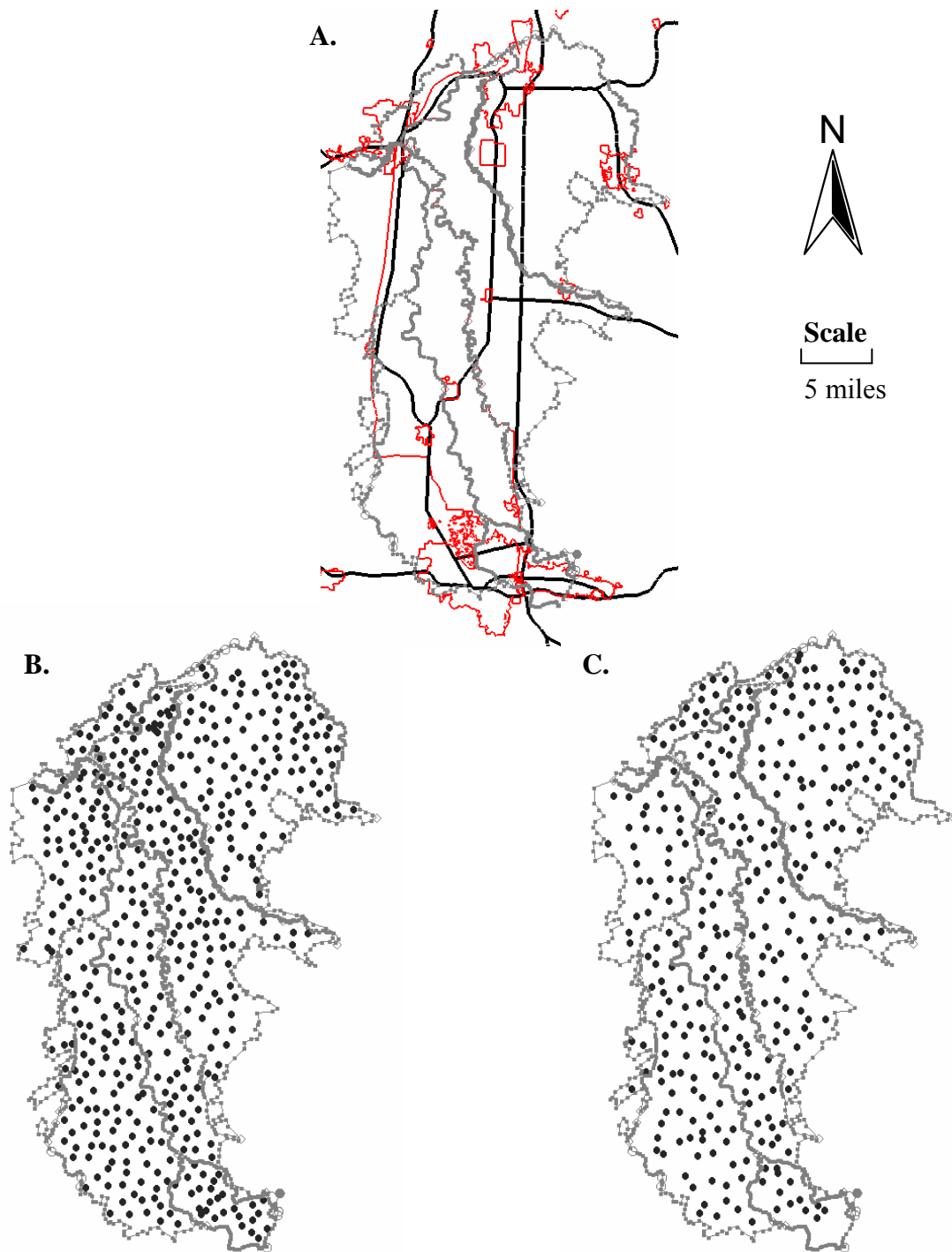
Figure 46: (A.) Major highways, city limits, and GWMA; (B.) Randomly selected cells in the MSHU; (C.) Randomly selected cells in the LSHU.
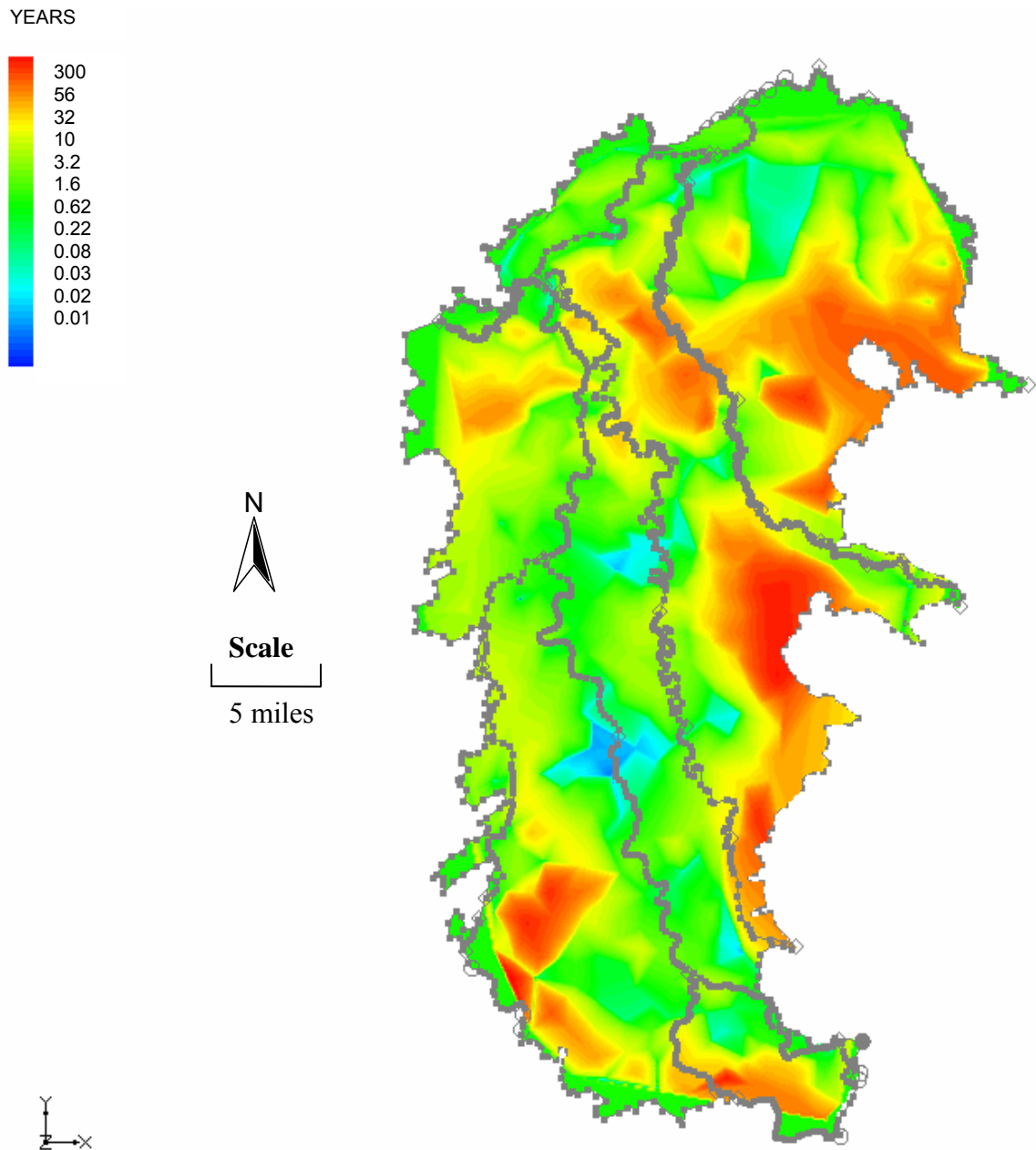
Figure 47: Spatial distribution of maximum travel times (numbers indicate the time it takes a water molecule to travel from the location indicated out of the aquifer) for the Middle Sedimentary hydrogeologic unit. This model simulation may not represent the exact maximum groundwater direction and travel time. Note: Contour coloring not uniformly spaced.
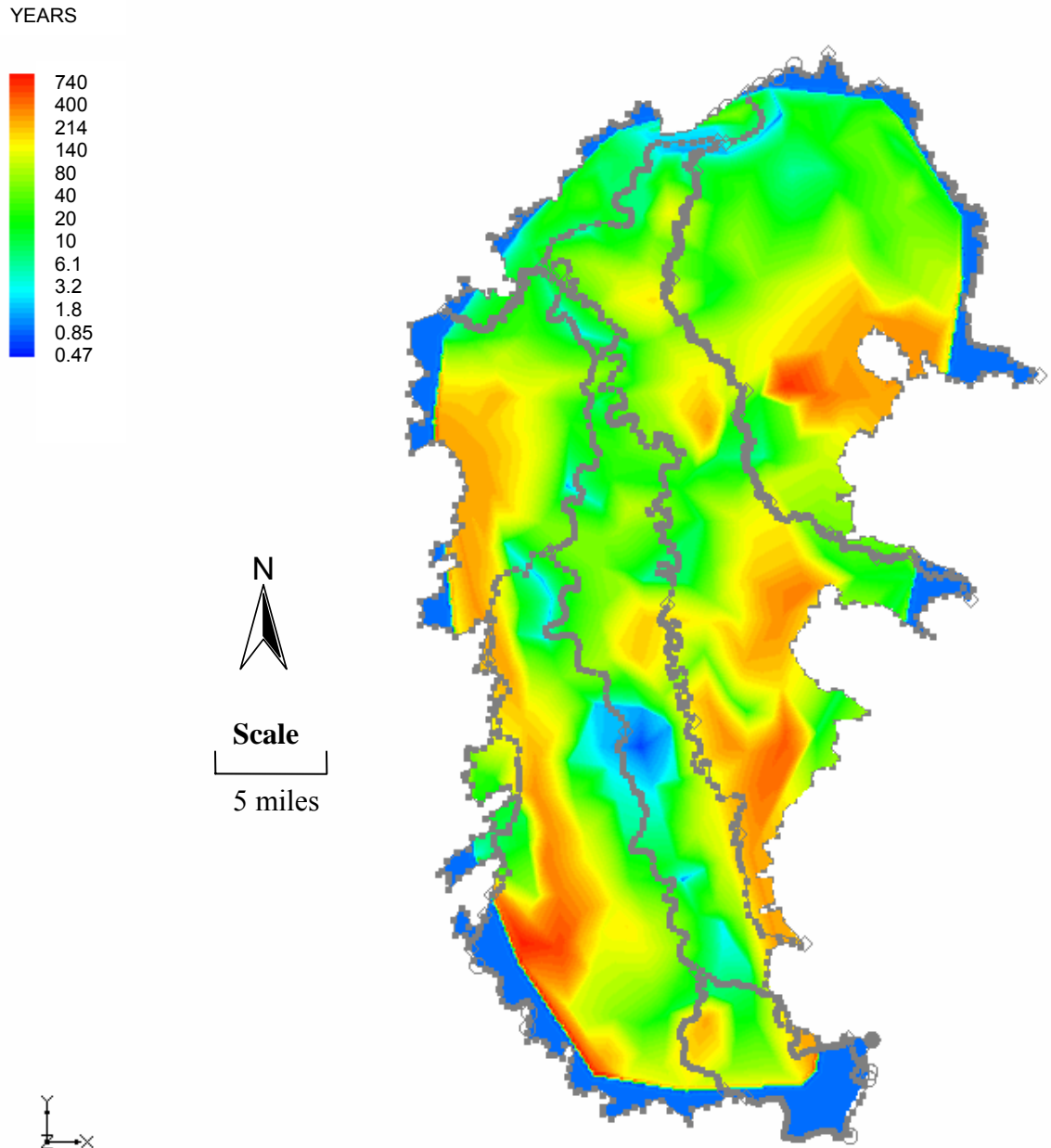
Figure 48: Spatial distribution of maximum travel times (numbers indicate the time it takes a water molecule to travel from the location indicated out of the aquifer) for the Lower Sedimentary hydrogeologic unit. This model simulation may not represent the exact maximum groundwater direction and travel time. Note: Contour coloring not uniformly spaced and blue outline near model edges due to interpolation errors.

4. DISCUSSION

Groundwater Chemistry and CFCs

Nitrate concentrations from 14 wells in the SWV ranged from 0.20 mg/L to 11.60 mg/L, with a mean concentration of 6.17 mg/L. Vick (2004) sampled 120 wells and found a mean nitrate concentration 4.81 mg/L. Studies by the ODEQ (Aitken et al., 2003; Eldridge, 2004) from 476 wells indicated nitrate concentrations from approximately 100 wells exceeding 7.0 mg/L, mostly in areas near Coburg, Junction City, Corvallis, Shedd, and Monroe. A study containing a high level of quality control by the U.S. Geological Survey sampled 30 wells in the SWV and found nitrate concentrations ranging from 3.0 mg/L to 10 mg/L in 6 wells and >10 mg/L nitrate in 4 wells. It has been shown in this study and others that groundwater nitrate concentrations in the SWV are commonly above 2 mg/L, indicating influence of anthropogenic activity ((Mueller and Helsel, 1996) and occasionally over the MCL of 10 mg/L, causing a potential health risk (U.S. Environmental Protection Agency, 2005).

Mean nitrate concentrations were greater from wells that did not penetrate Willamette Silt (8.21 mg/L) compared to wells that did penetrate Willamette Silt (2.84 mg/L). Eldridge (2004) and Vick (2004) also found this same relationship. Past studies in the SWV looked at the attenuation capabilities of the low-permeability, regionally extensive Willamette Silt. In areas where there is a reduction-oxidization (RedOx) boundary near the base of the Willamette Silt, it is thought that biochemical reactions occur where autotrophic denitrification converts nitrate into N_2O or N_2 (Iverson, 2002) and/or denitrification during ferrous iron reduction converting nitrate to nitrite abiotically (Argihi, 2004; Vick, 2004). Since the vadose zone is generally thicker where the

Willamette Silt is present and the flow of water in the unsaturated zone is usually at least one order of magnitude smaller than the groundwater flow velocity (Zoellman et al., 2001), more time is allowed for attenuation to occur. The Willamette Silt also has low dissolved oxygen concentrations and electron donors which assist denitrification. Overall lesser nitrate concentrations from wells where Willamette Silt is present in this study and others suggest that the geochemical "redoxcline" reduces nitrate concentrations to some extent and is therefore important information for local groundwater management.

The SWV contains a variety of geologic units (with varying degrees of permeability), supports a variety of land uses (mostly agricultural, followed by commercial/industrial and residential), and differing soil types and differing well characteristics that likely account for the spatial variation of nitrate concentrations of this area. Understanding of the factors that control the distribution of nitrate concentrations, nitrate transport mechanisms, and nitrate source locations are important to regional water management. Further study is needed to fully understand these factors. If denitrification does not occur and nitrate is not taken up by local crops or converted into some other form of nitrogen, excess nitrate enters the groundwater system.

Mean chloride concentrations were greater from wells where Willamette Silt is present (116.37 mg/L) compared to wells where Willamette Silt is not present (5.04 mg/L). Septic systems, pesticides, fertilizers, and marine sedimentary rock can introduce chloride into groundwater. The elevated chloride concentrations from wells that penetrated Willamette Silt are likely due to its' longer residence time and weathering reactions that occur within MSHU and Willamette Silt.

Table 19: Summary of groundwater chemistry for wells where the WSHU is present and wells where the WSHU is not present.

Parameter	Wells where Willamette Silt is present (mean)	Wells where Willamette Silt is not present (mean value)	Total number of samples
Nitrate	2.84 mg/L	**8.21 mg/L**	14
Chloride	**116.37** mg/L	5.04 mg/L	14
Sulfate	**10.32** mg/L	6.63 mg/L	14
DO	1.74 mg/L	**5.71 mg/L**	14
pH	**7.12**	6.76	14
SEC	**836** μS/cm	393 μS/cm	14

Mean sulfate concentrations were slightly greater from samples collected from wells where Willamette Silt is present (10.32 mg/L) compared to wells where Willamette Silt is not present (6.63 mg/L). Sulfate is RedOx sensitive (Hinkle, 1997), reacting under reducing or oxidizing conditions. Following reduction of oxygen, nitrate, manganese, and ferric iron in the saturated zone, sulfate is reduced (Korom, 1992). Greater sulfate concentrations where Willamette Silt exists suggest little or no reduction of sulfate occurs up gradient these sampling locations. Vick (2004) found a statistically significant trend between nitrate and sulfate (P-value <0.05). Sulfate based fertilizes are likely sources.

Mean dissolved oxygen (DO) concentrations were greater from samples collected from wells where Willamette Silt is not present (5.71 mg/L) compared to wells where

Willamette Silt is present (1.74 mg/L). Reducing conditions (<1.0 mg/L, Hinkle, 1997)

do exist at or near wells sampled beneath the Willamette Silt. This suggests that

denitrification may be occurring in the Willamette Silt. Figure 22 shows a correlation

between nitrate and dissolved oxygen (R^2 = 0.8035); Figure 23 shows a correlation

between nitrate and dissolved oxygen and well depth. In contrast, a past study by Vick

(2004) showed a weak statistical trend between nitrate and dissolved oxygen

concentrations (P-value = 0.1531).

Mean pH levels were slightly greater from samples collected from wells where

Willamette Silt is present (7.12) compared to samples collected from wells where

Willamette Silt is not present (6.76). An increase in pH, a decrease in nitrate

concentrations, and carbonate minerals precipitating out of solution was found near the

RedOx boundary at some sites in the Willamette Valley (Iverson, 2002; Arighi, 2004).

The mean pH levels slightly greater in wells that penetrated Willamette Silt may support

denitrification near a RedOx boundary. Vick (2004) found a statistically significant trend

(P-value <0.05) in nitrate and pH, as well as a statistically significant greater pH levels in

the Willamette Silt than all other geologic units.

Mean specific electrical conductance values are greater from samples collected

from wells where Willamette Silt is present (836 µS/cm) compared to wells where

Willamette Silt is not present (393 µS/cm). A portion of the greater value of specific

electrical conductance where Willamette Silt exists may be explained by chemical

weathering that may control denitrification (Argihi, 2004). This reaction results in an

increase in groundwater pH and specific electrical conductance due to loss of H^+. Vick

(2004) uses this reaction to explain, at least in part, the increased pH and specific

electrical conductance values from samples collected where Willamette Silt exists. Vick (2004) also found the greatest specific electrical conductance values from samples collected where Willamette Silt exists.

Concentration of CFCs in groundwater samples were used to determine a CFC-model age for 10 sampling locations. In the Coburg area, wells were sampled as close to one another as possible from wells that had open intervals up to 87 ft (26.5 m) below land surface (see Table 11 and Figure 26). CFC-model ages did not increase with well depth, as one would expect. This may be due to horizontal and vertical advection and dispersion, causing mixing of groundwater. One explanation for similar groundwater ages throughout the entire thickness of the sampled aquifer is a large vertical component of groundwater flow during and after recharge. Local recharge into the permeable sand and gravel aquifer may "push" older water ahead of younger water, mixing along the way until horizontal flow dominates, thus transporting relatively young water deep into the aquifer.

CFC samples collected in the Harrisburg area along a groundwater flow path showed no down gradient increase in groundwater age (see Table 11 and Figure 27). However, a transect along a groundwater flow path in the northern portion of the SWV does demonstrate an increase in CFC-model age along the flow path (Hinkle, 2005). This maybe due to the small number of samples ($N = 5$) collected for this study along the groundwater flow path. Also, shallow well depths may have resulted in sampling water above the true groundwater flow path.

CFC-model ages determined from wells where Willamette Silt is present were greater (19 years to >50 years) than CFC-model ages determined from wells where

Willamette Silt does not exist (13 years to 20 years). An estimated travel time of 25

years from the ground surface to a well 75 ft (23 m) deep for nitrate was made for the

Willamette Valley by Brandi-Dohrn (1998). Iverson (2002) estimated a conservative

travel time of approximately 23 years through the Willamette Silt where Willamette Silt

is 60 ft thick. Given the number of factors that can affect CFC-model age (see Section

3.6 and Table 10), this study has developed reasonable groundwater age estimates given

the current understanding of geological and hydrological information of the SWV.

CFC-model ages and groundwater ion concentrations can be used to reconstruct

past loading and determine long-term concentration trends. A correlation between

average CFC-model ages (used when CFC-model ages were assigned a range of ages, see

Table 11), nitrate concentration, and DO concentration was found in samples collected

from wells where Willamette Silt is present and where Willamette Silt is not present (see

Figure 49 and Figure 50). CFC samples collected from wells where Willamette Silt is

present indicate a correlation between average CFC-model ages, nitrate concentration,

sulfate concentration, and dissolved oxygen concentration (see Figure 49). CFC samples

collected from wells where Willamette Silt is not present indicate a correlation between

CFC model age, nitrate concentration, and dissolved oxygen concentration (see Figure

50). Another correlation represented on Figure 50 is CFC-model age, chloride, and

sulfate concentrations.
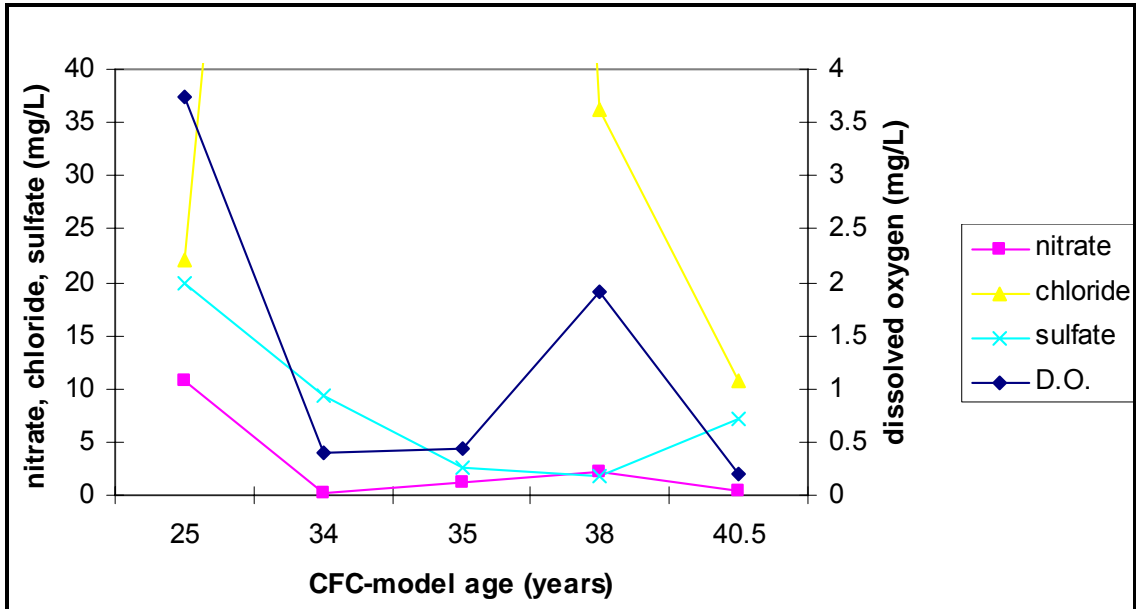
Figure 49: CFC-model age vs. nitrate, chloride, sulfate, and dissolved oxygen concentrations for samples collected where Willamette Silt is present. Lines shown are meant to guide the eye, not to interpolate between samples.
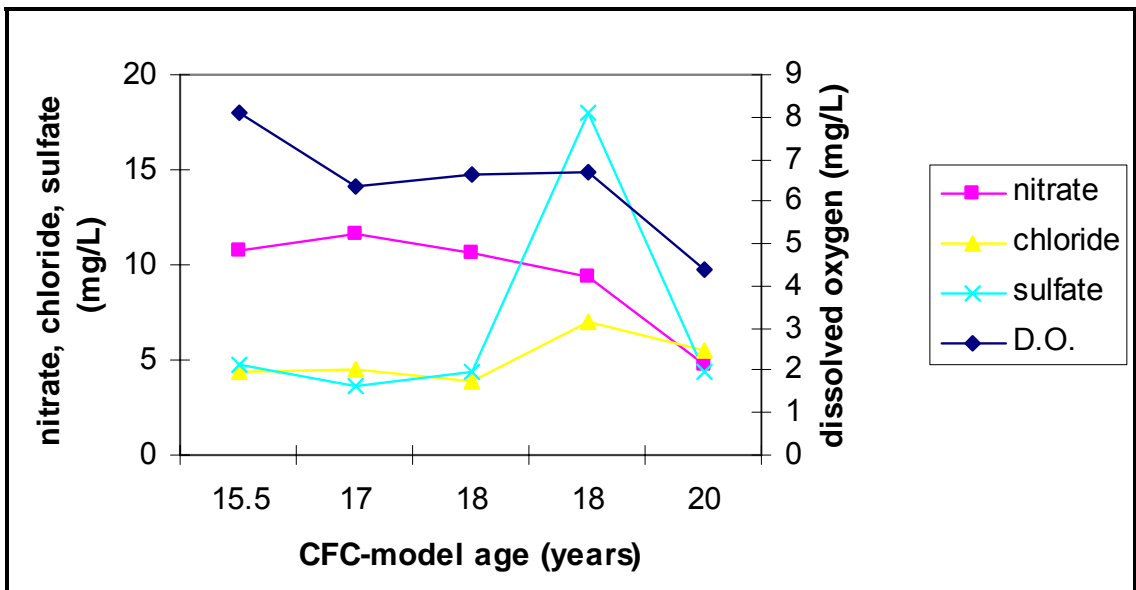
Figure 50: CFC-model age vs. nitrate, chloride, sulfate, and dissolved oxygen concentrations for samples collected where no Willamette Silt is present. Lines shown are meant to guide the eye, not to interpolate between samples.

The correlation between dissolved oxygen and nitrate concentrations indicated the possibility that denitrification may occur where Willamette Silt is present and where Willamette Silt is not present. If denitrification is not affecting nitrate concentrations, then the negative slope of nitrate concentration vs. time indicates groundwater nitrate concentrations may increase in the future. An increase in fertilizer application rates from 1945 to 1985 may also explain the greater nitrate concentrations of younger water. Sulfate concentrations track nitrate concentration where Willamette Silt exists, suggesting these RedOx sensitive species are altered with time. Chloride and sulfate concentrations are likely affected by anthopogenic sources.

Nitrate concentration and dissolved oxygen concentration show a decrease as groundwater age increases, indicating that the increase in nitrogen fertilizer application from 1945 to 1985 (Alexander and Smith, 1990) and steady increase in population within the SWV (OCS Climate Service, 2005) may be increasing groundwater nitrate levels. This data suggests that future groundwater nitrate concentrations may increase.

Future work using CFC-model ages and groundwater ion concentrations would be useful to determine past contaminant loading. Bohlke and Denver (1995) and Johnston (1994) used CFC and ^{3}H/^{3}He dating to reconstruct past nitrate loads to unconfined aquifers beneath agricultural land. This type of study would be beneficial to predict current and future contaminate loading to the local aquifer. ^{3}H/^{3}He dating of groundwater would be useful to check the accuracy of and add confidence to the CFC-model ages determined during this study and those determined in Hinkle (2005). Future sampling of CFCs at a variety of locations to determine CFC-model ages would greatly enhance understanding of groundwater flow in the SWV and aid in model calibration.

Model Parameters

Complexities exist when dealing with slug tests (see Section 3.3.2), however, they are relatively fast and inexpensive when compared to pump tests, and generally produce reasonable results. Major problems encountered while conducting the 12 slug tests included the inability to install a pressure transducer into the well casing (wellhead access difficulties), instantaneous addition or removal of water from wells with limited access, and the ability to record accurate manual measurements using an electric tape when access was limited and hydraulic conductivity high, causing the water levels in the wells to return to static levels quickly. Nonetheless, analysis using the Bouwer-Rice method resulted in reasonable estimations of K_x-values (3.95 x 10^{-2} ft/d to 4.29 x 10^2 ft/d; 3.59 x 10^{-8} m/s to 4.62 x 10^{-4} m/s). More slug tests conducted in the SWV within all hydrogeologic units (especially the WSHU and USHU) would better estimate K_x-values resulting in a more accurate groundwater model.

Three pump tests were conducted at two locations where the requirements (see Section 3.3.1) were met to develop accurate data collection. Pump test #1 and Pump test #2 were conducted at the same location. Less than expected drawdown was observed in the nearest monitoring well which made determining aquifer parameters and storage coefficients somewhat difficult. Precipitation and rising river levels during Pump test #3 resulted in even lesser drawdown than Pump test #1. However, analysis using the Neuman, Theis Match-Point, and Theis Recovery Methods produced reasonable results. These include K_x-values from 1.02 x 10^2 ft/d to 1.75 x 10^3 ft/d (3.59 x 10^{-4} m/s to 7.22 x 10^{-3} m/s), K_v-values from 9.87 x 10^{-1} ft/d to 1.00 ft/d (3.48 x 10^{-6} m/s to 3.84 x 10^{-6} m/s), and storage coefficients from 0.05 to 0.15. All hydraulic conductivity values are typical

of an unconfined sand and gravel aquifer. More pump tests conducted in the SWV within

the USHU, MSHU, and LSHU with large production wells (>500 gal/min) during the

summer when recharge and river fluctuations vary little would better estimate K_x- and K_y-

values and storativity values, resulting in a more accurate groundwater flow model.

Specific capacity (*sc*) data used to assign K_x-values to the model were

underestimated. During the model calibration process, K_x-values for the MSHU were

multiplied by 14 and K_x-value for the LSHU was multiplied by 8. The underestimation

of the initial K_x-values is likely a result of the low constant in $T = 158.48sc$ (where $T =$

transmissivity (ft^2/d) and $sc =$ (gal/min/ft); $R^2 = 0.61$) compared to the constants cited in

literature of 1500 or 2000 (Dawson and Istok, 1991), low number of wells ($N = 9$) with

both specific capacity and aquifer test information, measurement error by the well

drillers, and short duration of specific capacity tests. Future work should focus on

recently drilled wells that likely contain longer specific capacity tests.

Limited data exist in the SWV to determine seepage (gain or loss) estimates of

rivers and lakes. Recent studies attempted to quantify seepage rates along the

Willamette, Middle Fork Willamette, and South Santiam Rivers during high and low flow

conditions (Lee and Risley, 2002; Conlon et al, 2005). Nearly all measured seepage rates

did not exceed the measurement error, therefore making seepage rates unable to be

conclusively determined. Average flow rates were calculated from 07/01/04 though

07/31/05 along 4 stream reaches in the study area using gage data and used to compare to

modeled seepage rates during calibration. Due to the transient nature of seepage flux

along all rivers and stream in the SWV (including the 4 stream reaches) and the inability

of past studies to conclusively measure seepage flux, little confidence exists in the

averaged flow and seepage rates. Reasonable agreement between simulated vs. observed seepage rates along these 4 stream reaches currently exist. Future work studying groundwater/surface water interactions is vital to quantifying seepage flux. When seepage flux along rivers and streams is better quantified, seepage can be used in confidence as a much needed additional model calibration target.

Groundwater pumping within the groundwater model was assumed to occur only in the MSHU due to time constrains. Groundwater pumping is known to occur in hydrogeologic units other than the MSHU (Conlon et al., 2005). Maximum evapotranspiration (ET) was estimated as one location in the SWV. ET can vary with crop type, temperature, and groundwater elevation. Future work to more accurately estimate and assign groundwater pumping and ET would result in a more accurate groundwater model.

Recharge rate was the most sensitive model parameter tested during the model sensitivity analysis (Section 3.7.6). The recharge rate to the saturated zone was based upon taking 27 percent of the precipitation amount from 07/01/04 though 07/31/05. During this time, the SWV only received about 28 in (71 cm) of rain, well below normal. Therefore, the spatially constant recharge rate is likely underestimated. A spatially constant recharge rate applied over the entire model assumes recharge to the aquifer is constant over the entire extent of the model. This is known not to be the case (Woodward et al., 1998; Lee and Risley, 2002; and Conlon et al., 2005). The application of an accurate, spatially heterogeneous recharge flux to the water table would improve model quality.

Hydraulic conductivity fields were assigned to each model layer as accurately as possible using all available data. The MSHU contained considerable variability with distance (determined from semi-variograms). Thus, effort was spent using ordinary kriging to interpolate K_x-values throughout this unit focusing on three geologically different zones (see Section 3.7.4.3 and Appendix I). The Lebanon Fan, or proximal fan facies, does not contain greater hydraulic conductivity than the distal fan facies. The Springfield Fan, also containing proximal fan facies, does contain greater hydraulic conductivity values than the distal fan facies. The distal fan facies contains the greatest values of hydraulic conductivity. This may be due to the greater amount of lesser quality specific capacity data that lies in the distal fan facies unit or because wells that contain high specific capacity values are within past river channels. The model would benefit from future work within the MSHU, as well as the USHU and LSHU to determine hydraulic conductivity fields that best represent the hydrogeological conditions of these units.

The model during this study was developed to simulate steady-state conditions, not unreasonable considering the sustained water level elevations throughout the past 60+ years (Piper, 1942). However, a transient model would better simulate the many seasonal fluxes and water elevation changes that occur in the SWV. This would require continued collection of groundwater level measurements for an extended period of time for model calibration. Future work to collect data, organize, and calibrate a transient groundwater model would enable transient questions to be addressed.

Model Implications

Due to increasing population and little available surface water in the SWV, water quantity issues will soon emerge and the groundwater model developed during this study can be used as a tool to make water use policy decisions. Water quality issues in the SWV currently exist. Section 3.7.9 illustrates simulations that can be used to address some of the current water quality issues in the SWV. Any number of site specific simulations can be run to address certain questions. The production of the maximum travel time maps for the MSHU and LSHU of the entire SWV will be helpful when considering groundwater and land use management.

Currently, one of the most difficult questions to answer by land and groundwater managers in response to the declaration of the GWMA is: "Using groundwater sampling, how can we demonstrate that the groundwater in the GWMA is improving?" Varying land use, geologic units, and soil types affect groundwater nitrate concentrations. Transient effects like wet winters and dry summers affect recharge rates, seepage rates, and water table elevations, all of which affect groundwater nitrate concentrations to varying degrees. Using the maximum travel time maps shown in Section 3.7.9 and CFC-model ages discussed in Section 3.6, local land and groundwater managers can help to determine when to sample groundwater, how to effectively manage land that overlies relatively old vs. relatively young groundwater, and approximately how long it will take before groundwater nitrate concentrations are reduced. According to the maximum travel time map and CFC-model ages, it may take 10's of years before groundwater nitrate concentrations are reduced in some areas when local stakeholders use Best Management Practices (BMPs).

Use of the groundwater model developed during this project should be conducted with full understanding of model assumptions, error, and scale limitations.

5. CONCLUSIONS and RECOMMENDATIONS

CONCLUSIONS

(1) Pump and slug tests conducted in the alluvial aquifer produced reasonable aquifer parameter estimates. However, more aquifer test data are needed to quantify the hydraulic conductivity field in a manner that makes sense geologically.

(2) Specific capacity data can be used to develop homogeneous and heterogeneous aquifer conditions. Analysis of more data specific capacity data would improve hydraulic conductivity estimates for all hydrogeologic units.

(3) Nitrate concentrations from this study ranged from 0.20 mg/L to 11.60 mg/L with a mean concentration of 6.17 mg/L. This study and past studies have shown some groundwater in the SWV is above the maximum contaminant level.

(4) Denitrification may be occurring in portions of the SWV as indicated by correlations between nitrate, dissolved oxygen, and sulfate concentrations. Further study is needed to characterize specifically where denitrification occurs.

(5) Nitrate and dissolved oxygen concentrations were greatest from wells where Willamette Silt is not present. Chloride, sulfate, pH, and SEC were greatest from wells where Willamette Silt is present.

(6) CFC-model age does not necessarily increase along a groundwater flow path or with depth below land surface in the SWV. More groundwater age dating is needed to fully understand the residence time of groundwater in the SWV.

(7) CFC-model ages were greater in areas where Willamette Silt is present (19 years to >50 years) compared to areas where Willamette Silt is not present (13 years to 20 years).

(8) CFC-model age vs. nitrate, chloride, sulfate, and dissolved oxygen concentrations were found useful to infer past contaminant loading, observe trends, and possibly predict future ion concentrations.

(9) CFC-model ages and MODFLOW-MODPATH were found useful in model calibration.

(10) This steady-state groundwater flow model can be used to determine groundwater flow direction, groundwater velocities, help educate stakeholders, and make management decisions. This model was developed to be used for medium to large scale (generally valley scale) applications.

(11) Local geology (unit and heterogeneity) affect recharge rates and groundwater flow in the SWV.

(12) If BMPs for the SWV are followed from today forward, it may take 10's of years before local groundwater nitrate concentrations are reduced. This is important when considering how long it may take to remediate the elevated nitrate concentrations in the SWV. This is also important to mention to stakeholders when discussing how long it takes to clean-up contaminated groundwater.

RECOMMENDATIONS

1) Further study and field work is necessary to better quantify and reduce uncertainty in aquifer parameter estimates.

2) Continue to monitor groundwater, especially near local nitrate sources (CAFOs, septic tanks, and where fertilization occurs).

3) It is recommended that farmers follow BMPs supported by local studies. These include proper timing of fertilizer application and amount and proper timing of irrigation and irrigation rate. Farmers and stakeholders can save money and drink clean water if they follow the recommendations outlined in Selker and Rupp (2004); Selker (2004); Feaga et al. (2004); Vick (2004); Kite-Powell (2003); and Western Oregon Irrigation Guides (2000).

4) Continued collection of groundwater samples to determine groundwater age and groundwater chemistry is recommended. A check on the determined CFC-model ages with the ^{3}H/^{3}He method would add confidence in using CFCs as an indicator of groundwater age in the SWV.

5) Future work to the groundwater model should include focus on recharge rate and K_x- and K_v-values (recharge most sensitive model parameter according to sensitivity analysis, however, the sensitivity analysis produced skeptical results and a greater range of uncertainty in K_x- and K_v-values exists), converting the current steady-state model to a transient model, and field work to constrain seepage rates along streams and rivers of the SWV.

BIBLIOGRAPHY

Aitken, G., J. Arendt, and A. Eldridge, 2003, Southern Willamette Valley Groundwater Assessment 2000-2001 Nitrate Study, Oregon Department of Environmental Quality, Salem, Oregon, 37 p. plus appendices.

Alexander, R.B., and R.A. Smith, 1990, County-level estimates of nitrogen and phosphorus fertilizer use in the United States, 1945-1985: U.S. Geological Survey Open-File Report 90-130, 12p.

Allison, I.S., 1933, New version of the Spokane Flood, Geological Survey of America Bulletin, v. 44, pp. 675-632.

Allison, I.S., 1935, Glacial erratics in the Willamette Valley, Geological Society of America Bulletin, v. 46, pp. 615-632.

Allison, I.S., 1953, Geology of the Albany Quadrangle, Oregon, Oregon Department of Geology and Mineral Industries Bulletin 37, 20p.

Allison, I.S., 1978, Late Pleistocene sediments and floods in the Willamette Valley, The Ore Bin, v.40, pp. 177-191.

Anderson, M. P., and W.W. Woessner, 1992. Applied Groundwater Modeling: Simulation of Flow and Advective Transport., Academic Press, 381 p.

Arighi, L., 2004, Quantification of the nitrate attenuation capacity of low permeability Missoula Flood Deposits in the Willamette Valley, Oregon: M.S. thesis, Department of Geosciences, Oregon State University, 99p.

Balster, C.A., and R.B. Parsons, 1968, Geomorphology and soils, Willamette Valley, Oregon, Oregon State University Agricultural Experiment Station Special Report 265, 31p.

Balster, C.A, and R.B. Parsons, 1969, Late Pleistocene stratigraphy, southern Willamette Valley, Oregon, Northwest Science, v. 43, pp. 116-129.

Benner, P.A., and J.R. Sedell, 1997, Upper Willamette River landscape: A historic perspective, in Laenen, A., and D.A. Dunnette, River quality dynamics and resotration, Lewis Publishers, New York, 260p.

Bastasch, R., 1998, Waters of Oregon: A source book on Oregon's water and water management, Oregon State University Press, Corvallis, Oregon, 288p.

Bohlke, J.K., and J.M. Denver, 1995, Combined use of groundwater dating, chemical, and isotopic analysis to resolve the history and fate of nitrate contamination in tow agricultural watersheds, Atlantic coastal plain, Maryland. Water Resources Research, v. 31, no. 9, pp. 2319-2339.

Bozevich, Jay, Eugene Water and Electric Board, personal communication July 15, 2005.

Brandi-Dohrn, F.M., 1993, Field evaluation of passive capillary samplers in monitoring the leaching of agrochemicals: M.S. thesis, Department of Bioengineering, Oregon State University, 100p.

Bretz, J.H., 1925a, The Spokane flood beyond the Channeled Scablands, Journal of Geology, v. 33, pp. 97-115.

Bretz, J.H., 1925b, The Spokane flood beyond the Channeled Scablands II, Journal of Geology, v. 77, pp. 236-259.

Broad, T.M., and D.D. Nebert, 1990, Oregon Water Supply and Use, in National Water Summary 1987, Hydrologic Events and Water Supply and Use: U.S. Geological Survey Water-Supply Paper 2350, pp. 425-432.

Bu, X., and M.J. Warner, 1995, Solubility of chlorofluorocarbon 113 in water and seawater, Deep-Sea Res. I, v. 42, pp. 1151-1161.

Bureau of Reclamation, The AgriMet Home Page. Retrieved December 10, 2004 from http://www.usbr.gov/gp/agrimet/.

Busenberg, E., and L.N. Plummer, 1991, Chlorofluorocarbons (CCl_3F and CCl_2F_2): use as an age dating tool and hydrologic tracer in shallow ground-water systems: U.S. Geological Survey Water Resources Investigations Report 91-4034, pp. 542-547.

Busenberg, E., and L.N. Plummer, 1992, Use of chlorofluorocarbons (CCl_3F and CCl_2F_2) as hydrologic tracers and age-dating tools: the alluvium and terrace system of central Oklahoma, Water Resources Research, v. 28, no. 9, pp. 2257-2283.

Canter, L.W., 1997, Nitrates in Groundwater, CRC Press Lewis Publishers, New York, 287p.

Clemo, T., 2005, Improved water table dynamics in MODFLOW, Ground Water, pp. 270-273.

Cole, D.L., and Oregon Department of Environmental Quality, Groundwater quality report for the Willamette Basin, Oregon, March 2004, DEQ Water Quality and Labor Divisions, 75p.

Conlon, T.D., K.C. Wozniak, D. Woodcock, N.B. Herrera, B.J. Fisher, D.S. Morgan, K.K. Lee, and S.R. Hinkle, 2005, Ground-Water Hydrology of the Willamette Basin, Oregon: U.S. Geological Survey Scientific Investigations Report 2005-5168, 83p., 1pl.

Cook, P.G., and D.K. Solomon, 1995, The transport of atmospheric trace gases to the water table: Implications for groundwater dating with chlorofluorocarbons and Krypton-85, Water Resources Research, v. 31, no. 2, pp. 263-270.

Cook. P.G., and D.K. Solomon, 1997, Recent advances in dating young groundwater: chlorofluorocarbons, ^{3}H/^{3}He and ^{85}Kr, Journal of Hydrology, v. 191, pp. 245-265.

Dawson, K.J., and J.D. Istok, 1991, Aquifer Testing: Design and analysis of pumping and slug tests, Lewis Publishers, Boca Raton, Florida, 344p.

Driscoll, F.G., 1986, Groundwater and wells, Johnson Division, St. Paul Minnesota, 1089p.

Eldridge, A., 2004, Southern Willamette Valley Groundwater Summary Report, January 30, 2004, Oregon Department of Environmental Quality, 26p.

Ekwurzel, B., P. Schlosser, W.M.S. Jr., L.N. Plummer, E. Busenberg, R.L. Michel, R. Weppernig, and M. Stute, 1994, Dating of shallow groundwater: Comparison of the transient tracers ^{3}H/^{3}He, chlorofluorocarbons, and ^{85}Kr, Water Resources Research, v. 30 no. 6, pp. 1693-1708.

Epler, N.A., 1990, Chlorofluoromethanes as tracers of recent ground water on Long Island, New York, NWMA Annual Meeting, Anaheim, CA, 8p.

Feaga, J., R. Dick, M. Louie, and J. Selker, 2004, Nitrate and groundwater: Why should we be concerned with our current fertilizer practices?, Oregon State University, Agricultural Experiment Station Special Report 1050, 21p.

Fetter, C. W., 2001, Applied Hydrogeology, Fourth Edition, Prentice-Hall, Inc., New Jersey, 598p.

Frank, F.J., 1973, Ground water in the Eugene-Springfield area, southern Willamette Valley, Oregon: U.S. Geological Survey Water Supply Paper 2018, 65p.

Frank, F.J., 1974, Ground water in the Corvallis-Albany area, central Willamette Valley, Oregon: U.S. Geological Survey Water-Supply Paper 2032, 48p.

Frank, F.J., 1976, Ground water in the Harrisburg-Halsey area, southern Willamette Valley, Oregon: U.S. Geological Survey Water-Supply Paper 2040, 45p.

Freeze, J.A., and J.A. Cherry, 1979, Groundwater, Englewood Cliffs, Prentice-Hall, New Jersey, 604p.

Gannett, M.W., and R.R. Caldwell, 1998, Geologic Framework of the Willamette Lowland Aquifer System, Oregon and Washington: U.S. Geological Survey Professional Paper 1424-A, 32p., 8pl.

Gannett, M.W., and D.G. Woodward, 1997, Groundwater and surface-water relations in the Willamette Valley, Oregon, in Laenen, A., and D.A. Dunnette, River quality dynamics and restoration, Lewis Publishers, New York, 260p.

Gardner, K.K., and R.M. Vogel, 2005, Predicting ground water nitrate concentration from land use, Ground Water, v. 43, no. 3, pp. 343-352.

Glenn, J.L., 1962, Gravel deposits in the Willamette Valley between Salem and Oregon City, Oregon, The Ore Bin, v. 24, no. 3, pp. 33-47.

Glenn, J.L., 1965, Late quaternary sedimentation and geologic history of the north Willamette Valley, Oregon, Geology Department, Oregon State University, P.h.D. dissertation, 231p.

Gonthier, J.B., 1985, Oregon Ground-Water Resources, in National Water Summary 1984, Hydrologic events, Selected Water-Quality Trends, and Ground-Water Resources: U.S. Geological Survey Water-Supply Paper 2275, pp. 355-360.

Graven, E.P., 1990, Structure and tectonics of the southern Willamette Valley, Oregon: M.S. thesis, Department of Geosciences, Oregon State University, 119p.

Harbaugh, A.W., E.R. Banta, M.C. Hill, and M.G. McDonald, 2000, MODFLOW-2000, the U.S. Geological Survey modular ground-water model, User guide to modularization concepts and the Ground-Water Flow Process, U. S. Geological Survey, Denver, Colorado, 121p.

Hill, M.C., 1998, Methods and guidelines for effective model calibration: U.S. Geological Survey Water-Resources Investigations Report 98-4005, 90p.

Hill, M.C., 2003, Preconditioned conjugate-gradient 2 (PCG2), a computer program for solving ground-water flow equations: U.S. Geological Survey Water-Resources Investigations Report 90-4048, 25p.

Hinkle, S.R., 1997, Quality of Shallow Ground Water in Alluvial Aquifers of the Willamette Basin, Oregon, 1993-95: U.S. Geological Survey Water-Resources Investigations Report 97-04082-B, 48p.

Hinkle, S.R., and D.T. Snyder, 1997, Comparison of chlorofluorocarbon-age dating with particle-tracking results of a regional ground-water flow model of the Portland Basin, Oregon and Washington: U.S. Geological Survey Water Supply Paper 2483, 45p.

Hinkle, S.R., 2005, Chlorofluorocarbon-based model ages for ground water in the Willamette Basin, Oregon, in Appendix B. of Ground-Water Hydrology of the Willamette Basin, Oregon, Conlon, T.D, K.C. Wozniak, D. Woodcock, N.B. Herrera, B.J. Fisher, D.S. Morgan, K.K. Lee, and S.R. Hinkle: U.S. Geological Survey Scientific Investigations Report 2005-5168, 83p., 1pl.

Hulse, D., Gregory, S., and Baker, J, 2002, Willamette River Basin Planning Atlas, Oregon State University Press, Corvallis, OR, 178p.

Iverson, J., 2002, Investigation of the hydraulic, physical, and chemical buffering capacity of Missoula Flood Deposits for water quality and supply in the Willamette Valley, Oregon: M.S. thesis, Department of Geosciences, Oregon State University, 147p.

Johnston, C.T., 1994, Geochemistry, isotropic composition, and age of groundwater from the Waterloo Moraine: implications for groundwater protection and management: M.S. thesis, University of Waterloo, Ontario.

Johnston, C.T., P.G. Cook, S.K. Frape, L.N. Plummer, E. Busenberg, and R.J. Blackport, 1998, Ground water age and nitrate distribution within a glacial aquifer beneath a thick unsaturated zone, Ground Water, v. 36, no. 1, pp. 171-180.

Kite-Powell, A.C., 2003, An analysis of well water quality and local residents' perceptions of drinking water quality in the southern Willamette Valley, Oregon: M.S. thesis, Department of Geosciences, Oregon State University, 101p.

Korom, S., 1992, Natural denitrification in the saturated zone: A review. Water Resources Research, v.28, no. 6, pp. 1657-1668.

Kruseman, G.P., and N.A. de Ridder, 2000, Analysis and Evaluation of Pumping Test Data, second edition, ILRI, The Netherlands, 377p.

Lapham, W.W., F.D. Wilde, and M.T. Koterba, 1995, Ground-water data-collection protocols and procedures for the National Water-Quality Assessment Program: Selection, installation, and documentation of wells, and collection of related data: U.S. Geological Survey Open-File Report 95-398, 9p.

Laenen, A., and J.C. Risley, 1997, Precipitation-runoff and streamflow routing models for the Willamette River Basin, Oregon: U.S. Geological Survey Water-Resources Investigations Report 95-4284, 197p.

Leavesley, G.H., R.W. Lichty, B.M. Troutman, and L.G. Saindon, 1983, Precipitation-runoff modeling system-User's manual: U.S. Geological Survey Water - Resources Investigations Report 95-4284, 197p.

Lee, K.K, and J.C. Risley, 2002, Estimates of ground-water recharge. base flow, and stream reach gains and losses in the Willamette River Basin, Oregon: U.S. Geological Survey Water-Resources Investigations Report 01-4215, 52p.

List, R.J., 1949, Smithsonian Meteorological Tables, Sixth edition, Smithsonian Institution Press, Washington, D.C., 527p.

Mattick, Michael, Oregon Water Resources Department, Watermaster District 2 Office, written communication August 10, 2005.

McDonald, M.G., and A.W. Harbaugh, 1988, A modular three-dimensional finite-difference ground-water flow model: U.S. Geological Survey Techniques of Water-Resources Investigations, Book 6, 875p.

McDonald, M.G., and A.W. Harbaugh, 2003, The history of MODFLOW, Ground Water, v. 41, no. 2, pp. 280-283.

McDowell, P.F., 1991, Quaternary stratigraphy and geomorphic surfaces of the Willamette Valley, Oregon, in Morrison, R.B., editor, Quaternary nonglacial geology; conterminous U.S., Geological Society of America, The Geology of North America, v. K-2, pp. 156-164.

Meier, P.M., J.Carrera, and X. Sanchez-Villa, 1999, A numerical study on the relationship between transmissivity and specific capacity in heterogeneous aquifers, Ground Water, v. 37, no. 4, pp. 611-617.

Mueller, D.K., and D.R. Helsel, 1996, Nutrients in the nation's waters-Too much of a good thing? U.S. Geological Survey Circular 1136.

NAAS, 2002, National Agricultural Statistics Service, 2002 Census of Agriculture, v. 1, chapt. 2: Oregon County Level Data. Table 8. Accessed online December 1, 2005 from National Agricultural Statistics Service website at: http:/www.nass.usda.gov/census/census02/volume1/or/index2.htm.

Nolan, Bernard T., 2001, Relating nitrogen sources and aquifer susceptibility to nitrate in shallow ground waters of the United States, Ground Water, v. 30, no. 2, pp. 290-299.

O'Connor, J.E., A. Sarna-Wojcicki, K.C. Wozniak, D.J. Polette, and R.J. Fleck, 2001, Origin, Extent, and Thickness of Quaternary Geologic Units in the Willamette Valley, Oregon, U. S. Geological Survey Professional Paper 1620, 52p., 1pl.

Oregon Climate Service. Retrieved June 25, 2005 from http://www.ocs.oregonstate.edu/index.html.

Oregon Department of Human Services and Oregon Department of Environmental Quality, Drinking Water Protection Plans. Retrieved August 30, 2005 from http://www.deq.state.or.us/wq/dwp.dwphome.htm

Oregon Department of Environmental Quality: Water Quality Division, 2001, Southern Willamette Valley Groundwater 2000-2001 Assessment, Portland, OR, 68pp.

Oregon Statewide DEM Downloads. Retrieved December 10, 2003 from http://buccaneer.geo.orst.edu/dem/.

Orzol, L.L., K.C. Wozniak, T.R. Meissner, and D.B. Lee, 2000, Ground-water and water-chemistry data for the Willamette Basin, Oregon, U.S. Geological Survey Water-Resources Investigations Report 99-4036, 140p.

Osiensky, J.L., and R.E. Williams, 1997, Potential inaccuracies in MODFLOW simulations involving the SIP and SSOR methods for matrix solution, Ground Water, v. 35, no. 2, pp. 229-232.

Penhallegon, Ross, Oregon State University Extension Service, written communication May 5, 2004.

Piper, A.M., 1942, Ground-water resources of the Willamette Valley, Oregon: U.S. Geological Survey Water-Supply Paper 890, 194p.

Plummer, L.N., 1999, Tracing and dating young ground water: U.S. Geological Survey Report FS-134-99, 7p.

Plummer, L.N., E. Busenberg, 1999, Chlorofluorocarbons, in P.G. Cook and A.L. Herczeg, editors, Environmental Tracers in Subsurface Hydrology, Kluwer Academic Publishers, Boston, pp. 441-478.

Plummer, L.N., R.L. Michel, E.M. Thurman, and P.D. Glynn, 1993, Environmental tracers for age dating young ground water, Regional Ground-Water Quality, edited by W.M. Alley, Van Nostrand Reinhold, New York, NY, pp. 255-294.

Population Research Center, Portland State University. Retrieved July 10, 2005 from http://www.pdx.edu/prc/.

Price, D., 1967, Geology and water resources in the French Prairie area, northern Willamette Valley, Oregon: U.S. Geological Survey Water Supply Paper 1833, 98p.

Prinn, R.G., R.F. Weiss, B.R. Miller, J. Huang, F.N. Alyea, D.M. Cunnold, P.J. Fraser, D.E. Hartley, and P.G. Simmonds, 1995, Atmospheric trends and lifetime of CH_3CCl_3 and global OH concentrations, Science, v. 269, pp. 187-192.

Puckett, L.J., 1994, Identifying the major sources of nutrient water pollution, Environmental Science and Technology, v. 29, no. 9, pp. 408A-414A.

Razack, M., and D. Huntley, 1991, Assessing transmissivity from specific capacity in a large and heterogeneous alluvial aquifer, Ground Water, v. 29, no. 6, pp. 856-861.

Reilly, T.E., L.N. Plummer, P.J. Phillips, and E. Busenberg, 1994, The use of simulation and multiple environmental tracers to quantify groundwater flow in a shallow aquifer, Water Resources Research, v. 30, no. 2, pp. 421-433.

Rinella, F.A., and M.L. Janet, 1998, Seasonal and Spatial Variability of Nutrients and Pesticides in Streams of the Willamette Basin, Oregon, 1993-95, U.S. Geological Survey Water-Resources Investigations Report 97-4082-C, 57p.

Roberts, M.C., 1984, The late Cenozoic history of an alluvial fill-The southern Willamette Valley, Oregon, in Mahaney, W.C., editor, Correlation of Quaternary chronologies, Norwich, Great Britain, Geo Books, pp. 491-504.

Schwartz, Frank W., Andrews, Charles B., Freyberg, David L., Kincaid, Charles B., Konikow, Leonard F., McKee, Chester R., McLaughlin, Dennis B., Mercer, James W., Quinn, Ellen J., Rao, P., Rittman, Bruce E., Runnells, Donald D., Walsh, William J., 1990, Ground Water Models, National Academy Press, Washington D.C., 301p.

Selker, J., 2004, Irrigation system maintenance, groundwater quality, and improved production, Oregon State University Extension Service EM 8862, 4p.

Selker, J., and D. Rupp, 2004, Groundwater and nitrogen management in Willamette Valley mint production, Oregon State University Extension Service EM 8861, 5p.

Siegel, D.I., and D.T. Jenkins, 1987, Isotopic analysis of groundwater flow systems in a wet alluvial fan, southern Nepal, Isotope Techniques in Water Resource Development, Proc. Symp., Vienna, 1987, pp. 475-482.

Solomon, D.K., S.L. Schiff, R.J. Poreda, and W.B. Clarke, 1993, A validation of the $^3H/^3He$ method for determining groundwater recharge, Water Resources Research, v. 29, no. 9, pp. 2951-2962.

Sotomayor, D., and C.W. Rice, 1996, Denitrification in soil profiles beneath grassland and cultivated soils, Soil Science Society of America Journal, v. 60, pp. 1822-1828.

Spalding, R.F., and M.E. Exner, 1993, Occurrence of nitrate in groundwater: A review, Journal of Environmental Quality, v. 22, no. 3, pp. 392-402.

Stute, M., and P. Schlosser, 2000, Tritium/^{3}He measurements as calibration tools in groundwater transport modelling, Tracers and Modelling in Hydrogeology, no. 262, pp. 33-38.

Uhrich, M.A., and Wentz, D.A., 1999, Environmental Setting of the Willamette Basin, Oregon, U.S. Geological Survey Water-Resources Investigations Report 97-4082-A, 19p.

U.S. Army Corps of Engineers. Retrieved July 30, 2005 from http://www.usace.army.mil/.

U.S. Environmental Protection Agency. Retrieved June 10, 2005 from http://www.epa.gov/safewater/mcl.html

United States Geological Survey, Oregon Real-Time Data. Retrieved July 30, 2005 from http://www.usgs.gov/state/state.asp?State=OR.

Vick, C.F., 2004, Chemical and isotropic patterns of nitrate variability in the southern Willamette, Valley, Oregon: M.S. Thesis, Bioengineering Department, Oregon State University, 125p.

Volk, C.M., J.W. Elkins, D.W. Fahey, G.S. Dutton, J.M. Gilligan, M. Loewenstein, J.R. Podolske, K.R. Chan, M.R. Gunson, 1997, Evaluation of source gas lifetimes from stratospheric observations, Journal of Geophysical Research-Atmosphere, v. 102, no, D21, pp. 25543-25564.

Warner, M.J., and R.F. Weiss, 1985, Solubilities of chlorofluorocarbons 11 and 12 in water and seawater, Deep-Sea Res., v. 32, pp. 1485-1497.

Weeks, E.P., D.E. Earp, and G.M. Thompson, 1982, Use of atmospheric fluorocarbons F-11 and F-12 to determine the diffusion parameters of the unsaturated zone in the southern high plains of Texas, Water Resources Research, v. 15, pp. 1365-1378.

Wentz, D.A., B.A. Bonn, K.D. Carpenter, S.R. Hinkle, M.L. Janet, F.A. Rinella, M.A. Uhrich, I.R. Waite, A. Laenen, and K.E. Bencala, 1998, Water Quality in the Willamette Basin, Oregon, 1991-95, U.S. Geological Survey Circular 1161, 34p.

Woodward, D.G., M.W. Gannett, and J.J. Vaccaro, 1998, Hydrogeologic Framework of the Willamette Lowland Aquifer System, Oregon and Washington: U.S. Geological Survey Professional Paper 1424-B, 82p, 1pl.

Wozniak, Karl, Oregon Water Resources Department, written communication December 10, 2003.

Yeats, R.S., E.P. Graven, K.S. Werner, C. Goldfinger, T.A. Popowski, 1996, Tectonics of the Willamette Valley, Oregon, in Rogers, A.M., T.J. Walsh, W.J. Kockelman, G.R. Priest, editors, Assessing earthquake hazards and reducing risk in the Pacific Northwest, v. 1: U.S. Geological Survey Professional Paper 1560, pp. 183-222.

Yeskis, D., and B. Zavala, 2002, Ground-water sampling guidelines for Superfund and RCRA Project Managers, U.S. Environmental Protection Agency 542-S-02-001, 51p.

Zimmerman, D.L., and Zimmerman, M.B., 1991, A comparison of spatial semivariogram estimators and corresponding ordinary kriging predictors, Technometrics, v. 33., no. 1, pp. 77-91.

Zoellmann, K., W. Kinzelbach, and C. Fulda, 2001, Environmental tracer transport (^{3}H and SF_6) in the saturated and unsaturated zones and its use in nitrate pollution management, Journal of Hydrology, v. 240, pp. 187-205.

Zuber, A., S.M. Weise, J. Motyka, K. Osenbruck, and K. Rozanski, 2004, Age and flow pattern of groundwater in a Jurassic limestone aquifer and related Tertiary sands derived from combined isotope, noble gas and chemical data, Journal of Hydrology, v. 286, pp. 87-112.

APPENDICES

APPENDIX A: Analytical Instruments for CAL and TTL and Analytical Methods for
TTL

Central Analytical Laboratory (CAL) Instrumentation:

Note: Below information found at:
http://cropandsoil.oregonstate.edu/Services/Plntanal/CAL/index.html.

1. The Perkin Elmer Optima 3000DV is an inductively-coupled plasma optical emission spectrometer with a diode array detector. The dual view is capable of viewing the plasma axially for improved detection limits, or radially to provide lower matrix effects and fewer spectral interferences. Routine analysis includes P, K, Ca, Mg, Mn, Fe, Cu, B and Zn and this instrument is capable of running any ICP analyte. Contact the lab for further information.

2. The Leco CNS-2000 Macro Analyzer simultaneously determines carbon, nitrogen and sulfur in solid samples. No digestion or extraction is required. Up to 2g of ground sample can be used for maximum accuracy in heterogeneous samples.

3. The Alpkem Flow Solution with digital and monochromater detectors provides automated analysis of Total Kjeldahl N, NH_4, NO_3, Total P, or ortho-P in soil, plant and water samples. The Random Access Sampler allows simultaneous analysis of 2 analytes and automatic dilution of off-scale samples. This instrument is used primarily for low level detection in water samples.

4. The Alpkem RFA 300 provides automated analysis of Total Kjeldahl N, NH_4, NO_3, Total P, or ortho-P in soil, plant and water samples. This instrument is used primarily for higher concentration levels in soil and plant samples.

5. Waters Capillary Ion Analysis System performs separations by applying an electrical field to the sample in a capillary filled with an electrolyte.

6. Perkin Elmer 4000 atomic absorption spectrometer.

7. Perkin Elmer 372 atomic absorption spectrometer.

The Tritium Laboratory (TTL) CFC's procedures and standards

Note: Information below as well as additional information on CFC's and sampling of CFC's found at: http://www.rsmas.miami.edu/groups/tritium/ and http://water.usgs.gov/lab/.

Brief Overview:
Water samples are analyzed for CFC's using a custom built purge-and-trap gas chromatograph with electron capture detection. Briefly, water samples are purged with inert gas to remove dissolved gases. The CFC's are adsorbed from the purging gas stream onto trap held at -10° C. Once the CFC's are purged and trapped, the trap is heated to release the CFC's onto a small volume focusing trap held at -15° C. After CFC transfer is complete, the focusing trap is heated releasing the CFC's into the gas chromatograph. Separation of the CFC's is achieved on a capillary column and the compounds are detected using a electron capture detector. This method is extremely sensitive and the limit of detection for CFC-11, CFC-12 and CFC-113 is 0.007, 0.01, and 0.01 $\times 10^{-12}$ moles per kilogram of water (pmol kg^{-1}), respectively. Precision values for all three CFC's are 2 % or less. The accuracy of CFC-derived recharge ages from these measurements is $\pm$ 3 years or less.

1. LOW LEVEL ANALYSIS OF CFC-11, CFC-12 AND CFC-113 BY PURGE-AND-TRAP GAS CHROMATOGRAPHY WITH ELECTRON CAPTURE DETECTION.
   A. Sample Introduction
   Samples are introduced into a 30 ml sample loop with a custom built apparatus that uses nitrogen to push the sample out from the bottom of the bottle.
   B. Purge-and-Trap
   CFC's are purged from the sample for 4 minutes with UHP N_2 flowing at a rate of 150 mL/min. The stream of nitrogen containing the CFC's is first passed over a trap containing magnesium perclorate (removes water vapor) and Ascarite (removes hydrogen sulfide, which can interfer with CFC-12). The dry, hydrogen sulfide free gas stream is then passed over a Porapak N trap held at -10^oC which quanitatively removes the CFC's from the N_2 purge gas stream. After the 4 minute purge the main trap is isolated and electrically heated to 140° C to release the CFC's from the trapping material. Purging efficiency is checked by isolating a water sample in the purge chamber after it has been purged once and purging it a second time. Purging efficiencies are generally > 99 %.
   C. Cryofocusing
   Because of the relatively large amount of gas used to purge a sample, the CFCs spread out on the main trap as they are being purged from the water sample. If the CFCs were injected into the gas chromatograph (GC) directly from the main trap the resulting peaks would broad, diffuse and difficult to accurately quantify. Therefore the CFC's are transferred from the hot main trap to a smaller volume cryofocusing trap packed with Porapak N and held at -15^oC. The main to cryofocusing trap transfer is accomplished with UHP He flowing at 13 mL/min for 1 minute. This results in the CFC's being trapped on the cryofocusing trap in a nice tight plug.

D. Gas Chromatography

After the CFC's have been transferred to the cryofocusing trap, the trap is flashed heated electrically to 160 ^{o}C and the CFC's are transferred to the gas chromatographic column with UHP He flowing at 5 mL/min. The following chromatographic conditions are used. Column: 30 m x 0.32 mm GasPro capilliary column. Carrier Gas: He flowing at 5 mL/min, with the flow rate controlled using a mass flow controller. Column temperature: 90°C for 1 min, then 10°C/min to110^{o}C, then 15°C/min to 170°C, hold at 170° C for 1 min. As the CFCs elute from the column they are detected using an electron capture detector. The limit of detection for this method is 0.010 picomoles/Kg for CFC-11, CFC-12 and CFC-113.

E. Standards and Blanks

Gas phase standards are prepared in our laboratory. The approximate concentration of CFC-11, CFC-12 and CFC-113 in these standards is 120, 270 and 80 picomoles of the respective CFC per mole of N_2 (parts-per-trillion). One standard containing all three compounds is used to construct a calibration curve by injecting different volumes of the standard. A fixed volume sample loop is loaded with the standard and the loaded sample loop is purged-and-trapped as described above. Various combinations of 5 different volume sample loops are used to construct a calibration curve consisting of at least 10 points. A calibration curve is run at least once a week. In order to ensure that the detector response to the CFCs remains stable with time, a single volume of standard is injected after every eight unknowns.

Standards containing such low CFC concentrations are not available from NIST, therefore the standards prepared in our laboratory are calibrated against standards obtained from the Scripps Institution of Oceanography and National Oceanographic and Atmospheric Administration's Climate Monitoring and Diagnostics Laboratory. Groups at these two laboratories maintain the currently accepted absolute calibration scales used in monitoring background atmospheric levels of CFCs. These two absolute calibration scales agree to within 2 % of each other.

System blanks are determined by loading the water sample loop with UHP N_2, and then purging-and-trapping the N_2 as described above. A blank is run after every eight unknowns. Blanks generally contain undetectable amounts of CFCs.

F. Update

Periodically, usually about every six weeks, all measurements for the preceding time period are recomputed, applying statistical tests, and scrutinized for flaws in quality. This includes all measurements of unknowns, blanks, purging efficiencies, standards, etc. Only after this step is the result considered final. The results, which include CFC concentrations and derived recharge ages, are then reported in Data Releases, one for each project or job.

2. SAMPLE IDENTIFICATION AND FLOW OF INFORMATION

Water samples for CFC analysis are received and inventoried using the accompanying packing list or chain of custody supplied by the client. A computer worksheet listing sample name, volume or weight, syringe or ampule number, salinity, temperature, sample collection date, and date of arrival into lab, as well as client information, is generated. At this time, each order is given a unique job number, and each sample decimal numbered

within that job. For example, the job-sample number (CFC#), 123.05 indicates the fifth sample in the listing for job 123. The computer input is proofread, and the worksheet and labels are printed. An abbreviated copy of the worksheet listing is given to the administrative personnel to be filed with the client's records. The worksheet is used by the preparation technician to keep track of the progress of the samples. Preliminary results are recorded on this sheet as they become available through the computer. From the time the worksheet is printed, the sample is referred to by its CFC#. Labels are attached to each sample container. Once the sample is ready to be analyzed the CFC# and all other sample information is entered into the computer that controls the gas chromatograph and collects the raw data. After the sample is analyzed the computer controlling the gas chromatograph generates a database which includes all of the entered sample information along with the raw CFC peak areas. This data base also contains the information needed to calculate calibration curves and blank and efficiency corrections.

Using these procedures, every sample can be easily traced from the moment it arrives in the lab to the final result.

APPENDIX B: Precision and Accuracy Table

Matrix	Parameter	Sample container	Sample Size	Max. holding time	Lab	Precision	Accuracy	Measurement Range
Water	nitrate	screw top, plastic bottle	250 mL	24 hours	CAL	±5 %	± 0.01 mg/L	0-30 mg/L
Water	sulfate	screw top, plastic bottle	250 mL	24 hours	CAL	±5 %	± 0.1 mg/L	0-10 mg/L
Water	chloride	screw top, plastic bottle	250 mL	24 hours	CAL	± 5%	± 1 mg/L	0-100 mg/L
Water	pH	screw top, plastic bottle	250 mL	24 hours	CAL	± 5%	± 0.5	3-10.5 units
Water	Dissolved Oxygen[1]	none	none	24 hours	none	± 20%	± 0.3 mg/L	0-20 mg/L
Water	Specific electrical conductance[2]	none	none	none	none	± 2%	± 1 µS/cm	0-1999 µS/cm
Water	CFC's (CFC-11, CFC-12, CFC-113)	metal caps w/foil liner, boston round clear glass bottle	125 mL	A few months	TTL	≤ 2%	± 2-4 years	0.007, 0.01, and 0.01 x10⁻¹² moles per kilogram of water, respectively

Table B 1: Precision and Accuracy Table
[1]Dissolved oxygen measured using YSI Model 52 DO meter
[2]SEC measured using HI 8733 conductivity meter

APPENDIX C: Field Forms

OWRD WATER LEVEL INVENTORY SHEET

page _____ of _____

OWRD Logid: _____

T/R-S ABC# _____ / _____ - _____

Site name _____

State Obs Well Number _____

StartCard _____
USGS siteid _____
Well Address _____

Well Tag on well L _____
Well Tag on log L _____
Surface csg diam (in field) _____

Maximum Well Depth _____
County _____
Basin _____

Water levels: Easy / OK / Difficult   Hang-ups: Y / N at _____
Tools needed _____

Measuring Point Sketch:

Measuring Points:

Date mm/dd/yyyy	MP #	ft +/- lsd****	Description

**** feet above (+) or below (-) land surface.

Water Levels:

Flowmeter Make/Serial # →

Date mm/dd/yyyy	Time hh:mm	PSI or PDF	Hold Or Airl L	Tape Missg	Cut Or PSI	Tape Strtch	WL BMP	MP #	MP Corr	WL BLSD	Meth *od*	Stat- us**	Meas by	Math Checked	Data Entered
Comments:															
Comments:															
Comments:															
Comments:															
Comments:															
Comments:															
Comments:															

* Method: A = Airline, G = Calibrated Gage, H = Uncalibrated Gage, M = Manometer, O = Observed, R = Reported, S = Steel Tape, T = E Tape, V = Calibrated E Tape
** Status: S = Static, R = Rising, P = Pumping, F = Flowing, A = Falling, D = Dry   *** Please note flowmeter units, make and serial number

02/13/2002

OWRD RECORDER WELL INVENTORY SHEET

page _____ of _____

OWRD logid: _____

Site name _____

State Obs Well Number _____ T/R-S ABC# _____ / _____ - _____

StartCard _____ Maximum Well Depth _____

USGS siteid _____ County _____

Basin _____

Well tag on well L _____

Well Tag on log L _____

Surface csg diam (in field) _____

Measuring Points:

Date	MP #	ft +/- lsd***	Description

*** feet above (+) or below (-) land surface.

Measuring Point Sketch:

Equipment Installed:

Date	Equipment Type / Serial #	Equipment Type / Serial #	Remarks

Water Levels:

Date mm/dd/yyyy	Time h:mm	PST PD T	Manual WL Measurements (show details) BMP	Me * ' BLS	St "	Meas by	Raw Sensor Readings Before	Raw Sensor Readings After	Sensor WL Measurement (Calculated from "life line" reading) BMP	BLS	Baro	Batt Volt	DataFile	Re- set Y/N	Remarks (Use xtra lines)

Method: A = Airline, G = Calibrated Gage, H = Uncalibrated Gage, M = Manometer, O = Observed, R = Reported, S = Steel Tape, T = E Tape, V = Calibrated E Tape

* Status: S = Static, R = Rising, P = Pumping, F = Flowing, D = Falling

07/03/2001

APPENDIX D: Letter Sent to Participating Stakeholders

OSU
Oregon State
UNIVERSITY

Department of Geosciences
Oregon State University
104 Wilkinson Hall • Corvallis, Oregon 97331-5506
Tel: (541) 737-1201 • Fax: (541) 737-1200 •
www.geo.oregonstate.edu

January 18, 2004

Thank-you very much for your willingness to participate this fall with the groundwater age and chemistry study conducted as part of my masters' degree research project. Your cooperation made for an enjoyable experience. Quality data was collected that will help local groundwater management personnel make better decisions to improve overall water quality in the Southern Willamette Valley.

The results of the groundwater chemistry analysis conducted for your well was recently completed at the Oregon State University Central Analytical Lab and are as follows:

Nitrate-Nitrogen (mg/L)	
pH	
Chloride (mg/L)	
Sulfate (mg/L)	

The Maximum Contaminant Level (MCL) set by the United States Environmental Protection Agency for nitrate is 10 mg/L for public water systems. The OSU Extension Service Well Water Program recommends that private well owners with nitrate levels above 2 mg/L learn more about protecting the safety of their drinking water. You may visit their website at http://wellwater.oregonstate.edu, Gail Andrews at 541-737-6494, or see the enclosed "fact sheet" for more information.

If you have any questions about these results or my research, please contact me at 541-231-1875 or at jeremycraner@hotmail.com . Thanks again for your help.

Sincerely,

Jeremy Craner

APPENDIX E: Water Level Measurement Procedures

U.S. GEOLOGICAL SURVEY, OFFICE OF GROUND WATER
STAND-ALONE PROCEDURE DOCUMENT

TITLE: *WATER-LEVEL MEASUREMENT USING AN ELECTRIC TAPE*

NUMBER: GWPD 4

PURPOSE: To measure the depth to the water surface below a measuring point using the electric tape method.

MATERIALS & INSTRUMENTS:
1. An electric tape, also known as an "M-scope", marked at 5-foot intervals with clamped-on metal bands (figure 1). Electric tapes are commonly mounted on a hand-cranked supply reel that contains space for the batteries and some device for signaling when the circuit is closed.

2. A steel tape graduated in feet, tenths and hundredths of feet.

3. Electric tape calibration and maintenace equipment log book.

4. Pencil and eraser.

5. Water level measurements (Field), Form 9-194 (table 1).

6. Two wrenches with adjustable jaws for removing well cap.

7. Common household chlorine bleach.

DATA ACCURACY & LIMITATIONS:
1. Independent electric tape measurements of static water levels using the same tape should agree within + or - 0.04 foot for depths of less than about 200 feet.

2. For depths of about 500 feet, the maximum difference of independent measurements using the same tape should agree within + or - 0.1 foot.

3. For depths in the 2,000 foot range, the repeatability of measurements using the same tape should agree within + or - 0.5 foot (Garber and Koopman, 1968, p. 11).

ADVANTAGES:
1. Superior when water is dripping into the well or condensing on the inside casing walls which may make it impossible to get a good water mark on the chalked tape.

2. Superior in wells that are being pumped, particularly with large-discharge pumps, where the splashing of the water surface makes consistent results by the wetted-tape method impossible.

3. Superior when a series of measurements are needed in quick succession, such as in aquifer tests, because the electric tape does not have to be removed from the well for each reading.

4. Safer to use in pumping wells because the water is sensed as soon as the probe reaches the water surface and there is less danger of lowering the tape into the pump impellers.

DISADVANTAGES:
1. Gives slightly less accurate results than a steel tape. See data accuracy.

2. Harder to keep calibrated than a steel tape. Electric connections need to be maintained in good order.

ASSUMPTIONS:
1. An established measuring point (MP) exists and the distance from the MP to land-surface datum (LSD) is known (table 1). See GWPD 3 for the technical procedure document on establishing a permanent MP.

2. The MP is clearly marked and described so that a person who has not measured the well will know where to measure from.

INSTRUCTIONS:
1. Before using an electric tape in the field, calibrated it by comparing the total length of the electric tape against the length of an acceptable steel tape. An acceptable steel tape is one that is maintained, in the office, for use only for calibrating tapes. Also, check the accuracy of the position of each 5-foot interval metal band to make sure that the bands have not moved. This is especially important if the electric tape has been used for a long time or after it has been pulled hard in attempting to free the line.

2. Check the circuitry of the electric tape before lowering the probe into the well by dipping the probe into water and observe if the indicator needle deflects, indicating that the circuit is closing.Note the position the indicator needle deflects during the circuitry check.

3. Make all readings using the same deflection point on the indicator scale so that water levels will be consistent between measurements.

4. Lower the electrode probe slowly into the well until contact with the water surface (figure 1) indicates that the circuit it closed. Place the nail of the index finger on the insulated wire at the MP when the indicator needle deflects to the point you chose during the circuitry testing.

5. Partly withdraw the electric tape from the well and record the foot mark of the nearest 5-foot tape band in the `NEAREST 5-FOOT TAPE BAND' column of the water level measurements field form (#2, table 1).

6. Measure the distance from the MP mark on the insulated wire to the nearest 5-foot tape band with a graduated steel tape and record that distance in the `DIFFERENCE BETWEEN MP MARK AND NEAREST 5-FOOT TAPE MARK' column of the water level measurements field form (#3, table 1).

7. To obtain the depth to water below the MP, subtract the distance between the MP mark and the next highest 5-foot tape band, or if the nearest 5-foot tape band is lower, add the distance to the MP mark to obtain the depth to water below the MP. Record this number in the `DEPTH TO WATER FROM MP' column of the water level measurements field form (#4, table 1).

8. Apply the MP correction to get the depth to water below or above LSD. If the MP is above land surface, its height is subtracted from the water level to obtain the depth to water below land surface. If the MP is below land surface precede the MP correction value with a minus (-) sign and subtract its height from the water level to obtain the depth to water below land surface. Subtract the MP correction (#5, table 1) from the depth to water from MP (#4, table 1) and record this number in the `DEPTH TO WATER CORRECTED FOR LSD' column of the water level measurements field form (#6, table 1). If the water level is above LSD, enter the water level in feet above land surface preceded by a minus sign (-)

9. Make a check measurement by repeating steps 4 through 8. If the check measurement does not agree with the original measurement within the accuracy given under data accuracy, continue to make check measurements until the reason for the lack of agreement is determined or until the results are shown to be reliable.

10. After completing the well measurement, disinfect the electric tape by pouring a small amount of common household chlorine bleach on a clean cloth and wiping down the part of the tape that was submerged below the water surface; this will avoid possible contamination of other wells.

11. Maintain the tape in good working condition by periodically checking the tape for breaks, kinks, and possible stretch due to the suspended weight of the tape and the tape weight. Do not let the tape rub across the top of the casing because the 5-foot metal bands can become displaced; consequently, placement of the bands should be checked frequently with a steel tape.

DATA RECORDING: All calibration and maintenance data associated with the electric tape being used are recorded in its calibration and maintenance equipment log book. All data are recorded in the water level measurements field form (Form 9-194) to the appropriate accuracy for the depth being measured. See data accuracy and limitations.

REFERENCES:
1. U.S. Geological Survey level 1 training, ground-water field techniques, 1994.

2. United States, Office of Water Data Coordination, 1977 -, National handbook of recommended methods for water-data acquisition: Office of Water Data Coordination, Geological Survey, U.S. Department of the Interior, Reston, Va., chap. 2, p. 1-149.

3. Ralph C. Heath, 1983, Basic ground-water hydrology: Water Supply Paper 2220, Washington, U. S. Government Printing Office, p 72-73, .

4. Garber, M. S., and Koopman, F. C., 1968, Methods of measuring water levels in deep wells: U. S. Geological Survey TWRI, book 8, chapter A1, Washington, U. S. Government Printing

Office, p. 6-11.

5. GWPD 3, establishing a permanent measuring point, 1995.

APPENDIX F: CFC Data and Calculations from TTL

Data Release CFC05-01, Job # CFC0023

Lab ID#	Client ID	Well Name	Sampling Date	Date received	Analysis Date	Recharge Salinity	Recharge Temp oC	Water Concentration Corrected for Stripping Efficiency					
								CFC12 pmol/kg	error pmol/kg	CFC11 pmol/kg	error pmol/kg	CFC113 pmol/kg	error pmol/kg
23.01		CFC11 Dave Malpass	10/25/04	12/16/04	12/20/04	0	8	10.3	0.21	0.27	0.01	0.01	0.01
0023.01D		CFC12 Dave Malpass	10/25/04	12/16/04	12/20/04	0	8	10.32	0.21	0.3	0.01	0.02	0.01
0023.01D2		CFC13 Dave Malpass	10/25/04	12/16/04	12/20/04	0	8	10.36	0.21	0.26	0.01	0.01	0.01
23.02		CFC21 Victor Knox	10/25/04	12/16/04	12/20/04	0	8	0.51	0.01	0.5	0.01	0.01	0.01
0023.02D		CFC22 Victor Knox	10/25/04	12/16/04	12/20/04	0	8	0.52	0.01	0.65	0.01	0.02	0.01
0023.02D2		CFC23 Victor Knox	10/25/04	12/16/04	12/20/04	0	8	0.49	0.01	0.58	0.01	0.02	0.01
23.03		CFC31 Louis Dornheckel	10/26/04	12/16/04	12/20/04	0	8	0.75	0.02	0.46	0.01	0	0.01
0023.03D		CFC32 Louis Dornheckel	10/26/04	12/16/04	12/20/04	0	8	0.75	0.02	0.5	0.01	0	0.01
0023.03D2		CFC33 Louis Dornheckel	10/26/04	12/16/04	12/20/04	0	8	0.79	0.02	0.5	0.01	0	0.01
23.04		CFC41 Duane Harge	10/26/04	12/16/04	12/20/04	0	8	2.55	0.05	2.51	0.05	0.11	0.01
0023.04D		CFC42 Duane Harge	10/26/04	12/16/04	12/20/04	0	8	2.54	0.05	2.46	0.05	0.12	0.01
23.05		CFC51 Harold Makos	11/09/04	12/16/04	12/21/04	0	8	3.85	0.08	5.01	0.1	0.3	0.01
0023.05D		CFC52 Harold Makos	11/09/04	12/16/04	12/21/04	0	8	3.85	0.08	5.08	0.1	0.3	0.01
0023.05D2		CFC53 Harold Makos	11/09/04	12/16/04	12/21/04	0	8	3.83	0.08	5.06	0.1	0.31	0.01
23.06		CFC61 Gray's	11/16/04	12/16/04	12/21/04	0	8	2.71	0.05	3.86	0.08	0.19	0.01
0023.06D		CFC62 Gray's	11/16/04	12/16/04	12/21/04	0	8	2.71	0.05	3.9	0.08	0.18	0.01
0023.06D2		CFC63 Gray's	11/16/04	12/16/04	12/21/04	0	8	2.73	0.06	3.93	0.08	0.19	0.01
23.07		CFC71 Emersons	11/16/04	12/16/04	12/21/04	0	8	4.4	0.09	5.77	0.12	0.35	0.01
0023.07D		CFC72 Emersons	11/16/04	12/16/04	12/21/04	0	8	4.46	0.09	5.79	0.12	0.37	0.01
0023.07D2		CFC73 Emersons	11/16/04	12/16/04	12/21/04	0	8	4.44	0.09	5.82	0.12	0.34	0.01
0023.08D		CFC82 Hanson	11/20/04	12/16/04	12/21/04	0	8	0.83	0.02	0.3	0.01	0.01	0.01
0023.08D2		CFC83 Hanson	11/20/04	12/16/04	12/21/04	0	8	0.82	0.02	0.26	0.01	0	0.01
23.09		CFC91 McKluskie	12/14/04	12/16/04	12/21/04	0	8	4.33	0.09	5.63	0.11	0.39	0.01
0023.09D		CFC92 McKluskie	12/14/04	12/16/04	12/21/04	0	8	4.3	0.09	5.65	0.11	0.36	0.01
0023.09D2		CFC93 McKluskie	12/14/04	12/16/04	12/21/04	0	8	4.29	0.09	5.64	0.11	0.35	0.01
23.1		CFC101 Funke Dist. Well	12/14/04	12/16/04	12/21/04	0	8	4.23	0.09	6.29	0.13	0.41	0.01
0023.10D		CFC102 Funke Dist. Well	12/14/04	12/16/04	12/21/04	0	8	4.23	0.09	6.28	0.13	0.37	0.01
0023.10D2		CFC103 Funke Dist. Well	12/14/04	12/16/04	12/21/04	0	8	4.19	0.08	6.28	0.13	0.36	0.01

D in column one indicates duplicate sample, there is no charge for this analysis.

Detection limit is 0.010 pmol/kg for CFC-12 and CFC-113 and 0.005 pmol/kg for CFC-11

Data Release CFC05-01, Job # CFC0023

Lab ID#	Client ID	Well Name	Sampling Date	Equivalent Atmospheric Concentration						CFC-Derived Recharge Age In years before sampling date					
				CFC12 pmol/mol	error pmol/mol	CFC11 pmol/mol	error pmol/mol	CFC113 pmol/mol	error pmol/mol	CFC12 years	error years	CFC11 years	error years	CFC113 years	error years
23.01	CFC11	Dave Malpass	10/25/04	1718	34.4	11.6	11.6	1.1	1.4	supersaturated		45	2	37	4
0023.01D	CFC12	Dave Malpass	10/25/04	1721	34.4	12.7	12.7	2.5	1.4	supersaturated		44	2	36	4
0023.01D2	CFC13	Dave Malpass	10/25/04	1727.2	34.5	11	11.1	below detection limit		supersaturated		46	2	below detection limit	
23.02	CFC21	Victor Knox	10/25/04	84.8	1.7	21.5	21.5	below detection limit		38	2	41	2	below detection limit	
0023.02D	CFC22	Victor Knox	10/25/04	86	1.7	27.7	27.7	2.2	1.4	38	2	39	2	36	4
0023.02D2	CFC23	Victor Knox	10/25/04	82.4	1.6	25	25	2.2	1.4	38	2	40	2	36	4
23.03	CFC31	Louis Dornheckel	10/26/04	125.2	2.5	19.6	19.6	below detection limit		35	2	41	2	below detection limit	
0023.03D	CFC32	Louis Dornheckel	10/26/04	125.7	2.5	21.4	21.4	below detection limit		35	2	41	2	below detection limit	
0023.03D2	CFC33	Louis Dornheckel	10/26/04	132.5	2.6	21.2	21.2	below detection limit		35	2	41	2	below detection limit	
23.04	CFC41	Duane Harge	10/26/04	426	8.5	107.6	107.6	14.9	1.4	19	2	31	2	28	2
0023.04D	CFC42	Duane Harge	10/26/04	423.1	8.5	105.3	105.3	16	1.4	19	2	31	2	27	2
23.05	CFC51	Harold Makos	11/09/04	641.7	12.8	214.4	214.5	40.7	1.4	supersaturated		20	2	20	2
0023.05D	CFC52	Harold Makos	11/09/04	642.2	12.8	217.4	217.4	40.5	1.4	supersaturated		20	2	20	2
0023.05D2	CFC53	Harold Makos	11/09/04	638.2	12.8	216.3	216.3	41.8	1.4	supersaturated		20	2	20	2
23.06	CFC61	Gray's	11/16/04	452.1	9	165.2	165.2	26.6	1.4	17	2	25	2	23	2
0023.06D	CFC62	Gray's	11/16/04	452.8	9.1	167	167	25.1	1.4	17	2	25	2	24	2
0023.06D2	CFC63	Gray's	11/16/04	455.6	9.1	168.1	168.1	26.5	1.4	17	2	25	2	23	2
23.07	CFC71	Emersons	11/16/04	733.6	14.7	247	247	48.3	1.4	supersaturated		17	2	19	2
0023.07D	CFC72	Emersons	11/16/04	744.5	14.9	247.8	247.9	50.7	1.4	supersaturated		17	2	18	2
0023.07D2	CFC73	Emersons	11/16/04	740.1	14.8	248.8	248.8	46.7	1.4	supersaturated		17	2	19	2
0023.08D	CFC82	Hanson	11/20/04	138.1	2.8	12.9	12.9	below detection limit		34	2	44	2	below detection limit	
0023.08D2	CFC83	Hanson	11/20/04	136.2	2.7	11	11	below detection limit		34	2	46	2	below detection limit	
23.09	CFC91	McKluskie	12/14/04	721.6	14.4	240.9	240.9	53.6	1.4	supersaturated		18	2	18	2
0023.09D	CFC92	McKluskie	12/14/04	716.7	14.3	241.7	241.7	49	1.4	supersaturated		17	2	19	2
0023.09D2	CFC93	McKluskie	12/14/04	715	14.3	241.2	241.2	48.1	1.4	supersaturated		18	2	19	2
23.1	CFC101	Funke Dist. Well	12/14/04	705.1	14.1	268.9	269	55.8	1.4	supersaturated		13	2	18	2
0023.10D	CFC102	Funke Dist. Well	12/14/04	705.1	14.1	268.7	268.7	50.3	1.4	supersaturated		13	2	18	2
0023.10D2	CFC103	Funke Dist. Well	12/14/04	698.5	14	268.8	268.8	49.8	1.4	supersaturated		13	2	18	2

D in column one indicates duplicate sample,	current atmospheric value for CFC-12 is ~ 546 pmol/mol	Supersaturated indicates the equilvalent atmospheric concentration
there is no charge for this analysis.	current atmospheric value for CFC-11 is ~ 258 pmol/mol	is above the maximum observed atmospheric concentration, implying that there are additional non-atmospheric sources of the CFC.
		max. atmospheric value for CFC-11 was ~ 272 pmol/mol in 1994
		current atmospheric value for CFC-113 is ~ 80 pmol/mol
		max. atmospheric value for CFC-113 was ~ 85 pmol/mol in 1994

Table F 1: CFC Calculations from TTL

Recharge temperature and elevation values were initially supplied to TTL and

CFC-model ages calculated by staff. All CFC concentrations are reported on the

SIO1998 absolute calibration scale (Prinn et al., 2000). The atmospheric histories of the

CFCs were obtained from Prinn et al., (2000). The temperature, salinity, and pressure

dependent CFC solubilities were obtained from Warner and Weiss (1985) and Bu and

Warner (1995). The atmospheric pressure at the given recharge elevation was estimated

with the following expression from List (1949):

$$\ln P = -H/8300$$

where P is the pressure in atmospheres and H is the elevation in meters.

Once the sample has been analyzed and the concentrations of CFC-11, CFC-12, and

CFC-113 in each water sample have been determined the recharged age is calculated as

follows (from TTL lab online information):

1) Using the temperature dependent solubility function and the measured

CFC concentration in the water,"equivalent atmospheric concentration"

for each CFC is calculated using the following equation:

$$C_{EA} = C_W/F$$

where C_W = measured CFC concentration in the water sample, F is the

temperature dependent solubility constant, and C_{EA} is the equivalent

atmospheric concentration.

2) The equivalent atmospheric concentration for each compound is then

compared to a plot of atmospheric CFC concentration versus time to

determine the year in which the sample was recharged.

3) The derived recharge age for each compound is then calculated by subtracting the year of recharge from the sampling date. The recharge ages derived from each compound are then compared to each other. If no problems are detected the ages derived from each compound are averaged to determine the CFC-derived recharge age.

APPENDIX G: Pump Test Data and Example Calculations
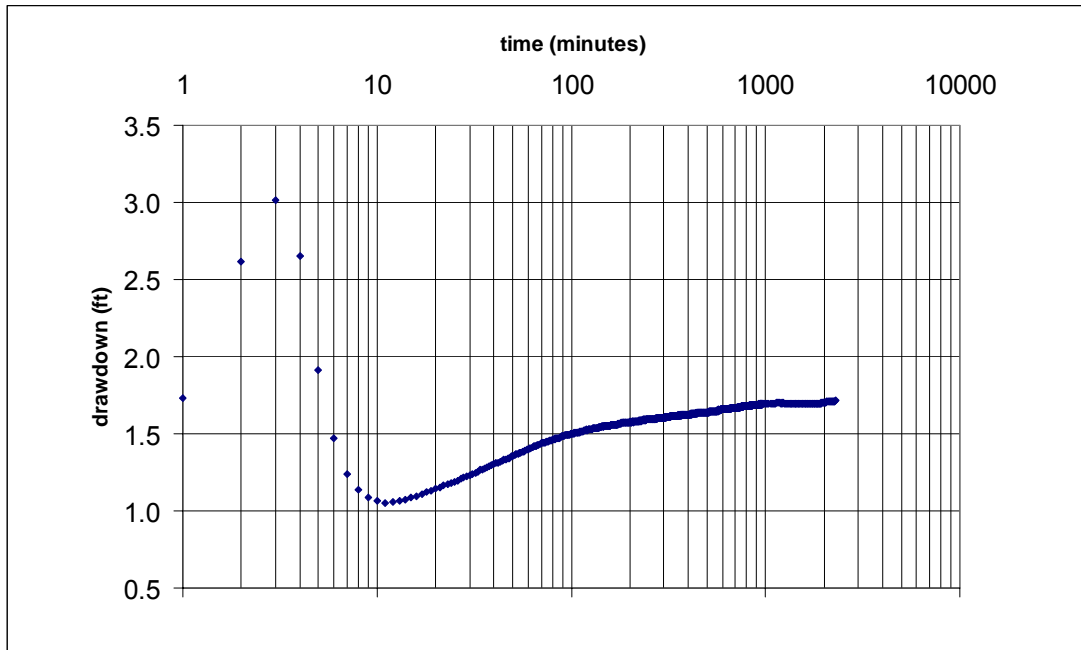
Figure G 1: Pumping well GR-2800 Drawdown vs. Time for Pump Test
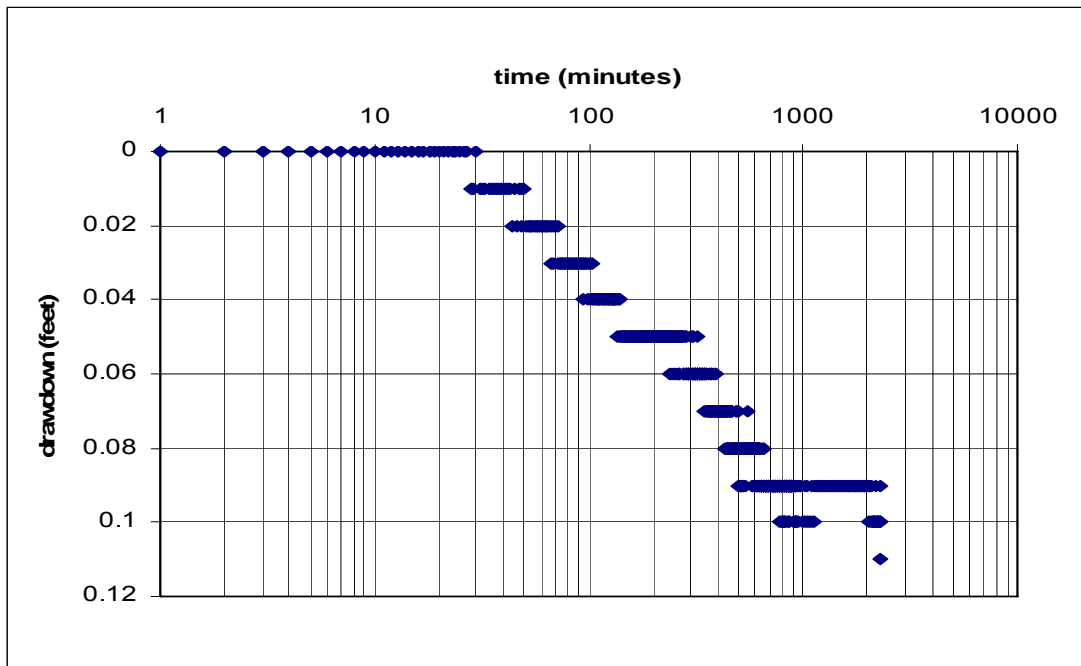
Figure G 2: Monitoring Well LINN 55017 Drawdown vs. Time for Pump Test #1
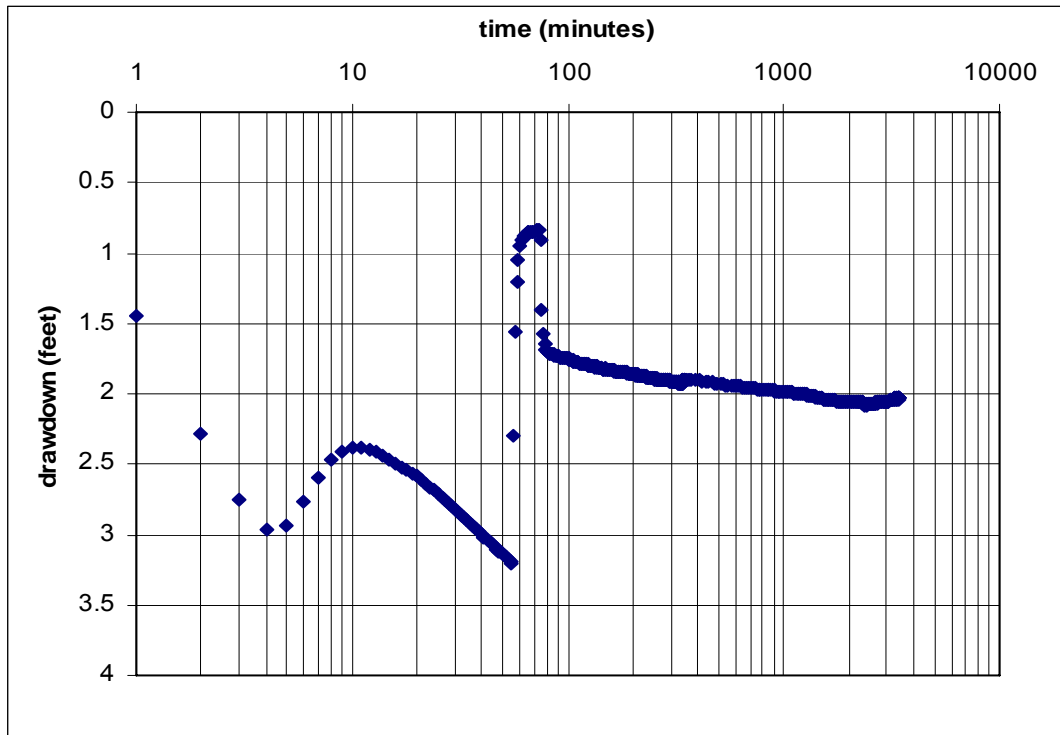
Figure G 3: Pumping Well GR-2800 Drawdown vs. Time for Pump Test #2
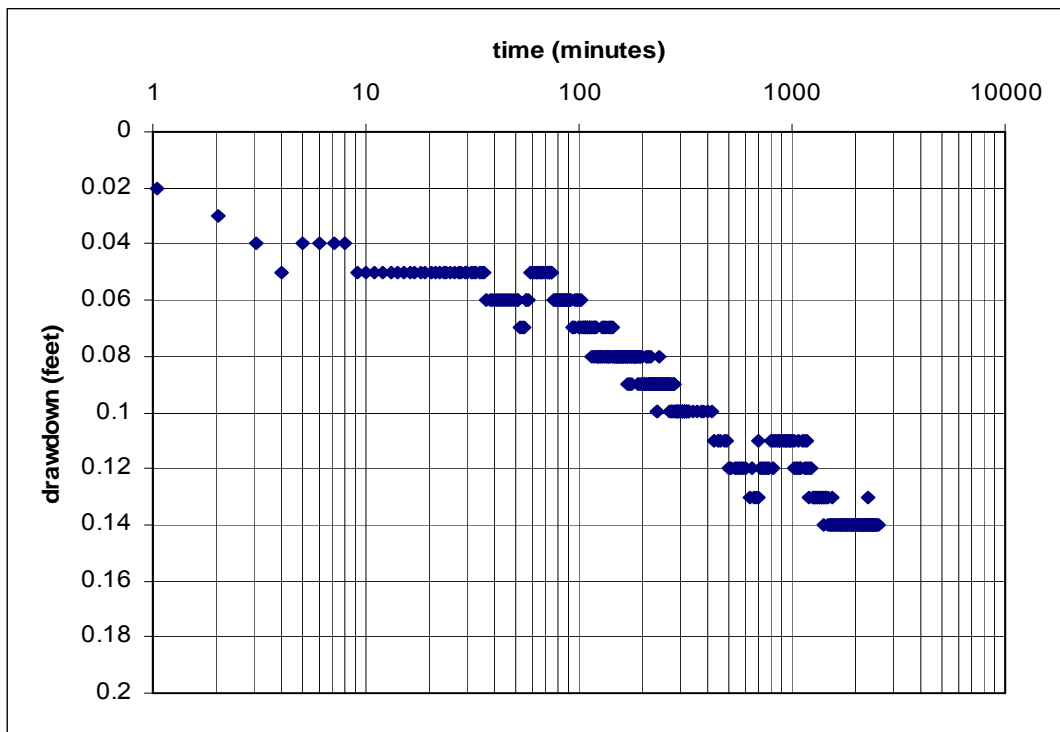
Figure G 4: Monitoring Well LINN 55017 Drawdown vs. Time For Pump Test #2
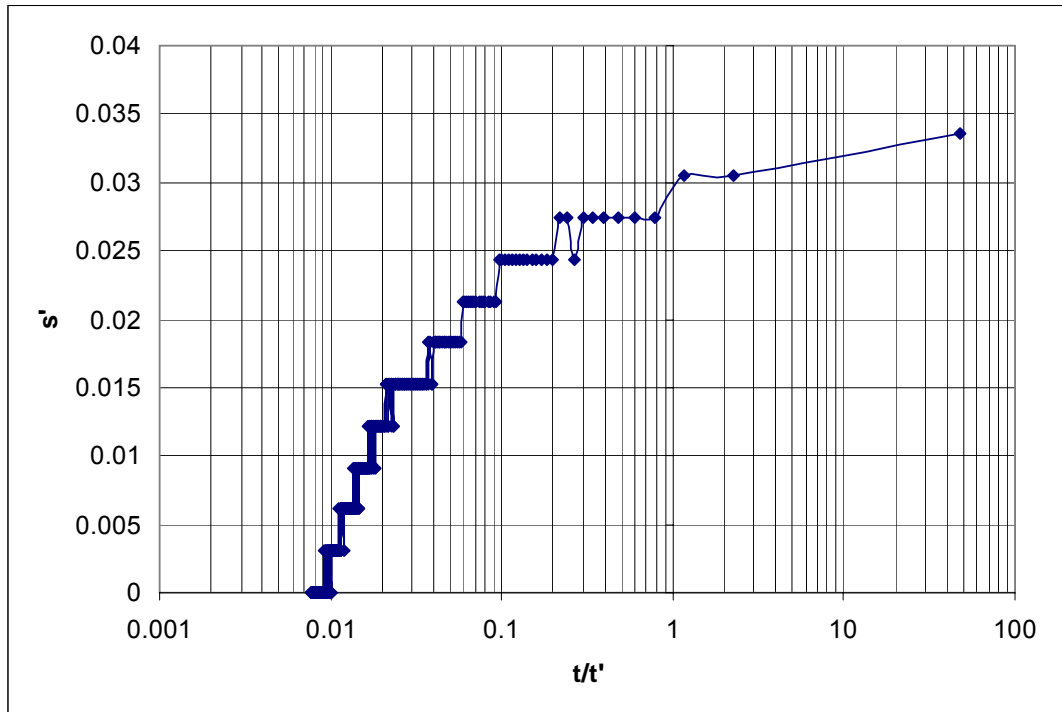
Figure G 5: Monitoring Well LINN 55017 s' vs. t/t' (Recovery Data) For Pump Test #2
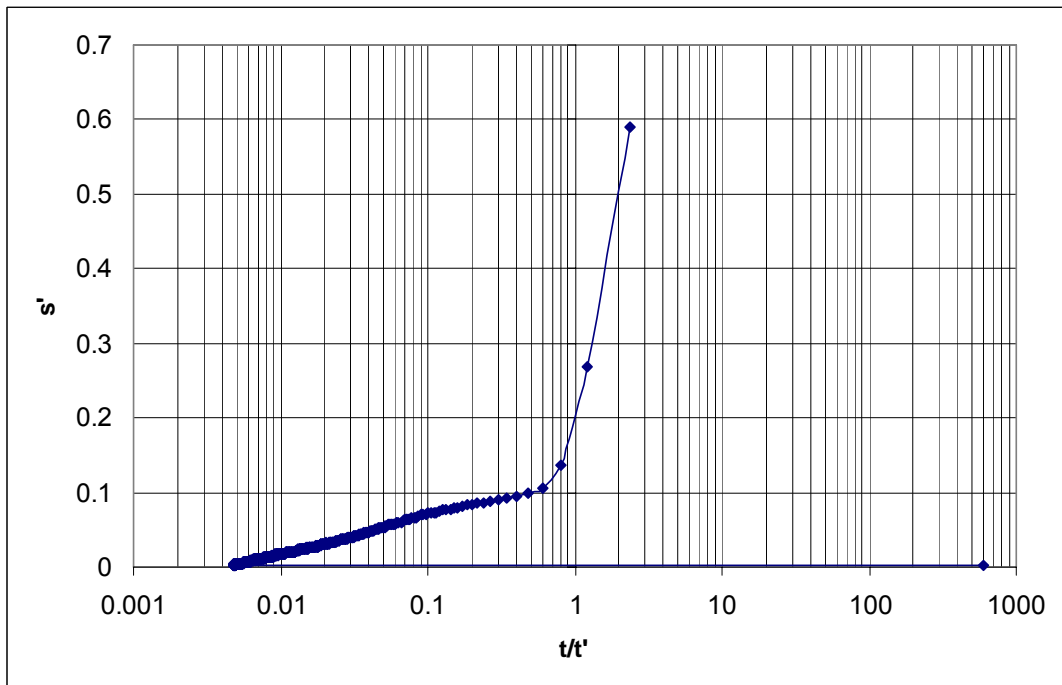
Figure G 6: Pumping Well GR-2800 s' vs. t/t' (Recovery Data) For Pump Test #2
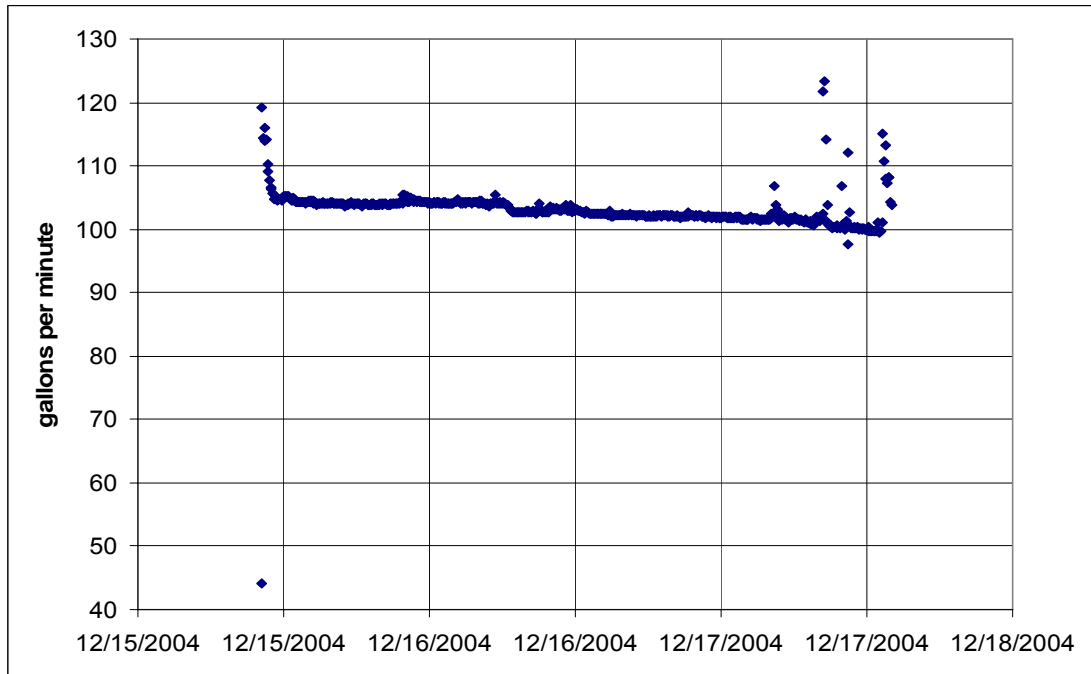
Figure G 7: Flow Rate of Pumping well during Pump Test #3
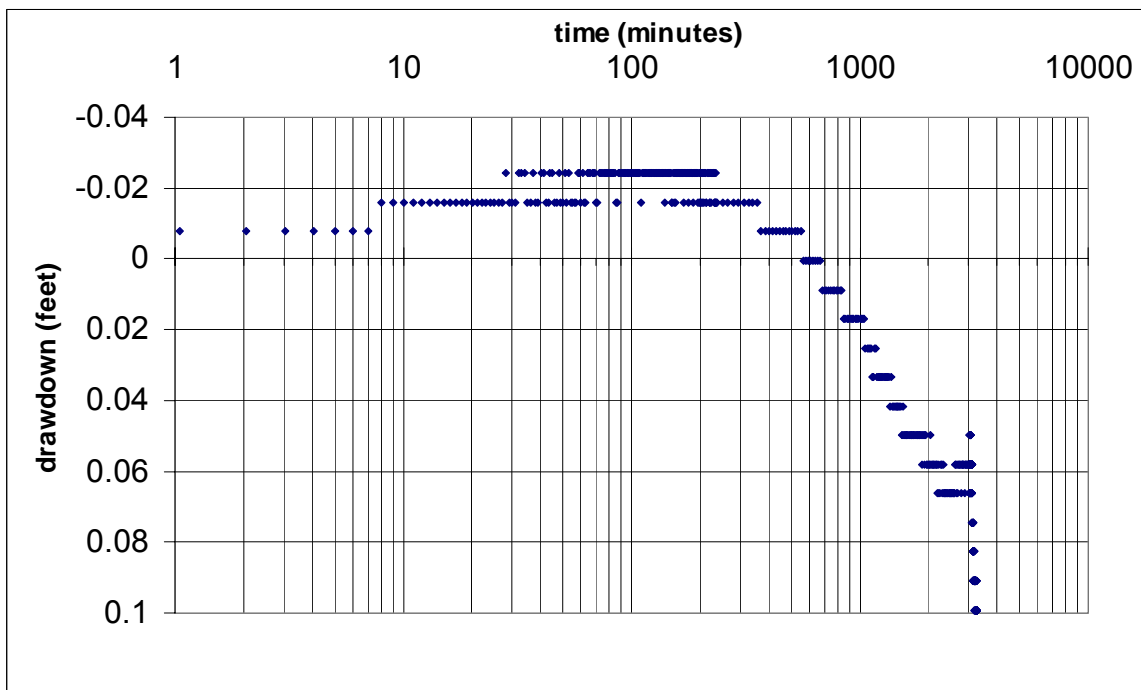
Figure G 8: Monitoring Well (Sullivan Well) Drawdown vs. Time For Pump Test #3
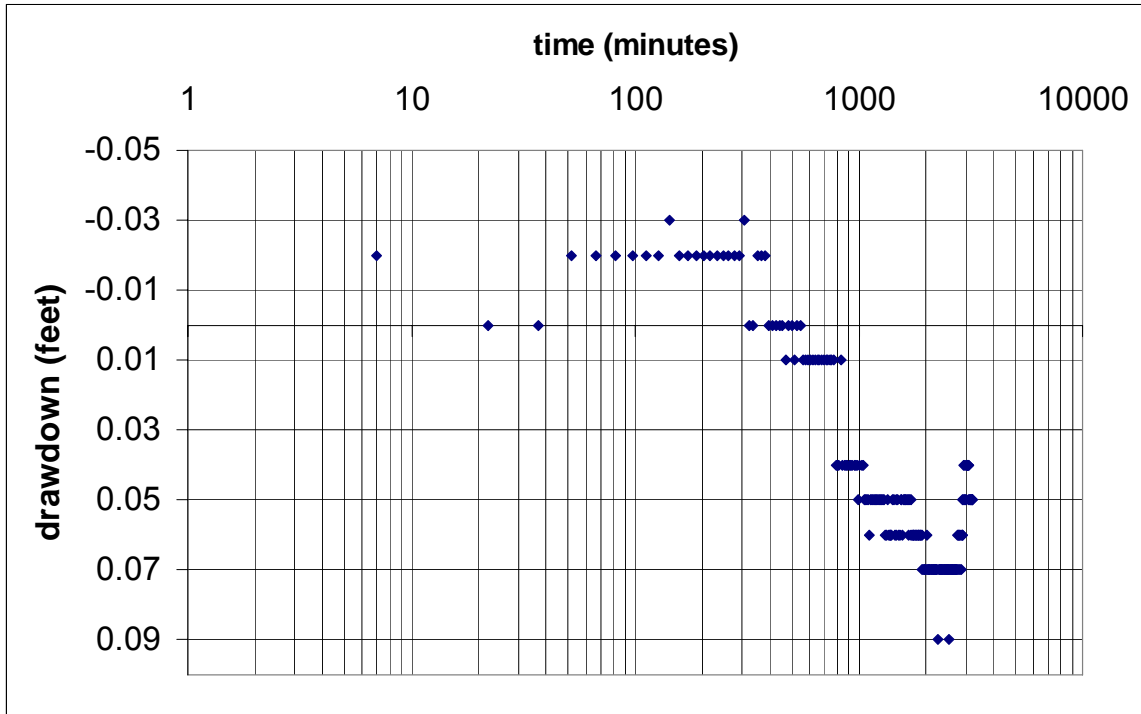
Figure G 9: Monitoring Well LANE 8069 Drawdown vs. Time For Pump Test #3

Figure G 10: Example Calculation Using the Neuman Method for LINN 55017 with Pump Test #1 Data
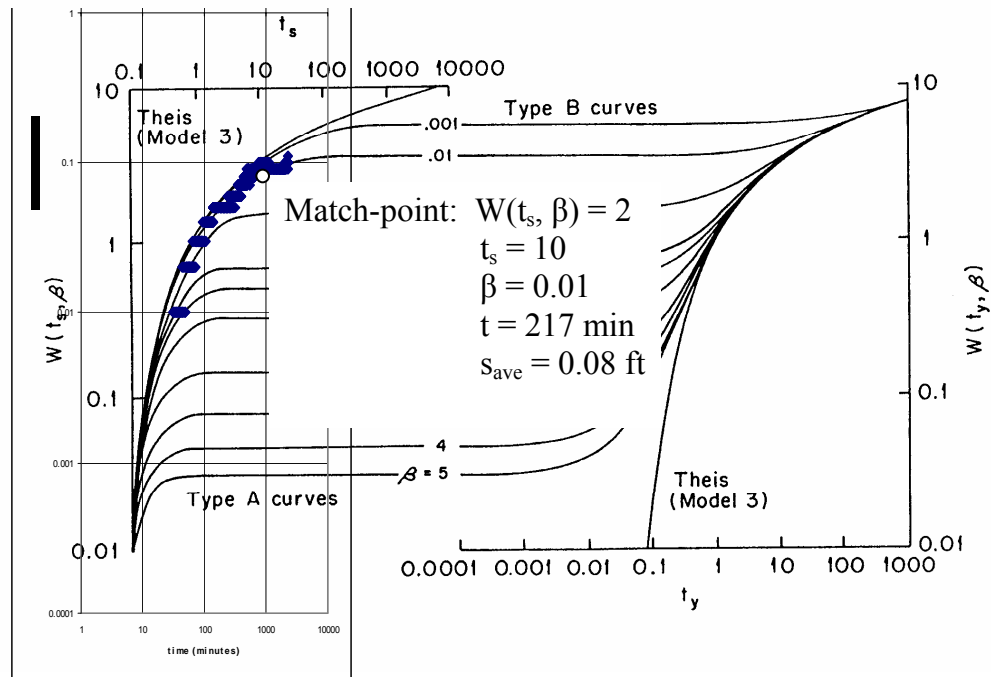
Model 13 from Dawson and Istok, (1991), did not use Model 15 due to $t > (2.5*10^3*r_c^2)/(T)$. All details and analysis can be found in Table G1.

$$T = \frac{Q*W(t_s, \beta)}{4\pi*s_{ave}} = \frac{90\,gpm*1/7.48*1440*2}{4\pi*0.08\,ft} = 36384.3827\,ft^2/day$$

$K_r = T/m = 36384.3827\,ft^2/day\,/\,22.95\,ft = 1585.376\,ft/day$

$$K_z = \frac{\beta K_r m^2}{r^2} = \frac{0.01*1585.376*22.95\,ft}{92\,ft^2} = 0.986557\,ft/day = 3.4804x10^{-6}\,m/s$$

$$S_s = \frac{Tt}{t_s mr^2} = \frac{36384.3827*217\,min}{10*22.95\,ft*92\,ft^2} = 0.00282263\ \ 1/ft$$

$S_y = S_s*m = 0.00282263*22.95ft = 0.064779$

Figure G 11: Example Calculation Using the Theis Match-point Method for Sullivan Well with Pump Test #3 Data

Match-point: s = 0.05 ft
t = 1718 min
W(u) = 1.04
1/u = 4
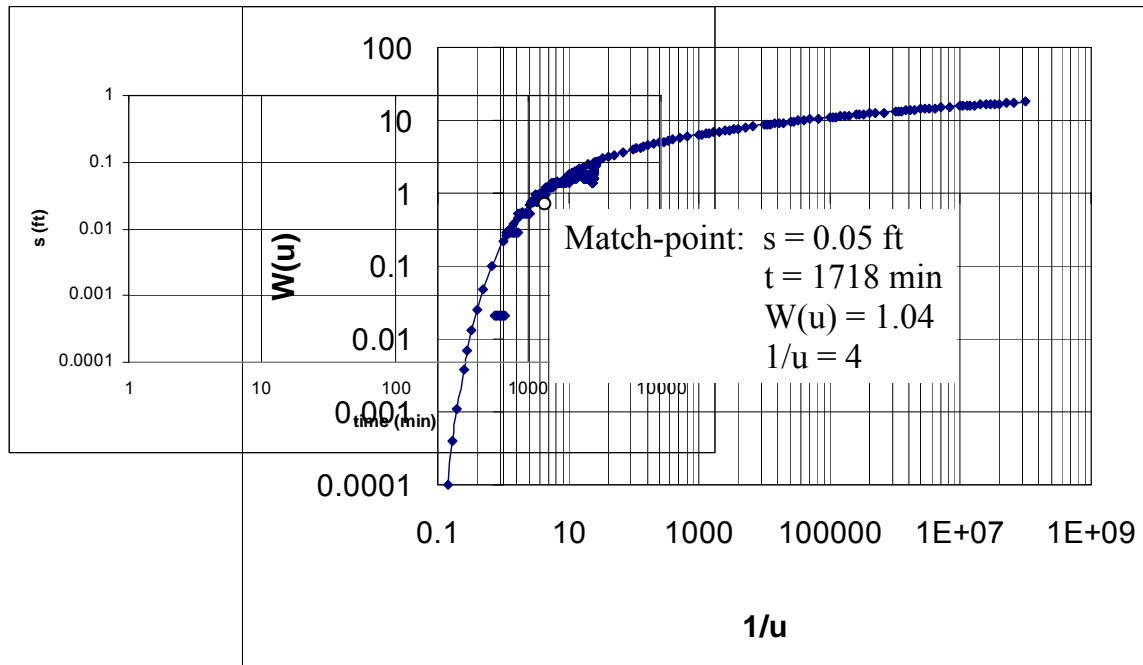
From Chapter 8 in Dawson and Istok, (1991). Other analysis can be found in Table G1.

Q = 103 gpm or 0.0065 m³/s
r = 251 ft

$$T = \frac{Q}{4\pi * s} x W(u) = \frac{103\,gpm * 1/7.48 * 1440 * 1.04\,ft}{4\pi * 0.05} = 32820.990\,ft^2 / day$$

K = T/b, where b = 50 ft so 32820.990/50 = 656.420 ft/day = 0.0023 m/s

$$S = \frac{4Tut}{r^2} = \frac{4 * 32820.990\,ft^2 / day * 1/4 * 1718\,min * 1/1440}{(251ft)^2} = 0.6215 \text{ too large}$$

Figure G 12: Example Calculation Using the Theis Recovery Method for LINN 55017 with Pump Test #2 Data
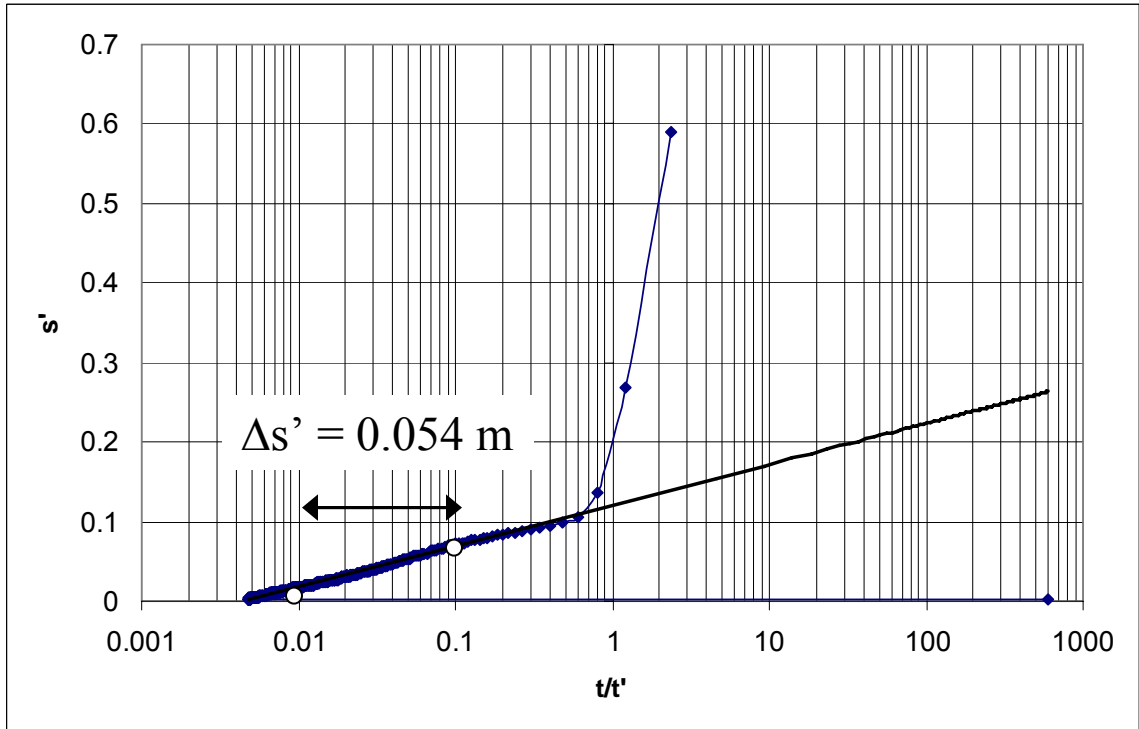
From Chapter 13 in Kruseman and de Ridder (2000). All recovery data analysis can be found in Table G1.

Δs' = 0.054 m
Q = 118 gpm or 643.217 m³/day

$$T = \frac{2.30Q}{4\pi\Delta s'} = \frac{2.30*643.217 m^3/day}{4\pi*0.054m} = 4360.798 m^2/day$$

K = T/b, where b = 7.0 *m*, so 4360.798/7.0 = 622.971 *m/day* or 0.0077 *m/s*

Note: Details regarding the Neuman match-point and Theis match-point (both used during pumping analysis) conceptual models and assumptions can be found in Chapters 18 and 19 of Dawson and Istok, (1991)

Details regarding the Theis Recovery Methods used during this study found in Kruseman and de Ridder, (2000)

TEST	OWRD well-log id	p = pumping; o = observation	r_w or r (ft)	m (ft)	W(t,B)	β		s (ft)	t (day)	T (ft²/day) [Eqn 18.19a]	T (ft²/day) [Eqn 19.18a]	K'_r (ft/day) [Eqn 19.16]	K'_r (m/s)	K_z (ft/day)	K_z (m/s)	S_s (1/ft) [Eqn 19.14]	S'_s	s (ft)	t (day)	$W_{(u)}$	1/u	T (ft²/day) [Eqn 8.5]	K (ft/day)	K (m/s)	S [Eqn 8.7]	Δs' (ft)	T (ft²/day) [Eqn 13.4]	K (ft/day)	K (m/s)
Test #1	GR-2800, no log	p	1.25	22.8	2	10	0.01	1.17	0.02	2.49E+03		1.09E+02	3.86E-04			0.107													
	LINN 55017	o	92	22.95	2	10	0.01	0.08	0.15		3.64E+04	1.59E+03	5.59E-03	0.99	3.48E-06	0.003	0.06												
	Q (gpm; m³/s) = 95; 0.0060)																												
Test #2	GR-2800, no log	p	1.25	22.8	2.5	100	0.01	1.94	0.41	2.33E+03		1.02E+02	3.59E-04			0.265													
	LINN 55017	o	92	22.95	2	10	0.01	0.09	0.17		4.02E+04	1.75E+03	6.18E-03	1.09	3.84E-06	0.004	0.08												
	Q (gpm; m³/s) = 118; 0.0074)																												
Test #3	LANE 8069	o	417	50														0.07	1.4	3	40	7.08E+04	1.42E+03	5.00E-03	0.05	0.05	2.35E+04	1.03E+03	3.62E-03
	Sullivan well	o	251	50														0.05	1.19	1.04		3.28E+04	6.56E+02	2.32E-03	0.62	0.03	4.69E+04	2.05E+03	7.22E-03
	Q (gpm; m³/s) = 103; 0.0065)																												

Equation references:
- Eqn. 18.19a; $s_w = Q/4\pi T \cdot W(t,\beta)$
- Eqn. 19.18a; $Q/4\pi T \cdot W(t,\beta)$
- Eqn. 19.16; $\beta = (r/2)^2 (K_z/K_r)$
- Eqn. 19.14; $t_s = (T \cdot t)/(S_s \cdot m \cdot r)$
- Eqn. 8.5; $T = (Q \cdot W_{(u)})/(4\pi \cdot s)$
- Eqn. 8.7; $S = (u \cdot 4 \cdot T \cdot t)/(r^2)$
- Eqn. 13.4; $\Delta s' = (2.30 \cdot Q)/(4\pi \cdot K \cdot m)$

Model 13: $t > (2.5 \times 10^3 \cdot r_c^2)/(T)$
Model 14: $t > (2.5 \times 10^3 \cdot r_c^2)/(T)$

Table G 1: Pump Test Analysis using the Neuman Match-Point, Theis Match-Point, and Theis Recovery Methods

APPENDIX H: Slug Test Data and Example Calculation
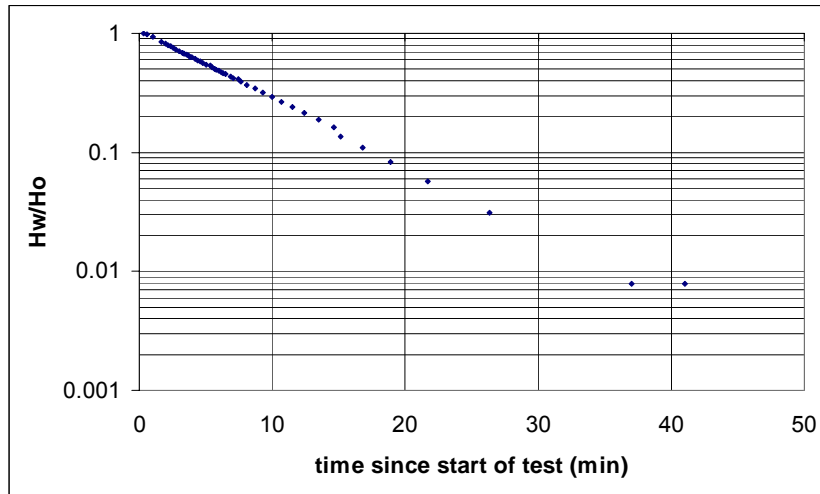
Figure H 1: Hw/Ho vs. Time for BENT 52470
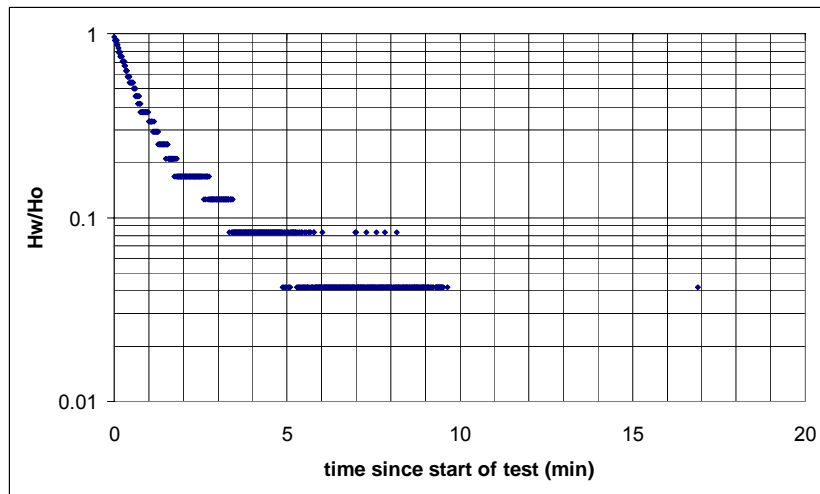
Figure H 2: Hw/Ho vs. Time for BENT 6612
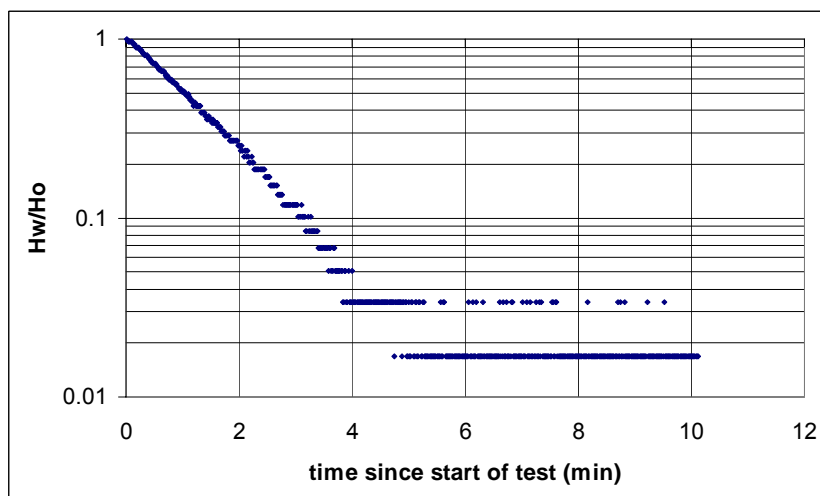
Figure H 3: Hw/Ho vs. Time for LANE 8725
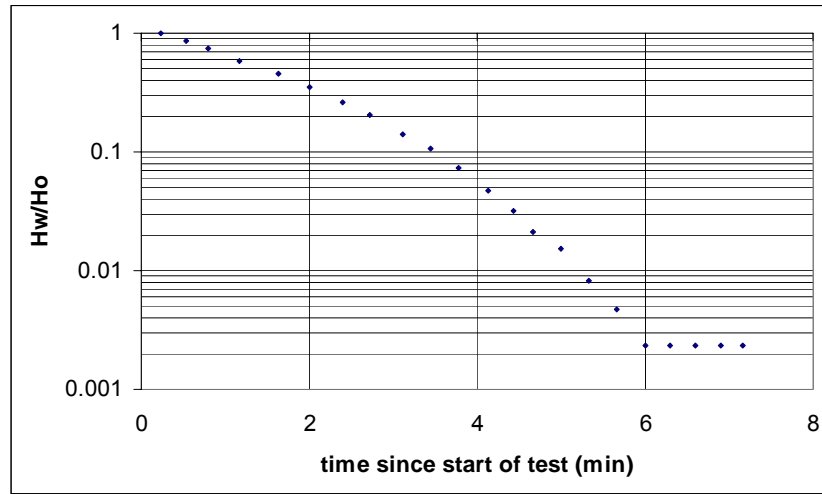
Figure H 4: Hw/Ho vs. Time for BENT 1192
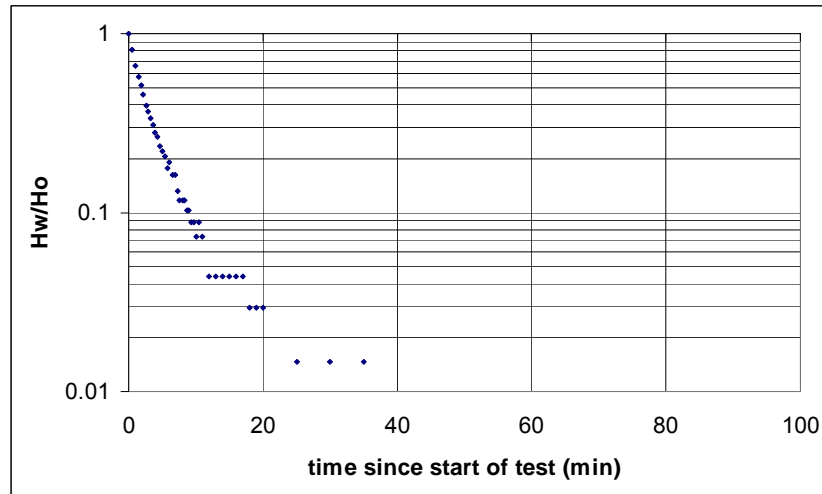
Figure H 5: Hw/Ho vs. Time for BENT 51799
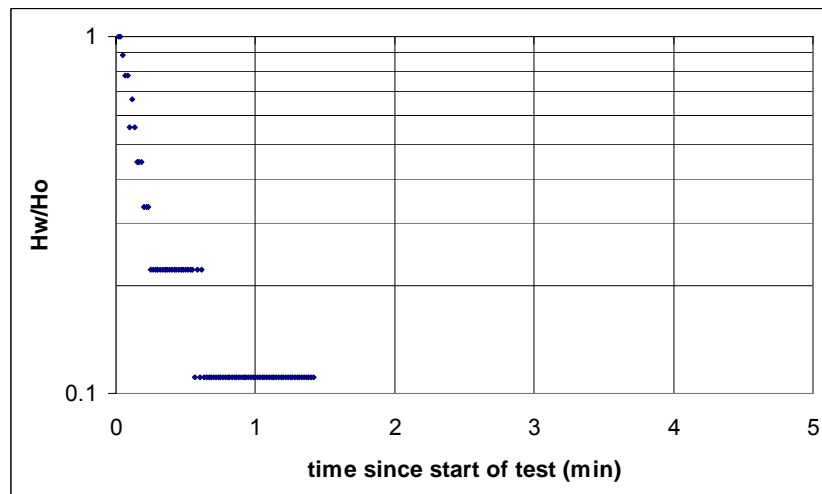
Figure H 6: Hw/Ho vs. Time for Funke Dist.
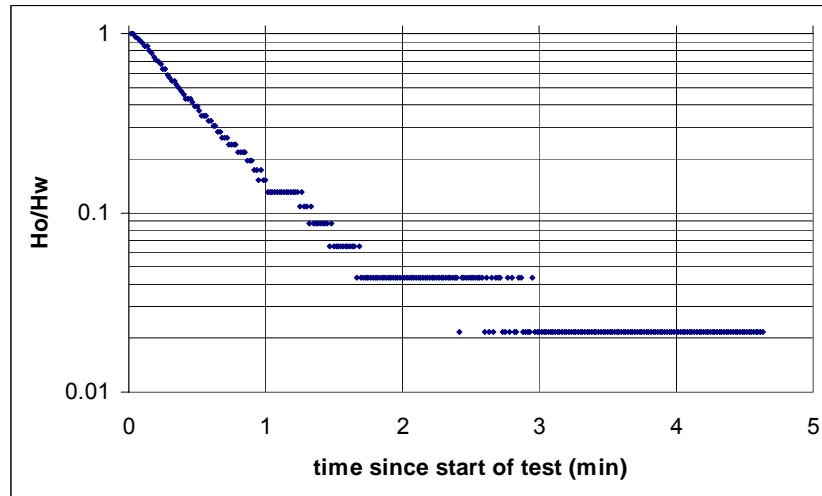
Figure H 7: Hw/Ho vs. Time for Funke phouse
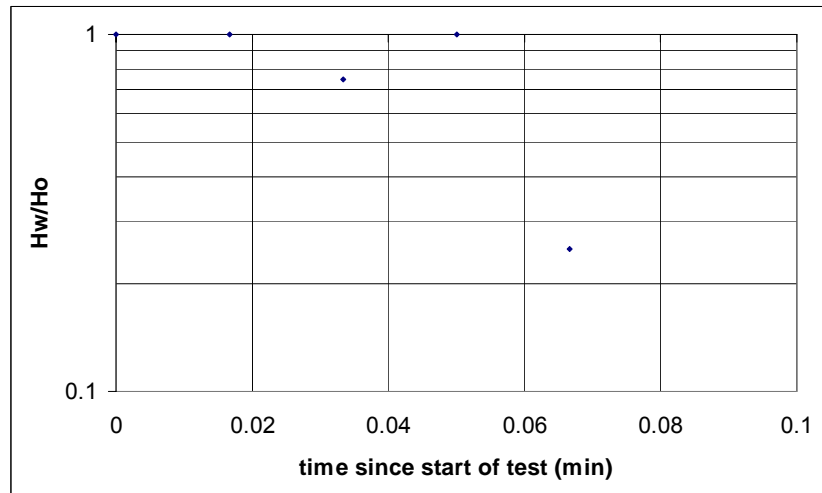
Figure H 8: Hw/Ho vs. Time for LANE 7590
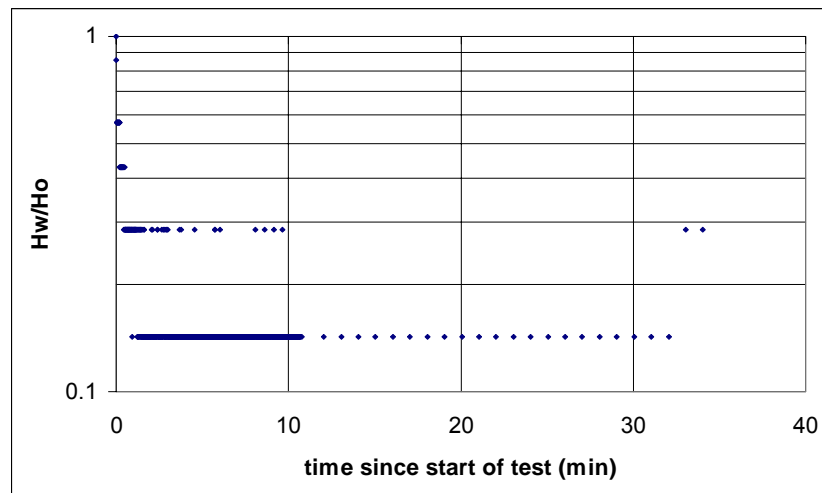
Figure H 9: Hw/Ho vs. Time for LANE 7596
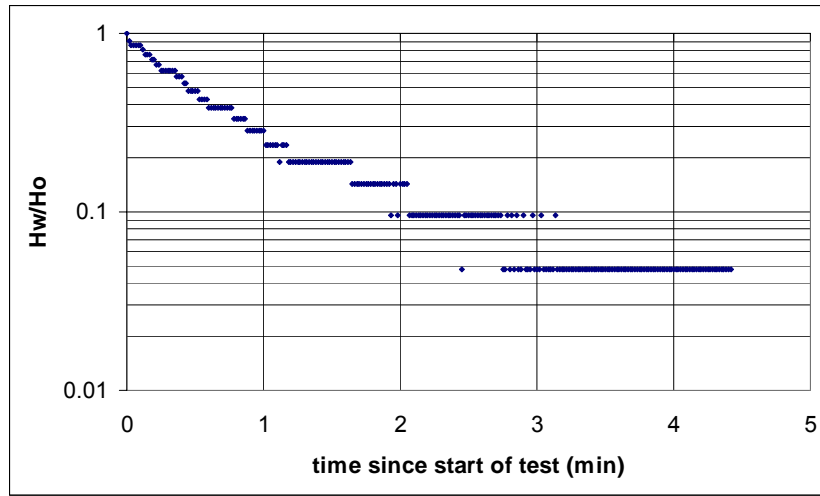
Figure H 10: Hw/Ho vs. Time for LINN 13770
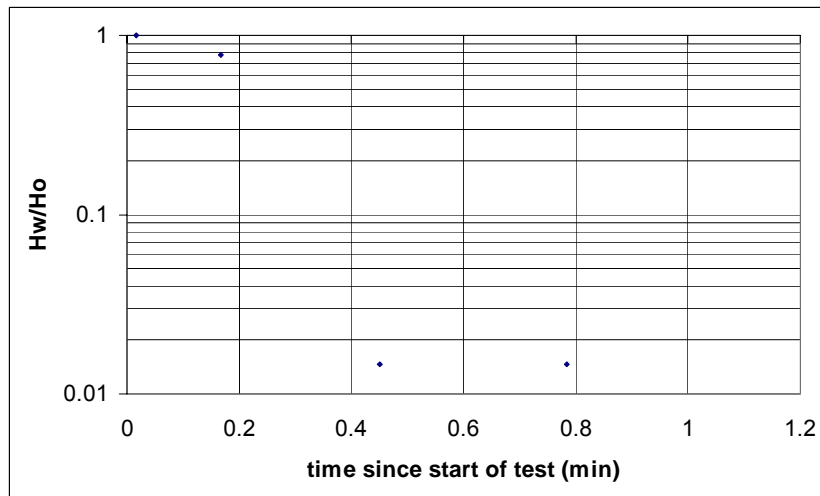
Figure H 11: Hw/Ho vs. Time for LINN 2476
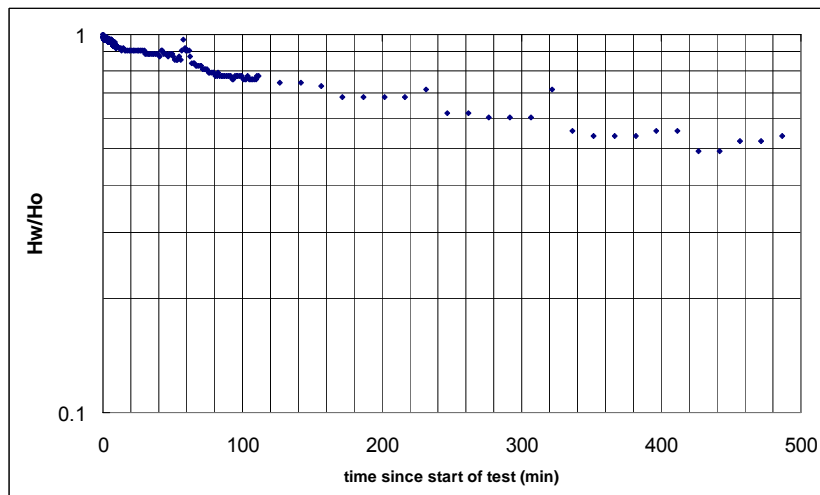
Figure H 12: Hw/Ho vs. Time for LANE 12120

Figure H 13: Example Calculation Using the Bouwer and Rice Analysis for LANE 8725
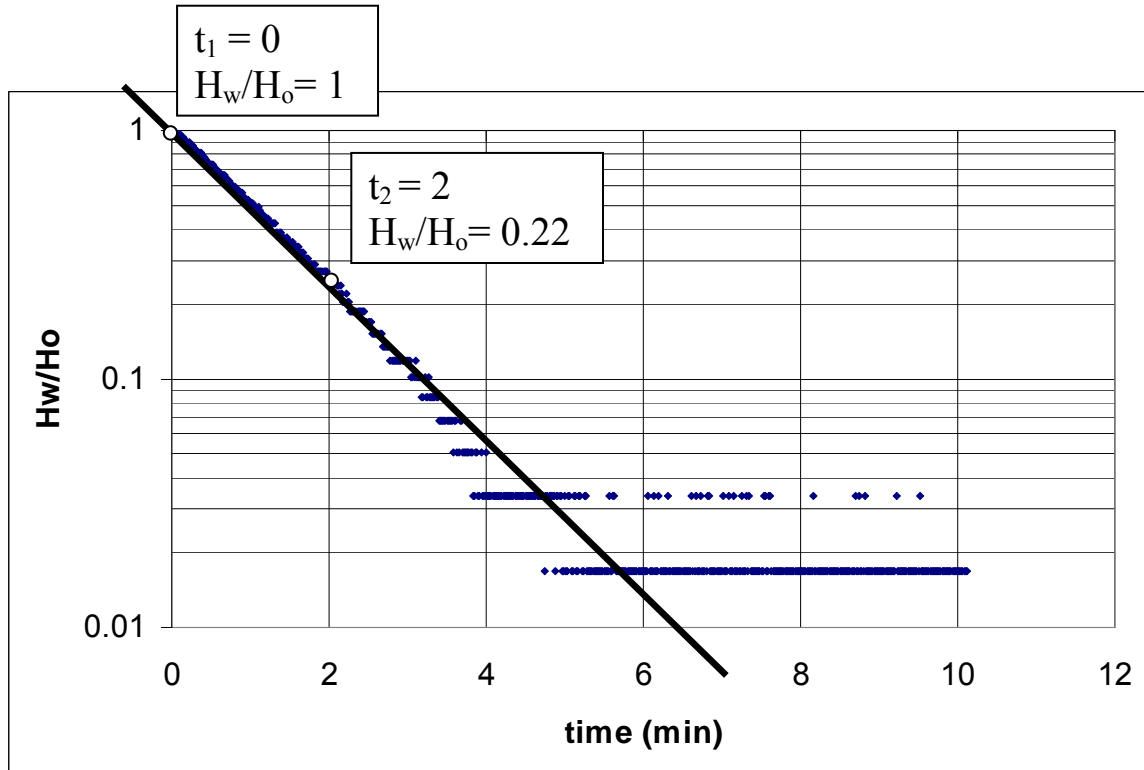
Example of Bouwer and Rice Analysis. All analysis found in Table H1.

$t_1 = 0$, $\ln(H_w/H_o) = 1$; $t_2 = 2$, $\ln(H_w/H_o) = 0.22$

$$K = \frac{r_c^2 \ln(R/r_w)}{2(l-d)t_L}$$

$$t_L = \frac{t_2 - t_1}{\ln(H_w/H_o)_2 - \ln(H_w/H_o)_1} = \frac{2-0}{\ln(0.22) - \ln(1)} = 1.3208\,\text{min} = 79.3\,\text{sec}$$

$$K = \frac{r_c^2 \ln(R/r_w)}{2(l-d)t_L} = \frac{(0.076m)^2(0.0810)}{2(8.516m - 8.440m)(79.3\,\text{sec})} = 3.89 \times 10^{-5}\,m/s$$

Note: Details regarding associated assumptions and conceptual model design found at Dawson and Istok, (1991)

English Units

OWRD well-log id	H_w (ft)	H_o (ft)	r_w (ft)	r_c (ft)	d (ft)	l (ft)	m (ft)	(l - d)/r_w	A	B	ln(m-l/r_w) <6?	ln (R/r_w)	$1/t_L = \ln(H_w/H_o)_1 - \ln(H_w/H_o)_2)/t_1 - t_2$ $1/t_L$ (1/day)	t_L (day)	Using eqn. 23.7 K (ft/day)
BENT 52470	variable	6.3	0.09	0.03	2.73	5.73	22.13	33.9	2.4	0.4	5.22	1.44	191.47	0.0052	4.48E-02
BENT 6612	variable	0.23	0.33	0.33	40.53	50.53	52.53	30	2.25	0.4	1.79	2.65	1158.75	0.0009	1.71E+01
LANE 8725	variable	0.59	0.25	0.25	27.69	27.94	97.94	1	1.9	0.25	5.63	0.08	1090.51	0.0009	1.10E+01
BENT 1192	variable	8.53	0.25	0.25	26.93	27.18	125	1	1.9	0.25	5.97	0.08	1394.7	0.0007	1.33E+01
BENT 51799	variable	0.68	0.25	0.25	67.79	87.79	187.79	80	3.85	0.7	5.99	1.89	363.77	0.0027	1.08E+00
Funke Dist. (have log, no well-log id)	variable	0.09	0.33	0.33	128.01	178.01	228.01	150	8.25	2.3	5.7	1.71	6369.43	0.0002	1.21E+01
Funke phouse (no log)	variable	0.46	0.25	0.25	64.13	64.38	147.38	1	1.9	0.25	5.81	0.08	2638.52	0.0004	2.60E+01
LANE 7590	variable	0.04	0.42	0.42	12.15	16.15	83.15	9.6	1.9	0.3	5.08	0.68	28969.55	0.0000	4.29E+02
LANE 7596	variable	0.63	0.25	0.25	248.35	249.35	289.35	4	1.85	0.25	5.08	0.35	3.56	0.2805	3.95E-02
LINN 13770	variable	0.21	0.42	0.42	31.37	41.37	43.37	24	2.1	0.4	1.57	2.48	1859.01	0.0005	4.01E+01
LINN 2476	variable	0.68	0.25	0.25	16.75	49.75	61.75	132	7.5	1.75	3.87	2.09	11052.44	0.0001	2.18E+01
LANE 12120	variable	0.63	0.25	0.25	248.35	249.35	289.35	4	1.85	0.25	5.08	0.35	3.56	0.2805	3.95E-02

SI Units

OWRD well-log id	H_w (m)	H_o (m)	r_w (m)	r_c (m)	d (m)	l (m)	m (m)	l - d/r_w	A	B	ln(m-l/r_w) <6?	ln (R/r_w)	$1/t_L$ (1/s)	t_L (s)	K (m/s)
BENT 52470	variable	1.92	0.03	0.01	0.83	1.75	6.75	33.7	2.4	0.4	5.22	1.43	0.00222	451.25	1.55E-07
BENT 6612	variable	0.07	0.1	0.1	12.35	15.4	16.01	30.3	2.25	0.4	1.8	2.66	0.01341	74.56	5.92E-05
LANE 8725	variable	0.18	0.08	0.08	8.44	8.52	29.85	1	1.9	0.25	5.63	0.08	0.01262	79.25	3.89E-05
BENT 1192	variable	2.6	0.08	0.08	8.21	8.28	38.1	1	1.9	0.25	5.97	0.08	0.01614	61.97	4.70E-05
BENT 51799	variable	0.21	0.08	0.08	20.66	26.76	57.24	80	3.85	0.7	5.99	1.89	0.00421	237.56	3.79E-06
Funke Dist. (have log, no well-log id)	variable	0.03	0.1	0.1	39.02	54.26	69.5	151.5	8.25	2.3	5.02	1.91	0.07391	13.53	4.68E-05
Funke phouse (no log)	variable	0.14	0.08	0.08	19.55	19.62	44.92	1	1.9	0.25	5.81	0.08	0.03054	32.74	9.18E-05
LANE 7590	variable	0.01	0.13	0.13	3.7	4.92	25.34	9.6	1.9	0.3	5.08	0.68	0.33530	2.98	1.52E-03
LANE 7596	variable	0.19	0.08	0.08	75.7	76	88.19	4	1.85	0.25	5.08	0.35	0.00004	24237.28	1.39E-07
LINN 13770	variable	0.06	0.13	0.13	9.56	12.61	13.22	24	2.1	0.4	1.57	2.48	0.02152	46.48	1.42E-04
LINN 2476	variable	0.21	0.08	0.08	5.11	15.16	18.82	132	7.5	1.75	3.87	2.09	0.12792	7.82	7.71E-05
LANE 12120	variable	0.19	0.08	0.08	75.7	76	88.19	4	1.85	0.25	5.08	0.35	0.00004	24237.28	1.39E-07

Table H 1: Slug Test Results using the Bouwer and Rice Method

APPENDIX I: Model Data

NOTE: Spatial locations reported in Oregon Lambert (projection) NAD 83 (datum). For information regarding conversion between Oregon Lambert and UTM projections see: http://www.oregon.gov/DAS/IRMD/GEO/coordination/projections/projections.shtml

OWRD well-log ID	x (oregon lambert ft)	y (oregon lambert ft)	K_x-value (ft/d)	Method	Source
LINN_11864	631387	992962.6875	1.7	sc*	Frank, (1976)
LINN_11949	642610.8125	979743.5	1.5	sc	Frank, (1976)
LANE_11424	640967.875	851466.9375	2.29	sc	SUB report**
BENT_1192	591559.0625	950251.25	13.34	slug test	this study
LINN_13770	619345	957271	40.09	slug test	this study
LINN_2476	619617	957911	21.85	slug test	this study
LINN_14047	633194.875	922827.625	1.63	sc	this study
LINN_8508	628479.1875	1048460	37.52	sc	this study
LINN_10562	639123.8125	1009944.25	3.39	sc	this study
BENT_961	628656.75	1065354.5	25.42	sc	this study
BENT_6693	576390.0625	968901.625	4.71	sc	this study
LINN_91	606282.4375	995042.375	12.11	sc	this study
LINN_1332	615396.625	1008651.5	10.59	sc	this study
LINN_2140	624593	944331.5	9.74	sc	this study
LINN_4146	613893.4375	1045311.813	9.93	sc	this study
LINN_8753	618987.6875	1037628.938	12.22	sc	this study
LINN_12089	627150	983550.0625	29.43	sc	this study
LINN_14111	613120.875	933607.75	1016.98	sc	this study
LINN_11952	630714.875	980948.125	25.42	sc	this study
LANE_5976	605870.625	927372.8125	30.27	sc	this study
LANE_8406	581579.3125	905982.875	6.36	sc	this study
LANE_6212	603958.9375	918260.25	12.46	sc	this study
LANE_7719	611039.875	907417.875	8.83	sc	this study
LINN_10841	595194.3125	1037560.188	26.48	sc	this study
LINN_14280	613855.125	1044073.938	31.78	sc	this study
LINN_8591	615670.1875	1045499.063	15.89	sc	this study
LINN_10484	618711.6875	1036112.375	6.05	sc	this study
BENT_1650	639135.0625	1070424.375	16.95	sc	this study
LINN_5147	640167.4375	1071438.5	7.95	sc	this study
LINN_1087	611940.3125	967904.125	7.82	sc	this study
LINN_13760	625714.9375	966109	5.04	sc	this study
LINN_13772	618386.9375	962225.3125	20.18	sc	this study
LINN_13823	602000.9375	951421.4375	29.43	sc	this study
LINN_1084	634281.125	946258.875	5.31	sc	this study
LINN_12022	606828.4375	994996.1875	4.54	sc	this study
BENT_6278	598040.4375	993445.125	29.1	sc	this study
BENT_6635	596533.4375	974528.9375	1059.36	sc	this study
LINN_10530	641641.375	1009995.813	35.86	sc	this study
LINN_10568	637709.6875	1007328.375	19.56	sc	this study

LINN_11853	640871.9375	989428.6875	38.14	sc	this study
LINN_13710	629695.0625	972199	14.45	sc	this study
BENT_6661	585758.125	970848.6875	31.16	sc	this study
LINN_12082	606542.1875	982644.6875	254.25	sc	this study
LINN_12064	611677.5	992417.5	7.53	sc	this study
LINN_14170	616637.1875	928134.6875	18.83	sc	this study
LINN_10457	611194.5	1021802.875	2.3	sc	this study
LINN_1288	614335.75	1045057.063	15.69	sc	this study
LANE_12461	608732.4375	853930.5	3.18	sc	this study
LINN_8596	614632.9375	1045466.625	8.07	sc	this study
LINN_14075	642247.0625	915521.1875	3.81	sc	this study
BENT_1567	635572.875	1070864.375	317.81	sc	this study

Table I 1: Initial hydraulic conductivity values and well information for the Middle Sedimentary hydrogeologic unit (not in Lebanon or Springfield Fans). Final optimized values were multiplied by 14.
*sc = specific capacity
**SUB report = Springfield Wellhead Protection Area Delineation Report, Lane County, Oregon, Cascade Earth Sciences, Ltd., 1996.

OWRD well-log ID	x (oregon lambert ft)	y (oregon lambert ft)	K_x-value (ft/d)	Method	Source
LINN_6902	674235.5	1043243.875	4.02	sc*	this study
LINN_7478	658492.25	1045288.938	0.92	sc	this study
LINN_10817	622646.875	1005071.438	11.24	sc	this study
LINN_12050	631470.75	998007.8125	84.75	sc	this study
LINN_50852	632128.125	1028752.125	8.47	sc	this study
LINN_6700	680982.75	1052808.375	29.43	sc	this study
LINN_50097	629901.125	1035779.813	26.48	sc	this study
LINN_10391	660970.8125	1029626.563	2.71	sc	this study
LINN_8062	680270	1018700.563	3.97	sc	this study
LINN_7378	640932.5	1055727.5	70.62	sc	this study
LINN_10719	626289	1021382.5	10.7	sc	this study
LINN_7398	635415.75	1051557.125	2.62	sc	this study
LINN_7400	634731.625	1051495.875	3.05	sc	this study
LINN_7399	634697.4375	1051598.75	9.6	sc	this study
LINN_10506	644321	1027996.625	7.43	sc	this study
LINN_10512	656646.375	1027496.375	5.3	sc	this study
LINN_7191	639874.25	1053609.375	19.86	sc	this study
LINN_1536	634327.375	1028740.938	5.53	sc	this study

Table I 2: Initial hydraulic conductivity values and well information for the Middle Sedimentary hydrogeologic unit (in Lebanon Fan). Final optimized values were multiplied by 14.
*sc = specific capacity

OWRD well-log ID	x (oregon lambert ft)	y (oregon lambert ft)	K_x-value (ft/d)	Method	Source
SP_1	659355.5625	852575.75	22	sc*	SUB report**
SP_2	660963.6875	852259.4375	12	sc	SUB report
MAIA	657759.875	852845.25	22	sc	SUB report
Q-Street	651169.25	852870.0625	4	sc	SUB report
Willamette_o	657306.9375	841030.4375	29	sc	SUB report
Weyerhaeuser	664565.4375	851617.25	675	sc	SUB report
COBURG_1	637766.0625	878808.6875	404.4	sc	LCOG, Coburg***
LANE_7553	637721.375	879166.375	26.24	sc	LCOG, Coburg
LANE_10784	659430.5625	847768.875	1.81	sc	SUB report
LANE_10977	637621.8125	876389.25	2.14	sc	SUB report
17S/3W-5aba	636814.125	876620.0625	1.51	sc	SUB report
LANE_10980	637160.3125	872581.6875	1.73	sc	SUB report
17S/3W-9dd	642698.625	867620.3125	3.03	sc	SUB report
LANE_11038	642583.25	868428	1.01	sc	SUB report
LANE_11122	646506.1875	861851.25	4.75	sc	SUB report
LANE_11292	638429.5	858505.1875	0.42	sc	SUB report
LANE_1034	651236.8125	848351.625	0.78	sc	SUB report
LANE_11567	656429	849505.4375	0.27	sc	SUB report
17S/4W-23cbd1	618237.75	859312.875	0.94	sc	SUB report
LANE_15287	660698.0625	842928.6875	0.42	sc	SUB report
17S/3W-9aaa	643275.5	871312.5	106.63	sc	SUB report
17S/4W-1acb	626199.0625	875235.5	33.9	sc	SUB report
17S/4W-12bdc	623776.0625	869927.9375	70.62	sc	SUB report
18S/2W-6dba	662428.8125	841544.125	12.22	sc	SUB report
Sullivan	615455.125	892350.6875	656	pump test	this study
LANE_8725	590818.625	888325.1875	11.04	slug test	this study
Funke_Dist	636908.5	878267.25	12.11	slug test	this study
Funke_Pumph	636889.5625	878380.75	26.02	slug test	this study
LANE_7590	634082.4375	883581.3125	429.2	slug test	this study
LANE_7596	636293.0625	880026.8125	0.04	slug test	this study
LANE_88	608247.6875	878600.0625	2.35	sc	this study
LANE_11804	611250.125	869346.3125	4.04	sc	this study
LANE_752	625851.375	893910.875	5.45	sc	this study
LANE_10761	660951.625	852257.1875	0.94	sc	this study
LANE_10801	666310.3125	849000	3.53	sc	this study
LANE_8056	602120.625	890040.5625	2.27	sc	this study
LANE_11276	636907.5	860959.25	1.67	sc	this study
LANE_3380	635196.25	893782.1875	12.73	sc	this study

Table I 3: Initial hydraulic conductivity values and well information for the Middle Sedimentary hydrogeologic unit (in Springfield Fan). Final optimized values were multiplied by 14.
*sc = specific capacity; ** SUB report = Springfield Wellhead Protection Area Delineation Report, Lane County, Oregon, Cascade Earth Sciences, Ltd., 1996.

***LCOG, Coburg = Coburg Wellhead Protection Area Delineation Report, Lane County, Oregon. Cascade Earth Science, Ltd., 1996.

OWRD well-log ID	x (oregon lambert ft)	y (oregon lambert ft)	K_x-value (ft/d)	Method	Source
I-5	645040.125	868213.5625	43	pump test/sc*	SUB report**
BENT_7065	581585.125	946885.625	20.25	pump test/sc	ODHS, Monroe***
LINN_14186	612364.0625	928627.6875	2.12	pump test/sc	ODHS, Harrisburg****
LINN_50455	612152.5	928065.4375	2.27	pump test/sc	ODHS, Harrisburg
LINN_55191	612461.1875	927962.5625	4.2	pump test/sc	ODHS, Harrisburg
LINN_56007	612191.0625	927962.5625	6.94	pump test/sc	ODHS, Harrisburg
LANE_4428	604778.75	913229.75	47.76	pump test	ODHS, Junction City*****
LANE_3357	605076.9375	912422.5	55.38	pump test	ODHS, Junction City
LANE_8367	604294.25	912769.25	20.16	sc	ODHS, Junction City
LANE_6385	605094.5	910861.6875	7.06	sc	ODHS, Junction City
LANE_6364	602358	911458.125	5.8	sc	ODHS, Junction City
LINN_13705	629518.8125	970073.125	1.72	sc	Frank, (1976)
LINN_13742	600583.8125	969143.25	44.23	sc	Frank, (1976)
MW2 (BENT 52470)	586774	1036118.188	0.04	slug test	this study
BENT_6612	592642.125	935322.5625	17.06	slug test	this study
BENT_51799	591570.4375	950302.375	1.08	slug test	this study
LANE_13051	592305.875	865945.9375	25.42	sc	this study
LANE_8029	609012.625	895777.6875	0.2	sc	this study
LINN_13576	634798.75	962499	1.22	sc	this study
BENT_2544	609440.1875	1063545.375	47.08	sc	this study
LANE_11099	648413.6875	864817.375	17.21	sc	this study
LANE_8712	595534.375	894605.875	23.84	sc	this study
LINN_1091	608682.625	956680.625	47.9	sc	this study
LINN_2123	612850.1875	933451.875	1.51	sc	this study
LINN_8756	621288.6875	1036971.188	10.28	sc	this study
LINN_10808	615350.3125	1008639.813	46.61	sc	this study
LINN_13545	655276.25	968616.0625	8.87	sc	this study
LINN_14614	680212	963194.5625	8.63	sc	this study
LINN_50854	649848.9375	1006531.813	0.45	sc	this study
LANE_6633	588117.625	918944	5.89	sc	this study
LINN_13680	634422.25	946264.4375	2.35	sc	this study

LINN_13739	603682.3125	971538.75	21.39	sc	this study
LINN_10769	611959.3125	1018009.125	4.24	sc	this study
LINN_7086	646523.125	1065788.625	13.04	sc	this study
LINN_10586	656941.125	1006580	0.72	sc	this study
BENT_1625	634964.3125	1071534.625	66.7	sc	this study
BENT_434	594522.5	1030513	2.12	sc	this study
LINN_13598	657738.5	965343.5	4.04	sc	this study
LINN_13627	637238.9375	957471.8125	74.78	sc	this study
LINN_10783	616950.75	1013026.313	22.95	sc	this study
LINN_11794	651434.1875	1003259.625	7.95	sc	this study
LINN_13557	641646.4375	971946.5625	8.83	sc	this study
LINN_13555	644084.5625	971790.1875	16.95	sc	this study
BENT_6834	586297.125	954565.5	35.31	sc	this study
BENT_6297	577330	987404.9375	2.18	sc	this study
BENT_4224	592587.1875	1041978.438	56.5	sc	this study
BENT_528	572840.625	1009881.813	6.15	sc	this study
LANE_52059	584795.125	878474.25	1	sc	this study
BENT_1591	637149.1875	1070409.375	12.36	sc	this study
LINN_50851	635988.75	973025	4.61	sc	this study
LANE_5101	599223.6875	912459.1875	1.93	sc	this study
LANE_4315	612147.9375	912726.9375	6.05	sc	this study
		geometric mean =	7.2439495		

Table I 4: Initial hydraulic conductivity values and well information for the Lower Sedimentary hydrogeologic unit. Final optimized values were multiplied by 8.
*pump test/sc = used both pump test and specific capacity information
** SUB report = Springfield Wellhead Protection Area Delineation Report, Lane County, Oregon, Cascade Earth Sciences, Ltd., 1996.
***ODHS, Monroe = Source Water Assessment Report, City of Monroe PWS #4100540, Oregon Department of Human Services and Oregon Department of Environmental Quality, 2002.
****ODHS, Harrisburg = Source Water Assessment Report, City of Harrisburg, Oregon Department of Human Services and Oregon Department of Environmental Quality, future publishing, pers. communication, Dennis Nelson.
*****ODHS, Junction City = Source Water Assessment Report, City of Junction City, Oregon Department of Human Services and Oregon Department of Environmental Quality, future publishing, pers. communication, Dennis Nelson.

Well	x (oregon lambert ft)	y (oregon lambert ft)	Land surface elevation amsl (ft)	Average well screen elevation (ft)	Date/Time	Water level BLSD (ft)	Average water level elevation amsl (ft) from 7/1/04 through 7/31/05	Hydro-geologic layer	Source
LANE_8725	590818.6226	888325.2070	341.0	313	recorder	recorder	336.63	3	this study*
BENT_6612	592642.1100	935322.5900	295.0	242	recorder	recorder	287.08	4	this study*
LINN_14047	633194.8962	922827.6250	325.9	282.9	OWRD net.	OWRD net.	320.9	3	OWRD*
LINN_10817	622646.8829	1005071.4200	250.0	169	OWRD net.	OWRD net.	242.4	3	OWRD*
LANE_8029	609012.6359	895777.7160	339.6	259.6	OWRD net.	OWRD net.	327.08	4	OWRD*
LINN_10562	639123.8048	1009944.2200	253.4	183.4	OWRD net.	OWRD net.	249.02	3	OWRD*
BENT_50297	577084.2587	1019217.0400	239.3	161.3	OWRD net.	OWRD net.	228.12	4	OWRD*
LINN_13576	634798.7400	962499.0160	288.5	216	OWRD net.	OWRD net.	282.99	4	OWRD*
LANE_51613	665629.4193	848321.7320	484.7	393.2	OWRD net.	OWRD net.	465.94	3	OWRD*
LINN_7478	658492.2477	1045288.9600	274.0	162	OWRD net.	OWRD net.	262.06	3	OWRD*
LINN_8508	628479.1599	1048460.0000	216.3	143.3	OWRD net.	OWRD net.	197.86	3	OWRD*
BENT_2544	609440.1695	1063545.3100	228.0	174.5	OWRD net.	OWRD net.	198.06	4	OWRD*
LANE_13051	592305.9044	865945.9650	386.0	302.5	OWRD net.	OWRD net.	364.44	4	OWRD*
LINN_11999	661631.9909	975029.2392	300.0	177	OWRD net.	OWRD net.	302.11	3	OWRD*
MW1	582670.0000	1039270.0000	252.5	236.6			239.46	3	this study*
					7/16/04 15:50	12.99			
					10/12/04 7:45	13.06			
					1/20/05 11:10	13.06			
					4/12/05 18:40	13.03			
					7/14/05 8:10	13.27			
					10/19/05 8:00	12.93			
MW2	586773.9800	1036118.2000	229.4	212.3			213.44	4	this study*
					7/16/04 15:20	15.61			
					10/12/04 8:00	15.99			
					1/20/05 11:30	16.15			
					4/12/05 18:35	16.09			
					7/14/05 8:15	15.96			
					10/19/05 8:18	16.03			
MW3	609940.2900	1023784.9000	226.1	207.6			208.77	3	this study*
					7/16/04 16:20	14.37			
					10/14/04 8:40	18.29			
					1/20/05 13:55	18.44			
					4/13/05 9:25	18.21			
					7/18/05 9:05	18.13			
					10/19/05 9:00	18.28			
MW4	596412.8200	990606.4700	249.1	223.2			224.73	3	this study*
					7/19/04 9:00	24.04			
					10/12/04 8:50	24.3			
					1/22/05 8:20	24.26			
					4/11/05 8:17	24.86			
					7/14/05 9:15	24.31			
					10/19/05 8:57	24.48			
MW5	594039.8500	934456.6900	297.5	276			283.23	3	this study*
					7/16/04 11:45	11.74			
					10/26/04 10:35	14.13			
					1/22/05 9:25	11.4			
					4/11/05 9:15	19.79			
					7/14/05 10:10	19.57			
					10/19/05 10:10	dry			
MW6	630786.8900	885456.7700	370.4	348.9			350.51	3	this study*
					7/20/04 9:10	20.04			
					10/12/04 13:45	20			
					1/22/05 15:36	20.1			
					4/11/05 15:45	19.4			
					7/18/05 15:40	20.12			
					10/19/05 15:15	20.34			

LINN_6700	681081.3100	1052753.8700	282.5	255			273.6	3	this study*
					7/21/04 13:45	13.25			
					10/14/04 10:50	8.44			
					1/25/05 14:05	7.13			
					4/12/05 16:25	6.76			
					7/19/05 10:25	7.83			
					10/22/05 10:45	8.17			
LINN_10391	660953.7300	1029590.6700	292.3	237.3			279.68	3	this study*
					7/21/04 15:00	17.2			
					10/14/04 10:20	15.57			
					1/20/05 15:00	9.53			
					4/12/05 16:50	8.18			
					7/19/05 10:55	12.93			
					10/22/05 0:00	15.71			
LINN_50097	629798.3700	1035644.8200	240.0	188			226.47	3	this study*
					7/6/04 16:49	14.6			
					7/21/04 15:45	19.51			
					10/14/04 9:55	17.71			
					1/20/05 14:30	8.87			
					4/12/05 17:15	6.94			
					7/18/05 11:40	12.93			
					10/22/05 10:00	16.17			
Phouse_hyslp	611804.2100	1062260.5700	226.0	166			193.57	4	this study*
					8/10/04 14:45	32.69			
					10/14/04 11:25	33.39			
					1/20/05 16:05	32.19			
					4/12/05 15:45	31.45			
					7/19/05 11:40	32.3			
					10/29/05 11:30	34.03			
Closet_hyslp	611814.5100	1062322.3600	226.0	167			194.22	4	this study*
					1/20/05 16:15	32.15			
					4/12/05 15:50	31.4			
					7/19/05 11:45	32.23			
					10/24/05 11:23	34.09			
LINN_14280	613883.8800	1044150.3700	230.0	185.5			194.03	3	this study*
					8/6/04 13:45	36.29			
					10/16/04 11:38	37.41			
					1/25/05 14:45	35.76			
					4/15/05 17:45	34.43			
					7/18/05 10:22	34.52			
					10/24/05 0:14	37.08			
GR-2291	598677.9300	1039155.1400	217.0	184			195.64	4	this study*
					8/10/04 17:00	27.54			
					10/14/04 8:00	21.32			
					1/20/05 13:00	18.65			
					4/13/05 9:00	17.93			
					7/18/05 8:35	20.64			
					10/22/05 9:35	21.32			
BENT_4231	599091.1000	1038600.3100	218.0	193.5			197.03	3	this study*
					8/10/04 16:00	22.89			
					10/14/04 8:05	21.78			
					1/20/05 13:25	18.97			
					4/13/05 9:10	20.22			
					7/18/05 8:50	20.67			
					10/22/05 9:15	21.84			
GR-2292	598630.7100	1038340.6000	217.7	192.7			198.59	3	this study*
					8/10/04 15:30	18.04			
					10/14/04 8:15	21.65			
					1/20/05 12:40	18.93			
					4/13/05 8:45	17.82			
					7/18/05 9:10	20.68			
					10/22/05 9:10	21.67			

LINN_10841	595207.2900	1037537.8700	206.4	172.4			182.88	3	this study*
					7/6/04 15:55	24.62			
					10/14/04 9:20	25.78			
					1/20/05 12:05	22.8			
					4/12/05 17:35	20.86			
					7/18/05 7:55	26.46			
					10/22/05 9:00	25.57			
BENT_5197	591144.7400	1025414.4600	235.0	195.5			225.65	3	this study*
					8/4/04 9:45	18.02			
					10/12/04 8:20	12			
					1/20/05 16:55	4.5			
					4/11/05 7:45	2.86			
					7/14/05 8:50	PUMPING			
					10/19/05 8:37	11.42			
LINN_10769	611998.7100	1018058.6900	247.5	207.5			228.51	4	this study*
					7/22/04 11:05	23.65			
					10/14/04 8:50	20.25			
					1/20/05 14:05	17.75			
					4/13/05 0:00	14.29			
					7/18/05 9:40	18.09			
					10/24/05 0:40	19.04			
LINN_13737	604177.4500	972281.9000	271.2	230.7			254.75	4	this study*
					7/20/04 16:40	12.75			
					10/12/04 16:05	19.09			
					1/25/05 13:00	18.12			
					4/13/05 10:00	15.85			
					7/18/05 18:35	17.62			
LINN_13770	619345.0100	957270.9800	285.2	242.2			276.46	3	this study*
					7/20/04 15:55	12.29			
					10/12/04 15:45	10.6			
					1/25/05 12:35	6.61			
					4/11/05 18:35	5.45			
					7/18/05 17:15	9.35			
					10/19/05 18:10	12.76			
LINN_2476	619617.0200	957911.0100	282.0	240.5			270.07	3	this study*
					7/20/04 15:22	13.84			
					10/12/04 15:40	14.36			
					1/25/05 12:40	10.39			
					4/11/05 18:45	9.13			
					7/18/05 17:20	11.77			
					10/19/05 18:00	13.83			
LANE_6633	588142.4700	918906.8000	310.7	254.2			304.22	4	this study*
					7/19/04 15:15	7.84			
					10/12/04 10:30	8.33			
					1/22/05 10:00	4.97			
					4/11/05 10:15	4.76			
					7/14/05 11:10	7.37			
					10/19/05 10:47	8.69			
LANE_59211	600426.9300	907695.6600	324.9	283.4			316.03	3	this study*
					7/19/04 13:40	13			
					10/12/04 11:50	12.97			
					1/22/05 12:17	5.09			
					4/11/05 12:15	4.4			
					7/18/05 15:05	6.75			
					10/19/05 12:14	9.54			
LANE_4237	611709.8600	908017.3600	330.9	271.9			319.47	4	this study*
					8/4/04 12:00	12.99			
					10/12/04 12:55	12.4			
					1/22/05 12:00	10.24			
					4/11/05 12:30	10.09			
					7/17/05 14:15	9.69			
					10/19/05 0:45	12.63			

LANE_51063	611329.6200	907347.4300	332.8	272.8			321.76	4	this study*
					7/19/04 11:30	7.86			
					10/12/04 13:15	13.64			
					1/22/05 12:50	11.44			
					4/11/05 12:50	11.21			
					7/17/05 14:00	14.63			
					10/19/05 13:30	14.31			
LANE_7719	611067.0800	907419.8600	332.7	294.2			318.27	3	this study*
					8/26/04 9:55	16.59			
					10/12/04 12:35	15.41			
					1/22/05 13:00	13.01			
					4/11/05 13:10	12.69			
					7/18/05 13:15	15.51			
					10/19/05 13:05	15.51			
LANE_12676	586837.1400	878377.4400	381.0	276			350.28	4	this study*
					8/4/04 13:45	32.79			
					10/12/04 11:05	28.65			
LANE_3203	586866.6200	878306.7000	381.0	366.5			371.05	3	this study*
					8/4/04 13:20	13.19			
					10/12/04 11:10	13.59			
					1/22/05 10:35	7.82			
					4/11/05 11:25	5.2			
					7/14/05 11:40	10.68			
					10/19/05 11:10	14.76			
LANE_7596	636293.0800	880026.8000	388.1	359.1			367.3	2	this study*
					8/4/04 16:45	22.99			
					1/22/05 16:50	19.82			
					4/11/05 16:45	19.58			
					7/14/05 18:15	19.5			
					10/19/05 16:15	22.55			
BENT_1192	591559.0800	950251.2300	278.0	239			264.12	3	this study*
					7/16/04 10:40	15.19			
					10/12/04 9:21	16.08			
					1/22/05 8:44	13			
					4/11/05 8:45	11.23			
					7/14/05 9:45	11.42			
					10/19/05 9:20	15.86			
BENT_51799	591570.4500	950302.3900	278.0	188			262.74	4	this study*
					7/19/04 17:10	19.79			
					10/12/04 9:30	15.87			
					1/22/05 9:00	13.14			
					4/11/05 8:50	12.22			
					7/14/05 9:55	20.31			
					10/19/05 9:27	15.79			
MW-02-04	638161.5000	867005.1000		342.8			389.77	3	EWEB*
					7/2/2004	392.41			
					7/9/2004	391.95			
					7/16/2004	391.54			
					7/23/2004	ND			
					7/30/2004	390.55			
					10/1/2004	388.81			
					10/8/2004	388.62			
					10/15/2004	388.54			
					10/22/2004	388.35			
					10/29/2004	388.3			
					1/7/2005	389.47			
					1/16/2005	389.17			
					1/21/2005	389.27			
					1/28/2005	389.17			
					4/1/2005	388.96			
					4/8/2005	389.41			
					4/15/2005	390.02			
					4/22/2005	390.63			
					4/29/2005	390.66			

Table I 5: Water level measurements used as model calibration targets. Digital data also included in Appendix J.
*Additional data is available for this regional area from each source, including the SUB (Springfield Utility Board, pers. communication, Chuck Davis). Data obtained from EWEB (Eugene Water and Electric Board) courtesy of Jay Bozevich. All data in area not used due to some spatial locations existing outside of model boundary and some low quality data.

APPENDIX J: GMS-MODFLOW Models, Water Level Measurements, GIS data, and
Raw Pump Test Data

Disk Contents:

Folder Pump test data: contains data collected during test 1, test 2, and test 3.

Folder Recorder wells: contains long-term water level data from recorder wells LANE 8725 and BENT 6612, and pressure transducer data from LANE 8069.

Folder Water level network: contains quarterly water level network data.

Folder project 10: contains final GMS-MODFLOW model with travel time data.

Folder GIS well location: contains well locations where slug tests, pump tests, groundwater age and chemistry, and water level measurements were collected. All data is projected in Oregon Lambert and NAD 83 datum.